Wave scattering from nontrivial boundary conditions

Dissertation
der Mathematisch-Naturwissenschaftlichen Fakultät
der Eberhard Karls Universität Tübingen
zur Erlangung des Grades eines
Doktors der Naturwissenschaften
(Dr. rer. nat.)

vorgelegt von

M. Sc. Jörg Alexander Nick

aus Horb am Neckar

Tübingen
2022

Gedruckt mit der Genehmigung der Mathematisch-Naturwissenschaftlichen Fakultät der Eberhard Karls Universität Tübingen.

Tag der mündlichen Qualifikation:	16.02.2023
Dekan:	Prof. Dr. Thilo Stehle
1. Berichterstatter:	Prof. Dr. Christian Lubich
2. Berichterstatter:	Prof. Dr. Markus Melenk
3. Berichterstatter:	Prof. Dr. Habib Ammari

Abstract

This dissertation studies the numerical approximation of time-dependent acoustic and electromagnetic wave scattering problems in the presence of non-standard boundary conditions. Of particular interest is the numerical treatment of generalized impedance boundary conditions, effective models that approximate the wave-material interaction of partially penetrable obstacles. Classical applications of such boundary conditions are the scattering of highly absorbing materials and perfectly reflecting obstacles with a thin coating. Moreover, acoustic boundary conditions are discussed in the context of the acoustic wave equation. Finally, a class of nonlinear boundary conditions is covered in the context of electromagnetic scattering.

Formulated on the time domain, these boundary conditions contain surface differential operators and temporal convolution operators. The resulting boundary value problems on exterior domains are reformulated to retarded boundary integral equations, which are themselves nonlocal in time and space, but fully formulated on the boundary. Several new fundamental properties of the time-harmonic classical potential operators and boundary operators for the acoustic wave equation and the Maxwell's equations are shown, in particular in view of their temporal counterparts. These theoretical results are the necessary preparations for the subsequent numerical analysis of these problems.

To derive numerical methods, the boundary integral equations are then discretized in time and space. The temporal discretization is carried out using the Runge–Kutta convolution quadrature method. Fully discrete schemes are derived by combining the time discretization with appropriate boundary element methods in space. Error bounds with specific convergence rates are shown for all boundary conditions.

The presentation of the linear boundary conditions is focused on emphasizing the similarities and differences of the acoustic and the electromagnetic settings. The error analysis for the nonlinear scattering problem substantially differs from the analysis of the linear boundary conditions and several new concepts are necessary to overcome the difficulties arising through the nonlinearity of the corresponding boundary integral equation. Numerical experiments illustrate the theoretical results and investigate practical aspects of the proposed methods.

Zusammenfassung

Die vorliegende Arbeit untersucht numerische Verfahren zur Simulation von akustischen und elektromagnetischen Wellen im Kontext von zeitabhängingen Streuproblemen, die an eine nichttriviale Randbedingung gekoppelt werden. Eine Vielzahl solcher Randbedingungen sind in der Praxis von Interesse, insbesondere wenn mehrere physikalische Skalen involviert sind. Effektive Randbedingungen beinhalten Modelle für dünne Schichten auf reflektierenden Materialien, oder beschreiben das Verhalten eines stark absorbierenden Mediums. Motiviert durch diese Anwendungen, behandelt die vorliegende Arbeit drei Klassen von Randbedingungen:

- akustische Streuprobleme mit einer abstrakten, linearen Randbedingung, die neben den beschriebenen Anwendungen auch akustische Randbedingungen beinhaltet,
- elektromagnetische Streuprobleme mit einer abstrakten linearen Randbedingung,
- elektromagnetische Streuprobleme mit einer nichtlinearen Randbedingung.

Zur Bearbeitung dieser Problemstellungen werden, basierend auf Repräsentationsformeln, zeitabhängige Randintegralgleichungen hergeleitet. Diese Gleichungen sind vollständig auf dem Rand des Streuobjekts formuliert und äquivalent zum ursprünglichen Streuproblem. Essenzielle Eigenschaften der zugrunde liegenden zeitabhängigen Randintegraloperatoren und Repräsentationsformeln werden mithilfe von Transmissionsproblemen gezeigt. Mithilfe dieser fundamentalen Resultate wird die Wohlgestelltheit der Randintegralgleichungen hergeleitet, womit die Wohlgestelltheit der jeweiligen Randwertprobleme insgesamt gezeigt wird.

Die Randintegralgleichungen werden in der Zeit durch Faltungsquadraturen basierend auf den Radau IIA Runge–Kutta Methoden diskretisiert. Die Stabilität der Semi-Diskretisierungen folgen aus den fundamentalen Eigenschaften der Randintegraloperatoren und allgemeinen Eigenschaften der Faltungsquadraturen. Komplementiert wird die Zeitdiskretisierung mit der Randelementmethode im Raum, um Volldiskretisierungen zu konstruieren, deren Lösungen effektiv berechnet werden können. Die resultierenden Verfahren berechnen in einem ersten Schritt die numerischen Lösungen auf dem Rand. Anschließend können die Approximationen durch diskrete Repräsentationsformeln an beliebigen Punkten im Gebiet ausgewertet werden.

Fehleranalysen leiten Konvergenzraten für die numerischen Approximationen her. Die Notation der Behandlung der linearen Randbedingungen für akustische und elektromagnetische Wellen wurde entsprechend angepasst, sodass Gemeinsamkeiten und Unterschiede herausgestellt werden. Für die nichtlinearen Randbedingungen wird eine Fehleranalyse mithilfe neuer Techniken basierend auf diskreten Transmissionsproblemen durchgeführt.

Alle numerischen Verfahren wurden implementiert und mit verschiedenen Parametern und Gittern getestet. Empirische Konvergenzraten illustrieren und komplementieren die theoretischen Ergebnisse. Visualisierungen der numerischen Approximationen zeigen den Nutzen der untersuchten Verfahren.

Danksagung

An erster Stelle möchte ich mich bei meinem Betreuer Prof. Dr. Christian Lubich bedanken, der in jederlei Hinsicht die vorliegende Arbeit ermöglicht hat. Deine durchgehende Bereitschaft (insbesondere mathematische) Hilfestellung zu leisten und deine uneingeschränkte Unterstützung für die Anliegen deiner Mitarbeiter haben meine Promotionszeit sehr erleichtert.

Herauszustellen ist mein Dank an Prof. Dr. Marlis Hochbruck und ihre Arbeitsgruppe, die im Zuge des SFB 1173 eine Schlüsselrolle meiner Promotion einnahm. Besonders gefreut haben mich die Einladungen nach Hirschegg und Bad Herrenalb, in denen ich „euch Karlsruher“ auch auf persönlicher Ebene kennenlernen durfte.

Ein ganz besonderer Dank gebührt Dr. Balázs Kovács, der mich bereits seit dem Beginn meines Studiums in wechselnden Rollen begleitet. Deine herausragende Lehre und Betreuung haben einen entscheidenden Beitrag zum Gelingen meines Studiums und meiner Promotion beigetragen. Danke für deine Unterstützung, für deine fachlichen Anregungen und die vielseitigen Diskussionen.

Die gute Atmosphäre in der Arbeitsgruppe, untermalt durch interessante Gespräche und kulturelle Kuriositäten, haben viele meiner Arbeitstage bereichert. Danke daher an alle Kolleginnen und Kollegen der Numerikgruppe, insbesondere an Gianluca Ceruti, Dominik Edelmann, Lukas Einkemmer, Guilherme Fiusa, Yanyan Shi, Dominik Sulz, Hanna Walach und Bin Wang, die ich während meiner Tübinger Zeit kennenlernen durfte.

Mein herzlicher Dank gebührt meiner Familie, besonders meinen Eltern, deren Unterstützung während meiner Studienzeit direkt zum Gelingen der vorliegenden Arbeit beigetragen hat. Bei meiner Partnerin Julia bedanke ich mich für den bedingungslosen Rückhalt, den sie mir durchwegs während der Promotion gegeben hat. Danke euch allen für die Bestärkungen, für die Begleitung durch Höhen und Tiefen, und euren Rat.

This work has been funded by the Deutsche Forschungsgemeinschaft (DFG, German Research Foundation) - Project-ID 58734477 - SFB 1173.

Contents

1. Introduction **1**
- 1.1. Notation and conventions . . . 3
- 1.2. Boundary conditions studied in this thesis . . . 6
  - 1.2.1. Time-dependent acoustic scattering . . . 6
  - 1.2.2. Time-dependent electromagnetic scattering . . . 9
  - 1.2.3. Electromagnetic scattering from nonlinear boundary conditions . . . 11
- 1.3. Contributions of this thesis . . . 12
- 1.4. Outline . . . 13

2. Acoustic scattering from GIBCs **17**
- 2.1. Traces, Sobolev spaces and a further Hilbert space $V \subset H^{-1/2}(\Gamma)$ . . . 17
  - 2.1.1. Setting of the transfer operator $Z(s)$ . . . 19
- 2.2. The transfer operators from (1.4)–(1.8) . . . 20
  - 2.2.1. Weak formulation of the generalized impedance boundary conditions . . . 23
- 2.3. The Helmholtz problem . . . 23
  - 2.3.1. Recap: Potential operators and representation formulas . . . 24
  - 2.3.2. Transmission problems and boundary operators . . . 26
  - 2.3.3. Time-harmonic boundary operators and the Calderón operator . . . 30
- 2.4. Time-harmonic boundary integral equations . . . 31
  - 2.4.1. Well-posedness of time-harmonic scattering with generalized impedance boundary conditions . . . 35
  - 2.4.2. Boundary integral equations for the inverted boundary condition . . . 36
  - 2.4.3. Bounds for the time-harmonic potential operators away from the boundary 38
- 2.5. Time-dependent acoustic wave equation with GIBCs . . . 39
- 2.6. Semi-discretization in time . . . 42
  - 2.6.1. Convolution quadrature for the scattering problem . . . 42
- 2.7. Full discretization . . . 45
- 2.8. Numerical experiments . . . 52
  - 2.8.1. Spherically symmetric scattering: an example with an accurate reference solution . . . 52
  - 2.8.2. Scattering of a plane wave from a halfpipe for different boundary conditions . . . 54

3. Electromagnetic scattering from GIBCs **61**
- 3.1. Tangential trace, trace space $\boldsymbol{X}_\Gamma$ and a further Hilbert space $\boldsymbol{V}_\Gamma \subset \boldsymbol{X}_\Gamma$ . . . 62
  - 3.1.1. Setting of the impedance operator . . . 63

3.2. The impedance operators (1.13)–(1.16) . . . 64
3.2.1. Weak formulation of the generalized impedance boundary condition . . . 66
3.3. Time-harmonic Maxwell's equations . . . 67
3.3.1. Recap: Potential operators and representation formulas . . . 68
3.3.2. Transmission problems and boundary operators . . . 69
3.3.3. Time-harmonic boundary operators and the Calderón operator . . . 73
3.4. Time-harmonic boundary integral equation . . . 74
3.4.1. Well-posedness of time-harmonic scattering with generalized impedance boundary conditions . . . 78
3.4.2. Bounds for the time-harmonic potential operators away from the boundary 79
3.5. Time-dependent Maxwell's equations with GIBCs . . . 82
3.6. Semi-discretization in time . . . 84
3.6.1. Convolution quadrature for the scattering problem . . . 84
3.7. Full discretization . . . 87
3.8. Numerical experiments . . . 93

4. Nonlinear electromagnetic scattering **99**
4.1. Problem setting . . . 99
4.1.1. Functional analytical setting of the nonlinear function $\boldsymbol{b}$ . . . 100
4.1.2. Weak formulation of the nonlinear boundary condition . . . 103
4.1.3. Time-dependent representation formulas and a time-dependent transmission problem . . . 103
4.2. Maxwell's equations with the nonlinear boundary condition . . . 105
4.2.1. Bounds on the solution of the boundary integral equation . . . 106
4.3. Semi-discretization in time by Runge–Kutta convolution quadrature . . . 108
4.3.1. Runge–Kutta convolution quadrature . . . 108
4.3.2. Auxiliary result: Time discrete transmission problem . . . 111
4.3.3. Convolution quadrature for the nonlinear boundary integral equation . . . 113
4.3.4. Error bounds for the semi-discretization in time . . . 114
4.4. Semi-discretization in space by the boundary element method . . . 119
4.4.1. Spatial semi-discretization: Quasi-optimality . . . 120
4.4.2. Spatial semi-discretization: Error rates . . . 122
4.5. Full discretization . . . 123
4.5.1. Error bounds for the full discretization . . . 124
4.5.2. Pointwise error bounds . . . 132
4.5.3. Unconditional estimates on the numerical solution . . . 136
4.6. Numerical experiments . . . 138

Appendices **147**
A. Temporal Sobolev spaces and operational calculus . . . 148
B. The convolution quadrature method . . . 149
C. Implementation of the convolution quadrature method . . . 151

1. Introduction

Wave phenomena are of paramount importance in science as well as engineering and their understanding is a crucial aspect in a large class of applications in modern technologies. The study of waves has therefore been a long-standing scientific endeavour and remains an active field of research. Mathematically, these phenomena are described by hyperbolic partial differential equations, which are also referred to as wave equations. When an incoming wave interacts with an obstacle, some material law governing the behaviour of the wave inside the scatterer must be coupled to the wave equation along the boundary of the impeding object. This problem setting is generally known as *wave scattering*. When the behaviour of the wave inside of the obstacle is mainly determined by a small scale effect near the boundary, the effects on the scattered wave are local, up to a defect depending on the difference in scales. Examples of such physical settings of interest are the electromagnetic scattering from obstacles with high conductivity or perfect conductors with a thin dielectric coating.

The general concept behind *generalized impedance boundary conditions (GIBC)* is then to replace a full model inside of the scatterer with an asymptotic model on the interface. Coupling these approximate boundary conditions with the wave equation of interest then yields effective models for wave diffraction, whose discretizations do not require the computational resolution of the small scale. Such models are particularly relevant when the boundary condition takes the explicit form of a surface boundary differential equation.

This dissertation provides numerical analysis for a large class of such boundary conditions in the context of time-dependent wave scattering. The covered boundary conditions investigated in this thesis fall into the following classes.

- **Highly absorbing obstacles:** These boundary conditions approximate the scattering from highly conductive obstacles, a medium in which electromagnetic waves are absorbed and decay rapidly. As a consequence, the waves penetrate only a thin layer inside of the scatterer, a phenomenon which is also referred to as the *skin effect*. The width of this thin layer then constitutes the small scale, which affects the wave on the normal scale, but is computationally expensive to resolve numerically. Boundary conditions which approximate the effect of imperfect conducters have been used extensively in the engineering literature, starting already before the advent of computers in the 1930s to model the interaction of radio waves with the surface of the earth [71].

- **Thin dielectric layers around perfect conductors:** This class of boundary condition considers obstacles whose material properties are accurately modeled by an ideal conductor with a thin dielectric layer of a small width. In this case, the physical width of the thin coating is the small scale, whose properties influence the overall behaviour of the wave. As a consequence of the difference in scale of the layer thickness and the magnitude of

the obstacle, the effects due to these material properties are well approximated by local operators, a fact reflected in the spatial locality of the operators arising in the boundary condition. The derivation of these models is a much more recent development than the development of strongly absorbing boundary conditions, starting in the 1990s with [32].

- **Acoustic boundary conditions:** This type of boundary condition simulates the interaction of acoustic waves with obstacles by assuming that each point on the scattering surface acts like a spring. The boundary condition is then derived by neglecting transverse tensions along neighboring points on the surface, which was proposed in [20].

- **Nonlinear boundary conditions for electromagnetic scattering:** The interaction of electromagnetic waves with obstacles whose material inhibits physical phenomena that are nonlinear, such as thin ferromagnetic coatings, is effectively modeled by the use of nonlinear boundary conditions, as demonstrated in [3], [39] and [40]. These models result from the coupling of Maxwell's equations with the Landau–Lifschitz–Gilbert equation on the surface of the scatterer and are beyond the scope of this dissertation. Nevertheless, the existence of applications for nonlinear boundary conditions motivates the study of a nonlinear model problem in this dissertation. The nonlinear boundary condition chosen for the present work is of a power-law form which was originally discussed in [66] and subsequent work of the authors in the context of quasi-static Maxwell's equations on a bounded domain. The final chapter of the present thesis studies this nonlinear boundary condition in the context of scattering problems.

The specific formulation of the addressed boundary conditions are technically more challenging than classical Dirichlet or Neumann boundary conditions, in particular when formulated in the time domain. Generally, these boundary conditions consist of operators associated to surface partial differential equations and of time-dependent convolution operators. The temporal differential operators are generally nonlocal in time and belong to the framework of fractional calculus, or more generally the operational calculus of Heaviside. Retarded boundary integral equations naturally cope with these difficulties and are therefore an attractive tool to overcome these difficulties, in particular in the context of wave scattering problems.

The domain of interest for wave scattering problems, in this context the exterior of the bounded scatterer, is naturally unbounded. Unbounded domains pose a challenge for the derivation of numerical methods. The literature concerning numerical analysis for partial differential equations on unbounded domains is mainly divided into the following two approaches.

The first approach is to truncate the domain by an artificial boundary. Undesirable reflections at the artificial boundary can be mitigated by approximate non-reflecting boundary conditions, such as perfectly matched layers [21]. Techniques of this type require the artificially truncated domain to be convex, in order to avoid waves that re-enter the domain of interest. The resulting boundary value problems, then formulated on a bounded domain, can be discretized by more classical approaches, such as finite differences or finite element techniques.

The second approach to treat wave problems on exterior domains, which is the method of choice throughout this thesis, is the use of boundary integral equations. The analytic foundations of these ideas for time-dependent problems originate from [8, 9, 52] and were later

extended in [47]. The key idea behind these techniques is the use of representation formulas, which explicitly formalize the relation of wave functions and their traces. Through a limit process towards the boundary, general conclusions on the traces of wave problems can be drawn and consequently lead to the derivation of boundary integral equations. These formulations are equivalent to the full scattering problem, but completely formulated on the boundary. The space discretization of these boundary integral equations is carried out with boundary elements, either by the Galerkin method or through collocation. Two approaches to discretize such time-dependent boundary integral equations are known to guarantee stability in the literature. Firstly, the space-time Galerkin approach (for example in [36] and [37]) and secondly, the convolution quadrature method, proposed in the original works [50] and [52]. These time discretizations of the temporal boundary integral equation rely purely on the evaluation of the corresponding time-harmonic operators and are generally known to possess good stability and approximation properties [52]. Consequently, these methods have been used in a large number of publications (see, for example, [7, 11, 17, 19, 38]). Particularly related to the present thesis is [62], which investigates the convolution quadrature method in the context of an impedance boundary condition. The numerical methods throughout this thesis are derived through a combination of the convolution quadrature method with Galerkin-based boundary element techniques.

Another research result is indispensable for the techniques in the present thesis, namely the analysis of the temporal Calderón operator of the wave equation. Crucial initial results have been obtained in [1], in which the authors couple a discontinuous finite element method inside the scatterer with boundary integral equations in the exterior domain and show a partial stability result, which in particular does not include error bounds. The same setting, with different numerical and analytical methods, is investigated in [16], which gives a complete numerical analysis for the described setting. Both works rely on the Calderón operator, whose positivity (see [16]) is the key to obtain the desired stability of the proposed schemes. Leveraging the favourable stability properties of boundary integral equations derived through the Calderón operator, provably convergent numerical methods for nonlinear boundary conditions in the context of the acoustic wave equation have been derived in [13] and [18]. The results of [16] have further been transferred to electromagnetic wave propagation problems in [46] (additionally note [58]). These publications motivated and prepared the investigations of the present thesis.

1.1. Notation and conventions

In order to discuss the boundary conditions investigated in this thesis in more detail, some basic terminology and notational conventions are required. This section gives the fundamental definitions necessary to provide a precise formulation of the problems of interest.

Domains and surfaces

All problems in this thesis are formulated on exterior domains $\Omega \subset \mathbb{R}^3$, assumed to be the complement of one or several scatterers. Wherever not explicitly stated otherwise, these domains

are assumed to be Lipschitz domains [29]. At several points in the thesis, stronger regularity is assumed for the domain, either for the ease of presentation or to enable the derivation of results relying on bounds for higher derivatives of exact solutions of the studied wave equations. Regularity assumptions on the domain naturally carry over to its boundary $\Gamma = \partial\Omega$.

The unit normal vector is denoted by $\nu \colon \Gamma \to \mathbb{R}^3$. This vector field is the normalized vector field defined on the boundary orthogonal to the tangent space, which by convention points into the exterior domain Ω.

Differential operators and vector calculus

We give a brief definition of fundamental differential operators, which are the building blocks indispensable to formulate strong forms of the wave equations and boundary conditions covered in this thesis.

Throughout the thesis, we denote vectors, vector-valued functions and operators acting on such functions with boldface symbols to separate them from scalar entities. Two vector products appear in the thesis for three-dimensional vectors $\boldsymbol{a}, \boldsymbol{b} \in \mathbb{C}^3$. The scalar product, denoted by $\cdot$ and also referred to as dot product, reads

$$\boldsymbol{a} \cdot \boldsymbol{b} = \overline{\boldsymbol{a}}^T \boldsymbol{b} = \sum_{i=1}^{3} \overline{\boldsymbol{a}_i} \boldsymbol{b}_i, \tag{1.1}$$

where $\overline{\boldsymbol{a}}$ is the componentwise complex conjugate of $\boldsymbol{a}$. The vector-valued cross product is denoted by $\times$ and is defined by

$$\boldsymbol{a} \times \boldsymbol{b} = \begin{pmatrix} \boldsymbol{a}_2 \boldsymbol{b}_3 - \boldsymbol{a}_3 \boldsymbol{a}_2 \\ \boldsymbol{a}_3 \boldsymbol{b}_1 - \boldsymbol{a}_1 \boldsymbol{a}_3 \\ \boldsymbol{a}_1 \boldsymbol{b}_2 - \boldsymbol{a}_2 \boldsymbol{a}_1 \end{pmatrix}.$$

Spatial differential operators on the domain Ω

These operations, combined with spatial partial derivatives, are the building blocks of the wave equations occuring in this thesis. The partial derivatives with regards to the spatial coordinates x_1, x_2 and x_3 are denoted by ∂_1, ∂_2 and ∂_3. The gradient then collects these partial derivatives and reads,

$$\nabla = \begin{pmatrix} \partial_1 \\ \partial_2 \\ \partial_3 \end{pmatrix}.$$

The divergence and **curl** operators are notationally the vector products with the gradient, where the multiplication in (1.1) is understood as the application of the partial derivatives.

The divergence operator is thus defined, for a vector field $v : \Omega \to \mathbb{C}^3$, by

$$\operatorname{div} v = \nabla \cdot v = \sum_{i=1}^{3} \partial_i v_i.$$

Composing the divergence of the gradient yields the Laplace operator

$$\Delta = \operatorname{div} \circ \nabla = \nabla \cdot \nabla.$$

The **curl** operator is notationally the concatenation of the gradient with the cross product, which gives the expression

$$\mathbf{curl}\, v = \nabla \times v = \begin{pmatrix} \partial_2 v_3 - \partial_3 v_2 \\ \partial_3 v_1 - \partial_1 v_3 \\ \partial_1 v_2 - \partial_2 v_1 \end{pmatrix}.$$

Spatial differential operators on the boundary Γ

Whereas the differential operators on the domain are the building blocks of the wave equations, analogous operators on the boundary $\Gamma = \partial\Omega$ play a similar role for the formulation of the studied boundary conditions. For functions and vector fields defined on the boundary, the surface gradient for a function $f : \Gamma \to \mathbb{C}$ is the gradient of some arbitrary local extension around the the surface projected to the tangent space, which reads for $f : \mathbb{R}^3 \to \mathbb{C}$

$$\nabla_\Gamma f = \nabla f - (\nabla f \cdot \nu)\, \nu \quad \text{on} \quad \Gamma.$$

Analogous to their counterparts in the domain, the divergence and the **curl** operators are now deduced from the components of the surface gradient.

The surface divergence of a vector field on the boundary $v_\Gamma : \Gamma \to \mathbb{C}^3$ is defined via

$$\operatorname{div}_\Gamma v_\Gamma = \nabla_\Gamma \cdot v_\Gamma.$$

As it bears no relevance to the topics covered in this thesis, the definition of the surface **curl** is omitted. The Laplace-Beltrami operator is defined as the surface divergence of the surface gradient, which reads

$$\Delta_\Gamma = \operatorname{div}_\Gamma \circ \nabla_\Gamma = \nabla_\Gamma \cdot \nabla_\Gamma.$$

Details on surface differential equations are found in [30].

Frequency domain and temporal convolutional operators

Finally, temporal convolutional operators generalize a large class of differential operators in time. The derivative in time, the most basic temporal convolutional operator, is denoted analogously to the partial derivatives in space by ∂_t.

Key to many of our observations is the *Laplace transform* $\mathcal{L}$. Given a temporal function $g : (0, \infty) \to \mathbb{R}$, its Laplace transform is defined via the integral

$$\widehat{g}(s) = (\mathcal{L}g)(s) \coloneqq \int_0^\infty e^{-st} g(t) \mathrm{d}t, \qquad \text{for all } \mathrm{Re}\, s > 0,$$

provided that the right-hand side is finite. The Laplace transform $\widehat{g}(s)$ is consequently, under sufficient regularity of g, a well-defined analytic function on $\mathbb{C}_+ = \{s \in \mathbb{C} \mid \mathrm{Re}\, s > 0\}$, the complex half space with real part.

Laplace transforms of quantities of interest or operators which act exclusively on Laplace transforms are also referred to as *time-harmonic*, or are said to be in the *Laplace domain*. Sometimes, these functions and operators are also said to be in the *frequency domain*.

Consider a function defined on the Laplace domain, namely some polynomially bounded $Z(s) : \mathbb{C} \to \mathbb{C}$, analytic on the half space $\mathbb{C}_+$. This analytic transfer function now defines a temporal convolutional operator via the Heaviside notation of operational calculus, which writes

$$Z(\partial_t) g = (\mathcal{L}^{-1} Z) * g. \tag{1.2}$$

This definition is a generalization of the classical notation of differential operators, namely the temporal convolution operator associated with the scalar multiplication $Z(s) = s$ (for g with vanishing initial conditions and sufficiently regular), corresponds to the time derivative ∂_t in the time domain. Under the same assumptions, this expression redefines the integral by setting $Z(s) = s^{-1}$. The expression (1.2) further gives a definition of the fractional derivative $\partial_t^{1/2}$, by inserting $Z(s) = s^{1/2}$.

1.2. Boundary conditions studied in this thesis

With these expressions at our disposal, we are in the position to formulate all wave equations and boundary conditions studied in this thesis, starting from the acoustic wave equation with generalized impedance boundary conditions. All of the boundary conditions are presented, in contrast to most of their original literature, in their first-order formulation. This will prove to be a convenient setting for the presentation throughout the thesis.

1.2.1. Time-dependent acoustic scattering

The *acoustic wave equation* (with wave speed set to $c = 1$ in appropriate physical units) reads

$$\begin{aligned} \partial_t p^{\mathrm{tot}} - \nabla \cdot \boldsymbol{v}^{\mathrm{tot}} &= 0 \\ \partial_t \boldsymbol{v}^{\mathrm{tot}} - \nabla p^{\mathrm{tot}} &= 0 \end{aligned} \qquad \text{in the exterior domain } \Omega. \tag{1.3}$$

The operators ∇ and $\nabla\cdot$ denote the gradient and the divergence as discussed in the previous section. The total wave $(p^{\mathrm{tot}}, \boldsymbol{v}^{\mathrm{tot}})$ is assumed to have initial support away from the boundary $\Gamma = \partial\Omega$ and to initially coincide with a closed form solution of the acoustic wave equation on

the whole space $\mathbb{R}^3$, which is referred to as the *incident wave* $(p^{\text{inc}}, \boldsymbol{v}^{\text{inc}})$. As the total wave and the incident wave are solutions of the acoustic wave equation, their differences $p := p^{\text{tot}} - p^{\text{inc}}$ and $\boldsymbol{v} := \boldsymbol{v}^{\text{tot}} - \boldsymbol{v}^{\text{inc}}$, referred to as *scattered waves*, again solve the acoustic wave equation. The objective is now to find the unknown scattered wave $(p, \boldsymbol{v})$ such that the total wave fulfills a specified boundary condition.

All boundary conditions studied in this context enforce a relation between the entities p^{tot} and $\boldsymbol{v}^{\text{tot}}$ along the boundary Γ. Since boundary conditions in the literature are often expressed in terms of the second-order formulation of the acoustic wave equation, the following identity is crucial for the conversion to the present notation. The Neumann trace of the acoustic pressure coincides with the derivative of an appropriate trace of the velocity field, namely

$$\partial_n p^{\text{tot}} = \nabla p^{\text{tot}} \cdot \boldsymbol{\nu} = \partial_t \boldsymbol{v}^{\text{tot}} \cdot \boldsymbol{\nu} \quad \text{on } \Gamma = \partial\Omega,$$

where the right-hand side is to be understood as the appropriate trace operator applied to the total velocity field.

Generalized impedance boundary conditions for acoustic scattering

Consider a perfectly reflecting material, which is coated by a thin-layer of a homogeneous material. The interaction of such a scatterer with an incoming acoustic wave is the objective of the generalized impedance boundary condition derived in [32]. This boundary condition is explicitly formulated as a surface partial differential equation, itself reminiscent of the acoustic wave equation, and reads

$$\partial_t \boldsymbol{v}^{\text{tot}} \cdot \boldsymbol{\nu} = \delta(\partial_t^2 p^{\text{tot}} - \Delta_\Gamma p^{\text{tot}}) \quad \text{on } \Gamma. \tag{1.4}$$

The small parameter $\delta \ll 1$ on the right-hand side is a physical property of the scattering problem and is proportional to the thickness of the thin-layer. Integration on both sides yields, in view of the Heaviside notation (1.2), the equivalent formulation

$$\boldsymbol{v}^{\text{tot}} \cdot \boldsymbol{\nu} = \delta(\partial_t p^{\text{tot}} - \partial_t^{-1} \Delta_\Gamma p^{\text{tot}}) \quad \text{on } \Gamma. \tag{1.5}$$

This formulation, where the left-hand side consists solely of the trace of the velocity field, will prove to be a convenient setting for the presentation.

A particularly interesting use of generalized impedance boundary conditions is the incorporation of small scale effects along the boundary, which is noticable through the presence of small parameters in the boundary condition. The magnitude of these parameters are in the order of the small physical scale arising in the problem of interest, for example the thickness of the coating in the boundary condition discussed above. To unify our notation, these small positive parameters are denoted by the same letter $\delta \ll 1$.

The first boundary condition dedicated to the scattering from strongly absorbing media is attributed to Leontovich (published in [48] and [49] (cited from [71]), although the initial discovery is assumed to be much earlier in the 1930s). Higher-order extensions of this boundary condition were developed by Rytov [61]. These extensions were based on an expansion of the wave inside and outside of the scatterer by a power series in terms of the small parameter δ

and omitting terms of at least a given order. A rigorous asymptotic analysis of this boundary condition in the time domain has been conducted much later in [55]. In the present context, this boundary condition is compactly formulated through the use of fractional calculus, which reads

$$\boldsymbol{v}^{\mathrm{tot}} \cdot \boldsymbol{\nu} = \frac{1}{\delta}\, \partial_t^{-1/2} p^{\mathrm{tot}} \quad \text{on } \Gamma. \tag{1.6}$$

This boundary condition approximates the effects of coupling the exterior acoustic wave equation to the damped wave equation

$$\partial_t^2 p^{\mathrm{tot}} + \frac{1}{\delta^2}\, \partial_t p^{\mathrm{tot}} - \Delta p^{\mathrm{tot}} = 0 \qquad \text{in the interior domain } \mathbb{R}^3 \setminus \overline{\Omega}.$$

Solutions to this damped wave equation decay exponentially in terms of the distance to the boundary. For δ small enough, the wave is consequently almost zero beyond a thin-layer inside the scatterer, which causes the skin-effect phenomenon. This boundary condition is also referred to as a first-order approximation, as its pertubation to the full problem is in the order of $\mathcal{O}(\delta^2)$, for sufficiently small δ. A second-order extension of the above boundary condition has been rigorously analyzed by [41] in the time-harmonic setting and reads, when translated to the time domain

$$\partial_t p^{\mathrm{tot}} \cdot \boldsymbol{\nu} = \frac{1}{\delta}\, \partial_t^{1/2} p^{\mathrm{tot}} - \mathcal{H} p^{\mathrm{tot}} \quad \text{on } \Gamma, \tag{1.7}$$

where $\mathcal{H}$ is the mean curvature of Γ. Whereas these boundary conditions were the original motivating examples for this thesis, another boundary condition is of particular interest to specifically model acoustic waves. Effective models for scatterers with a vibrating surface are *acoustic boundary conditions*; see [20]. These boundary conditions are typically formulated as the following coupled system

$$\begin{aligned} m\, \partial_t^2 w + \alpha\, \partial_t w + k\, w + \partial_t p^{\mathrm{tot}} &= 0 \\ \partial_t w &= -\partial_t \boldsymbol{v}^{\mathrm{tot}} \cdot \boldsymbol{\nu} \end{aligned} \qquad \text{on } \Gamma, \tag{1.8}$$

completed by vanishing initial conditions for w and $\partial_t w$. The physical constants $m > 0$, $\alpha \geq 0$ and $k > 0$ are the given mass, damping and stiffness parameters, respectively.

We formulate the described problems as a general first-order system, which fits well into the framework of time-dependent boundary integral equations. The presented boundary conditions (1.4)–(1.8) are special cases of the following abstract generalized impedance boundary condition

$$\boldsymbol{v}^{\mathrm{tot}} \cdot \boldsymbol{\nu} = Z(\partial_t) p^{\mathrm{tot}} \quad \text{on } \Gamma. \tag{1.9}$$

Generally, this boundary condition thus enforces some linear relation between the traces of the two quantities occuring in the first-order formulation of the wave equation, which is analogous to the subsequently discussed treatment of electromagnetic scattering. The temporal convolution operator $Z(\partial_t)$ is assumed to fulfill a positivity condition, which is shown for all stated boundary conditions in the subsequent chapter.

Interest in these boundary conditions was the starting point of this thesis, yet the main practical interest is found in applications based on their electromagnetic counterparts, which are introduced in the following section.

1.2.2. Time-dependent electromagnetic scattering

Our attention turns towards electromagnetic wave propagation, mathematically described by the *time-dependent Maxwell's equations*. The total electromagnetic fields, consisting of the electric field $\boldsymbol{E}^{\text{tot}}(\boldsymbol{x}, t)$ and the magnetic field $\boldsymbol{H}^{\text{tot}}(\boldsymbol{x}, t)$, both vector fields with three components, are strong solutions to Maxwell's equations, if

$$\begin{aligned} \varepsilon\, \partial_t \boldsymbol{E}^{\text{tot}} - \mathbf{curl}\, \boldsymbol{H}^{\text{tot}} &= 0 \\ \mu\, \partial_t \boldsymbol{H}^{\text{tot}} + \mathbf{curl}\, \boldsymbol{E}^{\text{tot}} &= 0 \end{aligned} \qquad \text{in the exterior domain } \Omega. \tag{1.10}$$

The free space is assumed to be a homogeneous medium, namely the electric permittivity ε and the magnetic permeability μ are assumed to be positive constants in Ω. Analogous to the acoustic case, this constitutes a first-order hyperbolic system of equations with two quantities of interest.

Throughout the thesis and for all studied wave equations, the wave speed c is assumed to be normalized, i.e. $c = 1$. This condition can safely be assumed and is equivalent to rescaling the time variable $t \to ct$. Under this (always achievable) assumption, the product of the permittivity ε and permeability μ is 1, since

$$\varepsilon\mu = c^{-2} = 1.$$

In order to completely eliminate any physical constants in the problem formulation we further use the rescaling $\mu\boldsymbol{H} \to \boldsymbol{H}$. This rescaled field is sometimes also referred to as the magnetic field $\boldsymbol{B}$. With these conventions, the time-dependent Maxwell's equations are free of the physical constants ε and μ, and read

$$\begin{aligned} \partial_t \boldsymbol{E}^{\text{tot}} - \mathbf{curl}\, \boldsymbol{H}^{\text{tot}} &= 0 \\ \partial_t \boldsymbol{H}^{\text{tot}} + \mathbf{curl}\, \boldsymbol{E}^{\text{tot}} &= 0 \end{aligned} \qquad \text{in the exterior domain } \Omega. \tag{1.11}$$

Generalized impedance boundary conditions for electromagnetic scattering

The time-dependent generalized impedance boundary condition studied in the context of electromagnetic wave propagation is structurally similar to the acoustic case and reads

$$\boldsymbol{E}_T^{\text{tot}} + \boldsymbol{Z}(\partial_t)\left(\boldsymbol{H}^{\text{tot}} \times \boldsymbol{\nu}\right) = 0 \quad \text{ on } \Gamma. \tag{1.12}$$

The additional subscript in $\boldsymbol{E}_T^{\text{tot}}$ denotes the tangential projection of total electric field $\boldsymbol{E}^{\text{tot}}$ on the tangent space of the surface Γ. Analogous to the acoustic setting, $\boldsymbol{Z}(\partial_t)$ is an abstract linear operator, which generally consists of a combination of temporal convolutions and surface differential operators. This operator is also referred to as the *time-dependent impedance operator*.

Several examples of $\boldsymbol{Z}(\partial_t)$ from the literature are of interest and presented in the following.

Obstacles with thin coating

The starting point of our investigations into generalized impedance boundary conditions is an effective boundary condition for a perfect conductor with a thin dielectric coating, which was introduced by Engquist & Nédélec [32, equation (4.9)] in the time-harmonic context. Consider a thin coating of a small depth $\delta \ll 1$, consisting of a dielectric material with electric permittivity ε^δ and magnetic permeability μ^δ around a perfectly conducting obstacle. Formulated in the time domain, the effective boundary condition is then given by (1.12) with

$$\boldsymbol{Z}(\partial_t) = \delta \left(\frac{\mu^\delta}{\mu} \partial_t - \left(\frac{\varepsilon^\delta}{\varepsilon} \right)^{-1} \partial_t^{-1} \nabla_\Gamma \operatorname{div}_\Gamma \right). \tag{1.13}$$

The temporal operator ∂_t^{-1} denotes integration in time and is a special case of the Heaviside notation (1.2). The above boundary condition is again a first-order approximation with respect to the parameter δ. For a fixed frequency, this boundary condition was treated by Ammari & Nédélec [5, 6] using boundary integral equations.

Multiple extensions of this boundary condition have been proposed subsequently, most notably a second-order approximate boundary condition for thin layers, for which a rigorous error analysis was in the time-harmonic regime by Haddar & Joly [40, Eq. (95)]. Transferred to the time domain, it corresponds to (1.12) with

$$\boldsymbol{Z}(\partial_t) = \delta \left(\frac{\mu^\delta}{\mu} \partial_t \left(1 + \delta \left(\mathcal{H} - \mathcal{C}\right)\right) - \left(\frac{\varepsilon^\delta}{\varepsilon} \right)^{-1} \partial_t^{-1} \nabla_\Gamma \left[\left(1 - \delta \mathcal{H}\right) \operatorname{div}_\Gamma \right] \right), \tag{1.14}$$

where $\mathcal{C}$ and $\mathcal{H}$ denote the curvature tensor and the mean curvature respectively. Other extensions of these boundary conditions include models to approximate the effects of inhomogeneous coatings, which were derived in [4], and the effects of multiple layers placed on top of each other, which is explored in [34] and [35].

Highly conductive obstacles

The oldest applications of impedance boundary conditions is the approximation of the interaction of highly conductive materials with electromagnetic waves. The mathematical literature, conducting rigorous analysis of such boundary conditions and deriving error estimates in terms of the small scale, is more recent [40], [41] and [42].

The boundary conditions of interest for highly conductive materials have been derived in the time-harmonic setting by Haddar, Joly & Nguyen [42]. Electromagnetic waves in a conductive medium decay rapidly, which limits the penetration depth of the wave. As in the acoustic case, this causes the wave to vanish mostly in the interior of the scatterer, creating the *skin-effect* in the electromagnetic setting. An asymptotic expansion, with respect to the (small) depth of the penetration then yields reduced models. In the original reference [42], the authors derive multiple boundary conditions in the time-harmonic setting, covering multiple orders up to order 3. To limit the scope of the thesis, only the first- and second-order boundary conditions, or respectively their corresponding impedance operators, are discussed.

The following impedance operator yields a first-order boundary condition to the described problem setting

$$\boldsymbol{Z}(\partial_t) = \delta\, \partial_t^{1/2}, \tag{1.15}$$

where δ is inversely proportional to the square root of the high conductivity. The fractional derivative $\partial_t^{1/2}$ is a special case of the Heaviside notation (1.2) and is defined as the convolution with the kernel $(\pi t)^{-1/2}$. First-order in this context refers again to the power in the small parameter δ, which is a small physical parameter since the conductivity of the material is assumed to be large. The time domain impedance operator corresponding to the second-order boundary conditions reads

$$\boldsymbol{Z}(\partial_t) = \delta\, \partial_t^{1/2} - \delta^2 \mu(\mathcal{H} - \mathcal{C}), \tag{1.16}$$

where again $\mathcal{C}$ and $\mathcal{H}$ denote the curvature tensor and the mean curvature respectively.

1.2.3. Electromagnetic scattering from nonlinear boundary conditions

Finally, a class of nonlinear boundary conditions coupled to Maxwell's equations are studied. This type of boundary condition is obtained by replacing the linear impedance operator $\boldsymbol{Z}$ by a nonlinear function $\boldsymbol{a}$ (or more generally a nonlinear operator). The *nonlinear boundary condition* enforces the following relation between the traces of the electromagnetic fields:

$$\boldsymbol{E}^{\text{tot}} \times \boldsymbol{\nu} + \boldsymbol{a}(\boldsymbol{H}^{\text{tot}} \times \boldsymbol{\nu}) \times \boldsymbol{\nu} = 0 \quad \text{on } \Gamma, \tag{1.17}$$

where $\boldsymbol{\nu}$ denotes the outer unit normal vector.

Despite the apparent similarity of this boundary condition and the generalized impedance boundary condition (1.12), serious challenges arise in the discussed analysis of this boundary condition. The nonlinearity impedes the application of time-harmonic results and requires consequently a separate analysis, in particular for the derivation of error estimates.

We restrict the type of nonlinearities covered to the following class of power-law type

$$\boldsymbol{a}(\boldsymbol{x}) = |\boldsymbol{x}|^{\alpha-1}\boldsymbol{x} \quad \text{for all } \boldsymbol{x} \in \mathbb{R}^3, \tag{1.18}$$

with the parameter $\alpha \in (0, 1]$. The study of this boundary condition stems from [66] and [67], in which numerical analysis for such boundary conditions is conducted on bounded domains. The nonlinearity further plays a key role in the evolution boundary condition studied in [70]. Well-posedness analysis and decay results are available for this boundary condition and can be found in [31]. As in the chapters before, $\boldsymbol{\nu}$ denotes the unit outward surface normal and the region of interest Ω is the exterior domain. We therefore note that the signs of $\boldsymbol{\nu}$ appearing in the boundary condition (1.17) change in comparison to analysis on the inner domain, compare for example the notation used in the mentioned references.

This formulation of the nonlinear boundary condition appears in the literature and is used in the original paper [57] of the same author. Instead of repeating the analysis there, we use the

following equivalent formulation of the boundary condition in this thesis

$$\boldsymbol{H}^{\mathrm{tot}} \times \boldsymbol{\nu} + \boldsymbol{b}(-\boldsymbol{E}^{\mathrm{tot}} \times \boldsymbol{\nu}) \times \boldsymbol{\nu} = 0 \quad \text{on } \Gamma = \partial\Omega. \tag{1.19}$$

The nonlinearity here is the inverse of $\boldsymbol{a}$, which is also a power-law type function and reads

$$\boldsymbol{b}(\boldsymbol{x}) = \boldsymbol{a}^{-1}(\boldsymbol{x}) = |\boldsymbol{x}|^{\frac{1-\alpha}{\alpha}} \boldsymbol{x} \quad \text{for all } \boldsymbol{x} \in \mathbb{R}^3. \tag{1.20}$$

1.3. Contributions of this thesis

The present thesis intends to give the first extended numerical analysis for a large class of non-standard boundary conditions in the context of acoustic and electromagnetic wave scattering problems. On the basis of time-dependent representation formulas, stable boundary integral equations are derived. Fundamental results for the time-dependent potential operators and boundary integral operators, namely time-harmonic frequency-specific bounds, are shown. Combining these results with assumptions on the studied boundary conditions gives stability results for the corresponding temporal boundary conditions. In particular, this includes a new general well-posedness result for generalized impedance boundary conditions in the context of time-dependent electromagnetic scattering.

Discretizing the boundary integral equations with the convolution quadrature method in time and boundary elements in space then yields fully discrete schemes. The chosen discretizations conserve crucial properties of the boundary integral equations, which is the foundation of the present error analysis. For all presented boundary conditions, a complete error analysis is conducted. Under regularity assumptions on the exact solutions, error bounds with explicit error rates are derived, both for the boundary data and the solution away from the scatterer. The error analysis conducted for the nonlinear boundary condition should be particularly emphasized, since it relies on a novel stability analysis based on time-discrete transmission problems. Several key results are shown in the process of the convergence analysis, which in particular includes a discrete partial integration inequality for the m-stage Radau IIA Runge–Kutta method. Numerical experiments illustrate the use of the proposed methods and complement the theoretical results.

These main results were first published in their respective original works of the same author, namely in

- [15], joint work with L. Banjai and Ch. Lubich, for the treatment of GIBCs in the context of acoustic scattering, which is presented in Chapter 2;
- [59], joint work with B. Kovács and Ch. Lubich, for the treatment of GIBCs in the context of electromagnetic scattering, which is presented in Chapter 3;
- [57] for the treatment of a nonlinear boundary condition in the context of electromagnetic scattering, which is presented in Chapter 4.

To present these results in a unified notation and further contribute to the scientific literature, substantial modifications are made to the original presentations. Throughout the thesis,

particular emphasis will be placed on the connections of the acoustic and the electromagnetic settings, where the notation is chosen to highlight similarities in the analysis. Results from [15], which considered the numerical analysis for acoustic scattering from GIBCs, were reformulated in a first-order setting. This change was motivated by the electromagnetic analysis conducted in [59] and clarifies the connections of both settings. Some fundamental results from [59], mainly with respect to time-harmonic bounds on boundary integral operators, are carried over to the acoustic setting in order to give a unified presentation of the two settings. These efforts to unify the analysis of the settings then culminates in error bounds whose proofs contain large passages that are word for word identical, thus emphasizing the structural similarities of the acoustic and electromagnetic scattering problems. To the knowledge of the author, such a presentation is in itself a new contribution, in particular in the context of time-dependent retarded boundary integral equations.

The nonlinear boundary condition was originally investigated in a formulation where the nonlinearity is applied to the magnetic field, which is also known as "$\boldsymbol{H}$-to-$\boldsymbol{E}$". In the present thesis, the techniques developed in the original paper [57] are used to treat the equivalent rearranged boundary condition (then "$\boldsymbol{E}$-to-$\boldsymbol{H}$"), where the nonlinearity is instead applied to the electric field. This change results in an equivalent scattering problem, however the resulting boundary integral equation and consequently the derived numerical methods differ. The structure of the original error analysis is transferred to this transformed discrete boundary integral equation to obtain error bounds for the alternative formulation. For this new scheme, the present analysis predicts slightly improved convergence rates in comparison with the original results. Numerical experiments compare the two methods.

1.4. Outline

The results of this dissertation are mainly divided into the following three chapters, each devoted to the study of a separate class of boundary conditions. These chapters are complemented by Appendices A–C, which formulate important notation and general approximation results that are omnipresent throughout the thesis.

Chapter 2: GIBCs for the acoustic wave equation

Our investigations start with the acoustic wave equation, to which the second chapter is dedicated. The analytic setting of the acoustic impedance operator and its connection to the setting of acoustic traces are discussed in Sections 2.1–2.2. In the subsequent Section 2.3, the fundamental operators associated to the Helmholtz problem are introduced and connected to a time-harmonic transmission problem. Time-harmonic bounds that explicitly formulate the dependence on the Laplace parameter s are derived and proven through an effective use of the jump conditions and Green's formula. These results are then used in Section 2.4 to derive time-harmonic boundary integral equations, whose solutions solve the time-harmonic acoustic scattering problem with the generalized impedance boundary condition. Section 2.5 transports the time-harmonic results to the time-dependent setting. In Section 2.6, the convolution quadrature method based on the m-stage Radau IIA method is employed to discretize the boundary

integral equation in time. Combining the semi-discrete scheme with a boundary element discretization in Section 2.7 yields a fully discrete scheme. An error analysis is conducted and error estimates with explicit convergence rates are shown, under regularity assumptions on the exact solution. Finally, Section 2.8 presents numerical experiments of the proposed scheme and provides convergence plots. The chapter closes with the visualization of scattered waves under several boundary conditions to demonstrate the use of the method.

Chapter 3: GIBCs for Maxwell's equations

The third chapter is devoted to transport the previous results to the setting of electromagnetic scattering and is therefore structurally similar to the previous chapter. Section 3.1 introduces the functional analytic framework used in the context of electromagnetic scattering. An abstract framework for the generalized impedance boundary conditions is presented. This abstract framework includes the presented boundary conditions, which is shown in Section 3.2. The subsequent Section 3.3 introduces the potential and boundary operators associated to the time-harmonic Maxwell's equations and a time-harmonic electromagnetic transmission problem is formulated. Time-harmonic bounds for the potential operators that are explicit in the Laplace parameter s are shown, in particular also for point evaluations of the potential operators. Using the tools introduced in these sections we derive time-harmonic boundary integral equations in Section 3.4. A well-posedness result shows the equivalence of the boundary integral equation and the time-harmonic scattering problem. Section 3.5 carries these results over to the time-dependent problem and derives time-dependent boundary integral equations for Maxwell's equations. Employing the convolution quadrature method based on the m-stage Radau IIA method in Section 3.6 then gives a time-discrete scheme, whose approximation properties are guaranteed by previously established time-harmonic results. Section 3.7 combines a Raviart–Thomas boundary element discretization with the convolution quadrature time discretization to obtain a fully discrete boundary integral equation. The notation and the analysis up to this point is carefully adjusted so that the error analysis required is almost identical to the error analysis conducted in the acoustic setting. The necessary arguments to obtain error estimates are nevertheless completely formulated, as closely to the previously covered acoustic case as possible. Finally, Section 3.8 demonstrates the use of the proposed method with numerical experiments.

Chapter 4: Nonlinear boundary conditions for Maxwell's equations

The final chapter investigates a nonlinear boundary condition in the context of electromagnetic scattering. Section 4.1 describes the problem setting and provides an appropriate functional analytic framework of the nonlinear operator associated to the power-law type nonlinearity. Nonlinear boundary integral equations are derived in Section 4.2 and a bound on the solution in terms of the incident fields is given. Section 4.3 uses the convolution quadrature method based on the m-stage Radau IIA Runge–Kutta method to discretize the temporal convolution operators in the nonlinear boundary integral equation. Several important auxiliary results for the error analysis are shown, including a discrete partial integration inequality and techniques surrounding a time-discrete electromagnetic transmission problem. A temporally discrete error

analysis demonstrates the use of energy techniques based on the time-discrete transmission problem and proves optimal order convergence rates in time.

Section 4.4 considers the time-continuous boundary integral equation with a spatial semi-discretization based on Raviart–Thomas elements. A stability result is shown through applying a strong monotonicity property of the nonlinearity and combined with interpolation estimates for the Raviart–Thomas boundary element spaces to obtain convergence rates for the semi-discretization in space.

Employing the convolution quadrature method and the Raviart–Thomas boundary element method of the previous sections together gives the full discretization described in Section 3.7. Combining the ideas of the previously conducted error analysis gives error bounds for the fully discrete solutions in the natural norms, under regularity assumptions on the exact solution. Furthermore, through the use of new bounds on the potential operators associated to the time-harmonic Maxwell's equations and a chain of Hölder inequalities, pointwise error bounds are shown for points away from the boundary. Finally, the numerical solution is shown to be bounded, without any regularity assumptions on the exact solution. Numerical experiments illustrate the use of the method and complement the theoretical results in Section 3.8.

2. Acoustic scattering from generalized impedance boundary conditions

Acoustic scattering theory is a natural starting point for this thesis. We start with a strong formulation of the acoustic scattering problem with a generalized impedance boundary condition, which is expressed in terms of the scattered wave. Consider the setting of Section 1.2.1 and let $p = p^{\text{tot}} - p^{\text{inc}}$ and $v = v^{\text{tot}} - v^{\text{inc}}$ denote the scattered fields, which are outgoing solutions of the acoustic wave equation with vanishing initial conditions.

The scattered acoustic wave equation with an abstract generalized impedance boundary condition, formulated for the *acoustic pressure* p and the *velocity field* v, is therefore the following boundary value problem

$$\partial_t p - \nabla \cdot v = 0 \qquad \text{in} \quad \Omega, \tag{2.1}$$

$$\partial_t v - \nabla p = 0 \qquad \text{in} \quad \Omega, \tag{2.2}$$

$$v \cdot \nu - Z(\partial_t) p = g^{\text{inc}} \qquad \text{on} \quad \Gamma. \tag{2.3}$$

Initially, p and v are assumed to vanish. The right-hand side of the boundary condition is fully determined by the incoming wave, through

$$g^{\text{inc}} = Z(\partial_t) p^{\text{inc}} - v^{\text{inc}} \cdot \nu. \tag{2.4}$$

The scattered wave (p, v) has finite wave speed $c = 1$, which together with its vanishing initial support implies that the support of the wave is finite at any time t. Consequently, the scattered wave is square integrable at any time t without the application of additional asymptotic boundary conditions for $|x| \to \infty$.

2.1. Traces, Sobolev spaces and a further Hilbert space $V \subset H^{-1/2}(\Gamma)$

The boundary condition relates the trace of the acoustic pressure p and the trace of the velocity field v along the boundary. For a scalar function $u : \overline{\Omega} \to \mathbb{C}$, the *Dirichlet trace* reads

$$\gamma u = u_{|\Gamma} \quad \text{on } \Gamma.$$

The *normal trace*, associated to the Neumann trace of the pressure in the context of the acoustic wave equation, is given for a vector field $\boldsymbol{v}: \overline{\Omega} \to \mathbb{C}^3$ by

$$\gamma_\nu \boldsymbol{v} = \boldsymbol{v}_{|\Gamma} \cdot \boldsymbol{\nu} \quad \text{on } \Gamma.$$

This trace is related to the classical definition of the Neumann trace through the expression

$$\partial_\nu u = \gamma_\nu \nabla u.$$

These trace operators provide a suitable setting for the described boundary conditions. To rigorously define these operators, some functional analytic spaces are required. Proofs and rigorous derivations associated to the following definitions are found in [33, Chapter I]. On the exterior domain Ω, we define the spaces of square integrable functions by

$$L^2(\Omega) = \left\{ u: \Omega \to \mathbb{C} \;\middle|\; \int_\Omega |u|^2 \,\mathrm{d}\boldsymbol{x} < \infty \right\}, \quad \boldsymbol{L}^2(\Omega) = \left\{ \boldsymbol{u}: \Omega \to \mathbb{C}^3 \;\middle|\; \int_\Omega |\boldsymbol{u}|^2 \,\mathrm{d}\boldsymbol{x} < \infty \right\}.$$

With these spaces, the general Sobolev space $H^k(\Omega)$ of integer order $k \geq 0$, is defined by

$$H^k(\Omega) = \{ u \in L^2(\Omega) \,|\, D^\alpha_{\boldsymbol{x}} u \in L^2(\Omega) \text{ for all } |\alpha| \leq k \},$$

where $D^\alpha_{\boldsymbol{x}}$ denotes the combination of spatial derivatives associated to the multi-index α (details are found e.g. in [33, Section I.1]). The above spaces are equipped with their natural norms $\|\cdot\|_{L^2(\Omega)}$, $\|\cdot\|_{\boldsymbol{L}^2(\Omega)}$ and $\|\cdot\|_{H^k(\Omega)}$, which make them Hilbert spaces.

Two spaces are particularly relevant in the context of the acoustic wave equation. First, the classical space $H^1(\Omega)$, which is defined by the above expression and reads

$$H^1(\Omega) = \{ u \in L^2(\Omega) \,|\, \nabla u \in \boldsymbol{L}^2(\Omega) \}.$$

Analogously, the Sobolev space associated to the divergence operator reads

$$\boldsymbol{H}(\mathrm{div}, \Omega) = \{ \boldsymbol{v} \in \boldsymbol{L}^2(\Omega) \,|\, \nabla \cdot \boldsymbol{v} \in L^2(\Omega) \}.$$

A key identity is Green's formula [33, Corollary 2.1], which implies, for the function $u \in H^1(\Omega)$ and the vector field $\boldsymbol{v} \in \boldsymbol{H}(\mathrm{div}, \Omega)$, the expression

$$\int_\Omega \nabla u \cdot \boldsymbol{v} + \overline{u} \, \nabla \cdot \boldsymbol{v} \,\mathrm{d}\boldsymbol{x} = \int_\Gamma \gamma_\nu \overline{\boldsymbol{v}} \, \gamma u \,\mathrm{d}\boldsymbol{x}. \tag{2.5}$$

We note that the complex conjugation of the gradient in the first summand is already included in the definition of the dot product (1.1). The right-hand side of this identity is the sesquilinear L^2-pairing on the boundary, which is for $\phi, \psi: \Gamma \to \mathbb{C}$ denoted by

$$(\phi, \psi)_\Gamma = \int_\Gamma \overline{\phi} \, \psi \,\mathrm{d}\boldsymbol{x}. \tag{2.6}$$

The traces extend to surjective bounded linear operators on the above spaces and map into

respective spaces on the boundary. For any order $k \geq 0$, we define the following Hilbert space

$$H^{k-1/2}(\Gamma) = \gamma\left(H^k(\Omega)\right).$$

These trace spaces become Hilbert spaces by equipping them with appropriate norms $\|\cdot\|_{H^{k-1/2}(\Gamma)}$. The dense embedding in $L^2(\Gamma)$ then implies, for $r \geq 0$, the dense chain of inclusions

$$H^r(\Gamma) \subset L^2(\Gamma) \subset H^{-r}(\Gamma),$$

where the duality between $H^{-r}(\Gamma)$ and $H^r(\Gamma)$ is formally obtained by extending the L^2-pairing (2.6). The Dirichlet trace extends, by construction, to a bounded surjective operator (details are found e.g. in [33, Section I.1])

$$\gamma : H^1(\Omega) \to H^{1/2}(\Gamma).$$

Furthermore, the normal trace extends to a bounded surjective operator

$$\gamma_\nu : \boldsymbol{H}(\mathrm{div}, \Omega) \to H^{-1/2}(\Gamma).$$

A complete derivation of these results is found in [33, Section I.2.2], where the continuity and surjectivity are shown in [33, Theorem 2.2 & Corollary 2.4].
An additional Hilbert space is necessary to treat the acoustic generalized impedance boundary condition, in order to account for the impedance operator $Z(s)$. Consider the dense subspace $V \subset H^{1/2}(\Gamma)$, assumed to be equipped with a (semi-)norm $|\cdot|_V$, which implies the full norm

$$\|\phi\|_V^2 = \|\phi\|_{H^{1/2}(\Gamma)}^2 + \|\phi\|_V^2 . \tag{2.7}$$

2.1.1. Setting of the transfer operator $Z(s)$

The subspace V provides a suitable setting for the transfer operator $Z(s)$. Specifically, the norm of this analytic family is assumed to be *polynomially bounded* in terms of the Laplace parameter s in the following way: there exists a real constant κ and, for any $\sigma > 0$, there exists a constant $C_\sigma < \infty$ such that

$$\|Z(s)\|_{V' \leftarrow V} \leq C_\sigma |s|^\kappa , \quad \mathrm{Re}\, s \geq \sigma > 0. \tag{2.8}$$

All boundary conditions presented in the introduction correspond to transfer operators which fulfill this bound for some $\kappa \leq 1$, a property that is therefore assumed in order to simplify the presentation throughout the chapter. Furthermore, the operator family $Z(s)$ is assumed to be of *positive type*: For every $\sigma > \sigma_0 \geq 0$, there exists a positive constant $c_\sigma^Z > 0$ such that

$$\mathrm{Re}\, \langle \psi, Z(s)\psi \rangle_\Gamma \geq c_\sigma^Z \,\mathrm{Re}\, s \left| s^{-1}\psi \right|_V^2 \quad \text{for all } \psi \in V \text{ and } \mathrm{Re}\, s \geq \sigma > \sigma_0, \tag{2.9}$$

where the anti-duality between V and V', denoted by $\langle \cdot, \cdot \rangle_\Gamma$, is the appropriate extension of the L^2-pairing.

2.2. The transfer operators from (1.4)–(1.8)

Lemma 2.1 (Thin coating). *The transfer operator corresponding to the boundary condition* (1.4) *is a well-posed operator on the space* $V = H^1(\Gamma)$*, equipped with the* δ*-dependent semi-norm*

$$|\phi|_V^2 = \delta \, \|\nabla \phi\|_{L^2(\Gamma)}^2 .$$

The full norm (2.7) *makes this space an appropriate setting of the transfer operator* $Z(s)\colon V \to V'$ *corresponding to the acoustic thin layer boundary conditions* (1.4)*, in the sense that* (2.8) *and* (2.9) *hold with* $\kappa = 1$ *and* $\sigma_0 = 0$ *respectively.*

Proof. From the general form of the abstract generalized impedance boundary condition (1.9) and the specific thin layer boundary condition (1.4), we read that the corresponding temporal transfer operator has the expression

$$Z(\partial_t) = \delta(\partial_t - \partial_t^{-1}\Delta_\Gamma).$$

The corresponding time-harmonic transfer operator, formally derived by taking the Laplace transform, has for all $s \in \mathbb{C}$ with $\operatorname{Re} s > 0$ the form

$$Z(s) = \delta\big(s - \Delta_\Gamma s^{-1}\big).$$

The setting of this operator is naturally $V = H^1(\Gamma)$, equipped with the δ-dependent semi-norm and norms stated. In these norms, the transfer operator $Z(s)$ satisfies the polynomial bound (2.8) with $\kappa = 1$ and a constant that is independent of δ for $0 < \delta \leq 1$, since

$$\|Z(s)\|_{V' \leftarrow V} = \sup_{\substack{\psi_1, \psi_2 \in V \\ \|\psi_1\|_V = \|\psi_2\|_V = 1}} |\langle \psi_2, Z(s)\psi_1 \rangle_\Gamma|$$

and, for $\operatorname{Re} s \geq \sigma > 0$ and arbitrary $\psi_1, \psi_2 \in V$, we estimate

$$\begin{aligned}
\Big|\big\langle \psi_2, \delta\big(s - \Delta_\Gamma s^{-1}\big)\psi_1 \big\rangle\Big| &\leq \Big|\delta\,|s|\,(\psi_2, \psi_1)_{L^2(\Gamma)} + \delta\,|s|^{-1}\,(\nabla_\Gamma \psi_2, \nabla_\Gamma \psi_1)_{\boldsymbol{L}^2(\Gamma)}\Big| \\
&\leq \delta\,|s|\,\|\psi_2\|_{L^2(\Gamma)}\,\|\psi_1\|_{L^2(\Gamma)} + \delta\,|s|^{-1}\,\|\nabla_\Gamma \psi_2\|_{\boldsymbol{L}^2(\Gamma)}\,\|\nabla_\Gamma \psi_1\|_{\boldsymbol{L}^2(\Gamma)} \\
&\leq |s|\,(\delta + \sigma^{-2})\,\|\psi_2\|_V\,\|\psi_1\|_V.
\end{aligned}$$

Furthermore, the transfer operator Z satisfies the positivity condition (2.9), because for $\psi \in V$ we obtain

$$\begin{aligned}
\operatorname{Re}\big\langle \psi, \delta\big(s - \Delta_\Gamma s^{-1}\big)\psi \big\rangle &= \delta \operatorname{Re} s\, \|\psi\|_{L^2(\Gamma)}^2 + \delta \operatorname{Re} \bar{s}\, \|s^{-1}\nabla_\Gamma \psi\|_{L^2(\Gamma)^3}^2 \\
&\geq \delta \operatorname{Re} s\, \|s^{-1}\nabla_\Gamma \psi\|_{L^2(\Gamma)^3}^2 \\
&= \operatorname{Re} s\, \big|s^{-1}\psi\big|_V^2.
\end{aligned}$$

□

Lemma 2.2 (Strong absorption). *The transfer operators corresponding to the boundary conditions (1.6)–(1.7) are well-posed operators on the space $V = L^2(\Gamma)$, equipped with the δ-dependent semi-norm*

$$|\phi|_V^2 = \delta^{-1} \|\phi\|_{L^2(\Gamma)}^2 .$$

The full norm (2.7) then makes this space an appropriate setting for the transfer operators $Z(s)\colon V \to V'$ corresponding to the highly absorbing boundary conditions (1.6) and (1.7). In the case of the first-order boundary condition (1.6), the polynomial bound (2.8) holds for $\kappa = -1/2$ and the positivity (2.9) holds for $\sigma_0 = 0$. For the second order boundary condition (1.7), we assume that the L^∞-norm of the mean curvature of Γ is bounded by some constant. Under this assumption, both properties hold for the parameters $\kappa = -1/2$ and $\sigma_0 = \max(0, 2\delta\mathcal{H}_{\max})^2$, where $\mathcal{H}_{\max}$ denotes the maximum of the mean curvature of the boundary Γ.

Proof. From the general form of the generalized impedance boundary condition (1.9), we find that the time-harmonic transfer operator associated to the boundary condition (1.6) is of the form

$$Z(s) = \delta^{-1} s^{-1/2},$$

whereas the second order formulation (with respect to δ) (1.7) corresponds to the family of transfer operators associated to the expression

$$Z(s) = \delta^{-1} s^{-1/2} - \mathcal{H} s^{-1}.$$

With the stated norm, we obtain for arbitrary boundary functions ψ_1, ψ_2 that are normalized by setting $\|\psi_1\|_V = \|\psi_2\|_V = 1$, the following estimate

$$\begin{aligned}
&\left| \left\langle \psi_2, \left(\delta^{-1} s^{-1/2} - \mathcal{H} s^{-1} \right) \psi_1 \right\rangle \right| \\
&\leq \left(\delta^{-1} |s|^{-1/2} + \|\mathcal{H}\|_{L^\infty(\Gamma)} |s|^{-1} \right) \|\psi_2\|_{L^2(\Gamma)} \|\psi_1\|_{L^2(\Gamma)} \\
&\leq \left(|s|^{-1/2} + \delta \|\mathcal{H}\|_{L^\infty(\Gamma)} |s|^{-1} \right) \leq \sigma^{-1} M,
\end{aligned}$$

where the final estimate holds for $\sigma < 1$. Consequently, both absorbing boundary conditions satisfy (2.8) with $\mu = 0$, $\sigma_0 = 0$ and constants M_σ independent of δ.

The analytic family associated to the first-order boundary condition (1.6) fulfills the positivity condition (2.9) with $\sigma_0 = 0$ since for $\operatorname{Re} s \geq \sigma$ we obtain

$$\operatorname{Re}\langle \psi, Z(s)\psi \rangle_\Gamma = \operatorname{Re} \frac{s^{1/2}}{\delta |s|} \|\psi\|_{L^2(\Gamma)}^2 \geq \operatorname{Re} \frac{\sigma^{1/2}}{|s|} \|\psi\|_V^2 \geq \sigma^{1/2} \operatorname{Re} s \left\| s^{-1} \psi \right\|_V^2 .$$

For the transfer operator corresponding to the boundary condition of second order (1.7), we have for $\operatorname{Re} s > 0$, with the maximum value of the mean curvature denoted by $\mathcal{H}_{\max}$, the

estimate

$$\begin{aligned}\operatorname{Re}\langle\psi, Z(s)\psi\rangle_\Gamma &\geq \left(\delta^{-1}\operatorname{Re} s^{-1/2} - \mathcal{H}_{\max}\operatorname{Re} s^{-1}\right)\|\psi\|^2_{L^2(\Gamma)} \\ &= |s|\left(\delta^{-1}\operatorname{Re} s^{1/2} - \mathcal{H}_{\max}\frac{\operatorname{Re} s}{|s|}\right)\|s^{-1}\psi\|^2_{L^2(\Gamma)} \geq \operatorname{Re} s\frac{\sigma^{1/2}}{2}\left|s^{-1}\psi\right|^2_V,\end{aligned}$$

where the final estimate uses $\operatorname{Re} s^{1/2} \geq 2\delta\mathcal{H}_{\max}$, which holds for $\operatorname{Re} s \geq \sigma_0 = \max(0, 2\delta\mathcal{H}_{\max})^2$. □

Lemma 2.3 (Acoustic boundary conditions). *The transfer operator associated to acoustic boundary conditions is a well-posed operator on the original trace space $V = H^{1/2}(\Gamma)$, equipped with the trivial semi-norm*

$$|\phi|^2_V = 0.$$

In this context, the polynomial bound (2.8) and the positivity condition (2.9) hold with $\kappa = 0$ and $\sigma_0 = 0$.

Proof. Integrating both equations of (1.8) on both sides and inserting the second identity into the first reveals that the boundary condition of interest is a special case of the abstract boundary condition (1.9) with the temporal transfer operator

$$Z(\partial_t) = \left(m\partial_t + \alpha + k\partial_t^{-1}\right)^{-1}.$$

An application of the Laplace transform then gives the analytic family of time-harmonic transfer operators, which reads

$$Z(s) = (ms + \alpha + ks^{-1})^{-1}.$$

This family of operators is bounded in terms of the stated norms, since for $\operatorname{Re} s > 0$ we have

$$\|Z(s)\|_{H^{-1/2}(\Gamma)\leftarrow H^{1/2}(\Gamma)} = \left|ms + \alpha + ks^{-1}\right|^{-1}\|\mathrm{Id}\|_{H^{-1/2}(\Gamma)\leftarrow H^{1/2}(\Gamma)} \leq \alpha^{-1}.$$

This transfer operator is of positive type in the stated form (2.9), since for $\operatorname{Re} s > 0$ we obtain

$$\operatorname{Re} Z(s) = \operatorname{Re}\,(ms + \alpha + ks^{-1})^{-1} = \operatorname{Re}\frac{(m\bar{s} + \alpha + k\bar{s}^{-1})}{\left|m\bar{s} + \alpha + k\bar{s}^{-1}\right|^2} \geq 0.$$

Inserting this identity into the left-hand side of (2.9) shows the stated positivity. □

Remark 2.1 (Neumann and Robin boundary conditions). *We note that the setting of the acoustic boundary condition also applies to Neumann boundary conditions (through setting $Z(s) = 0$) and Robin boundary conditions (through setting $Z(s) = c$ for some positive constant c).*

2.2.1. Weak formulation of the generalized impedance boundary conditions

Testing the boundary condition by inserting the time-invariant continuous boundary function ϕ on Γ into the L^2-pairing yields

$$(\phi, \gamma_v \boldsymbol{v})_\Gamma - (\phi, Z(\partial_t)\gamma p)_\Gamma = \left(\phi, g^{\mathrm{inc}}\right)_\Gamma .$$

From the strong formulation of the temporal convolution operator $Z(\partial_t)$, we derive a family of weak time-harmonic operators $Z(s) : V \to V'$ such that the duality coincides with the $L^2(\Gamma)$ inner product when the regularity of the trace γp is sufficient:

$$\langle v, Z(\partial_t)\gamma p\rangle_\Gamma = (v, Z(\partial_t)\gamma p)_\Gamma , \quad v \in V.$$

Moreover, the right-hand side depending on the incident wave is understood as an element in the dual V', through the expression

$$\langle v, g^{\mathrm{inc}}\rangle_\Gamma = \left(v, g^{\mathrm{inc}}\right)_\Gamma , \quad v \in V. \tag{2.10}$$

Inserting these identities into the tested boundary condition then reveals the *w*eak formulation of the boundary condition (1.9): find

$$p \in L^2(0,T; H^1(\Omega)) \cap H^1(0,T; L^2(\Omega))$$

and

$$\boldsymbol{v} \in \boldsymbol{L}^2(0,T; \boldsymbol{H}(\mathrm{div}, \Omega)) \cap \boldsymbol{H}^1(0,T; \boldsymbol{L}^2(\Omega)),$$

solution to the acoustic wave equations with vanishing initial support, such that their traces $\gamma_v \boldsymbol{v} \in L^2(0,T; H^{-1/2}(\Gamma))$ and $\gamma p \in H^\kappa_0(0,T; H^{1/2}(\Gamma))$ fulfill for almost every $t \in (0,T)$

$$\langle v, \gamma_v \boldsymbol{v}\rangle_\Gamma - \langle v, Z(\partial_t)\gamma p\rangle = \langle v, g^{\mathrm{inc}}\rangle_\Gamma \quad \text{for all } v \in V. \tag{2.11}$$

The weak formulation of the boundary condition therefore weakly enforces a relation between the traces of solutions to the first-order formulation of the acoustic wave equation. Under the stated regularity assumptions, all of the terms in the weak formulation of the boundary condition are finite. For $g^{\mathrm{inc}} \in H^3_0(0,T;V')$, the above described formulation is well-posed in the stated regularities. In the case of general positive κ in (2.8), the necessary temporal regularity grows linearly, specifically $g^{\mathrm{inc}} \in H^{2+\kappa}_0(0,T;V')$. In the following sections, such a well-posedness result is given, with the stated regularities. The techniques and results developed in the process of deriving this result further take a central role in the subsequent numerical analysis.

2.3. The Helmholtz problem

We recall some basic notions of time-harmonic potential equations, which will be the foundation of our construction of solutions of time-dependent wave equations throughout this paper.

With time-dependent problems in mind, we start with the careful study of their time-harmonic counterparts. Frequency-specific bounds are then the key to a temporal well-posedness result.

Let us begin by applying the Laplace transform to the acoustic wave equation in the first-order formulation (2.1)–(2.2). Under the assumption of vanishing initial conditions, we obtain a first-order formulation of the Helmholtz problem, which reads for $\operatorname{Re} s > 0$

$$\begin{aligned} s\widehat{p} - \nabla \cdot \widehat{\boldsymbol{v}} &= 0 \\ s\widehat{\boldsymbol{v}} - \nabla \widehat{p} \quad &= 0 \end{aligned} \qquad \text{on} \quad \Omega. \tag{2.12}$$

In the literature, the Helmholtz problem is often formulated in terms of the Fourier parameter ω (see e.g. [26]), which is related to the Laplace parameter s through the identity $s = -i\omega$.

Completing these equations with asymptotic boundary conditions for $|\boldsymbol{x}| \to \infty$ renders solutions of the Helmholtz problem unique. Solutions defined through the representation formulas discussed in the subsequent sections always automatically satisfy these conditions by construction. With these decay conditions, the solutions of the Helmholtz problem are ensured to fulfill $\widehat{p} \in H^1(\Omega)$ and $\widehat{\boldsymbol{v}} \in \boldsymbol{H}(\operatorname{div}, \Omega)$.

2.3.1. Recap: Potential operators and representation formulas

We repeat the classical notation of potential operators and representation formulas for the Helmholtz problem, used e.g. in [16, 47, 64]. The notation in the present setting is slightly adapted, motivated by the notation used in [1].

The *fundamental solution* of the Helmholtz equation is given by the radial outgoing scalar solution centered at the origin

$$\widehat{p}_{\text{radial}}(\boldsymbol{z}) = G(s, \boldsymbol{z}) = \frac{e^{-s|\boldsymbol{z}|}}{4\pi\,|\boldsymbol{z}|} \quad \text{for} \quad \boldsymbol{z} \in \mathbb{R}^3 \setminus \{0\},$$

which solves the time-harmonic system (2.12) in the role of $\widehat{p}$, when complemented with

$$\widehat{\boldsymbol{v}}_{\text{radial}}(\boldsymbol{z}) = \frac{\nabla G(s, \boldsymbol{z})}{s} \quad \text{for} \quad \boldsymbol{z} \in \mathbb{R}^3 \setminus \{0\}.$$

The superposition of point sources along all points located on the boundary Γ defines the *single layer potential operator*, which reads

$$\left(S(s)\varphi\right)(\boldsymbol{x}) = \int_\Gamma \gamma_{\boldsymbol{y}} \widehat{p}_{\text{radial}}(\boldsymbol{x} - \boldsymbol{y})\, \varphi(\boldsymbol{y})\, \mathrm{d}\Gamma_{\boldsymbol{y}} \qquad \boldsymbol{x} \in \mathbb{R}^3 \setminus \Gamma.$$

The single layer potential is complemented by the *double layer potential operator*, which is defined by the superposition of all velocity fields along the boundary, which reads

$$\left(\mathcal{D}(s)\psi\right)(\boldsymbol{x}) = \int_\Gamma \gamma_{\nu_{\boldsymbol{y}}} \widehat{\boldsymbol{v}}_{\text{radial}}(\boldsymbol{x} - \boldsymbol{y})\psi(\boldsymbol{y})\, \mathrm{d}\Gamma_{\boldsymbol{y}} \qquad \boldsymbol{x} \in \mathbb{R}^3 \setminus \Gamma.$$

Note that this definition differs slightly from the conventions in the literature by a factor of s (cf. [47, Section 3]). Due to this particular form of the double layer potential, we obtain representation formulas with a consistent scaling of the potential operators.

The fundamental properties of these operators are presented in terms of *transmission problems*, for which we introduce some additional notation. Throughout this thesis, we consider boundary value problems on exterior domains Ω and we will only be interested in the approximation of solutions in these domains. Nevertheless, it will turn out to be essential for the analysis to pose some auxiliary problems on the complete space, decomposed into an exterior domain Ω^+ (which for our purposes coincides with the domain of interest Ω), an interior domain Ω^- describing the inside of the scatterer, and the boundary Γ at the interface of the interior domain and the exterior domain.

The trace operators γ and γ_ν are readily extended on the interior domain Ω^-, where ν remains the outer normal vector pointing in the exterior domain Ω^+. Trace operators, applied in the context of transmission problems, are denoted by an additional superscript to denote their respective domain, namely by writing γ^+, γ^-,γ_ν^+ and γ_ν^-, respectively. For functions which are defined on both the interior domain and exterior $\mathbb{R}^3$, we introduce *jumps* and *averages*, which derive from the traces and are defined by

$$\begin{aligned} [\gamma] &= \gamma^+ - \gamma^-, & \{\gamma\} &= \tfrac{1}{2}\left(\gamma^+ + \gamma^-\right), \\ [\gamma_\nu] &= \gamma_\nu^+ - \gamma_\nu^-, & \{\gamma_\nu\} &= \tfrac{1}{2}\left(\gamma_\nu^+ + \gamma_\nu^-\right). \end{aligned}$$

The bounds on the respective traces naturally extend to the jumps and averages. Of great interest are the composition of these trace operators with the potential operators, which reveals the behaviour of the representation formulas when the boundary Γ is approached.

Concatenating the jumps and the potential operators reveals the *jump conditions*, which for the respective traces read

$$\begin{aligned} [\gamma] \circ s\mathcal{S}(s) &= 0, & [\gamma] \circ s\mathcal{D}(s) &= \mathrm{Id}, \\ [\gamma_\nu] \circ \nabla\mathcal{S}(s) &= -\mathrm{Id}, & [\gamma_\nu] \circ \nabla\mathcal{D}(s) &= 0. \end{aligned}$$

With this notation, we are now in the position to formulate the time-harmonic transmission problem. Let $(\widehat{\varphi}, \widehat{\psi}) \in H^{-1/2}(\Gamma) \times H^{1/2}(\Gamma)$ be some arbitrary boundary functions in the trace space [1] and let $\widehat{p}$ and $\widehat{v}$ on $\mathbb{R}^3 \setminus \Gamma$ be defined by

$$\widehat{p} = s\mathcal{S}(s)\widehat{\varphi} + s\mathcal{D}(s)\widehat{\psi}, \tag{2.13}$$

$$\widehat{v} = \nabla\mathcal{S}(s)\widehat{\varphi} + \nabla\mathcal{D}(s)\widehat{\psi}. \tag{2.14}$$

Four potential operators have emerged, namely the single layer potential, the double layer potential and their gradients. These operators map boundary densities onto the fields in the domain and will ultimately be used to numerically recover the fields $\widehat{p}$ and $\widehat{v}$ away from the

[1] The notation $(\widehat{\varphi}, \widehat{\psi})$ is used, when these functions appear as the boundary densities of the time-harmonic acoustic fields $(\widehat{p}, \widehat{v})$. The hats indicate that these functions are Laplace transforms of time-dependent quantities of interest. Whenever a generic function from the trace space is denoted, without a relation to a time-dependent function of interest, the hats are omitted.

boundary. The construction and the jump conditions of the potential operators then imply, for the quantities of the representation formulas (2.13)–(2.14), the following transmission problem

$$s\widehat{p} - \nabla \cdot \widehat{v} = 0 \qquad \text{in} \quad \mathbb{R}^3 \setminus \Gamma, \tag{2.15}$$

$$s\widehat{v} - \nabla \widehat{p} = 0 \qquad \text{in} \quad \mathbb{R}^3 \setminus \Gamma, \tag{2.16}$$

$$-[\gamma_\nu]\widehat{v} = \widehat{\varphi}, \tag{2.17}$$

$$[\gamma]\widehat{p} = \widehat{\psi}. \tag{2.18}$$

For arbitrary boundary data of appropriate regularity, there exist associated acoustic fields $(\widehat{p}, \widehat{v})$ such that the above described transmission problem holds, however, at this point the regularity of these fields is unclear. This technique of associating a transmission problem to arbitrary boundary functions of sufficient regularity is omnipresent in the subsequent proofs of this thesis in the context of acoustic, electromagnetic, time-harmonic, time-dependent and time-discrete problems.

Until this point, the results presented in this section were restricted to the established theory surrounding the well-known potential operators associated to the Helmholtz problem. In the following, we use these identities to give s-explicit estimates on the quantities of interest and show fundamental inequalities, which play a key role in the subsequent sections.

2.3.2. Transmission problems and boundary operators

The expression on the right-hand side of the representation formulas (2.13)–(2.14), more precisely the linear map $(\widehat{\varphi}, \widehat{\psi}) \mapsto (\widehat{p}, \widehat{v})$, extends to a linear operator from the trace space

$$H^{-1/2}(\Gamma) \times H^{1/2}(\Gamma) \quad \text{to} \quad H^1(\mathbb{R}^3 \setminus \Gamma) \times \boldsymbol{H}(\mathrm{div}, \mathbb{R}^3 \setminus \Gamma).$$

Moreover, this operator is bounded by a constant which depends polynomially on the Laplace parameter s, which is crucial for the subsequent analysis of the temporal counterpart.

The following lemma gives such an estimate, by exploiting the trace theorem and Green's formula.

Lemma 2.4. *Let $(\widehat{\varphi}, \widehat{\psi}) \in H^{-1/2}(\Gamma) \times H^{1/2}(\Gamma)$ be complex-valued boundary functions in the trace spaces. Consider $(\widehat{p}, \widehat{v})$, defined through the representation formulas (2.13)–(2.14), and therefore the solution of the associated time-harmonic acoustic transmission problem (2.15)–(2.18) for $\operatorname{Re} s > 0$. Then, the following inequality holds*

$$\left\| \begin{pmatrix} \widehat{p} \\ \widehat{v} \end{pmatrix} \right\|_{H^1(\mathbb{R}^3\setminus\Gamma)\times\boldsymbol{H}(\mathrm{div},\mathbb{R}^3\setminus\Gamma)} \leq C_\Gamma \frac{|s|^2 + 1}{\operatorname{Re} s} \left\| \begin{pmatrix} \widehat{\varphi} \\ \widehat{\psi} \end{pmatrix} \right\|_{H^{-1/2}(\Gamma)\times H^{1/2}(\Gamma)}, \tag{2.19}$$

where the constant is the maximum of the operator norms of the occuring traces

$$C_\Gamma = \max\left(\|\{\gamma\}\|_{H^{1/2}(\Gamma)\leftarrow H^1(\mathbb{R}^3\setminus\Gamma)}, \|\{\gamma_\nu\}\|_{H^{-1/2}(\Gamma)\leftarrow \boldsymbol{H}(\mathrm{div},\mathbb{R}^3\setminus\Gamma)} \right). \tag{2.20}$$

Proof. Let us start by inserting solutions of the time-harmonic Helmholtz problem (2.12) into Green's formula (2.5), which yields on the exterior and interior domains respectively

$$\begin{aligned}\pm\int_\Gamma \overline{\left(\gamma_\nu^\pm \widehat{v}\right)}\,\gamma^\pm \widehat{p}\,\mathrm{d}\boldsymbol{x} &= \int_{\Omega^\pm} \nabla\widehat{p}\cdot\widehat{\boldsymbol{v}} + \overline{(\widehat{p})}\,(\nabla\cdot\widehat{\boldsymbol{v}})\,\mathrm{d}\boldsymbol{x}\\ &= \int_{\Omega^\pm} \bar{s}\,|\widehat{\boldsymbol{v}}|^2 + s\,|\widehat{p}|^2\,\mathrm{d}\boldsymbol{x}.\end{aligned}$$

Note that the conjugation of the first summand on the right-hand side is included in the notation of the dot product, which is defined through $\boldsymbol{a}\cdot\boldsymbol{b} = \overline{\boldsymbol{a}}^T\boldsymbol{b}$ on $\mathbb{C}^3$. Summation of the identity on the inner domain and the exterior domain yields

$$\mathrm{I} := \int_{\mathbb{R}^3\setminus\Gamma} \bar{s}\,|\widehat{\boldsymbol{v}}|^2 + s\,|\widehat{p}|^2\,\mathrm{d}\boldsymbol{x} = \left(\gamma_\nu^+\widehat{\boldsymbol{v}},\gamma^+\widehat{p}\right)_\Gamma - \left(\gamma_\nu^-\widehat{\boldsymbol{v}},\gamma^-\widehat{p}\right)_\Gamma. \tag{2.21}$$

The time-harmonic acoustic fields are readily rewritten in terms of their counterpart by inserting (2.12). Using the separation $\mathrm{I} = (1-\theta)\mathrm{I} + \theta\mathrm{I}$ and inserting the Helmholtz problem in the second summand reformulates the left-hand side to the expression

$$\begin{aligned}\mathrm{I} = \int_{\mathbb{R}^3\setminus\Gamma}\Big((1-\theta)\bar{s}\,|\widehat{\boldsymbol{v}}|^2 + \theta s\left|s^{-1}\nabla\cdot\widehat{\boldsymbol{v}}\right|^2\\ + (1-\theta)s\,|\widehat{p}|^2 + \theta\bar{s}\left|s^{-1}\nabla\widehat{p}\right|^2\Big)\,\mathrm{d}\boldsymbol{x}.\end{aligned}$$

The real part of both sides then simplifies the s-dependency to

$$\begin{aligned}\mathrm{Re}\,\mathrm{I} = \mathrm{Re}\,s\int_{\mathbb{R}^3\setminus\Gamma}\Big((1-\theta)\,|\widehat{\boldsymbol{v}}|^2 + \theta\left|s^{-1}\nabla\cdot\widehat{\boldsymbol{v}}\right|^2 &\qquad (2.22)\\ + (1-\theta)\,|\widehat{p}|^2 + \theta\left|s^{-1}\nabla\widehat{p}\right|^2\Big)\,\mathrm{d}\boldsymbol{x}. &\qquad (2.23)\end{aligned}$$

The parameter θ is free and chosen in such a way that the preceding factors of the summands agree, which is achieved by setting $(1-\theta) = \theta\,|s|^{-2}$. Rearranging this requirement leads to the choice of $\theta = 1/(1+|s|^{-2})$, for which we obtain

$$\mathrm{Re}\,\mathrm{I} = \frac{\mathrm{Re}\,s}{|s|^2+1}\left(\|\widehat{p}\|^2_{H^1(\mathbb{R}^3\setminus\Gamma)} + \|\widehat{\boldsymbol{v}}\|^2_{\boldsymbol{H}(\mathrm{div},\mathbb{R}^3\setminus\Gamma)}\right). \tag{2.24}$$

The real part of I therefore simplifies, up to the given preceding factor, to the left-hand side of the stated bound (2.19). Moreover, taking the real part of (2.21) gives

$$\mathrm{Re}\,\mathrm{I} = \mathrm{Re}\left(\gamma_\nu^+\widehat{\boldsymbol{v}},\gamma^+\widehat{p}\right)_\Gamma - \mathrm{Re}\left(\gamma_\nu^-\widehat{\boldsymbol{v}},\gamma^-\widehat{p}\right)_\Gamma.$$

Rewriting the right-hand side of this expression in terms of the jumps and averages through

adding intermediate terms yields

$$\begin{aligned}\operatorname{Re} \mathrm{I} &= \operatorname{Re}\, \left([\gamma_\nu]\widehat{v}\,,\, \{\gamma\}\widehat{p}\right)_\Gamma + \operatorname{Re}\left([\gamma]\widehat{p}\,,\, \{\gamma_\nu\}\widehat{v}\right)_\Gamma \\ &= \operatorname{Re}\, \left(-\widehat{\varphi}, \{\gamma\}\widehat{p}\right)_\Gamma + \operatorname{Re}\left(\widehat{\psi}, \{\gamma_\nu\}\widehat{v}\right)_\Gamma .\end{aligned} \tag{2.25}$$

Applying the duality estimate on the right-hand side and subsequently the Cauchy–Schwarz inequality on $\mathbb{R}^2$ yields

$$\begin{aligned}\operatorname{Re} \mathrm{I} &\leq \|\widehat{\varphi}\|_{H^{-1/2}(\Gamma)}\, \|\{\gamma\}\widehat{p}\|_{H^{1/2}(\Gamma)} + \left\|\widehat{\psi}\right\|_{H^{1/2}(\Gamma)} \|\{\gamma_\nu\}\widehat{v}\|_{H^{-1/2}(\Gamma)} \\ &= \begin{pmatrix} \|\widehat{\varphi}\|_{H^{-1/2}(\Gamma)} \\ \left\|\widehat{\psi}\right\|_{H^{1/2}(\Gamma)} \end{pmatrix} \cdot \begin{pmatrix} \|\{\gamma\}\widehat{p}\|_{H^{1/2}(\Gamma)} \\ \|\{\gamma_\nu\}\widehat{v}\|_{H^{-1/2}(\Gamma)} \end{pmatrix} \\ &\leq \left(\|\widehat{\varphi}\|^2_{H^{-1/2}(\Gamma)} + \left\|\widehat{\psi}\right\|^2_{H^{1/2}(\Gamma)}\right)^{1/2} \left(\|\{\gamma\}\widehat{p}\|^2_{H^{1/2}(\Gamma)} + \|\{\gamma_\nu\}\widehat{v}\|^2_{H^{-1/2}(\Gamma)}\right)^{1/2}.\end{aligned} \tag{2.26}$$

In the following, we estimate the second factor above through the bound on the traces γ and γ_ν. The time-harmonic acoustic fields $\widehat{p}$ and $\widehat{v}$ are, by [63, Theorem 3.16], in the local Sobolev spaces $H^1_{\mathrm{loc}}(\mathbb{R}^3 \setminus \Gamma)$ and $\boldsymbol{H}_{\mathrm{loc}}(\mathrm{div}, \mathbb{R}^3 \setminus \Gamma)$ respectively. Moreover, the exponential decay in terms of the distance away from the boundary for $\operatorname{Re} s > 0$ implies that these quantities are in the spaces $H^1(\mathbb{R}^3 \setminus \Gamma)$ and $\boldsymbol{H}(\mathrm{div}, \mathbb{R}^3 \setminus \Gamma)$ respectively. The operator norms for the traces then finally yield

$$\operatorname{Re} \mathrm{I} = \left(\|\widehat{\varphi}\|^2_{H^{-1/2}(\Gamma)} + \left\|\widehat{\psi}\right\|^2_{H^{1/2}(\Gamma)}\right)^{1/2} \left(\|\widehat{p}\|^2_{H^1(\mathbb{R}^3\setminus\Gamma)} + \|\widehat{v}\|^2_{\boldsymbol{H}(\mathrm{div},\mathbb{R}^3\setminus\Gamma)}\right)^{1/2}.$$

Inserting (2.24) on the left-hand side and dividing through the second factor the right-hand side yields the stated bound. □

Setting the boundary densities in Lemma 2.4 successively to zero gives bounds on the potential operators, which is formulated in the following Lemma.

Lemma 2.5. *For $\operatorname{Re} s > 0$, the scalar potential operators extend by density to a family of bounded linear operators on their respective spaces, which fulfill the bounds*

$$\begin{aligned}\|s\mathcal{S}(s)\|_{H^1(\mathbb{R}^3\setminus\Gamma)\leftarrow H^{-1/2}(\Gamma)} &\leq C_\Gamma \frac{|s|^2+1}{\operatorname{Re} s}, \\ \|s\mathcal{D}(s)\|_{H^1(\mathbb{R}^3\setminus\Gamma)\leftarrow H^{1/2}(\Gamma)} &\leq C_\Gamma \frac{|s|^2+1}{\operatorname{Re} s}.\end{aligned}$$

The identical bound holds for the potential operators composed with the gradients, which fulfill

$$\begin{aligned}\|\nabla\mathcal{S}(s)\|_{\boldsymbol{H}(\mathrm{div},\mathbb{R}^3\setminus\Gamma)\leftarrow H^{-1/2}(\Gamma)} &\leq C_\Gamma \frac{|s|^2+1}{\operatorname{Re} s}, \\ \|\nabla\mathcal{D}(s)\|_{\boldsymbol{H}(\mathrm{div},\mathbb{R}^3\setminus\Gamma)\leftarrow H^{1/2}(\Gamma)} &\leq C_\Gamma \frac{|s|^2+1}{\operatorname{Re} s}.\end{aligned}$$

The constant C_Γ is the maximum operator norm of the traces, as defined by (2.20).

All operator norms discussed in this section are bounded by the same constant, namely the preceding factor appearing in the bound (2.19) associated to the transmission problem. Note that the scaling of the scalar potentials $\mathcal{S}(s)$ and $\mathcal{D}(s)$ improves their frequency dependent bound to

$$\|\mathcal{S}(s)\|_{H^1(\mathbb{R}^3\setminus\Gamma)\leftarrow H^{-1/2}(\Gamma)} \leq C_\Gamma \frac{|s|+|s|^{-1}}{\operatorname{Re} s}$$

and analogously for $\mathcal{D}(s)$. The bounds on the scaled operators $s\mathcal{S}(s)$ and $s\mathcal{D}(s)$ are however, due to their appearance in the representation formulas (2.13)–(2.14), more relevant.

We turn our attention towards the transmission problem (2.15)–(2.18), which holds for arbitrary functions given through the representation formulas (2.13)–(2.14). The unknown time-harmonic acoustic scattered fields $\widehat{p}$ and $\widehat{v}$ only operate on the exterior domain of interest $\Omega = \Omega^+$, but solve an appropriate transmission problem when extended by zero in the inside of the scatterer Ω^-. In this case, the jumps and averages reduce to the exterior traces. Inserting the boundary data of the scattered fields into the representation formulas therefore recovers the scattered fields at any point, namely it holds that

$$\widehat{p} = s\mathcal{S}(s)\left(-\gamma_\nu \widehat{v}\right) \quad + s\mathcal{D}(s)\left(\gamma \widehat{p}\right), \tag{2.27}$$
$$\widehat{v} = \nabla\mathcal{S}(s)\left(-\gamma_\nu \widehat{v}\right) + \nabla\mathcal{D}(s)\left(\gamma \widehat{p}\right). \tag{2.28}$$

Throughout this thesis, we attempt to solve the boundary value problems of interest in a two step approach. First, the boundary data of the scattered waves are determined by appropriate boundary integral equations. Then, conclusions on the scattered wave are drawn from the representation formula. The previously established time-harmonic bounds of Lemma 2.4 can be sharpened when the corresponding solution of the transmission problem vanishes in one of the domains, which is proven in the next lemma.

Lemma 2.6. *Consider the situation of Lemma 2.4 and assume further that the interior traces $\gamma^- \widehat{p}$ and $\gamma_\nu^- \widehat{v}$ vanish, consequently reducing the boundary densities to $\widehat{\varphi} = -\gamma_\nu \widehat{v}$ and $\widehat{\psi} = \gamma \widehat{p}$. Then, the following bound holds*

$$\left\| \begin{pmatrix} \widehat{p} \\ \widehat{v} \end{pmatrix} \right\|_{H^1(\Omega)\times \boldsymbol{H}(\operatorname{div},\Omega)} \leq \left(\frac{|s|^2+1}{2\operatorname{Re} s} \right)^{1/2} \left\| \begin{pmatrix} \widehat{\varphi} \\ \widehat{\psi} \end{pmatrix} \right\|_{H^{-1/2}(\Gamma)\times H^{1/2}(\Gamma)}.$$

Furthermore, we have the following stronger bound for the weaker L^2-norm

$$\left\| \begin{pmatrix} \widehat{p} \\ \widehat{v} \end{pmatrix} \right\|_{L^2(\Omega)\times \boldsymbol{L}^2(\Omega)} \leq \left(\frac{1}{2\operatorname{Re} s} \right)^{1/2} \left\| \begin{pmatrix} \widehat{\varphi} \\ \widehat{\psi} \end{pmatrix} \right\|_{H^{-1/2}(\Gamma)\times H^{1/2}(\Gamma)}.$$

Proof. The proof of the first bound is identical to that of Lemma 2.4 down to (2.25), which now implies the bound $\operatorname{Re} \mathrm{I} \leq \frac{1}{2}\left(\|\widehat{\varphi}\|^2_{H^{-1/2}(\Gamma)} + \|\widehat{\psi}\|^2_{H^{1/2}(\Gamma)}\right)$ and yields the stated result. The stated L^2-bound follows readily from applying the argument directly to (2.21) instead of (2.24). □

2.3.3. Time-harmonic boundary operators and the Calderón operator

In view of the derivation of boundary integral equations, we are interested in the representation formulas for x approaching the boundary. In the following, we define the boundary operators as averages of the potential operators associated to the transmission problem (2.15)–(2.18). The boundary integral operators are consequently defined by the compositions

$$\begin{aligned} V(s) &= \{\gamma\} \circ s\mathcal{S}(s), & K(s) &= \{\gamma\} \circ s\mathcal{D}(s), \\ K^T(s) &= \{\gamma_\nu\} \circ \nabla\mathcal{S}(s), & W(s) &= \{\gamma_\nu\} \circ \nabla\mathcal{D}(s). \end{aligned} \tag{2.29}$$

Explicit expressions are found e.g. in [47, Section 3]. These operators are the building blocks of the *acoustic Calderón operator*, which is defined by the boundary integral operators through

$$C(s) = \begin{pmatrix} V(s) & K(s) \\ -K^T(s) & -W(s) \end{pmatrix}. \tag{2.30}$$

The sign structure of this block operator derives from the representation formulas. Moreover, applying the averages on both sides of the representation formulas (2.13)–(2.14) reveals, by construction, the jump conditions of the Calderón operator, which read

$$C(s) \begin{pmatrix} -[\gamma_\nu]\widehat{v} \\ [\gamma]\widehat{p} \end{pmatrix} = \begin{pmatrix} \{\gamma\}\widehat{p} \\ -\{\gamma_\nu\}\widehat{v} \end{pmatrix}. \tag{2.31}$$

The application of the Calderón operator therefore transforms the jumps of the transmission problem into the averages, which gives time-harmonic bounds through Lemma 2.4 and even more directly through Lemma 2.5.

Lemma 2.7. *The Calderón operator forms an analytic family of bounded linear operators on the complex half space with positive real part. For* $\operatorname{Re} s \geq 0$*, we further have the bound*

$$\|C(s)\|_{H^{1/2}(\Gamma)\times H^{-1/2}(\Gamma) \leftarrow H^{-1/2}(\Gamma)\times H^{1/2}(\Gamma)} \leq C_\Gamma^2 \frac{|s|^2 + 1}{\operatorname{Re} s},$$

and by extension we obtain the same bound on the boundary integral operators defined by (2.29), on their respective spaces. The constant is again the maximum of the trace operator norms, specifically given by (2.20).

The L^2-pairing is extended to the anti-duality between $H^{-1/2}(\Gamma) \times H^{1/2}(\Gamma)$ and $H^{1/2}(\Gamma) \times H^{-1/2}(\Gamma)$ through

$$\left\langle \begin{pmatrix} \varphi \\ \psi \end{pmatrix}, \begin{pmatrix} v \\ \eta \end{pmatrix} \right\rangle_\Gamma = \langle \varphi, v \rangle_\Gamma + \langle \psi, \eta \rangle_\Gamma,$$

for appropriate boundary functions.

As was shown in [16], the Calderón operator $C(s)$ is positive with respect to this extension of the L^2-pairing. In the following lemma, we give an explicit proof of this property, with a slightly modified s-dependency in comparison to the original result.

Lemma 2.8 (essentially [16, Lemma 3.1]). *The Calderón operator* (2.30) *satisfies the positivity bound*

$$\operatorname{Re}\left\langle \begin{pmatrix} \widehat{\varphi} \\ \widehat{\psi} \end{pmatrix}, C(s) \begin{pmatrix} \widehat{\varphi} \\ \widehat{\psi} \end{pmatrix} \right\rangle_{\Gamma} \geq \frac{1}{c_{\Gamma}^2} \frac{\operatorname{Re} s}{|s|^2+1} \left(\|\widehat{\varphi}\|^2_{H^{-1/2}(\Gamma)} + \|\widehat{\psi}\|^2_{H^{1/2}(\Gamma)} \right),$$

The constant c_Γ is the maximum of the norms of the jump operators associated to the traces

$$c_{\Gamma} = \max\left(\|[\gamma]\|_{H^{1/2}(\Gamma) \leftarrow H^1(\mathbb{R}^3 \setminus \Gamma)}, \|[\gamma_{\boldsymbol{\nu}}]\|_{H^{-1/2}(\Gamma) \leftarrow \boldsymbol{H}(\operatorname{div}, \mathbb{R}^3 \setminus \Gamma)} \right). \tag{2.32}$$

Proof. Let $(\widehat{\varphi}, \widehat{\psi}) \in H^{-1/2}(\Gamma) \times H^{1/2}(\Gamma)$ and further let the time-harmonic fields defined through the representation formulas (2.13)–(2.14) be denoted by $\widehat{p} \in H^1(\mathbb{R}^3 \setminus \Gamma)$ and $\widehat{\boldsymbol{v}} \in \boldsymbol{H}(\operatorname{div}, \mathbb{R}^3 \setminus \Gamma)$. The result is then given by the following compact chain of inequalities

$$\begin{aligned}
&\left\| \begin{pmatrix} \widehat{\varphi} \\ \widehat{\psi} \end{pmatrix} \right\|^2_{H^{-1/2}(\Gamma) \times H^{1/2}(\Gamma)} = \left\| \begin{pmatrix} -[\gamma_{\boldsymbol{\nu}}]\widehat{\boldsymbol{v}} \\ [\gamma]\widehat{p} \end{pmatrix} \right\|^2_{H^{-1/2}(\Gamma) \times H^{1/2}(\Gamma)} && \text{by (2.17)–(2.18)} \\
&\leq c_{\Gamma}^2 \left(\|\widehat{p}\|^2_{H^1(\mathbb{R}^3 \setminus \Gamma)} + \|\widehat{\boldsymbol{v}}\|^2_{\boldsymbol{H}(\operatorname{div}, \mathbb{R}^3 \setminus \Gamma)} \right) && \text{by def. of } c_{\Gamma} \\
&= c_{\Gamma}^2 \frac{|s|^2+1}{\operatorname{Re} s} \operatorname{Re} \left\langle \begin{pmatrix} -[\gamma_{\boldsymbol{\nu}}]\widehat{\boldsymbol{v}} \\ [\gamma]\widehat{p} \end{pmatrix}, \begin{pmatrix} \{\gamma\}\widehat{p} \\ -\{\gamma_{\boldsymbol{\nu}}\}\widehat{\boldsymbol{v}} \end{pmatrix} \right\rangle_{\Gamma} && \text{by (2.24)–(2.25)} \\
&= c_{\Gamma}^2 \frac{|s|^2+1}{\operatorname{Re} s} \operatorname{Re} \left\langle \begin{pmatrix} -[\gamma_{\boldsymbol{\nu}}]\widehat{\boldsymbol{v}} \\ [\gamma]\widehat{p} \end{pmatrix}, C(s) \begin{pmatrix} -[\gamma_{\boldsymbol{\nu}}]\widehat{\boldsymbol{v}} \\ [\gamma]\widehat{p} \end{pmatrix} \right\rangle_{\Gamma} && \text{by (2.31)} \\
&= c_{\Gamma}^2 \frac{|s|^2+1}{\operatorname{Re} s} \operatorname{Re} \left\langle \begin{pmatrix} \widehat{\varphi} \\ \widehat{\psi} \end{pmatrix}, C(s) \begin{pmatrix} \widehat{\varphi} \\ \widehat{\psi} \end{pmatrix} \right\rangle_{\Gamma} && \text{by (2.17)–(2.18).}
\end{aligned}$$

□

2.4. Boundary integral equation for the Helmholtz problem under time-harmonic generalized impedance boundary conditions

The previous results prepare a path to develop well-posed and stable boundary integral equations for the Helmholtz problem with $\operatorname{Re} s > 0$. We turn our attention towards the time-harmonic scattering from the generalized impedance boundary condition, which completes the first-order formulation of the Helmholtz problem in and reads

$$\langle v, \gamma_{\boldsymbol{\nu}} \widehat{\boldsymbol{v}} \rangle_{\Gamma} - \langle v, Z(s) \gamma \widehat{p} \rangle = \langle v, g^{\mathrm{inc}} \rangle_{\Gamma} \quad \text{for all } v \in V, \tag{2.33}$$

where $Z(s)$ satisfies the framework (2.8)–(2.9) and the data g^{inc} is assumed to be at least in V'. The unknown solution to the Helmholtz problem on the exterior domain Ω, fulfilling the weak formulation of the boundary condition, is extended by zero inside the scatterer in the interior domain Ω^-.

Applying the properties of the transmission problem to the extended exterior solution then reveals the representation formulas (2.27)–(2.28) and the jump conditions of the Calderón op-

erator (2.31) simplify to

$$C(s)\begin{pmatrix} -\gamma_v \widehat{v} \\ \gamma \widehat{p} \end{pmatrix} = \frac{1}{2}\begin{pmatrix} \gamma \widehat{p} \\ -\gamma_v \widehat{v} \end{pmatrix}. \tag{2.34}$$

We follow ideas from [13] and [18], which eliminate the Dirichlet trace on the right-hand side by introducing a skew-symmetric block operator. This defines the shifted Calderón operator $C_{\mathrm{imp}}(s)$, which reads

$$C_{\mathrm{imp}}(s)\begin{pmatrix} -\gamma_v \widehat{v} \\ \gamma \widehat{p} \end{pmatrix} = \begin{pmatrix} 0 \\ -\gamma_v \widehat{v} \end{pmatrix}, \quad \text{where} \quad C_{\mathrm{imp}}(s) = C(s) + \begin{pmatrix} 0 & -\frac{1}{2}\mathrm{Id} \\ \frac{1}{2}\mathrm{Id} & 0 \end{pmatrix}. \tag{2.35}$$

The traces on the left-hand side are also referred to as the boundary densities and denoted by

$$\widehat{\varphi} = -\gamma_v \widehat{v}, \qquad \widehat{\psi} = \gamma \widehat{p}. \tag{2.36}$$

Testing both sides of the shifted jump conditions with test functions $(v, \xi) \in H^{-1/2}(\Gamma) \times V$ yields

$$\left\langle \begin{pmatrix} v \\ \xi \end{pmatrix}, C_{\mathrm{imp}}(s)\begin{pmatrix} \widehat{\varphi} \\ \widehat{\psi} \end{pmatrix} \right\rangle_{\Gamma} = \langle \xi, -\gamma_v \widehat{v} \rangle_{\Gamma}.$$

The boundary integral equation in weak form is now given by inserting the boundary condition on the right-hand side and rearranging all unknown quantities to the left-hand side.

Time-harmonic boundary integral equation: *Let* $\operatorname{Re} s > 0$ *and further let* $\widehat{g}^{\mathrm{inc}} \in V'$*. The boundary data* $(\widehat{\varphi}, \widehat{\psi}) \in H^{-1/2}(\Gamma) \times V$ *weakly solves the time-harmonic boundary integral equations if for all* $(v, \xi) \in H^{-1/2}(\Gamma) \times V$ *it holds that*

$$\left\langle \begin{pmatrix} v \\ \xi \end{pmatrix}, C_{\mathrm{imp}}(s)\begin{pmatrix} \widehat{\varphi} \\ \widehat{\psi} \end{pmatrix} \right\rangle_{\Gamma} + \langle \xi, Z(s)\widehat{\psi} \rangle_{\Gamma} = \langle \xi, -g^{\mathrm{inc}} \rangle_{\Gamma}. \tag{2.37}$$

The components of the left-hand side of the boundary integral equation are collected in the analytic operator family

$$A(s) : H^{-1/2}(\Gamma) \times V \to H^{1/2}(\Gamma) \times V',$$

namely for all $(\varphi, \psi) \in H^{-1/2}(\Gamma) \times V$ and $(v, \xi) \in H^{-1/2}(\Gamma) \times V$ we define the evaluation of $A(s)$ through

$$\left\langle \begin{pmatrix} v \\ \xi \end{pmatrix}, A(s)\begin{pmatrix} \varphi \\ \psi \end{pmatrix} \right\rangle_{\Gamma} = \left\langle \begin{pmatrix} v \\ \xi \end{pmatrix}, C_{\mathrm{imp}}(s)\begin{pmatrix} \varphi \\ \psi \end{pmatrix} \right\rangle_{\Gamma} + \langle \xi, Z(s)\psi \rangle_{\Gamma}, \tag{2.38}$$

where the anti-duality $\langle \cdot, \cdot \rangle$ on functions with two components is between $H^{-1/2}(\Gamma) \times V$ and $H^{1/2}(\Gamma) \times V'$. With this operator family, the boundary integral equation simplifies to the fol-

lowing formulation: find $(\widehat{\varphi}, \widehat{\psi}) \in H^{-1/2}(\Gamma) \times V$ such that

$$\left\langle \begin{pmatrix} v \\ \xi \end{pmatrix}, A(s) \begin{pmatrix} \widehat{\varphi} \\ \widehat{\psi} \end{pmatrix} \right\rangle_\Gamma = \langle \eta, -g^{\mathrm{inc}} \rangle_\Gamma \qquad \text{for all } (v, \xi) \in H^{-1/2}(\Gamma) \times V.$$

Moreover, dropping the universal dual pairing with arbitrary test functions yields the compact notation

$$A(s) \begin{pmatrix} \widehat{\varphi} \\ \widehat{\psi} \end{pmatrix} = \begin{pmatrix} 0 \\ -g^{\mathrm{inc}} \end{pmatrix}. \tag{2.39}$$

This operator $A(s)$ describes the complete boundary integral equation for our time-harmonic scattering problem and inherits crucial bounds of $C(s)$ and $Z(s)$. In the following, we collect these bounds and coercivity results of the analytic operator family $A(s)$ for appropriate impedance operators $Z(s)$ fulfilling the polynomially bound (2.8) and the positivity condition (2.9).

Lemma 2.9 (Boundedness)**.** *Let $Z(s) : V \to V'$ satisfy the polynomial bound (2.8) with the real-valued rate $\kappa \leq 1$ (as shown to hold in Lemmas 2.1–2.3 for all presented boundary conditions). The operator family $A(s)$ defined by (3.41) then form an analytic family of bounded linear operators on the complex half-space with positive real part. For all $\sigma > 0$, there further exists a constant C_σ such that for all $\operatorname{Re} s \geq \sigma$ it holds that*

$$\|A(s)\|_{H^{1/2}(\Gamma)\times V' \leftarrow H^{-1/2}(\Gamma)\times V} \leq C_\sigma \frac{|s|^2}{\operatorname{Re} s},$$

where the constant C_σ grows at most polynomially in σ^{-1}.

Proof. The statement is a direct consequence of the triangle inequality applied to the Calderón operator $C(s)$ and the transfer operator $Z(s)$. The bounds on $C(s)$ proven in Lemma 2.7 readily extend to the stated spaces due to the continuous embedding $V \subset H^{1/2}(\Gamma)$. Furthermore, the identities $\mathrm{Id}_{H^{1/2}(\Gamma)\leftarrow V}$ and $\mathrm{Id}_{V' \leftarrow H^{-1/2}(\Gamma)}$ are bounded due to the chain of continuous embeddings of $V \subset H^{1/2}(\Gamma) \subset H^{-1/2}(\Gamma) \subset V'$. □

Lemma 2.10 (Coercivity)**.** *The analytic family of operators $A(s)$ has the following positivity property: For every $\sigma > \sigma_0 \geq 0$, there exists a positive constant $c_\sigma > 0$ such that for all $\operatorname{Re} s \geq \sigma$, we have*

$$\operatorname{Re} \left\langle \begin{pmatrix} \varphi \\ \psi \end{pmatrix}, A(s) \begin{pmatrix} \varphi \\ \psi \end{pmatrix} \right\rangle \geq c_\sigma \frac{\operatorname{Re} s}{|s|^2 + 1} \left(\|\varphi\|^2_{H^{-1/2}(\Gamma)} + \|\psi\|^2_V \quad \right)$$

for all boundary densities $(\varphi, \psi) \in H^{-1/2}(\Gamma) \times V$. The anti-duality on the left-hand side is naturally extended to $H^{-1/2}(\Gamma) \times V$ and $H^{1/2}(\Gamma) \times V'$ respectively. The constant in the lower bound has the explicit form $c_\sigma = \min(c_\Gamma^{-2}, c_\sigma^Z)$, where c_Γ is the maximum of the norms of the trace operators as defined in (2.20) and c_σ^Z is the constant from the positivity bound on $Z(s)$ in (2.9).

Proof. Coercivity bounds on the Calderón operator and the transfer operator are already established and the remaining shift is skew-hermitian since

$$\operatorname{Re}\left\langle \begin{pmatrix}\varphi\\ \psi\end{pmatrix}, \begin{pmatrix}0 & -\frac{1}{2}I\\ \frac{1}{2}I & 0\end{pmatrix}\begin{pmatrix}\varphi\\ \psi\end{pmatrix}\right\rangle = \frac{1}{2}\operatorname{Re}\left(-\langle\varphi,\psi\rangle + \langle\psi,\varphi\rangle\right) = 0.$$

We conclude, by applying the coercivity of the Calderón operator from Lemma 2.8 and the assumed positivity condition (2.9) on the transfer operator, which yields for $\operatorname{Re} s \geq \sigma > 0$

$$\begin{aligned}\operatorname{Re}\left\langle \begin{pmatrix}\varphi\\ \psi\end{pmatrix}, A(s)\begin{pmatrix}\varphi\\ \psi\end{pmatrix}\right\rangle &\geq \operatorname{Re}\left\langle \begin{pmatrix}\varphi\\ \psi\end{pmatrix}, C(s)\begin{pmatrix}\varphi\\ \psi\end{pmatrix}\right\rangle + \operatorname{Re}\langle\psi, Z(s)\psi\rangle\\ &\geq \frac{1}{c_\Gamma^2}\frac{\operatorname{Re} s}{|s|^2+1}\left(\|\varphi\|^2_{H^{-1/2}(\Gamma)} + \|\psi\|^2_{H^{1/2}(\Gamma)}\right) + \frac{c_\sigma^Z \operatorname{Re} s}{|s|^2}|\psi|_V^2\\ &= c_\sigma \frac{\operatorname{Re} s}{|s|^2+1}\left(\|\varphi\|^2_{H^{-1/2}(\Gamma)} + \|\psi\|^2_V\right),\end{aligned}$$

where $c_\sigma = \min\left(c_\Gamma^{-2}, c_\sigma^Z\right) > 0$. □

This coercivity result has direct consequences for the boundary integral equation (3.41), a fact that is described in the following proposition.

Theorem 2.1 (Well-posedness of the time-harmonic boundary integral equation)**.** *Let* $\operatorname{Re} s \geq \sigma > \sigma_0 \geq 0$ *and consider the boundary integral equation* (3.41) *with the boundary operator* $A(s)$*. For incident waves of sufficient regularity, in particular fulfilling* $\widehat{g}^{\text{inc}} \in V'$*, there exists a unique solution* $(\widehat{\varphi}, \widehat{\psi}) \in H^{-1/2}(\Gamma) \times V$*, which is bounded by*

$$\left\| \begin{pmatrix}\widehat{\varphi}\\ \widehat{\psi}\end{pmatrix}\right\|_{H^{-1/2}(\Gamma)\times V} \leq C_\sigma \frac{|s|^2}{\operatorname{Re} s}\left\|\widehat{g}^{\text{inc}}\right\|_{V'}. \tag{2.40}$$

The constant depends is explicitly given by the inverse of the constant in the coercivity result 2.10, i.e. $C_\sigma = c_\sigma^{-1} = \max(c_\Gamma^2, 1/c_\sigma^Z)$.

Proof. The bounds on $A(s)$ from Lemma 2.9–2.10 provide the conditions of Lax-Milgram Lemma, which implies the well-posedness of the inverse boundary integral operator and the bound

$$\left\|A^{-1}(s)\right\|_{H^{-1/2}(\Gamma)\times V \leftarrow H^{1/2}(\Gamma)\times V'} \leq C_\sigma \frac{|s|^2}{\operatorname{Re} s}. \tag{2.41}$$

The stated result is the consequence of applying this bound to the time-harmonic boundary integral equation (2.39). □

Remark 2.2. *The dependency of the incident wave is measured through the abstract norm associated to the vector space* V'*. However, since* $\|\phi\|_{H^{1/2}(\Gamma)} \leq \|\phi\|_V$ *for all* $\phi \in V$*, we obtain for more regular data*

$\widehat{g}^{\mathrm{inc}} \in H^{-1/2}(\Gamma)$ *the estimate*

$$\left\|\widehat{g}^{\mathrm{inc}}\right\|_{V'} = \sup_{\|\phi\|_V=1} \left\langle \phi, \widehat{g}^{\mathrm{inc}} \right\rangle_\Gamma \leq \sup_{\|\phi\|_{H^{1/2}(\Gamma)}\leq 1} \left(\phi, \widehat{g}^{\mathrm{inc}}\right)_\Gamma = \left\|\widehat{g}^{\mathrm{inc}}\right\|_{H^{-1/2}(\Gamma)}.$$

The data $\widehat{g}^{\mathrm{inc}} = Z(s)\widehat{p}^{\mathrm{inc}} - \widehat{v}^{\mathrm{inc}}$ *is sufficiently regular for the above bound for sufficiently smooth incident waves* $\widehat{p}^{\mathrm{inc}}$ *and* $\widehat{v}^{\mathrm{inc}}$*, sufficiently smooth boundaries* Γ *and the described transfer operators* $Z(s)$ *of Lemmas 2.1–2.3.*

2.4.1. Well-posedness of time-harmonic scattering with generalized impedance boundary conditions

Combining the previously established results with regards to the time-harmonic boundary integral equation gives the following well-posedness result for the time-harmonic scattering problem.

Theorem 2.2 (Well-posedness of the time-harmonic acoustic scattering problem)**.** *Consider the Helmholtz problem (2.12) for* $\operatorname{Re} s \geq \sigma > \sigma_0 \geq 0$*, completed with the generalized impedance boundary condition (2.33), where* $Z(s)$ *satisfies the polynomial bound (2.8) and the positivity condition (2.9). Furthermore, we assume the incident wave to be of sufficient regularity such that* $\widehat{g}^{\mathrm{inc}} \in V'$*. Under these conditions, the following statements hold.*

(a) The time-harmonic scattering problem has the unique solution

$$(\widehat{p}, \widehat{v}) \in H^1(\Omega) \times \boldsymbol{H}(\mathrm{div}, \Omega),$$

given by the representation formulas (2.13)–(2.14). The boundary data is uniquely determined by $(\widehat{\varphi}, \widehat{\psi}) = (-\gamma_\nu \widehat{v}, \gamma \widehat{p}) \in H^{-1/2}(\Gamma) \times V$*, the solution to the boundary integral equation (2.38). Consequently, the boundary data is bounded in terms of the incident wave, as described in Theorem 2.1.*

(b) The solutions are bounded by

$$\|\widehat{p}\|_{H^1(\Omega)} + \|\widehat{v}\|_{\boldsymbol{H}(\mathrm{div},\Omega)} \leq C_\sigma \frac{|s|^3}{(\operatorname{Re} s)^{3/2}} \left\|\widehat{g}^{\mathrm{inc}}\right\|_{V'},$$

where C_σ *depends polynomially on* σ^{-1} *and on the boundary* Γ *through norms of the traces. Moreover, in the case of the transfer operators discussed in Lemmas 2.1 and 2.2, the constant is independent of* δ*.*

Proof. Let $(\widehat{\varphi}, \widehat{\psi}) \in H^{-1/2}(\Gamma) \times V$ be the unique and bounded solution to the boundary integral equation (2.38), whose existence and uniqueness is provided by Theorem 2.1.

We define $\widehat{p}, \widehat{v} \in H^1(\mathbb{R}^3 \setminus \Gamma) \times \boldsymbol{H}(\mathrm{div}, \mathbb{R}^3 \setminus \Gamma)$ via the representation formulas (2.13)–(2.14), such that the transmission problem (2.15)–(2.18) holds. Expressing the functions $(\widehat{\varphi}, \widehat{\psi})$ in terms of the jumps of $(\widehat{p}, \widehat{v})$ by means of (2.17)–(2.18) and applying the jump conditions of the Calderón operator yields

$$C_{\mathrm{imp}}(s)\begin{pmatrix}\widehat{\varphi}\\ \widehat{\psi}\end{pmatrix} = C(s)\begin{pmatrix}\widehat{\varphi}\\ \widehat{\psi}\end{pmatrix} + \frac{1}{2}\begin{pmatrix}-\widehat{\psi}\\ \widehat{\varphi}\end{pmatrix} = \begin{pmatrix}\{\gamma\}\widehat{p}\\ -\{\gamma_\nu\}\widehat{v}\end{pmatrix} - \frac{1}{2}\begin{pmatrix}[\gamma]\widehat{p}\\ [\gamma_\nu]\widehat{v}\end{pmatrix} = \begin{pmatrix}\gamma^-\widehat{p}\\ \gamma_\nu^+\widehat{v}\end{pmatrix}.$$

Inserting this identity on the left-hand side of the boundary integral equation (2.38) yields

$$\gamma^- \widehat{p} = 0, \tag{2.42}$$

$$\gamma_\nu^+ \widehat{v} + Z(s)\widehat{\psi} = \widehat{g}^{\mathrm{inc}}. \tag{2.43}$$

The application of Green's formula in the inner domain and using (2.42) implies

$$\operatorname{Re} s \int_{\Omega^-} |\widehat{v}|^2 + |\widehat{p}|^2 \, \mathrm{d}\boldsymbol{x} = -\int_\Gamma \gamma_\nu^- \widehat{v}\, \gamma^- \widehat{p} \, \mathrm{d}\boldsymbol{x} = 0. \tag{2.44}$$

Consequently, $(\widehat{p}, \widehat{v})|_{\Omega^+}$ vanish in the inner domain and the boundary data reduces to $(\widehat{\varphi}, \widehat{\psi}) = (-\gamma_\nu \widehat{v}, \gamma \widehat{p})$, thus proving (a). Inserting this identity further for $\widehat{\psi}$ in (2.43) shows that the outer traces fulfill the weak formulation of the generalized impedance boundary condition (2.11).

Given that the inner traces vanishes, we are in the position of Lemma 2.6, which together with the bound of Theorem 2.1 yields the remaining statement (b) of the theorem. □

Remark 2.3. *The L^2- bound of Lemma 2.6 implies the additional L^2- bound*

$$\|\widehat{p}\|_{L^2(\Omega)} + \|\widehat{v}\|_{L^2(\Omega)} \leq C_\sigma \frac{|s|^2}{(\operatorname{Re} s)^{3/2}} \left\|\widehat{g}^{\mathrm{inc}}\right\|_{V'}. \tag{2.45}$$

2.4.2. Boundary integral equations for the inverted boundary condition

Transfer operators fulfilling the stated framework (2.8)–(2.9) are, as a consequence of the Lax–Milgram theorem, invertible. Applying the inverse operator to the generalized impedance boundary condition is therefore a well-posed operation and yields an equivalent boundary condition, which reads

$$\gamma \widehat{p} - Z(s)^{-1} \gamma_\nu \widehat{v} = \widehat{g}_-^{\mathrm{inc}}. \tag{2.46}$$

The right-hand side collects again terms, which only depend on the incident wave and is of the form $\widehat{g}_-^{\mathrm{inc}} = Z(s)^{-1}\gamma_\nu \widehat{v}^{\mathrm{inc}} - \gamma \widehat{p}^{\mathrm{inc}}$.

The boundary integral equation discussed previously has been derived by inserting the boundary condition into the trace of the velocity field $\widehat{v}$, which appears by using a shift and the jump conditions of the Calderón operator. Repeating this approach by changing the sign of the shift yields the operator

$$C_{\mathrm{imp}}^-(s) \begin{pmatrix} -\gamma_\nu \widehat{v} \\ \gamma \widehat{p} \end{pmatrix} = \begin{pmatrix} \gamma \widehat{p} \\ 0 \end{pmatrix}, \quad \text{where} \quad C_{\mathrm{imp}}^-(s) = C(s) - \begin{pmatrix} 0 & -\frac{1}{2} I \\ \frac{1}{2} I & 0 \end{pmatrix}. \tag{2.47}$$

The remaining right-hand side only depends on the trace of the acoustic pressure, in which the rearranged boundary condition (2.46) is inserted to obtain

$$C_{\mathrm{imp}}^-(s) \begin{pmatrix} \widehat{\varphi} \\ \widehat{\psi} \end{pmatrix} = \begin{pmatrix} -Z(s)^{-1}\widehat{\varphi} + \widehat{g}_-^{\mathrm{inc}} \\ 0 \end{pmatrix}.$$

Addition with the unknown term $Z(s)^{-1}\widehat{\varphi}$ in the first component on both sides yields the boundary integral equation

$$A^-(s)\begin{pmatrix}\widehat{\varphi}\\ \widehat{\psi}\end{pmatrix} = \begin{pmatrix}\widehat{g}_-^{\mathrm{inc}}\\ 0\end{pmatrix}, \quad \text{where} \quad A^-(s) = C^-_{\mathrm{imp}}(s) + \begin{pmatrix}Z(s)^{-1} & 0\\ 0 & 0\end{pmatrix}. \tag{2.48}$$

The analysis conducted so far, in particular Theorem 2.1, is readily transported to this boundary integral equation, for operator families $Z(s)$ whose inverse $Z(s)^{-1}$ is itself admissible in the sense of an appropriate counterpart of the polynomial bound (2.8) (which is already implied by the Lax–Milgram Lemma) and the positivity condition (2.9).

The Helmholtz problem under the generalized impedance boundary condition consequently admits two distinct boundary integral equations, the properties of which are determined by the transfer operator $Z(s)$ and its inverse $Z(s)^{-1}$. A direct application of this insight is the following consideration. The dependence on the small parameter δ is at this point in the thesis unclear and clarified in the subsequent sections. It is however natural, that any defect measured in the semi-norm chosen to treat the absorbing boundary condition (1.6) , which has the form $|\psi|_V = \delta^{-1/2}\|\psi\|_{L^2(\Gamma)}$, can only be bounded by an estimate which depends unfavourably on the factor $\delta^{-1/2}$. This is a drawback of the present boundary integral equation, as the boundary condition is particularly interesting for very small δ. The alternative approach described in this section completely avoids this difficulty and instead works with the inverse impedance operator, which is simply given by

$$Z(s)^{-1} = \delta s^{1/2}.$$

This transfer operator is polynomially bounded with the rate $\kappa = 1/2$ and fulfills the positivity condition (2.9) with the semi-norm $|\cdot|_V = \delta^{1/2}\|\cdot\|_{L^2(\Gamma)}$ installed on the Hilbert space $V = H^{1/2}(\Gamma)$. The positivity condition is obtained for the semi-norm by

$$\operatorname{Re}\left\langle \widehat{\varphi}, Z(s)^{-1}\widehat{\varphi}\right\rangle = \operatorname{Re} s\left(\delta\|\widehat{\varphi}\|^2_{L^2(\Gamma)}\right) = |s|^2\operatorname{Re} s\left|s^{-1}\widehat{\varphi}\right|_V \geq \sigma^2\operatorname{Re} s\left|s^{-1}\widehat{\varphi}\right|_V, \tag{2.49}$$

which holds for all $\operatorname{Re} s \geq \sigma$ and $\widehat{\varphi} \in V$. The alternative boundary integral equation (2.48) then yields a formulation based on this positivity condition, which subsequently gives favourable results in the following sections for strongly absorbing boundary conditions with the transfer operator as described in Lemma 2.2.

With this positivity, we obtain that the inverse of the operator family

$$A^-(s):\ V \times H^{1/2}(\Gamma) \to V' \times H^{-1/2}(\Gamma),$$

described in (2.48) with the transfer operator is $Z(s) = \delta^{-1}s^{1/2}$, is well defined. Moreover, the positivity of this operator family, as given in (2.49), shows the following bound of the inverse operator for $\operatorname{Re} s \geq \sigma > 0$

$$\left\|\left(A^-(s)\right)^{-1}\right\|_{V'\times H^{-1/2}(\Gamma)\leftarrow V\times H^{1/2}(\Gamma)} \leq C_\sigma\frac{|s|^2}{\operatorname{Re} s}, \tag{2.50}$$

where the constant depends on σ and Γ. The operator family $A^-(s)$ therefore shares the crucial properties of the boundary integral equation operator $A(s)$ described in Lemmas 2.9–2.10.

2.4.3. Bounds for the time-harmonic potential operators away from the boundary

Point evaluations of the potential operators fulfill bounds with a more favourable dependence on the real part of the Laplace parameter s than the previously established bounds of Lemma 2.5.

Such an estimate for the single layer potential operator is provided by [14, Lemma 7]. The same argument is accessible for the double layer potential operator and gives the following result.

Lemma 2.11. *Let $\boldsymbol{x} \in \mathbb{R}^3 \setminus \Gamma$ be an arbitrary point, away from the boundary with the positive distance $d = \operatorname{dist}(\boldsymbol{x}, \Gamma) > 0$. The point evaluation for the single and double layer potential operators $\mathcal{S}(s), \mathcal{D}(s)$ evaluated at this point satisfies the following bound:*

$$\begin{aligned} |(\mathcal{S}(s)\varphi)(\boldsymbol{x})| &\leq C\,|s|\,e^{-d\operatorname{Re}s}\,\|\varphi\|_{H^{-1/2}(\Gamma)}\,, \\ |(\mathcal{D}(s)\psi)(\boldsymbol{x})| &\leq C\,|s|\,e^{-d\operatorname{Re}s}\,\|\psi\|_{H^{1/2}(\Gamma)}\,, \end{aligned}$$

for $\operatorname{Re}s \geq \sigma > 0$, and for any $(\widehat{\varphi}, \widehat{\psi}) \in H^{-1/2}(\Gamma) \times H^{1/2}(\Gamma)$. The s-independent constant C only depends on $\sigma, \boldsymbol{x}$ and Γ.

Moreover, differentiating the point evaluations at any point is bounded directly by repeating the proof of the above Lemma with the differentiated fundamental solution, which gives the following Lemma.

Lemma 2.12. *Let k be some positive integer order of differentiation and consider an arbitrary partial derivative, corresponding to the coordinate $j = 1, 2, 3$. Further let $\boldsymbol{x} \in \mathbb{R}^3 \setminus \Gamma$ be an arbitrary point and consider the differentiated point evaluation for the single and double layer potential operators $\mathcal{S}(s), \mathcal{D}(s)$. Then, we have the following bounds*

$$\begin{aligned} \left|\left(\partial_{x_j}^k \mathcal{S}(s)\varphi\right)(\boldsymbol{x})\right| &\leq C\,|s|^{1+k}\,e^{-d\operatorname{Re}s}\,\|\varphi\|_{H^{-1/2}(\Gamma)}\,, \\ \left|\left(\partial_{x_j}^k \mathcal{D}(s)\psi\right)(\boldsymbol{x})\right| &\leq C\,|s|^{1+k}\,e^{-d\operatorname{Re}s}\,\|\psi\|_{H^{1/2}(\Gamma)}\,, \end{aligned}$$

for $\operatorname{Re}s \geq \sigma > 0$, and for any $(\varphi, \psi) \in H^{-1/2}(\Gamma) \times H^{1/2}(\Gamma)$. The s-independent constant C only depends on $k, \sigma, \boldsymbol{x}$ and Γ. Arbitrary combinations of the partial derivatives fulfill the identical bound, where k then corresponds to the overall order of differentiation.

Taking the above estimate and integrating over all points away from the boundary by at least a distance $d > 0$, gives the following bound.

Lemma 2.13. *Consider the domain away from the boundary by at least some fixed distance $d > 0$ with positive distance from the boundary $\Omega_d = \{\boldsymbol{x} \in \Omega \mid \operatorname{dist}(\boldsymbol{x}, \Gamma) > d\}$. The single and double layer potential operators $\mathcal{S}(s), \mathcal{D}(s)$, restricted on this domain, then satisfy the following bound: For any*

$\sigma > 0$, there exists a constant C_σ such that, for all $\operatorname{Re} s \geq \sigma$, we have

$$\begin{aligned}\|s\mathcal{S}(s)\|_{H^1(\Omega_d)\leftarrow H^{-1/2}(\Gamma)} &\leq C_\sigma |s|^3 e^{-d\operatorname{Re} s},\\ \|s\mathcal{D}(s)\|_{H^1(\Omega_d)\leftarrow H^{1/2}(\Gamma)} &\leq C_\sigma |s|^3 e^{-d\operatorname{Re} s}.\end{aligned}$$

The s-independent constant C_σ only depends on $\sigma, \boldsymbol{x}$ and Γ. In view of the representation formulas, the following bounds for the potential operators composed with the gradients are of interest

$$\begin{aligned}\|\nabla\mathcal{S}(s)\|_{\boldsymbol{H}(\operatorname{div},\Omega_d)\leftarrow H^{-1/2}(\Gamma)} &\leq C_\sigma |s|^3 e^{-d\operatorname{Re} s},\\ \|\nabla\mathcal{D}(s)\|_{\boldsymbol{H}(\operatorname{div},\Omega_d)\leftarrow H^{1/2}(\Gamma)} &\leq C_\sigma |s|^3 e^{-d\operatorname{Re} s}.\end{aligned}$$

Proof. Let $\varphi \in H^{-1/2}(\Gamma)$ be an arbitrary boundary function. Consider the square of this

$$\begin{aligned}\|\mathcal{S}(s)\varphi\|^2_{H^1(\Omega_d)} &= \int_{\Omega_d} |(\mathcal{S}(s)\varphi)(\boldsymbol{x})|^2 + |(\nabla\mathcal{S}(s)\varphi)(\boldsymbol{x})|^2 \,\mathrm{d}\boldsymbol{x}\\ &\leq C_\sigma \|\varphi\|^2_{H^{-1/2}(\Gamma)} |s|^4 \int_{\Omega_d} e^{-2\operatorname{dist}(\boldsymbol{x},\Gamma)\operatorname{Re} s}\,\mathrm{d}\boldsymbol{x}.\end{aligned}$$

The stated result for the single layer potential operator $\mathcal{S}(s)$ is then obtained by estimating the final integral, which decays exponentially with respect to the distance to the boundary. To estimate the integral on the right-hand side, we let $R > 0$ be large enough such that the ball B_R with radius R encloses the scatterer $\Gamma \subset B_R$, and its complement is a subset of Ω_d. Then, separating the integral domain yields the chain of inequalities

$$\begin{aligned}\int_{\Omega_d} e^{-2\operatorname{dist}(\boldsymbol{x},\Gamma)\operatorname{Re} s}\,\mathrm{d}\boldsymbol{x} &= \int_{\Omega_d\cap B_R} e^{-2\operatorname{dist}(\boldsymbol{x},\Gamma)\operatorname{Re} s}\,\mathrm{d}\boldsymbol{x} + \int_{\Omega_d\setminus B_R} e^{-2\operatorname{dist}(\boldsymbol{x},\Gamma)\operatorname{Re} s}\mathrm{d}\boldsymbol{x}\\ &\leq \int_{\Omega_d\cap B_R} e^{-2d\operatorname{Re} s}\,\mathrm{d}\boldsymbol{x} + e^{-2d\operatorname{Re} s}\int_{\mathbb{R}^3\setminus B_R} e^{-2(\|\boldsymbol{x}\|-R)\operatorname{Re} s}\,\mathrm{d}\boldsymbol{x}\\ &\leq \frac{4}{3}\pi R^3 e^{-2d\operatorname{Re} s} + e^{-2d\operatorname{Re} s} 4\pi\int_R^\infty r^2 e^{-2(r-R)\operatorname{Re} s}\,\mathrm{d}r\\ &\leq e^{-2d\operatorname{Re} s}\left(\frac{4}{3}\pi R^3 + 4\pi\frac{2\sigma^2R^2+2\sigma R+1}{4\sigma^3}\right).\end{aligned}$$

Taking the square root on both sides yields the bound for the single-layer potential operator.

Repeating this argument structure for the remaining potential operators gives the stated results. □

2.5. Time-dependent acoustic wave equation with generalized impedance boundary conditions

This section is devoted to leverage the Laplace domain results of the previous section, to give corresponding results to the time-dependent scattering problem, which are the overall objective of this chapter.

This approach, to derive properties of time-dependent problems via intermediate Laplace domain results, is notationally already present in the Heaviside notation (1.2) and follows the proposed framework of [52]. The foundation of this analysis are the frequency explicit bounds that have been derived in the previous section for all operators arising in relation to the time-harmonic acoustic scattering.

We begin with a time-dependent formulation of the boundary integral equation (2.38), obtained by formally replacing the Laplace transform variable s by the time differentiation operator ∂_t. In view of a future boundary element discretization, we further test the equation by time invariant test functions, which yields the following weak formulation.

Time-dependent boundary integral equation: *The time-dependent boundary densities, denoted by $(\varphi, \psi) : [0, T] \to H^{-1/2}(\Gamma) \times V$ with sufficient temporal regularity (to be specified in the subsequent sections) are said to be solutions of the time-dependent acoustic boundary integral equation, if for almost every time $t \in [0, T]$ and for all $(v, \xi) \in H^{-1/2}(\Gamma) \times V$, it holds that*

$$\left\langle \begin{pmatrix} v \\ \xi \end{pmatrix}, C_{\mathrm{imp}}(\partial_t) \begin{pmatrix} \varphi \\ \psi \end{pmatrix} \right\rangle_\Gamma + \langle \xi, Z(\partial_t)\psi \rangle_\Gamma = -\langle \xi, g^{\mathrm{inc}} \rangle_\Gamma. \tag{2.51}$$

The right-hand side $g^{\mathrm{inc}} : [0, T] \to V'$ is the time-dependent counterpart of the time-harmonic right-hand side of (2.38), which is assumed to be of the regularity $g^{\mathrm{inc}} \in H^r_0(0, T; V')$ with sufficiently large r. Some background on temporal Hilbert spaces and convolutional operators is introduced in Appendix A.

Through the operator family $A(s) : H^{-1/2}(\Gamma) \times V \to H^{1/2}(\Gamma) \times V'$, which effectively collects the time-harmonic boundary integral equation, we obtain the following compact representation of the time-dependent boundary integral equation (2.51) by

$$A(\partial_t) \begin{pmatrix} \varphi \\ \psi \end{pmatrix} = \begin{pmatrix} 0 \\ -g^{\mathrm{inc}} \end{pmatrix}. \tag{2.52}$$

In the interest of deriving properties of the time-dependent boundary densities (φ, ψ) we rewrite this boundary integral equation by using the temporal operator associated to the operator family $A(s)^{-1}$ for $\operatorname{Re} s > \sigma_0$, which by (2.41) constitutes a well-posed bounded operator family. Consequently, the temporal convolution operator $A^{-1}(\partial_t)$ is also well-defined by (A.3), and by the composition rule of operational calculus (A.2) we obtain the identities

$$A^{-1}(\partial_t)A(\partial_t) = \mathrm{Id}_{H^{-1/2}(\Gamma)\times V} \quad \text{and} \quad A(\partial_t)A^{-1}(\partial_t) = \mathrm{Id}_{H^{1/2}(\Gamma)\times V'}.$$

Applying the operator $A^{-1}(\partial_t)$ on both sides of the temporal boundary integral equation yields a closed form of the time-dependent boundary data, which reads

$$\begin{pmatrix} \varphi \\ \psi \end{pmatrix} = A^{-1}(\partial_t) \begin{pmatrix} 0 \\ -g^{\mathrm{inc}} \end{pmatrix}. \tag{2.53}$$

We are now in the position to apply the bound (A.3) from [52, Lemma 2.1] on the temporal convolution operator $A^{-1}(\partial_t)$, where the necessary Laplace domain bounds are supplied by

Theorem 2.1 with the exponent $\kappa = 2$.

Consequently, we obtain the well-posedness of the temporal boundary integral equation, complemented by a bound of the exact solution in terms of the incident wave, which is described in the following Theorem.

Theorem 2.3 (Well-posedness of the time-dependent boundary integral equation)**.** *Consider the boundary integral equation* (2.51) *and let* $g^{\text{inc}} \in H_0^{r+3}(0,T;V')$ *with* $r \geq 0$*. There exists a unique solution* $(\varphi,\psi) \in H_0^{r+1}(0,T;H^{-1/2}(\Gamma)\times V)$ *and it is bounded by*

$$\left\| \begin{pmatrix} \varphi \\ \psi \end{pmatrix} \right\|_{H_0^{r+1}(0,T;H^{-1/2}(\Gamma)\times V)} \leq C_T \left\| g^{\text{inc}} \right\|_{H_0^{r+3}(0,T;V')}. \tag{2.54}$$

The constant C_T *depends on norm of the trace operators and on the final time* T*. For transfer operators with* $\sigma_0 = 0$ *in* (2.8)–(2.9)*, the dependence on the final time is furthermore only polynomial.*

The boundary densities φ, ψ of Theorem 2.3 uniquely identify the time-dependent scattered fields p and $\boldsymbol{v}$, which are recovered by the temporal representation formulas

$$p = \partial_t \mathcal{S}(\partial_t)\varphi + \partial_t \mathcal{D}(\partial_t)\psi, \tag{2.55}$$
$$\boldsymbol{v} = \nabla \mathcal{S}(\partial_t)\varphi + \nabla \mathcal{D}(\partial_t)\psi. \tag{2.56}$$

The following theorem shows that the solution (φ,ψ) is in fact the boundary data to the time-dependent scattering problem of interest, namely the acoustic wave equation (1.3) with the time-dependent generalized impedance boundary condition (1.9). In combination with Theorem 2.3, this yields a well-posedness result of this temporal scattering result, which is complemented by a bound on the scattered wave in terms of the incoming wave.

The theorem is consequently the time-dependent counterpart of the time-harmonic well-posedness result from Theorem 2.2 and is proven by transporting the results from the Laplace domain to the time domain.

Theorem 2.4 (Well-posedness of the time-dependent scattering problem)**.** *Consider the acoustic wave equation* (1.3)*, complemented the generalized impedance boundary condition* (2.11)*, where* $Z(s)$ *satisfies the conditions* (2.8)–(2.9) *with* $\kappa \leq 1$ *and with* $g^{\text{inc}} \in H_0^{r+3}(0,T;V')$ *for some arbitrary real-valued* $r \geq 0$*.*

(a) Let p *and* $\boldsymbol{v}$ *be defined through the representation formulas* (2.55)–(2.56)*, where* φ *and* ψ *are solution to the boundary integral equation* (2.52)*. These fields are the unique solution to the time-dependent scattering problem with the generalized impedance boundary conditions and are further at least of the regularity*

$$(p,\boldsymbol{v}) \in H_0^r(0,T;H^1(\Omega)\times \boldsymbol{H}(\operatorname{div},\Omega)) \cap H_0^{r+1}(0,T;L^2(\Omega)\times \boldsymbol{L}^2(\Omega)).$$

The traces of this solution are uniquely determined by the boundary integral equation of Theorem 2.3,

$$(\varphi,\psi) = (-\gamma_\nu \boldsymbol{v}, \gamma p) \in H_0^{r+1}(0,T;H^{-1/2}(\Gamma)\times V).$$

(b) The scattered wave fulfills the bound

$$\|p\|_{H_0^r(0,T;H^1(\Omega))} + \|\boldsymbol{v}\|_{H_0^r(0,T;\boldsymbol{H}(\mathrm{div},\Omega))} \leq C_T \|g^{\mathrm{inc}}\|_{H_0^{r+3}(0,T;V')},$$

and the same bound holds for the norm $H_0^{r+1}(0,T;(L^2(\Omega)\times \boldsymbol{L}^2(\Omega))$ norms. The constant C_T depends on T (polynomially if $\sigma_0 = 0$ in (2.9)) and on the norms of the trace operators.

Proof. This proof was essentially formulated in [59, Theorem 4.2], in the analogous electromagnetic setting.

We start by extending the data $g^{\mathrm{inc}} \in H_0^{r+3}(0,T;V')$ on the right-hand side from the interval $[0,T]$ to a function in $H^r(\mathbb{R};V')$ on the whole real line, with support in $[0,\widetilde{T}]$, where $\widetilde{T} > T$ is chosen such that the H^r-norm of the extension of g^{inc} is equivalent to the H^r norm of the original data g^{inc} (only defined on $[0,T]$).

Let $(p,\boldsymbol{v})$ be defined by the time-dependent boundary integral equation (2.52) and the time-dependent representation formulas (2.55)–(2.56). The stated regularity is the consequence of (A.3), used with the time-harmonic bounds given in Theorem 2.2. These bounds hold on every finite time interval $(0,\bar{T})$, with at most exponential growth in $\bar{T}$ of the norm with an arbitrary exponent $\sigma_1 > \sigma_0$. The Laplace transform $(\widehat{p}(s),\widehat{\boldsymbol{v}}(s))$ then exists for $\mathrm{Re}\, s > \sigma_0$, and it is obtained by the solution to the time-harmonic boundary integral equation (2.39) and the time-harmonic representation formulas (2.13)–(2.14).

The well-posedness result of the time-harmonic scattering problem described in Theorem 2.2 then implies that the Laplace transforms $(\widehat{p}(s),\widehat{\boldsymbol{v}}(s))$ are indeed the unique solution to the time-harmonic scattering problem with the time-harmonic generalized impedance boundary conditions. The application of the inverse Laplace transform then shows that the temporal quantities $(p,\boldsymbol{v})$ solve the time-dependent scattering problem (2.1)–(2.2) under the generalized impedance boundary condition (2.3). Finally, the uniqueness of the time-dependent solution $(p,\boldsymbol{v})$ follows from the uniqueness of the traces and the well-posedness of the time-dependent acoustic wave equation with a given trace. □

2.6. Semi-discretization in time by Runge–Kutta convolution quadrature

2.6.1. Convolution quadrature for the scattering problem

Applying the convolution quadrature method to discretize the temporal operators of (2.52) gives the following time-discrete convolution equation

$$A(\partial_t^\tau)\begin{pmatrix}\varphi^\tau\\ \psi^\tau\end{pmatrix} = \begin{pmatrix}0\\ -g^{\mathrm{inc}}\end{pmatrix}. \tag{2.57}$$

The treatment of this formulation is structurally identical to the analytic treatment of the boundary integral equation, enabled through the discrete counterpart of the composition rule, as for-

mulated in (B.9), which implies the identities

$$A^{-1}(\partial_t^\tau)A(\partial_t^\tau) = \mathrm{Id}_{H^{-1/2}(\Gamma)\times V} \quad \text{and} \quad A(\partial_t^\tau)A^{-1}(\partial_t^\tau) = \mathrm{Id}_{H^{1/2}(\Gamma)\times V'}.$$

In view of this identity, we obtain the following direct representation of the temporal semi-discretization

$$\begin{pmatrix} \varphi^\tau \\ \psi^\tau \end{pmatrix} = A^{-1}(\partial_t^\tau) \begin{pmatrix} 0 \\ -g^{\mathrm{inc}} \end{pmatrix}. \tag{2.58}$$

This representation is crucial, both for the error analysis and for practical computations, since it rewrites the numerical approximation as a forward application of an understood temporal convolution operator. The subsequent error analysis then revolves around the application of general convolution quadrature results, in particular Lemma B.1. This approach has particularly favourable properties with regards to the stability of the resulting temporal semi-discretization.

The time-discrete numerical solution is recovered on the whole domain Ω through the temporal representation formulas discretized by the convolution quadrature method, which read

$$p^\tau = \partial_t \mathcal{S}(\partial_t^\tau)\varphi^\tau \; + \partial_t \mathcal{D}(\partial_t^\tau)\psi^\tau, \tag{2.59}$$
$$\boldsymbol{v}^\tau = \nabla \mathcal{S}(\partial_t^\tau)\varphi^\tau + \nabla \mathcal{D}(\partial_t^\tau)\psi^\tau. \tag{2.60}$$

These fields are therefore characterized directly in terms of the boundary data g^{inc} via the composite operator $\mathcal{U}(\partial_t)$ defined through

$$\begin{pmatrix} p^\tau \\ \boldsymbol{v}^\tau \end{pmatrix} = \mathcal{U}(\partial_t^\tau) g^{\mathrm{inc}} \quad \text{of} \quad \begin{pmatrix} p \\ \boldsymbol{v} \end{pmatrix} = \mathcal{U}(\partial_t) g^{\mathrm{inc}}, \tag{2.61}$$

where the composite operator is explicitly given by the composition of solving the discrete boundary integral equation and insert the result into the representation formulas, which reads

$$\mathcal{U}(s) = \begin{pmatrix} s\mathcal{S}(s) & s\mathcal{D}(s) \\ \nabla \mathcal{S}(s) & \nabla \mathcal{D}(s) \end{pmatrix} A(s)^{-1} \begin{pmatrix} 0 \\ \mathrm{Id} \end{pmatrix} : V' \to H^1(\Omega) \times \boldsymbol{H}(\mathrm{div}, \Omega).$$

This operator family is polynomially bounded through Theorem 2.4 (b), namely for any $\sigma > \sigma_0$ there exists a constant C_σ such that, for all $\operatorname{Re} s \geq \sigma$, it holds that

$$\|\mathcal{U}(s)\|_{H^1(\Omega)\times \boldsymbol{H}(\mathrm{div},\Omega) \leftarrow V'} \leq C_\sigma \frac{|s|^3}{(\operatorname{Re} s)^{3/2}}.$$

Moreover, for points away from the boundary with at least some minimum fixed distance d we obtain bounds with a more favourable dependence on the real part $\operatorname{Re} s$. As a consequence of the bounds on the potential operators described in Lemma 2.11–2.13, we further have for $\operatorname{Re} s \geq \sigma > \sigma_0 \geq 0$

$$\|\mathcal{U}(s)\|_{C^1(\overline{\Omega_d})\times \boldsymbol{C}^1(\overline{\Omega_d})^3 \leftarrow V'} + \|\mathcal{U}(s)\|_{H^1(\Omega_d)\times \boldsymbol{H}(\mathrm{div},\Omega_d) \leftarrow V'} \leq C_\sigma \, |s|^5 \, e^{-d \operatorname{Re} s},$$

where $\Omega_d = \{\boldsymbol{x} \in \Omega : \ \operatorname{dist}(\boldsymbol{x}, \Gamma) > d\}$ with $d > 0$ denotes all points in the domain with at least the fixed distance d from the boundary.

Remark 2.4. *The discrete velocity field $\boldsymbol{v}^\tau$ is* **curl***-free, just as the exact continuous velocity field $\boldsymbol{v}$. This identity directly follows from observing that the generating function $\sum_{n\geq 0} \boldsymbol{v}^n \zeta^n$ is itself directly characterized by time-harmonic representation formulas for $|\zeta| < 1$.*

With these bounds, we obtain error bounds for the semi-discretization by applying the general convolution quadrature result formulated in Lemma B.1 to the operator family $\mathcal{U}(s)$.

Proposition 2.1 (Error bound of the semi-discretization in time)**.** *In the setting of Theorem 2.4, consider the semi-discretization in time (2.57), discretized by Runge–Kutta convolution quadrature based on the Radau IIA method with m stages. Let p^τ and $\boldsymbol{v}^\tau$ further denote the solutions of the discrete representation formulas (2.59)–(2.60). Let $r > 2m + 3$ and assume that the regularity of the incident wave implies $g^{inc} \in \boldsymbol{C}^r([0,T], \boldsymbol{V}_\Gamma{}')$, with g^{inc} initially vanishing together with its first $r-1$ time derivatives.*

Under these conditions, the approximations of the semi-discrete electromagnetic fields $p^n = \left[(p^\tau)^{n-1}\right]_m$ and $\boldsymbol{v}^n = \left[(\boldsymbol{v}^\tau)^{n-1}\right]_m$ fulfill the following error bounds at the time $t_n = n\tau \in [0,T]$:

$$\left\| \begin{pmatrix} p^n - p(t_n) \\ \boldsymbol{v}^n - \boldsymbol{v}(t_n) \end{pmatrix} \right\|_{H^1(\Omega)\times \boldsymbol{H}(\operatorname{div},\Omega)} \leq C\, \tau^{m-1/2}\, M(g^{inc}, t_n).$$

On the domain away from the boundary by at least some fixed distance $d > 0$, namely the domain $\Omega_d = \{\boldsymbol{x} \in \Omega \ : \ \operatorname{dist}(\boldsymbol{x}, \Gamma) > d\}$ a corresponding bound of the full classical order $2m-1$ holds:

$$\left\| \begin{pmatrix} p^n - p(t_n) \\ \boldsymbol{v}^n - \boldsymbol{v}(t_n) \end{pmatrix} \right\|_{H^1(\Omega_d)\times \boldsymbol{H}(\operatorname{div},\Omega_d)\cap C^1(\overline{\Omega}_d)\times \boldsymbol{C}^1(\overline{\Omega}_d)^3} \leq C_d\, \tau^{2m-1}\, M(g^{inc}, t_n).$$

An equivalent bound holds for point evaluations at any point $\boldsymbol{x} \in \Omega$. The constant originates from Lemma B.1 and has the explicit form

$$M(g,t) = \|g^{(r)}(0)\|_{V'} + \int_0^t \|g^{(r+1)}(t')\|_{V'}\, \mathrm{d}t'.$$

The constants C and C_d in the error bounds depend on the final time T and on the boundary Γ, but are crucially independent of n, τ and g^{inc}. As indicated by the index, C_d additionally depends on the distance d. In particular, for the scattering problems associated to the boundary conditions (1.4)–(1.7), both C and C_d are independent of the small parameter δ.

In the context of acoustic scattering from a sound-soft obstacle, full-order convergence away from the boundary for the Runge–Kutta convolution quadrature time discretization was first observed and proved in [14].

2.7. Full discretization

Consider a family of regular triangulations of the boundary Γ with maximal mesh widths h. On these triangulations, we define the following boundary element spaces

$$X_h \subset H^{-1/2}(\Gamma), \quad V_h \subset V \subset H^{1/2}(\Gamma).$$

In the present chapter, we make the following choices for these spaces. For the integer order $k \leq 1$, we let X_h be the boundary element space of discontinuous piecewise polynomial basis functions of degree $k-1$ and V_h to be the boundary element space of globally continuous piecewise polynomials of degree k.

Let I_{X_h} and I_{V_h} denote the boundary interpolation operators as defined in Section 4.3 of the monograph [63]. For a regular family of triangulations, the results [63, Theorem 4.3.20, Theorem 4.3.22] provide the following approximation results for the interpolation operator.

Lemma 2.14. *Consider the subspaces $X_h \subset H^{-1/2}(\Gamma)$ and $V_h \subset V$, chosen as the discontinuous polynomial boundary elements of order $k-1$ and the continuous polynomial boundary elements of order $k \geq 1$ respectively. Then, there exists a constant C such that for all $\xi \in H^{k+1}(\Gamma)$ we have*

$$\begin{aligned} \left\| I^r_{X_h} \xi - \xi \right\|_{H^{-1/2}(\Gamma)} &\leq C\, h^{k+1/2} \left\| \xi \right\|_{H^k(\Gamma)}, \\ \left\| I^r_{V_h} \xi - \xi \right\|_{H^r(\Gamma)} &\leq C\, h^{k+1-r} \left\| \xi \right\|_{H^{k+1}(\Gamma)}, \end{aligned} \tag{2.62}$$

where the second estimate holds for arbitrary $r \in [0,1]$. The constant C only depends on the boundary Γ.

In view of the setting of the boundary integral equation, we are interested in bounds on the interpolation error on the functional analytic settings associated to the transfer operators of the boundary conditions studied.

Lemma 2.15. *Let $\xi \in H^{k+1}(\Gamma)$ be some arbitrary boundary function and consider the boundary element space V_h consisting of piecewise continuous polynomials of order k, where $I_{V_h}\xi$ denotes the interpolation of ξ. For the norm associated to the thin-layer boundary condition, as described by Lemma 2.1*

$$\left\| \mathrm{I}_{V_h} \xi - \xi \right\|_V = \left(\left\| \mathrm{I}_{V_h} \xi - \xi \right\|^2_{H^{1/2}(\Gamma)} + \delta \left\| \mathrm{I}_{V_h} \xi - \xi \right\|^2_{H^1(\Gamma)} \right)^{1/2} \leq C \left(h^{k+1/2} + \delta^{1/2} h^k \right). \tag{2.63}$$

For the norm associated to the strongly absorbing boundary condition, described by Lemma 2.2, we have

$$\left\| \mathrm{I}_{V_h} \xi - \xi \right\|_V = \left(\left\| \mathrm{I}_{V_h} \xi - \xi \right\|^2_{H^{1/2}(\Gamma)} + \delta^{-1} \left\| \mathrm{I}_{V_h} \xi - \xi \right\|^2_{L^2(\Gamma)} \right)^{1/2} \leq C \left(h^{k+1/2} + \delta^{-1/2} h^{k+1} \right). \tag{2.64}$$

Finally, the interpolation error for the trace space associated to the acoustic boundary condition, described by Lemma 2.3, is directly estimated through

$$\left\| \mathrm{I}_{V_h} \xi - \xi \right\|_V = \left\| \mathrm{I}_{V_h} \xi - \xi \right\|_{H^{1/2}(\Gamma)} \leq C h^{k+1/2}. \tag{2.65}$$

The constant C is independent of ξ and h, but depends on k and Γ.

Formulating the weak formulation of (2.57) and the restriction onto the finite dimensional subspace $X_h \times V_h$ yields the following full discretization:

$$\left\langle \begin{pmatrix} v_h \\ \xi_h \end{pmatrix}, A(\partial_t^\tau) \begin{pmatrix} \varphi_h^\tau \\ \psi_h^\tau \end{pmatrix} \right\rangle_\Gamma = \langle v_h, g^{\text{inc}} \rangle_\Gamma \qquad \text{for all } (v_h, \xi_h) \in (X_h \times V_h)^m. \tag{2.66}$$

The solution to these discrete schemes are approximations to the boundary densities, which are denoted by

$$\begin{aligned} \varphi_h^\tau &= \left((\varphi_h^\tau)^n\right)_{n\geq 0} \quad \text{with} \quad (\varphi_h^\tau)^n = \left((\varphi_h^\tau)_i^n\right)_{i=1}^m \in X_h^m, \\ \psi_h^\tau &= \left((\psi_h^\tau)^n\right)_{n\geq 0} \quad \text{with} \quad (\psi_h^\tau)^n = \left((\psi_h^\tau)_i^n\right)_{i=1}^m \in V_h^m. \end{aligned}$$

Through the time-discrete representation formulas, these approximations imply fully discrete solutions away from the boundary. Inserting the fully discrete boundary densities into (2.59)–(2.60) therefore reveals the numerical approximations in the domain Ω via

$$p_h^\tau = \partial_t^\tau \mathcal{S}(\partial_t^\tau)\varphi_h^\tau + \partial_t^\tau \mathcal{D}(\partial_t^\tau)\psi_h^\tau, \tag{2.67}$$

$$\boldsymbol{v}_h^\tau = \nabla \mathcal{S}(\partial_t^\tau)\varphi_h^\tau + \nabla \mathcal{D}(\partial_t^\tau)\psi_h^\tau. \tag{2.68}$$

The following theorem gives error bounds for these approximations, where the various bounds of the potential operators Lemma 2.5, Lemma 2.11 and Lemma 2.13 imply corresponding error bounds.

Theorem 2.5 (Error bound of the full discretization)**.** *Consider the boundary integral equation in the setting of Theorem 2.4 under the conditions stated there. In this setting, consider the approximations with the following discretizations:*

- *Convolution quadrature time discretization based on the Radau IIA Runge–Kutta method with $m \geq 2$ stages employed for the boundary integral equation (2.66) and the discrete representation formulas (2.59)–(2.60); and*

- *boundary element space discretization $X_h \times V_h$, consisting of discontinuous piecewise polynomials of order $k-1$ and continuous piecewise polynomials of order k respectively, applied to the boundary integral equation (2.66).*

In addition to the assumptions of Theorem 2.4, we assume $g^{inc} \in C^r([0,T], V')$ for some $r > 2m+3$ and further assume that g^{inc} vanishes at $t = 0$ together with its first $r-1$ time derivatives. Moreover, the exact solution (φ, ψ) of the boundary integral equation (2.52) is assumed to be in $C^{10}([0,T], H^{k+1}(\Gamma)^2)$ and vanish at $t = 0$ together with its time derivatives.
The error rates depend on the functional analytic setting of the boundary condition, as described by Lemmas 2.1–2.3. The following error bounds are therefore referenced to their functional analytic setting through their corresponding Lemma. Under these conditions, the following error bounds hold for the

approximations $p_h^n = \left[(p_h^\tau)^{n-1}\right]_m$ *and* $\boldsymbol{v}_h^n = \left[(\boldsymbol{v}_h^\tau)^{n-1}\right]_m$ *in time and space at* $t_n = n\tau \in [0,T]$*:*

$$\begin{aligned}
\left\| \begin{pmatrix} p_h^n - p(t_n) \\ \boldsymbol{v}_h^n - \boldsymbol{v}(t_n) \end{pmatrix} \right\|_{H^1(\Omega)\times \boldsymbol{H}(\mathrm{div},\Omega)} &\leq C\big(\tau^{m-1/2} + h^{k+1/2} + \delta^{1/2} h^k\big) && \text{Lemma 2.1,} \\
&\leq C\big(\tau^{m-1/2} + h^{k+1/2} + \delta^{-1/2} h^{k+1}\big) && \text{Lemma 2.2,} \\
&\leq C\big(\tau^{m-1/2} + h^{k+1/2}\big) && \text{Lemma 2.3.}
\end{aligned}$$

On the domain of points away from the boundary by at least a fixed distance $d > 0$*, namely the domain* $\Omega_d = \{x \in \Omega : \operatorname{dist}(x,\Gamma) > d\}$*, corresponding bounds for the full classical order* $2m-1$ *in time hold:*

$$\begin{aligned}
&\left\| \begin{pmatrix} p_h^n - p(t_n) \\ \boldsymbol{v}_h^n - \boldsymbol{v}(t_n) \end{pmatrix} \right\|_{H^1(\Omega_d)\times \boldsymbol{H}(\mathrm{div},\Omega_d)} + \left\| \begin{pmatrix} p_h^n - p(t_n) \\ \boldsymbol{v}_h^n - \boldsymbol{v}(t_n) \end{pmatrix} \right\|_{C^1(\overline{\Omega}_d)\times \boldsymbol{C}^1(\overline{\Omega}_d)} \\
&\leq C_d\big(\tau^{2m-1} + h^{k+1/2} + \delta^{1/2} h^k\big) && \text{Lemma 2.1,} \\
&\leq C_d\big(\tau^{2m-1} + h^{k+1/2} + \delta^{-1/2} h^{k+1}\big) && \text{Lemma 2.2,} \\
&\leq C_d\big(\tau^{2m-1} + h^{k+1/2}\big) && \text{Lemma 2.3.}
\end{aligned}$$

The constants C *and* C_d *in the error bounds depend on the final time* T*, on the boundary* Γ*, on the incident waves through* g^{inc} *and on higher Sobolev norms of the exact solution* (φ, ψ)*, but are crucially independent of* h*,*n *and* τ*. As indicated by the index,* C_d *additionally depends on the distance* d*. In particular, for the impedance operators (1.4)–(1.7), both* C *and* C_d *are independent of the small parameter* δ*.*

Proof. The proof is separated into three parts (a)–(c), starting from analyzing the time-harmonic space discretization, extending these results to the time-dependent space discretization and finally showing the stated bounds for the time-dependent full discretization. In order to simplify the presentation, we reduce the present the arguments for the thin-layer boundary condition, with the corresponding functional analytic setting of Lemma 2.1.

(a) *(Discretized time-harmonic boundary integral equation).* Consider the time-harmonic boundary integral equation (2.37), for $\operatorname{Re} s \geq \sigma > \sigma_0 \geq 0$. The spatially discrete solution operator of the time-harmonic boundary integral equation, which maps $\widehat{g} \mapsto (\widehat{\varphi}_h, \widehat{\psi}_h)$, is denoted by $L_h(s) : V' \to X_h \times V_h$ and defined by the Galerkin approximation in $X_h \times V_h$

$$\left\langle \begin{pmatrix} v_h \\ \xi_h \end{pmatrix}, A(s) \begin{pmatrix} \widehat{\varphi}_h \\ \widehat{\psi}_h \end{pmatrix} \right\rangle_\Gamma = \langle v_h, \widehat{g} \rangle_\Gamma \qquad \forall\, (v_h, \xi_h) \in X_h \times V_h. \tag{2.69}$$

By the bound of $A(s)$ in Lemma 2.9, the coercivity estimate of Lemma 2.10 and the Lax–Milgram Lemma, we obtain the bound

$$\|L_h(s)\|_{X_h\times V_h \leftarrow V'} \leq \frac{1}{c_\sigma} \frac{|s|^2}{\operatorname{Re} s}. \tag{2.70}$$

Additionally, consider the Ritz projection associated to the bilinear form on the left-hand side,

denoted by $\mathcal{R}_h(s) : H^{-1/2}(\Gamma) \times V \to X_h \times V_h$. This operator projects the boundary densities $(\widehat{\varphi}, \widehat{\psi}) \in H^{-1/2}(\Gamma) \times V$ into the boundary element space $(\widehat{\varphi}_h, \widehat{\psi}_h) \in X_h \times V_h$ and is defined by the formulation

$$\left\langle \begin{pmatrix} v_h \\ \xi_h \end{pmatrix}, A(s) \begin{pmatrix} \widehat{\varphi}_h \\ \widehat{\psi}_h \end{pmatrix} \right\rangle_\Gamma = \left\langle \begin{pmatrix} v_h \\ \xi_h \end{pmatrix}, A(s) \begin{pmatrix} \widehat{\varphi} \\ \widehat{\psi} \end{pmatrix} \right\rangle_\Gamma \qquad \forall\, (v_h, \xi_h) \in X_h \times V_h.$$

By employing the bounds Lemmas 2.9 and 2.10 on $A(s)$ and applying the Lax–Milgram Lemma, we obtain that the above problem is well-posed. Applying Céa's Lemma further yields an estimate of the projection error in terms of the approximation properties of the underlying boundary element space

$$\left\| \begin{pmatrix} \widehat{\varphi}_h \\ \widehat{\psi}_h \end{pmatrix} - \begin{pmatrix} \widehat{\varphi} \\ \widehat{\psi} \end{pmatrix} \right\|_{H^{-1/2}(\Gamma)\times V} \leq \frac{C_\sigma |s|^4}{c_\sigma (\operatorname{Re} s)^2} \inf_{(v_h,\xi_h)\in X_h\times V_h} \left\| \begin{pmatrix} v_h \\ \xi_h \end{pmatrix} - \begin{pmatrix} \widehat{\varphi} \\ \widehat{\psi} \end{pmatrix} \right\|_{H^{-1/2}(\Gamma)\times V}.$$

The best-approximation on the right-hand side is the subject of Lemma 2.14 and applying the bounds therein shows that the associated error operator

$$\mathcal{E}_h(s) = R_h(s) - \mathrm{Id}$$

is a bounded operator from $H^{k+1}(\Gamma)^2$ to $\boldsymbol{V}_\Gamma \times \boldsymbol{X}_\Gamma$ that fulfills, for $\operatorname{Re} s \geq \sigma > \sigma_0 \geq 0$,

$$\|\mathcal{E}_h(s)\|_{H^{-1/2}(\Gamma)\times V \leftarrow H^{k+1}(\Gamma)^2} \leq \widetilde{C}_\sigma \frac{|s|^4}{(\operatorname{Re} s)^2} \left(h^{k+1/2} + \delta^{1/2} h^k \right). \tag{2.71}$$

(b) *(Error of the spatial semi-discretization).* We turn our attention towards the spatial semi-discretization of the time-dependent boundary integral equation (2.52), which reads

$$\left\langle \begin{pmatrix} v_h \\ \xi_h \end{pmatrix}, A(\partial_t) \begin{pmatrix} \varphi_h \\ \psi_h \end{pmatrix} \right\rangle_\Gamma = \langle v_h, g^{\mathrm{inc}} \rangle_\Gamma \qquad \forall\, (v_h, \xi_h) \in X_h \times V_h. \tag{2.72}$$

The unique solution of the above system is characterized directly by the discussed operators transferred to the time domain, namely it holds that

$$\begin{pmatrix} \varphi_h \\ \psi_h \end{pmatrix} = L_h(\partial_t) g^{\mathrm{inc}} = R_h(\partial_t) \begin{pmatrix} \varphi \\ \psi \end{pmatrix},$$

where $(\varphi, \psi)^\top = A^{-1}(\partial_t)(g^{\mathrm{inc}}, 0)^\top$ is the solution to the fully continuous boundary integral equation (2.52). We collect the potential operators and their sign structure from the representation formulas in a block operator, which is denoted by

$$\mathcal{W}(s) = \begin{pmatrix} s\mathcal{S}(s) & s\mathcal{D}(s) \\ \nabla\mathcal{D}(s) & \nabla\mathcal{S}(s), \end{pmatrix}$$

and set

$$U_h(s) = \mathcal{W}(s) L_h(s) : V' \to H^1(\Omega) \times \boldsymbol{H}(\mathrm{div}, \Omega). \tag{2.73}$$

Employing the established bounds of the operators $\mathcal{W}(s)$ and $L_h(s)$, namely the bounds from Lemma 2.5 and (2.70), implies the bound

$$\|U_h(s)\|_{H^1(\Omega)\times \boldsymbol{H}(\mathrm{div},\Omega)\leftarrow V'} \leq \bar{C}_\sigma \frac{|s|^4}{(\operatorname{Re} s)^2}. \tag{2.74}$$

The temporal convolution operator $U_h(\partial_t)$ is therefore well-defined and extends to a bounded operator via (A.3). Consequently, the spatial semi-discretization of the scattering problem is characterized by the evaluation of this operator on the right-hand side, namely

$$\begin{pmatrix} p_h \\ \boldsymbol{v}_h \end{pmatrix} = U_h(\partial_t) g^{\mathrm{inc}}.$$

By employing the analogous identity for the fully continuous densities (2.61), its error is rewritten as

$$\begin{aligned} \begin{pmatrix} p_h \\ \boldsymbol{v}_h \end{pmatrix} - \begin{pmatrix} p \\ \boldsymbol{v} \end{pmatrix} &= \mathcal{U}_h(\partial_t) g^{\mathrm{inc}} - \mathcal{U}(\partial_t) g^{\mathrm{inc}} = \mathcal{W}(\partial_t) \begin{pmatrix} \varphi_h \\ \psi_h \end{pmatrix} - \mathcal{W}(\partial_t) \begin{pmatrix} \varphi \\ \psi \end{pmatrix} \\ &= \mathcal{W}(\partial_t)(R_h - \mathrm{Id}) \begin{pmatrix} \varphi \\ \psi \end{pmatrix} = \mathcal{W}(\partial_t)\, \mathcal{E}_h(\partial_t) \begin{pmatrix} \varphi \\ \psi \end{pmatrix}. \end{aligned}$$

Using the bounds of Lemma 2.5 for the complete potential operator $\mathcal{W}(s)$, the bound (2.71) for the error operator $\mathcal{E}_h(s)$, in combination with (A.3) (with $\kappa = 2$ and $\kappa = 4$ respectively) yields that their time-dependent counterparts extend to well-posed bounded operators on the spaces stated there. Further using the embedding $H^1(0,T;H) \subset C([0,T],H)$, which holds for any Hilbert space H, we obtain the following error bound for the spatial semi-discretization

$$\begin{aligned} &\max_{0\leq t\leq T} \left\| \begin{pmatrix} p_h(t) \\ \boldsymbol{v}_h(t) \end{pmatrix} - \begin{pmatrix} p(t) \\ \boldsymbol{v}(t) \end{pmatrix} \right\|_{H^1(\Omega)\times \boldsymbol{H}(\mathrm{div},\Omega)} \\ &\leq C \left\| \begin{pmatrix} p_h \\ \boldsymbol{v}_h \end{pmatrix} - \begin{pmatrix} p \\ \boldsymbol{v} \end{pmatrix} \right\|_{\boldsymbol{H}^1_0(0,T;H^1(\Omega)\times \boldsymbol{H}(\mathrm{div},\Omega))} \qquad (2.75) \\ &\leq c_T \left\| \mathcal{E}_h(\partial_t) \begin{pmatrix} \varphi \\ \psi \end{pmatrix} \right\|_{H^3_0(0,T;X_h\times V_h)} \leq C_T \left(h^{k+1/2} + \delta^{1/2} h^k \right) \left\| \begin{pmatrix} \varphi \\ \psi \end{pmatrix} \right\|_{H^7_0(0,T;H^{k+1}(\Gamma)^2)}. \qquad (2.76) \end{aligned}$$

Repeating the argument with the pointwise bounds away from the boundary given by Lemmas 2.11 and 2.12 instead of Lemma 2.5, yields the analogous result

$$\begin{aligned} &\max_{0\leq t\leq T} \left\| \begin{pmatrix} p_h(t) \\ \boldsymbol{v}_h(t) \end{pmatrix} - \begin{pmatrix} p(t) \\ \boldsymbol{v}(t) \end{pmatrix} \right\|_{C^1(\overline{\Omega}_d)\times \boldsymbol{C}^1(\overline{\Omega}_d)} \\ &\qquad \leq C_T \left(h^{k+1/2} + \delta^{1/2} h^k \right) \left\| \begin{pmatrix} \varphi \\ \psi \end{pmatrix} \right\|_{H^8_0(0,T;H^{k+1}(\Gamma)^2)}. \end{aligned} \tag{2.77}$$

An identical bound holds for any point evaluation $\boldsymbol{x} \in \Omega$.

(c) *(Error of the full discretization).* We decompose the total error into the differences

$$\begin{pmatrix} p_h^n \\ v_h^n \end{pmatrix} - \begin{pmatrix} p^n \\ v^n \end{pmatrix} \quad + \quad \begin{pmatrix} p^n \\ v^n \end{pmatrix} - \begin{pmatrix} p(t_n) \\ v(t_n) \end{pmatrix}.$$

The second summand of the above expression is the error of the temporal semi-discretization, bounded by the stated orders in their respective norms in Proposition 2.1. Our focus is therefore on the first difference, which is rewritten by the operators introduced in the first part of this proof via

$$\begin{aligned} \mathcal{W}(\partial_t^\tau)\mathcal{E}_h(\partial_t^\tau)\begin{pmatrix} \varphi \\ \psi \end{pmatrix} = \left(\mathcal{W}(\partial_t^\tau)\mathcal{E}_h(\partial_t^\tau)\begin{pmatrix} \varphi \\ \psi \end{pmatrix} - \mathcal{W}(\partial_t)\mathcal{E}_h(\partial_t)\begin{pmatrix} \varphi \\ \psi \end{pmatrix}\right) \\ + \ \mathcal{W}(\partial_t)\mathcal{E}_h(\partial_t)\begin{pmatrix} \varphi \\ \psi \end{pmatrix}. \end{aligned}$$

The summand in the last row is the error of the spatial semi-discretization and therefore bounded in the part (b) by (2.75).

The remaining difference written on the right-hand side is a defect due to the convolution quadrature method, which is accessible by the general approximation result of Lemma B.1. The established bounds on $\mathcal{W}(s)\mathcal{E}_h(s)$ ensure that the approximation property of Lemma B.1 holds with the constants $M_\sigma \leq C_\sigma h^{k+1}$, $\kappa = 6$ and $\nu = 3$.

Choosing $q = 2$ and $r = 10 > 2q - 1 + \kappa$, gives a convergence in time of order $\min(2q - 1, q + 1 - \kappa + \nu) = q - 2 = 0$. The error term is therefore shown to be of the overall order $\mathcal{O}(h^{k+1/2} + \delta^{1/2}h^k)$ in the $H^1(\Omega) \times \boldsymbol{H}(\mathrm{div}, \Omega)$-norm. Combining the defects yields overall the stated $\mathcal{O}(\tau^{m-1/2} + h^{k+1/2} + \delta^{1/2}h^k)$ error bound in the $H^1(\Omega) \times \boldsymbol{H}(\mathrm{div}, \Omega)$ norm.

We turn our attention towards the full-order error bound away from the boundary. To derive full-order error bounds for points away from the boundary, we rewrite the total error by

$$\begin{pmatrix} p_h^n \\ v_h^n \end{pmatrix} - \begin{pmatrix} p_h(t_n) \\ v_h(t_n) \end{pmatrix} \quad + \quad \begin{pmatrix} p_h(t_n) \\ v_h(t_n) \end{pmatrix} - \begin{pmatrix} p(t_n) \\ v(t_n) \end{pmatrix}.$$

Contrasting the argument structure before, the second difference is now the error of the spatial semi-discretization studied in part (b). The remaining first difference is a convolution quadrature defect for the transfer operator $U_h(s)$ of (2.73). For points away from the boundary, this operator decays exponentially in terms of the real part of s, which leads to favourable convergence properties of the convolution quadrature scheme. In particular, stronger convergence bounds are obtained by rewriting the remaining error as

$$\begin{pmatrix} p_h^n \\ v_h^n \end{pmatrix} - \begin{pmatrix} p_h(t_n) \\ v_h(t_n) \end{pmatrix} = \left[\left(U_h(\partial_t^\tau)g^{\mathrm{inc}}\right)^{n-1}\right]_m - U_h(\partial_t)g^{\mathrm{inc}}(t_n),$$

which is bounded by the full classical order through Lemma B.1, by employing the exponentially decaying bounds from Lemmas 2.11–2.13.

□

The proof of the above theorem further implies the following corollary, in which a convergence result is formulated for the boundary densities, namely the boundary data of the numerical solution. The concrete result is given by following the arguments of the previous proof, where the complete operator (2.73) simplifies to $L_h(s)$.

Corollary 2.1. *Consider the setting and assumptions of Theorem 2.5. The following error bounds hold for the approximations $\varphi_h^n = \big[(\varphi_h^\tau)^{n-1}\big]_m$ and $\psi_h^n = \big[(\psi_h^\tau)^{n-1}\big]_m$ in time and space at $t_n = n\tau \in [0,T]$*

$$\begin{aligned}\left\| \begin{pmatrix} \varphi_h^n - \varphi(t_n) \\ \psi_h^n - \psi(t_n) \end{pmatrix} \right\|_{H^{-1/2}(\Gamma)\times V} &\leq C\big(\tau^m + h^{k+1/2} + \delta^{1/2} h^k\big) && \text{Lemma 2.1,} \\ &\leq C\big(\tau^m + h^{k+1/2} + \delta^{-1/2} h^{k+1}\big) && \text{Lemma 2.2,} \\ &\leq C\big(\tau^m + h^{k+1/2}\big) && \text{Lemma 2.3.}\end{aligned}$$

The constant C in the error bounds depend on the final time T, on the boundary Γ, on the incident waves through g^{inc} and on higher Sobolev norms of the exact solution (φ, ψ), but are independent of h,n and τ. For the transfer operators (1.4)–(1.7), C is independent of the small parameter δ.

Remark 2.5 (Convergence of the inverted formulation for strongly absorbing boundary conditions)**.** *For the strongly absorbing boundary condition of Lemma 2.2, the convergence results predict an unfavourable dependence on the parameter δ for the numerical approximation defined through the full discretized boundary integral equation (2.66). This difficulty is circumvented by instead using the full discretization of the inverted formulation as sketched in Section 2.4.2 in the time-harmonic domain, whose temporal full discretization reads*

$$\left\langle \begin{pmatrix} v_h \\ \xi_h \end{pmatrix}, A^-(\partial_t^\tau) \begin{pmatrix} \varphi_-^{\tau,h} \\ \psi_-^{\tau,h} \end{pmatrix} \right\rangle_\Gamma = \langle v_h, g_-^{\mathrm{inc}} \rangle_\Gamma \qquad \text{for all } \ (v_h, \xi_h) \in (X_h \times V_h)^m, \tag{2.78}$$

where $A^-(s) : V \times H^{1/2}(\Gamma) \to V' \times H^{-1/2}(\Gamma)$ is the operator family described in (2.48), with $Z(s) = \delta^{-1} s^{1/2}$. Following the proof of Theorem 2.5, in particular with the bound (2.50), then analogously gives the following result, in the setting and under the assumptions of Theorem 2.5.

The numerical approximations obtained by inserting $(\varphi_-^{\tau,h}, \psi_-^{\tau,h})$ into the discrete representation formulas (2.67)–(2.68) are denoted by $p_-^{n,h} = \big[(p_-^{\tau,h})^{n-1}\big]_m$ and $\boldsymbol{v}_-^{n,h} = \big[(\boldsymbol{v}_-^{\tau,h}\big]_m$ at the time $t_n = n\tau \in [0,T]$. Then, in the case of the transfer operator described in Lemma 2.2 corresponding to the boundary condition (1.6), we have the following error bound

$$\left\| \begin{pmatrix} p_-^{n,h} - p(t_n) \\ \boldsymbol{v}_-^{n,h} - \boldsymbol{v}(t_n) \end{pmatrix} \right\|_{H^1(\Omega)\times \boldsymbol{H}(\mathrm{div},\Omega)} \leq C\big(\tau^{m-1/2} + h^{k+1/2}\big).$$

As before, for the domain $\Omega_d = \{x \in \Omega \,:\, \mathrm{dist}(x,\Gamma) > d\}$ with $d > 0$, a corresponding bound of the

full classical order $2m-1$ *in time holds:*

$$\left\| \begin{pmatrix} p_-^{n,h} - p(t_n) \\ \boldsymbol{v}_-^{n,h} - \boldsymbol{v}(t_n) \end{pmatrix} \right\|_{H^1(\Omega_d)\times \boldsymbol{H}(\mathrm{div},\Omega_d)} + \left\| \begin{pmatrix} p_-^{n,h} - p(t_n) \\ \boldsymbol{v}_-^{n,h} - \boldsymbol{v}(t_n) \end{pmatrix} \right\|_{C^1(\overline{\Omega}_d)\times \boldsymbol{C}^1(\overline{\Omega}_d)}$$
$$\leq C_d\big(\tau^{2m-1} + h^{k+1/2}\big).$$

The constants C *and* C_d *are subject to the same dependencies as the error constants in Theorem 2.5 and crucially independent of the parameter* δ*.*

2.8. Numerical experiments

We conclude our investigations into the acoustic scattering with some practical computations. All numerical experiments in this section were conducted using continuous piecewise linear boundary element functions for V_h and discontinuous piecewise constant boundary element functions for X_h. For the time discretization, the convolution quadrature method based on the Radau-IIA Runge–Kutta method with 2- and 3-stages is used. With these choices, the experiments of the original work [15], which were conducted with multistep based convolution quadratures and a coupling of continuous linear elements, are repeated here. The convolution quadrature weights are approximated via the trapezoidal rule over a complex contour, as discussed in the original paper [51] and in C.10. The boundary integral operators are realized by the C++ library Bempp (see [68]), which provides a Python interface. The implementation that has been used for these experiments is available under [56].

2.8.1. Spherically symmetric scattering: an example with an accurate reference solution

We begin with the scattering from a sphere, namely we choose Ω to be the exterior of the unit sphere. The interaction of a spherically symmetric incident wave p^{inc}, given by the expression

$$p^{\mathrm{inc}}(\boldsymbol{x},t) = \frac{e^{-5(|\boldsymbol{x}|-(3-t))^2}}{|\boldsymbol{x}|},$$

is observed on the time interval $[0,4]$. Constant functions on the sphere are eigenfunctions of all the boundary operators and are further eigenfunctions of the time-harmonic transfer operators described in Lemmas 2.1–2.3. Consequently, the scattered wave p and the corresponding boundary densities (φ,ψ) is therefore constant on the unit sphere, i.e. itself spherically symmetric. The relation between the traces of scattered field on the boundary Γ and evaluations of p in the domain Ω then simplifies to the identity

$$p(\boldsymbol{x},t) = \frac{1}{|\boldsymbol{x}|}p(\boldsymbol{y},t-(|\boldsymbol{x}|-1)) = \frac{1}{|\boldsymbol{x}|}\psi(\boldsymbol{y},t-(|\boldsymbol{x}|-1)), \qquad \text{for all } |\boldsymbol{y}|=1. \tag{2.79}$$

Furthermore, the boundary integral equation (2.52) simplifies in this fully spherically symmetric case. Through eliminating φ in (2.52) we obtain

$$(L(\partial_t) + Z(\partial_t))\,\psi = -Z(\partial_t)p^{\mathrm{inc}} + \gamma_\nu v^{\mathrm{inc}}, \tag{2.80}$$

where the operator in the first summand is, up to a differentiation in time, the temporal exterior Dirichlet-to-Neumann operator. The corresponding operator family in the frequency domain is therefore the scaled exterior Dirichlet-to-Neumann operator, namely

$$L(s) = W(s) - (\frac{1}{2}I - K^T(s))V(s)^{-1}(\frac{1}{2}I - K(s)) = -s^{-1}\mathrm{DtN}(s). \tag{2.81}$$

Since this operator is a composition of the boundary operators, constant functions remain eigenfunctions of this operator family. Moreover, the corresponding eigenvalue is given by

$$L(s)\widehat{\psi} = \left(1 + \frac{1}{s}\right)\widehat{\psi}. \tag{2.82}$$

More details on spherical harmonics for the boundary operators associated with the Helmholtz problem are found in [54]. With this identity, the boundary integral equation (2.80) simplifies to a temporal convolution equation, which is computationally cheap to solve with a fine time step size. For the present computation, a reference density ψ^{ref} was computed with $N = 2^{14}$ steps by employing the convolution quadrature method based on the 3-stage Radau IIA Runge–Kutta method. The reference solution is then evaluated at an arbitrary point $\boldsymbol{P} \in \Omega$ away from the sphere through (2.79). As the boundary condition, we employ the strongly absorbing boundary condition (1.7), with $\delta = 10^{-2}$.

Since pointwise error bounds are predicted by Theorem 2.5, the numerical approximations are compared to the reference solution away from the boundary, which was set to $\boldsymbol{P} = (2, 0, 0)$ for our computations. The error computed here is the maximum error in time, namely

$$\max_{0 \le n \le N} \left| p_h^\tau(\boldsymbol{P}, t_n) - p^{\mathrm{ref}}(\boldsymbol{P}, t_n) \right|.$$

Mutually fixing h and τ respectively then gives the convergence plots of Figures 2.1–2.2, by varying the mesh sizes $h_j = 2^{-j}$ for $j = 0, \ldots, 4$ and the number of time steps $N_j = 2^j$ for $j = 4, \ldots, 11$. As the time discretization, the convolution quadrature method based on the 2-stage Radau IIA Runge–Kutta method is employed.

Throughout the thesis, the effects of boundary approximation are neglected. Despite these additional pertubations in the numerical scheme, the predicted convergence rates of Theorem 2.5 accurately describe the error behaviour of the method, indicating that the neglected error terms are of higher order. For small τ and h, the error curves flatten out as expected, since the space- or time-discretization error respectively becomes the leading part in the full discretization error.

The formulation of the inverted boundary condition (2.78)

The convergence plots were repeated for to the inverted formulation of the boundary integral equation, as described in Remark 2.5. All parameters have been chosen to coincide with the previous experiments, to compare the two schemes (2.66) and (2.78). The small parameter $\delta = 10^{-2}$ has an unfavourable dependence on the error bounds of the numerical approximation defined by (2.66) and a favourable dependence on the error bounds of the numerical approximation defined by (2.78). This numerical experiment reveals that the methods are practically identical, as their convergence plots Figures 2.3–2.4 essentially coincide with the original convergence plots in Figures 2.1–2.2. The unfavourable dependence with respect to δ in the error bounds for the strongly absorbing boundary conditions (1.6)–(1.7) therefore seems to be an artifact of the analysis and not an inherent property of the method, at least in the present setting.

2.8.2. Scattering of a plane wave from a halfpipe for different boundary conditions

Consider a halfpipe shape with a length of 1, a width of 0.5 and a height of 0.5 (as seen from above in Figures 2.5–2.6), embedded in a homogeneous medium. An incoming planar wave, initially almost vanishing on the boundary, traverses the free space and interacts with the boundary condition enforced at the scatterer. The present computations are conducted with the closed form of the planar incoming wave

$$p^{\mathrm{inc}}(x,t) = e^{-100(\boldsymbol{x}\cdot\boldsymbol{a}-(t-t_0))^2},$$

where the parameters $t_0 = 1$ and $\boldsymbol{a} = (0,-1,0)$ are chosen. The interaction of the wave with the scatterer is then observed until the final time $T = 5$.

Three different generalized impedance boundary conditions are employed at the surface and visualized in the columns of Figure 2.5–2.6:

- The thin-layer boundary condition (1.4) with $\delta = 0.1$
- The strongly absorbing boundary condition (1.6) with $\delta = 0.1$
- The acoustic boundary condition (1.8) with $m = \alpha = k = 1$

The surface of the scatterer is approximated by a triangulation containing around 10^3 nodes, on which the same boundary element spaces as in the previous experiment are employed. For the time discretization, the convolution quadrature method based on the 3-stage Radau IIA Runge–Kutta multistage method is used with $N = 200$ steps.

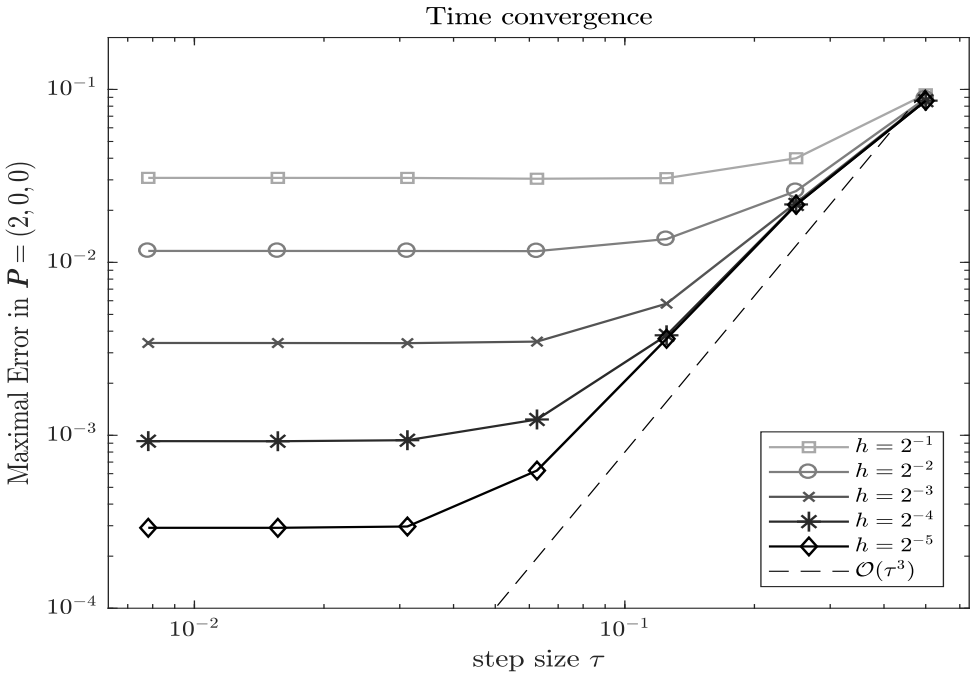

Figure 2.1.: Time convergence plot for the full discretization (2.66) with the 2-stage Radau IIA Runge–Kutta method.

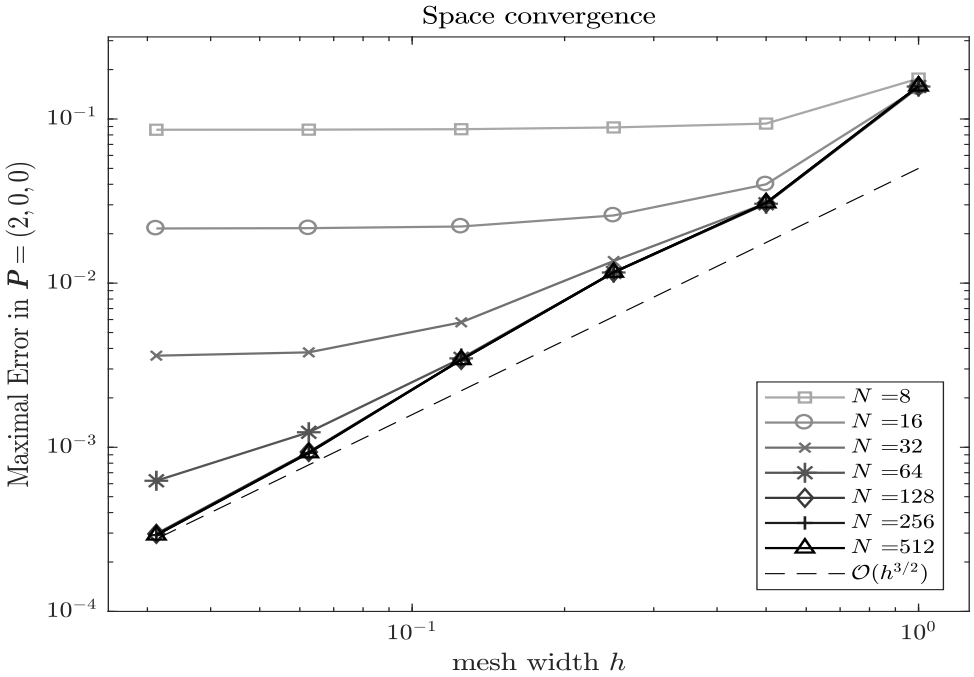

Figure 2.2.: Space convergence plot for the full discretization (2.66), based on the boundary element method with piecewise linear continuous boundary elements and piecewise constant discontinuous boundary elements.

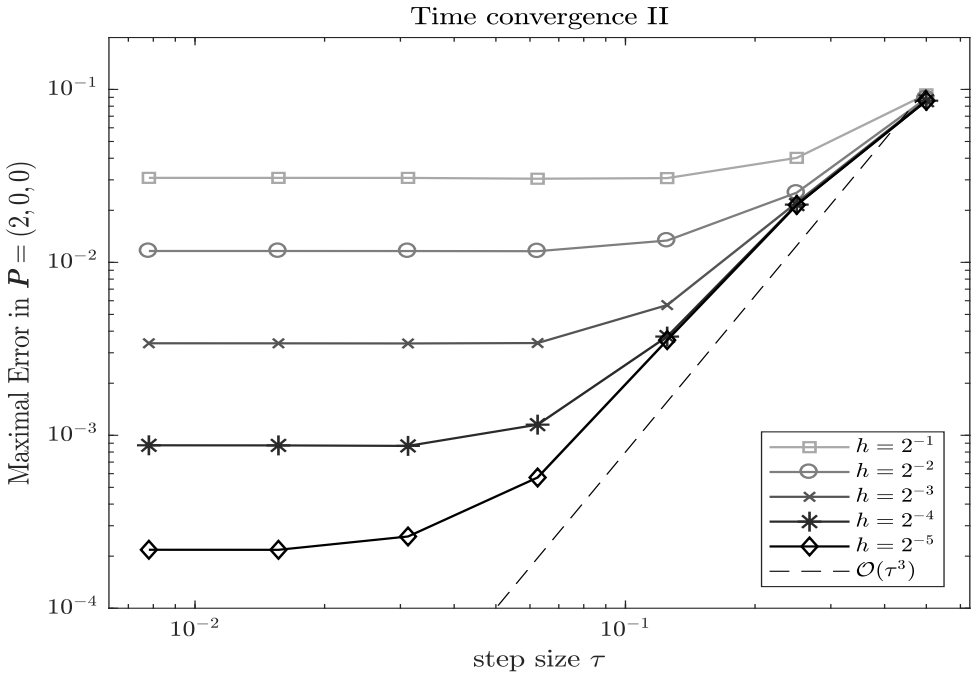

Figure 2.3.: Time convergence plot for the alternative full discretization (2.78), based on the 2-stage Radau IIA Runge–Kutta method.

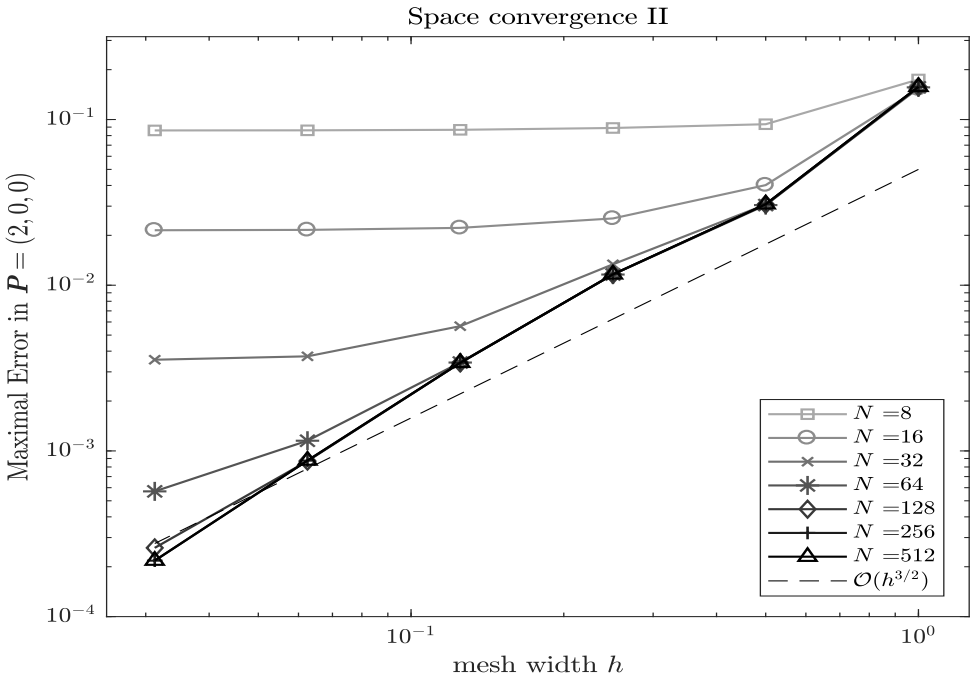

Figure 2.4.: Space convergence plot for the alternative full discretization (2.78), based on the boundary element method with piecewise linear continuous boundary elements and piecewise constant discontinuous boundary elements.

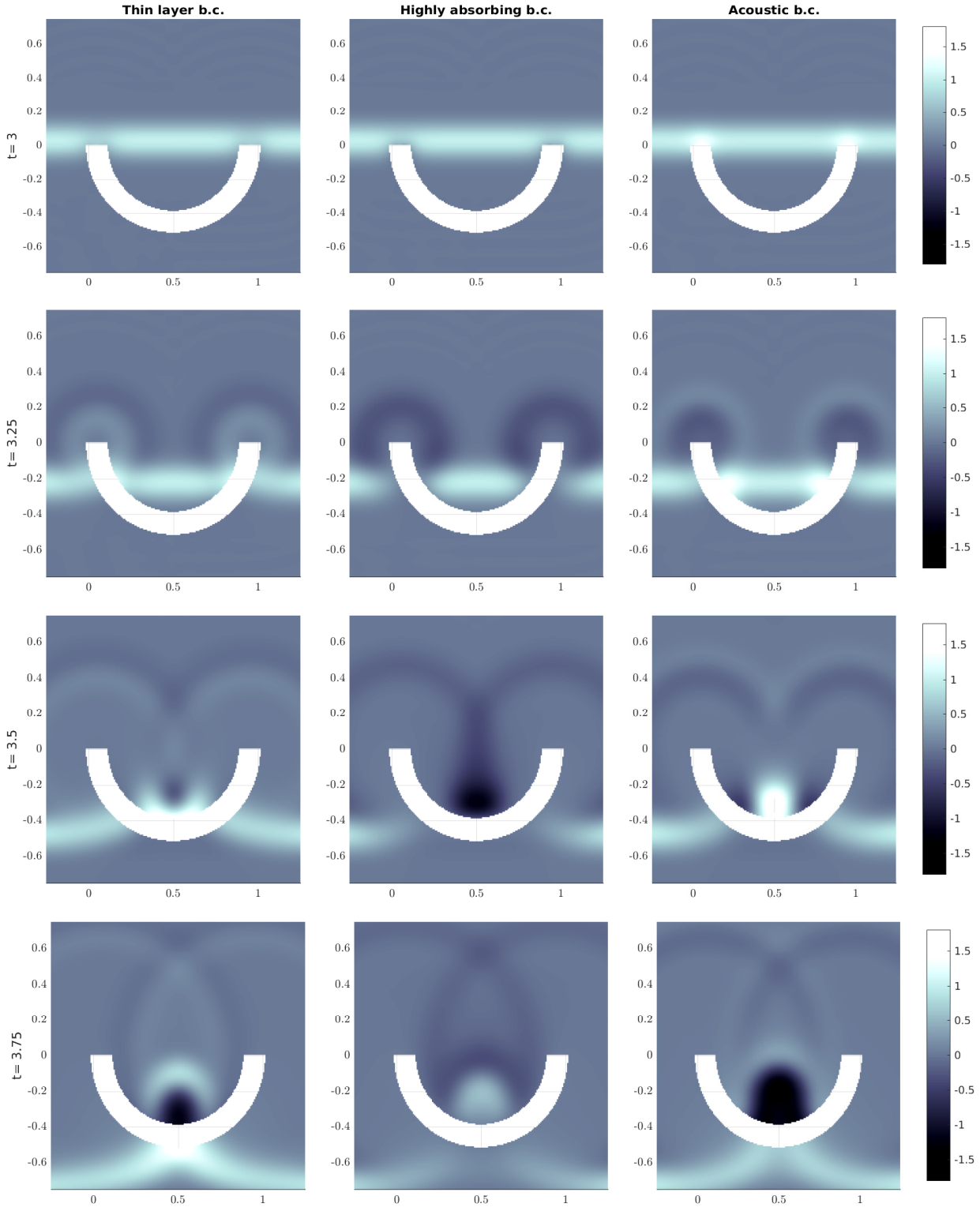

Figure 2.5.: Several boundary conditions, employed at the described halfpipe scatterer, interact with an incoming plane wave. Shown is the plane $x_3 = 0.25$, the middle of the scatterer, at several time points.

Figure 2.6.: Several boundary conditions, employed at the described halfpipe scatterer, interact with an incoming plane wave. Shown is the plane $x_3 = 0.25$, the middle of the scatterer, at several time points.

3. Electromagnetic scattering from generalized impedance boundary conditions

Electromagnetic scattering theory is a natural topic of interest, as a large class of practical applications fo the theory of wave scattering is found in the context of electromagnetic phenomena. The sections of this chapter are set up in parallel to the previous chapter to highlight the similarities of acoustic and electromagnetic phenomena. Technical details and proofs vary, but nevertheless lead to several analogous theorems, through which the qualitative similarity of the phenomena will become apparent.

A fitting point to start this chapter is the problem setting, formulated in its strong form. Let $\left(\boldsymbol{E}^{\text{inc}}, \boldsymbol{H}^{\text{inc}}\right)$ be an incident electromagnetic wave, which is assumed to solve the time-dependent Maxwell's equations on $\mathbb{R}^3$. The initial support of the incident wave is assumed to be away from the boundary Γ and fully in the exterior domain Ω. The objective of this chapter is to compute and investigate the scattered fields $\boldsymbol{E} = \boldsymbol{E}^{\text{tot}} - \boldsymbol{E}^{\text{inc}}$ and $\boldsymbol{H} = \boldsymbol{H}^{\text{tot}} - \boldsymbol{H}^{\text{inc}}$, which together are an outgoing solution to Maxwell's equations and ensure that the total electromagnetic fields fulfill the specified boundary conditions. The *electric field* $\boldsymbol{E}$ and the *magnetic field* $\boldsymbol{H}$ therefore solve the following initial boundary value problem of Maxwell's equations:

$$\partial_t \boldsymbol{E} - \mathbf{curl}\, \boldsymbol{H} = 0 \qquad \text{in} \quad \Omega, \tag{3.1}$$

$$\partial_t \boldsymbol{H} + \mathbf{curl}\, \boldsymbol{E} = 0 \qquad \text{in} \quad \Omega, \tag{3.2}$$

$$\boldsymbol{E}_T + \boldsymbol{Z}(\partial_t)\,(\boldsymbol{H} \times \boldsymbol{\nu}) = \boldsymbol{g}^{\text{inc}} \quad \text{on} \quad \Gamma, \tag{3.3}$$

where the tangential component of the electric field $\boldsymbol{E}$ is denoted by $\boldsymbol{E}_T$, and given through the expression $\boldsymbol{E}_T = (\boldsymbol{I} - \boldsymbol{\nu}\boldsymbol{\nu}^\top)\boldsymbol{E} = -(\boldsymbol{E} \times \boldsymbol{\nu}) \times \boldsymbol{\nu}$. The right-hand side on the boundary condition is completely determined by the incident waves and takes the form

$$\boldsymbol{g}^{\text{inc}} = -\left(\boldsymbol{E}_T^{\text{inc}} + \boldsymbol{Z}(\partial_t)(\boldsymbol{H}^{\text{inc}} \times \boldsymbol{\nu})\right) \quad \text{on } \Gamma. \tag{3.4}$$

Since the initial support of the incident waves is away from the boundary, we further impose vanishing initial values at $t = 0$ in Ω for the electromagnetic scattered fields $\boldsymbol{E}$ and $\boldsymbol{H}$.

3.1. Tangential trace, trace space X_Γ and a further Hilbert space $V_\Gamma \subset X_\Gamma$

The *tangential trace* is the key quantity in the electromagnetic boundary conditions of interest and defined, for a continuous vector field $v : \overline{\Omega} \to \mathbb{C}^3$, by the expression

$$\gamma_T v = v|_\Gamma \times \nu \qquad \text{on } \Gamma,$$

where the exterior unit surface normal is denoted by ν and is pointing into the exterior domain Ω. The field $v|_\Gamma$ can either be understood as the restriction of the field v to the boundary Γ, or its tangential component, which is given by projecting v into the tangent space via $v_T = (I - \nu\nu^\top)v|_\Gamma = -(\gamma_T v) \times \nu$.

A key identity of the present analysis is Green's formula for the **curl** operator. For sufficiently regular vector fields $u, v : \overline{\Omega} \to \mathbb{C}^3$, it reads

$$\int_\Omega (\mathbf{curl}\, u \cdot v - u \cdot \mathbf{curl}\, v)\, \mathrm{d}x = \int_\Gamma (\gamma_T u \times \nu) \cdot \gamma_T v \, \mathrm{d}x, \tag{3.5}$$

where the dot $\cdot$ denotes again the Euclidean inner product (1.1). The right-hand side in this formulation is already slightly rewritten from the original Green's formula (compare for example in contrast [26, Section 2.1]), which is attributed to the identity

$$\int_\Gamma (\gamma_T u \times \nu) \cdot \gamma_T v \, \mathrm{d}x = \int_\Gamma (u|_\Gamma \times \nu) \cdot v|_\Gamma \, \mathrm{d}x.$$

A rigorous definition for Green's formula on Lipschitz domains is given and derived in [24]. Either way, the right-hand side of Green's formula for the **curl** operator defines a skew-hermitian sesquilinear form for continuous tangential vector fields on the boundary, which is denoted for $\phi, \psi : \Gamma \to \mathbb{C}^3$ by

$$[\phi, \psi]_\Gamma = \int_\Gamma (\phi \times \nu) \cdot \psi \, \mathrm{d}x. \tag{3.6}$$

We turn our attention towards the functional analytic setting of the tangential trace operator γ_T. The natural Sobolev space describing the spatial regularity of electromagnetic fields in the domain Ω is $H(\mathbf{curl}, \Omega)$, namely

$$H(\mathbf{curl}, \Omega) = \{v \in L^2(\Omega) \,:\, \mathbf{curl}\, v \in L^2(\Omega)\}.$$

The tangential trace extends to a continuous operator from $H(\mathbf{curl}, \Omega)$ into an appropriate trace space X_Γ. This Hilbert space, which is also referred to as the proper trace space, is equipped with an appropriate norm $\|\cdot\|_{X_\Gamma}$.

In the following, the definition of this space is roughly sketched, following the original works from Alonso & Valli [2] for smooth domains and Buffa, Costabel & Sheen [25] for Lipschitz domains. We further refer the reader to the surveys [26, Sect. 2.2] and [54, Sect. 5.4].

For the real positive order $r \geq 0$, we define the Hilbert space

$$\boldsymbol{H}^r_\times(\Gamma) = \gamma_T \left(\boldsymbol{H}^{r+1/2}(\Omega) \right).$$

These spaces are subspaces of the tangential $\boldsymbol{L}^2(\Gamma)$ space, which is defined by

$$\boldsymbol{L}^2_T(\Gamma) = \left\{ \boldsymbol{\phi} \in \boldsymbol{L}^2(\Gamma) \mid \boldsymbol{\phi} \cdot \boldsymbol{\nu} = 0 \right\}.$$

This space, equipped with its natural scalar product $(\cdot,\cdot)_\Gamma$, serves as an appropriate pivot space such that with the dense embedding $\boldsymbol{H}^r_\times(\Gamma) \subset \boldsymbol{L}^2_T(\Gamma)$, we have the set of inclusions

$$\boldsymbol{H}^r_\times(\Gamma) \subset \boldsymbol{L}^2_T(\Gamma) \subset \boldsymbol{H}^{-r}_\times(\Gamma),$$

where $\boldsymbol{H}^{-r}_\times(\Gamma)$ denotes the dual space to $\boldsymbol{H}^r_\times(\Gamma)$, where the dual pairing is chosen to coincide with the scalar product installed on the pivot space $\boldsymbol{L}^2_T(\Gamma)$. Finally, we have the necessary spaces in place to give a definition of the proper trace space, which reads

$$\boldsymbol{X}_\Gamma = \{ \boldsymbol{\phi} \in \boldsymbol{H}^{-1/2}_\times(\Gamma) \mid \operatorname{div}_\Gamma \boldsymbol{\phi} \in H^{-1/2}(\Gamma) \}.$$

The norms associated to the spaces $\boldsymbol{H}^r_\times(\Gamma)$ are rather convoluted and their specific forms do not enter in our analysis. For curvilinear polyhedra, a specific form of the norm $\|\cdot\|_{\boldsymbol{H}^{1/2}_\times}$ has been given in [24]. Nevertheless, the associated norm to the trace space enters in the analysis and is denoted by $\|\cdot\|_{\boldsymbol{X}_\Gamma}$. Subsequent sections naturally yield computationally useful characterizations of this norm, by leveraging boundary operators arising in the context of time-harmonic Maxwell's equations.

With this notation in place, the tangential trace extends to a bounded surjective operator (see [25, Theorem 4.1])

$$\gamma_T : \boldsymbol{H}(\mathbf{curl}, \Omega) \to \boldsymbol{X}_\Gamma.$$

The anti-symmetric pairing (3.6) extends to a non-degenerate continuous bilinear form on the trace space $\boldsymbol{X}_\Gamma$, which renders it to be its own dual [23, Theorem 2]. In other words, the dual of $\boldsymbol{X}_\Gamma$ is itself, with the skew-symmetric form acting as the dual pairing.

A further Hilbert space is required for the treatment of the generalized impedance boundary conditions, which must be reconciled with the above setting of traces of Maxwell's equations. Consider a dense subspace of the trace space $\boldsymbol{V}_\Gamma \subset \boldsymbol{X}_\Gamma$, assumed to be equipped with a (semi-)norm $|\cdot|_{\boldsymbol{V}_\Gamma}$, which naturally equips the space with the full norm

$$\|\boldsymbol{\phi}\|^2_{\boldsymbol{V}_\Gamma} = \|\boldsymbol{\phi}\|^2_{\boldsymbol{X}_\Gamma} + |\boldsymbol{\phi}|^2_{\boldsymbol{V}_\Gamma}. \tag{3.7}$$

3.1.1. Setting of the impedance operator

The subspace $\boldsymbol{V}_\Gamma$ is tailored to the impedance operator, such that the underlying analytic family of time-harmonic impedance operators $\boldsymbol{Z}(s)$ extends to linear operators on these spaces. In particular, the operator norm of the weakly formulated impedance operator must be polyno-

mially bounded in terms of the frequency in the following way: for every positive $\sigma > 0$, there exists a positive constant $C_\sigma < \infty$ such that

$$\|\boldsymbol{Z}(s)\|_{\boldsymbol{V}_\Gamma' \leftarrow \boldsymbol{V}_\Gamma} \leq C_\sigma \, |s|^\kappa, \qquad \operatorname{Re} s \geq \sigma > 0. \tag{3.8}$$

Throughout this chapter we always have $\kappa \leq 1$, and for convenience we assume this (inessential) bound of κ in the following. The operator family $\boldsymbol{Z}$ is assumed to be of *positive type*: for every $\sigma > \sigma_0 \geq 0$, there exists $c_\sigma > 0$ such that the following bound from below holds

$$\operatorname{Re}\langle \boldsymbol{\phi}, \boldsymbol{Z}(s)\boldsymbol{\phi}\rangle_\Gamma \geq c_\sigma \operatorname{Re} s \, |s^{-1}\boldsymbol{\phi}|^2_{\boldsymbol{V}_\Gamma} \quad \text{for all } \boldsymbol{\phi} \in \boldsymbol{V}_\Gamma \text{ and } \operatorname{Re} s \geq \sigma > \sigma_0, \tag{3.9}$$

where the anti-duality between $\boldsymbol{V}_\Gamma$ and $\boldsymbol{V}_\Gamma{}'$ is the extended $\boldsymbol{L}^2$-pairing and denoted by $\langle \cdot, \cdot \rangle_\Gamma$. The conditions imposed here are very close to the setting of the acoustic impedance operator discussed in the previous chapter.

3.2. The impedance operators (1.13)–(1.16)

The impedance operators formulated in the introduction are special cases of the abstract framework above, which is shown in the following lemmas.

In addition to the Sobolev space of tangential, square integrable vector fields $\boldsymbol{L}^2_T(\Gamma)$, we introduce the additional vector space

$$\boldsymbol{H}(\operatorname{div}_\Gamma, \Gamma) = \{\boldsymbol{\phi} \in \boldsymbol{L}^2_T(\Gamma) \, : \, \operatorname{div}_\Gamma \boldsymbol{\phi} \in L^2(\Gamma)\}.$$

Lemma 3.1 (Thin coating)**.** *The impedance operator is well-posed and positive on the space*

$$\boldsymbol{V}_\Gamma = \boldsymbol{X}_\Gamma \cap \boldsymbol{H}(\operatorname{div}_\Gamma, \Gamma),$$

which is equipped with the following δ-dependent semi-norm

$$|\boldsymbol{\phi}|^2_{\boldsymbol{V}_\Gamma} = \delta\big(\|\boldsymbol{\phi}\|^2_{\boldsymbol{L}^2(\Gamma)} + \|\operatorname{div}_\Gamma \boldsymbol{\phi}\|^2_{L^2(\Gamma)}\big).$$

The above expression is a complete norm, but the semi-norm notation is nevertheless used to differentiate the term from the full norm, as defined via (3.7). The impedance operator $\boldsymbol{Z}(s) : \boldsymbol{V}_\Gamma \to \boldsymbol{V}_\Gamma{}'$ corresponding to the thin layer boundary conditions (1.13) and (1.14) then satisfy the bound (3.8) with $\kappa = 1$ and the positivity condition (3.9), with C_σ and $c_\sigma > 0$ independent of the small parameter δ. For the second-order boundary condition (1.14), the expressions $1 + \delta\,(\mathcal{H} - \mathcal{C})$ and $1 - \delta\mathcal{H}$ are assumed to be bounded from below by a positive constant, which is always achieved for small enough δ on sufficiently regular boundaries Γ. With this assumption, we further have $\sigma_0 = 0$ in the positivity assumption (3.9).

Proof. We restrict the proof to (1.13), as the extension to (1.14) is straightforward. The physical constants describing the material of the thin layer ε^δ and μ^δ are assumed to be positive and constant on the whole boundary. To simplify the terms in this proof, we simply show the

stated properties for the transfer operator

$$\boldsymbol{Z}(s) = \delta\big(s - s^{-1}\nabla_\Gamma \operatorname{div}_\Gamma\big),$$

where the material constants have been set to one. The anti-duality between $\boldsymbol{V}_\Gamma$ and $\boldsymbol{V}_\Gamma{}'$ is obtained by testing the above expression by some test function of appropriate regularity in the $\boldsymbol{L}^2$-pairing and applying Green's formula. Consequently, the anti-duality is to be understood as follows: for $\boldsymbol{\phi}, \boldsymbol{\psi} \in \boldsymbol{V}_\Gamma$ we write

$$\langle \boldsymbol{\phi}, \boldsymbol{Z}(s)\boldsymbol{\psi}\rangle_\Gamma = \delta s\big(\boldsymbol{\phi}, \boldsymbol{\psi}\big)_\Gamma + \delta s^{-1}\big(\operatorname{div}_\Gamma \boldsymbol{\phi}, \operatorname{div}_\Gamma \boldsymbol{\psi}\big)_\Gamma, \tag{3.10}$$

where the round brackets denote the L^2 inner product on the surface, taken anti-linear in the first argument. This expression fulfills, with the notation $m(|s|) = \max(|s|, |s|^{-1})$, the following chain of estimates

$$\begin{aligned}
|\langle \boldsymbol{\phi}, \boldsymbol{Z}(s)\boldsymbol{\psi}\rangle_\Gamma| &\le m(|s|)\,\delta\big(\|\boldsymbol{\phi}\|_{\boldsymbol{L}^2(\Gamma)}\,\|\boldsymbol{\psi}\|_{\boldsymbol{L}^2(\Gamma)} + \|\operatorname{div}_\Gamma \boldsymbol{\phi}\|_{L^2(\Gamma)}\,\|\operatorname{div}_\Gamma \boldsymbol{\psi}\|_{L^2(\Gamma)}\big)\\
&\le m(|s|)\,\delta\big(\|\boldsymbol{\phi}\|_{\boldsymbol{L}^2(\Gamma)} + \|\operatorname{div}_\Gamma \boldsymbol{\phi}\|_{L^2(\Gamma)}\big)\big(\|\boldsymbol{\psi}\|_{\boldsymbol{L}^2(\Gamma)} + \|\operatorname{div}_\Gamma \boldsymbol{\psi}\|_{L^2(\Gamma)}\big)\\
&\le 2\,m(|s|)\,|\boldsymbol{\phi}|_{\boldsymbol{V}_\Gamma}\,|\boldsymbol{\psi}|_{\boldsymbol{V}_\Gamma}\\
&\le 2\,m(|s|)\,\|\boldsymbol{\phi}\|_{\boldsymbol{V}_\Gamma}\,\|\boldsymbol{\psi}\|_{\boldsymbol{V}_\Gamma}.
\end{aligned}$$

In particular, we obtain the polynomial bound (3.8) with $\kappa = 1$. Furthermore, by setting $\boldsymbol{\phi} = \boldsymbol{\psi}$ and for all $\operatorname{Re} s \ge \sigma > 0$, we obtain the following bound from below

$$\begin{aligned}
\operatorname{Re}\langle \boldsymbol{\phi}, \boldsymbol{Z}(s)\boldsymbol{\phi}\rangle_\Gamma &= \delta\,(\operatorname{Re} s)\,\|\boldsymbol{\phi}\|^2_{\boldsymbol{L}^2(\Gamma)} + \delta\,\frac{\operatorname{Re} s}{|s|^2}\,\|\operatorname{div}_\Gamma \boldsymbol{\phi}\|^2_{L^2(\Gamma)}\\
&\ge \delta(\operatorname{Re} s)\sigma^2\|s^{-1}\boldsymbol{\phi}\|^2_{\boldsymbol{L}^2(\Gamma)} + \delta(\operatorname{Re} s)\|s^{-1}\operatorname{div}_\Gamma \boldsymbol{\phi}\|^2_{L^2(\Gamma)}\\
&\ge \min(\sigma^2, 1)\,(\operatorname{Re} s)\,|s^{-1}\boldsymbol{\phi}|^2_{\boldsymbol{V}_\Gamma},
\end{aligned}$$

which yields (3.9). □

Lemma 3.2 (Highly conductive obstacle)**.** *By setting $\boldsymbol{V}_\Gamma = \boldsymbol{X}_\Gamma \cap \boldsymbol{L}^2(\Gamma)$ and, in (3.7), the weighted norm*

$$|\boldsymbol{\phi}|^2_{\boldsymbol{V}_\Gamma} = \delta\|\boldsymbol{\phi}\|^2_{\boldsymbol{L}^2(\Gamma)},$$

the impedance operators (1.15) and (1.16) become well-posed operators $Z(s) : \boldsymbol{V}_\Gamma \to \boldsymbol{V}_\Gamma{}'$ for $\operatorname{Re} s > 0$, which further satisfy the bound (3.8) with $\kappa = 1/2$ and the positivity condition (3.9), with M_σ and $c_\sigma > 0$ independent of the small parameter δ. In the case of (1.15), we further have $\sigma_0 = 0$ in the positivity property (3.9). For (1.16), the positivity of (3.9) is still obtained with $\sigma_0 = \max(0, 2\mu\delta C_\Gamma)^2$, with the constant $C_\Gamma = \sup_{x\in\Gamma}(\mathcal{H}(\boldsymbol{x}) - \mathcal{C}(\boldsymbol{x}))$, which is finite for sufficiently regular Γ.

Proof. We restrict the presentation of the result to the first-order boundary condition (1.15), as the proof for (1.16) is a straightforward extension. In that case, the transfer operator is

$$\boldsymbol{Z}(s) = \delta\, s^{1/2},$$

for which the anti-duality between $\boldsymbol{V}_\Gamma$ and $\boldsymbol{V}_\Gamma{}'$ is defined for $\boldsymbol{\phi}, \boldsymbol{\psi} \in \boldsymbol{V}_\Gamma$, as the weighted L^2-pairing

$$\langle \boldsymbol{\phi}, \boldsymbol{Z}(s)\boldsymbol{\psi}\rangle_\Gamma = \delta s^{1/2}(\boldsymbol{\phi}, \boldsymbol{\psi})_\Gamma. \tag{3.11}$$

As a direct consequence of the Cauchy–Schwarz inequality, we obtain

$$|\langle \boldsymbol{\phi}, \boldsymbol{Z}(s)\boldsymbol{\phi}\rangle_\Gamma| \leq |s|^{1/2}\|\boldsymbol{\phi}\|_{\boldsymbol{V}_\Gamma}\|\boldsymbol{\phi}\|_{\boldsymbol{V}_\Gamma},$$

which gives the polynomial bound (3.8) with the order $\kappa = 1/2$. The positivity is directly obtained by the following chain of inequalities from below, which for $\operatorname{Re} s \geq \sigma > 0$ read

$$\operatorname{Re}\langle \boldsymbol{\phi}, \boldsymbol{Z}(s)\boldsymbol{\phi}\rangle_\Gamma \geq \delta(\operatorname{Re} s^{1/2})\,\|\boldsymbol{\phi}\|^2_{\boldsymbol{L}^2(\Gamma)} \geq \sigma^{3/2}(\operatorname{Re} s)|s^{-1}\boldsymbol{\phi}|^2_{\boldsymbol{V}_\Gamma},$$

which yields (3.9).

The polynomial bound for (1.16) follows in the same way as before. For the positivity, we use the estimate

$$\begin{aligned}\operatorname{Re}\langle \boldsymbol{\phi}, \boldsymbol{Z}(s)\boldsymbol{\phi}\rangle_\Gamma &= \operatorname{Re}\left(\delta s^{1/2}(\boldsymbol{\phi}, \boldsymbol{\phi})_\Gamma - \delta^2\mu(\boldsymbol{\phi}, (\mathcal{H}-\mathcal{C})\boldsymbol{\phi})_\Gamma\right)\\ &\geq \operatorname{Re}\left(s^{1/2} - \delta\mu C_\Gamma\right)|s|^2\,|s^{-1}\boldsymbol{\phi}|^2_{\boldsymbol{V}_\Gamma} \geq \operatorname{Re} s\frac{\sigma^{3/2}}{2}|s^{-1}\boldsymbol{\phi}|^2_{\boldsymbol{V}_\Gamma},\end{aligned}$$

where the last inequality holds for $\operatorname{Re} s^{1/2} \geq 2\delta\mu C_\Gamma$, with the constant C_Γ purely determined by the boundary through $C_\Gamma = \sup_{\boldsymbol{x}\in\Gamma}(\mathcal{H}(\boldsymbol{x}) - \mathcal{C}(\boldsymbol{x}))$. This assumptions alway holds under the condition $\operatorname{Re} s \geq \sigma_0 = \max(0, 2\mu\delta C_\Gamma)^2$. □

3.2.1. Weak formulation of the generalized impedance boundary condition

The choice of the anti-duality is not as clear as in the acoustic context. We clarify the role of the two dual pairings, respectively on $\boldsymbol{X}_\Gamma$ and $\boldsymbol{V}_\Gamma$, by deriving a weak formulation of the boundary condition (3.3). Assuming sufficient regularity of the boundary traces and taking the $\boldsymbol{L}^2(\Gamma)$ inner product $(\cdot,\cdot)_\Gamma$ with an arbitrary continuous tangential vector field $\boldsymbol{\phi}$ on Γ yields the intermediate formulation

$$(\boldsymbol{\phi}, \boldsymbol{E}_T)_\Gamma + (\boldsymbol{\phi}, \boldsymbol{Z}(\partial_t)\gamma_T\boldsymbol{H})_\Gamma = (\boldsymbol{\phi}, \boldsymbol{g}^{\mathrm{inc}})_\Gamma. \tag{3.12}$$

In the following, we rearrange this boundary condition to purely depend on the tangential traces of the electromagnetic fields.

For vector fields $\boldsymbol{E}$ with well-defined tangential traces, we employ the pointwise identity $\boldsymbol{E}_T \times \boldsymbol{\nu} = \boldsymbol{E} \times \boldsymbol{\nu} = \gamma_T\boldsymbol{E}$ to obtain the following identity with regards to the bilinear forms

$$(\boldsymbol{\phi}, \boldsymbol{E}_T)_\Gamma = (\boldsymbol{\phi} \times \boldsymbol{\nu}, \boldsymbol{E}_T \times \boldsymbol{\nu})_\Gamma = (\boldsymbol{\phi} \times \boldsymbol{\nu}, \gamma_T\boldsymbol{E})_\Gamma = [\boldsymbol{\phi}, \gamma_T\boldsymbol{E}]_\Gamma,$$

where the right-hand side is the anti-symmetric pairing (3.6). Through the strong formulation of the temporal convolution operator $\boldsymbol{Z}(\partial_t)$, which in general includes surface differential operators, the analytic family of weak operator $\boldsymbol{Z}(s) : \boldsymbol{V}_\Gamma \to \boldsymbol{V}_\Gamma{}'$ is constructed.

The duality then coincides with the $\boldsymbol{L}^2(\Gamma)$ inner product when restricted to tangential vector fields $\gamma_T \boldsymbol{H}$ of sufficient regularity:

$$\langle \boldsymbol{v}, \boldsymbol{Z}(\partial_t)\gamma_T \boldsymbol{H}\rangle_\Gamma = (\boldsymbol{v}, \boldsymbol{Z}(\partial_t)\gamma_T \boldsymbol{H})_\Gamma, \qquad \boldsymbol{v} \in \boldsymbol{V}_\Gamma.$$

The previous lemmas provided precisely this treatment for the concrete examples (1.13)–(1.16) in (3.10) and (3.11). Analogously, the tangential vector field $\boldsymbol{g}^{\mathrm{inc}}$ is understood as an element in the dual $\boldsymbol{V}_\Gamma{}'$, by association with the following functional on $\boldsymbol{V}_\Gamma$

$$\langle \boldsymbol{v}, \boldsymbol{g}^{\mathrm{inc}}\rangle_\Gamma = (\boldsymbol{v}, \boldsymbol{g}^{\mathrm{inc}})_\Gamma, \qquad \boldsymbol{v} \in \boldsymbol{V}_\Gamma.$$

These identities and the tested boundary condition (3.12) yield the *weak formulation of the boundary condition* (3.3): find $\boldsymbol{E}, \boldsymbol{H} \in \boldsymbol{L}^2(0,T;\boldsymbol{H}(\mathbf{curl},\Omega)) \cap \boldsymbol{H}^1(0,T;\boldsymbol{L}^2(\Omega))$, solutions to the time-dependent Maxwell's equations with vanishing initial conditions, such that their tangential traces $\gamma_T \boldsymbol{E} \in \boldsymbol{L}^2(0,T;\boldsymbol{X}_\Gamma)$ and $\gamma_T \boldsymbol{H} \in \boldsymbol{H}^\kappa_0(0,T;\boldsymbol{V}_\Gamma)$, with κ from (3.8) fulfill for almost every $t \in (0,T)$

$$[\boldsymbol{v}, \gamma_T \boldsymbol{E}]_\Gamma + \langle \boldsymbol{v}, \boldsymbol{Z}(\partial_t)\gamma_T \boldsymbol{H}\rangle_\Gamma = \langle \boldsymbol{v}, \boldsymbol{g}^{\mathrm{inc}}\rangle_\Gamma \qquad \text{for all } \boldsymbol{v} \in \boldsymbol{V}_\Gamma. \tag{3.13}$$

This weak formulation thus weakly enforces a relation between the tangential traces of the electromagnetic fields $\boldsymbol{E}$ and $\boldsymbol{H}$. All expressions on both sides are finite under the stated regularity assumptions on $\gamma_T \boldsymbol{E}, \gamma_T \boldsymbol{H}$ and $\boldsymbol{g}^{\mathrm{inc}}$.

The above formulation is well-posed in the stated regularities if $\boldsymbol{g}^{\mathrm{inc}}$ is sufficiently differentiable in time, namely $\boldsymbol{g}^{\mathrm{inc}} \in \boldsymbol{H}^3_0(0,T;\boldsymbol{V}_\Gamma{}')$. In the case of general positive κ, the necessary temporal regularity scales accordingly with $\boldsymbol{g}^{\mathrm{inc}} \in \boldsymbol{H}^{2+\kappa}_0(0,T;\boldsymbol{V}_\Gamma{}')$. The subsequent two sections will be devoted to proof a well-posedness and stability result in the stated Hilbert spaces. Techniques and arguments that are developed in the process of the stability analysis will later be crucial in the analysis of the applied numerical methods.

3.3. Time-harmonic Maxwell's equations

As before in the acoustic chapter, we will turn to the time-harmonic problem, which is structurally simpler and offers valuable insights in the time-dependent problem of interest. In contrast to classical theory, we study a range of frequencies, in particular on a complete complex half space.

The *time-harmonic Maxwell's equations* read, for $s \in \mathbb{C}$ with $\operatorname{Re} s > 0$,

$$s\widehat{\boldsymbol{E}} - \mathbf{curl}\,\widehat{\boldsymbol{H}} = 0 \quad \text{in } \Omega, \tag{3.14}$$

$$s\widehat{\boldsymbol{H}} + \mathbf{curl}\,\widehat{\boldsymbol{E}} = 0 \quad \text{in } \Omega. \tag{3.15}$$

These equations are completed with asymptotic conditions for $|\boldsymbol{x}| \to \infty$, to ensure that the scattered wave is an outgoing wave. Solutions constructed through the representation formula automatically satisfy these conditions. The imposed conditions ensure that the strong solutions decay sufficiently fast for the fields to fulfill $\widehat{\boldsymbol{E}}, \widehat{\boldsymbol{H}} \in \boldsymbol{H}(\mathbf{curl},\Omega)$.

We briefly sketch the structure of this section. Starting from the fundamental solution and potential operators, representation formulas for the time-harmonic Maxwell's equations are presented. Through these formulas, the relation between the solution fields $\widehat{\boldsymbol{E}}$ and $\widehat{\boldsymbol{H}}$ and their tangential traces become apparent.

The representation formulas sit at the heart of our analysis and a series of lemmas is devoted to thoroughly investigate their properties. Essential estimates, which are explicit in s for $\operatorname{Re} s > 0$, are shown for operators in the context of the time-harmonic Maxwell's equations.

Based on the representation formulas, boundary integral equations for the tangential traces of $\widehat{\boldsymbol{E}}$ and $\widehat{\boldsymbol{H}}$ fulfilling the time-harmonic generalized impedance boundary conditions are derived. Well-posedness results and s-explicit bounds are shown in appropriate norms. As a consequence of the representation formulas, the time-harmonic scattering problem with the associated generalized impedance boundary conditions is shown to be well-posed and a stability result with s-explicit bounds is given.

These results, obtained for all frequencies on a complex half space, then yield the well-posedness of the time-dependent scattering problem in the subsequent Section 3.5. The specific powers from the s-explicit bounds further take a crucial role in the subsequent error analysis.

3.3.1. Recap: Potential operators and representation formulas

The following subsection describes the basic terminology and standard notions that are used in the context of time-harmonic Maxwell's equations. As such, these results are not original and can be found, with more details, in the survey [26] and the reference [54]. The fundamental solution of the time-harmonic Maxwell's equations reads

$$G(s, \boldsymbol{x}) = \frac{e^{-s|\boldsymbol{x}|}}{4\pi\,|\boldsymbol{x}|}, \qquad \operatorname{Re} s > 0,\ \boldsymbol{x} \in \mathbb{R}^3 \setminus \{0\}.$$

The *electromagnetic single layer potential* operator is denoted by $\boldsymbol{\mathcal{S}}(s)$. Applied to a complex-valued boundary function $\boldsymbol{\varphi}$ of sufficient regularity for the expressions to be finite, and evaluated at a point $\boldsymbol{x} \in \mathbb{R}^3 \setminus \Gamma$ away from the boundary, it reads

$$\boldsymbol{\mathcal{S}}(s)\boldsymbol{\varphi}(\boldsymbol{x}) = -s \int_\Gamma G(s, \boldsymbol{x}-\boldsymbol{y})\boldsymbol{\varphi}(\boldsymbol{y})\mathrm{d}\boldsymbol{y} + s^{-1}\nabla \int_\Gamma G(s, \boldsymbol{x}-\boldsymbol{y})\operatorname{div}_\Gamma \boldsymbol{\varphi}(\boldsymbol{y})\mathrm{d}\boldsymbol{y}.$$

The *electromagnetic double layer potential* operator is denoted by $\boldsymbol{\mathcal{D}}(s)$ and is given in the same context by

$$\boldsymbol{\mathcal{D}}(s)\boldsymbol{\varphi}(\boldsymbol{x}) = \mathbf{curl} \int_\Gamma G(s, \boldsymbol{x}-\boldsymbol{y})\boldsymbol{\varphi}(\boldsymbol{y})\mathrm{d}\boldsymbol{y}.$$

By construction, the potential operators fulfill the relations

$$s\boldsymbol{\mathcal{S}}(s) - \mathbf{curl} \circ \boldsymbol{\mathcal{D}}(s) = 0, \qquad s\boldsymbol{\mathcal{D}}(s) + \mathbf{curl} \circ \boldsymbol{\mathcal{S}}(s) = 0. \tag{3.16}$$

For any boundary function $\boldsymbol{\varphi}$ of appropriate regularity, the fields $\widehat{\boldsymbol{E}} = \boldsymbol{\mathcal{S}}(s)\boldsymbol{\varphi}$ and $\widehat{\boldsymbol{H}} = \boldsymbol{\mathcal{D}}(s)\boldsymbol{\varphi}$ solve the time-harmonic Maxwell's equations (3.14)–(3.15) on $\mathbb{R}^3 \setminus \Gamma$. Likewise, due to the inherent anti-symmetry of Maxwell's equations, the same statement holds for the fields $\widehat{\boldsymbol{E}} = \boldsymbol{\mathcal{D}}(s)\boldsymbol{\varphi}$ and $\widehat{\boldsymbol{H}} = -\boldsymbol{\mathcal{S}}(s)\boldsymbol{\varphi}$. Note that without the appropriate rescaling and assumptions on ε and μ, as discussed in the introduction, these constants would enter into the formulas above.

In the previous chapter, transmission problems were the key tool to prove significant results for the time-harmonic problem. In the same way, this section relies heavily on electromagnetic transmission problems, formulated on the whole space $\mathbb{R}^3 \setminus \Gamma$. Jumps and averages for the tangential traces are defined as in the previous chapter by

$$[\boldsymbol{\gamma}_T] = \boldsymbol{\gamma}_T^+ - \boldsymbol{\gamma}_T^-, \qquad \{\boldsymbol{\gamma}_T\} = \tfrac{1}{2}\left(\boldsymbol{\gamma}_T^+ + \boldsymbol{\gamma}_T^-\right).$$

The composition of the jumps with the potential operators reveals the *jump relations*, which read

$$[\boldsymbol{\gamma}_T] \circ \boldsymbol{\mathcal{S}}(s) = 0, \qquad [\boldsymbol{\gamma}_T] \circ \boldsymbol{\mathcal{D}}(s) = -\mathbf{Id}. \tag{3.17}$$

Analogously to the previous chapter, a time-harmonic transmission problem is associated to any pair of boundary densities of appropriate regularity.

The identities (3.16) and the jump relations (3.17) imply that any given boundary densities $(\widehat{\boldsymbol{\varphi}}, \widehat{\boldsymbol{\psi}})$ from the trace space $\boldsymbol{X}_\Gamma \times \boldsymbol{X}_\Gamma$ are associated to electromagnetic fields by

$$\widehat{\boldsymbol{E}} = -\boldsymbol{\mathcal{S}}(s)\widehat{\boldsymbol{\varphi}} + \boldsymbol{\mathcal{D}}(s)\widehat{\boldsymbol{\psi}}, \tag{3.18}$$

$$\widehat{\boldsymbol{H}} = -\boldsymbol{\mathcal{D}}(s)\widehat{\boldsymbol{\varphi}} - \boldsymbol{\mathcal{S}}(s)\,\widehat{\boldsymbol{\psi}}, \tag{3.19}$$

which are fields that solve the transmission problem

$$s\widehat{\boldsymbol{E}} - \mathbf{curl}\,\widehat{\boldsymbol{H}} = 0 \qquad \text{in} \quad \mathbb{R}^3 \setminus \Gamma, \tag{3.20}$$

$$s\widehat{\boldsymbol{H}} + \mathbf{curl}\,\widehat{\boldsymbol{E}} = 0 \qquad \text{in} \quad \mathbb{R}^3 \setminus \Gamma, \tag{3.21}$$

$$[\boldsymbol{\gamma}_T]\widehat{\boldsymbol{H}} = \widehat{\boldsymbol{\varphi}}, \tag{3.22}$$

$$-[\boldsymbol{\gamma}_T]\widehat{\boldsymbol{E}} = \widehat{\boldsymbol{\psi}}. \tag{3.23}$$

Up to this point, this section was restricted to the presentation of established operators and identities, which hold for boundary densities of sufficient regularity. The next section provides bounds in terms of the appropriate norms, which in particular gives a rigorous setting for the previously defined operators.

3.3.2. Transmission problems and boundary operators

The right-hand side of the representation formula, namely the operator associated to the linear map $(\widehat{\boldsymbol{\varphi}}, \widehat{\boldsymbol{\psi}}) \mapsto (\widehat{\boldsymbol{E}}, \widehat{\boldsymbol{H}})$, extends by density to a bounded linear operator from the trace space $\boldsymbol{X}_\Gamma{}^2$ to $\boldsymbol{H}(\mathbf{curl}, \Omega)^2$. The following lemma proves this and further provides an s-explicit bound. A related result can be found in [27, Lemma 6.4].

Lemma 3.3. *Let $(\widehat{\boldsymbol{\varphi}}, \widehat{\boldsymbol{\psi}}) \in \boldsymbol{X}_\Gamma{}^2$ be some complex-valued boundary functions in the trace space. There exist time-harmonic electromagnetic fields $(\widehat{\boldsymbol{E}}, \widehat{\boldsymbol{H}})$, that are defined by the representation formulas (3.18)–(3.19), which solve the transmission problem (3.20)–(3.23) for $\operatorname{Re} s > 0$ and are bounded by*

$$\left\| \begin{pmatrix} \widehat{\boldsymbol{E}} \\ \widehat{\boldsymbol{H}} \end{pmatrix} \right\|_{\boldsymbol{H}(\mathbf{curl}, \mathbb{R}^3 \setminus \Gamma)^2} \leq C_\Gamma \frac{|s|^2 + 1}{\operatorname{Re} s} \left\| \begin{pmatrix} \widehat{\boldsymbol{\varphi}} \\ \widehat{\boldsymbol{\psi}} \end{pmatrix} \right\|_{\boldsymbol{X}_\Gamma{}^2}, \tag{3.24}$$

where the constant $C_\Gamma = \|\{\gamma_T\}\|_{\boldsymbol{X}_\Gamma \leftarrow \boldsymbol{H}(\mathbf{curl}, \mathbb{R}^3 \setminus \Gamma)}$ is the operator norm of the tangential trace operator.

Proof. Inserting solutions of the time-harmonic Maxwell's equations (3.14)–(3.15) into Green's formula (3.5)–(3.6) yields

$$\begin{aligned} \pm \left[\gamma_T^\pm \widehat{\boldsymbol{H}}, \gamma_T^\pm \widehat{\boldsymbol{E}} \right]_\Gamma &= \int_{\Omega^\pm} \left(\mathbf{curl}\, \widehat{\boldsymbol{H}} \cdot \widehat{\boldsymbol{E}} - \widehat{\boldsymbol{H}} \cdot \mathbf{curl}\, \widehat{\boldsymbol{E}} \right) \mathrm{d}\boldsymbol{x} \\ &= \int_{\Omega^\pm} \left(\bar{s} \left| \widehat{\boldsymbol{E}} \right|^2 + s \left| \widehat{\boldsymbol{H}} \right|^2 \right) \mathrm{d}\boldsymbol{x}. \end{aligned} \tag{3.25}$$

Note that $\Omega^\pm$ refers to the inner and exterior domain respectively. The conjugation of the Laplace parameter in the first summand stems from the anti-linearity of the inner product, which has been defined via $\boldsymbol{a} \cdot \boldsymbol{b} = \overline{\boldsymbol{a}}^\top \boldsymbol{b}$ on $\mathbb{C}^3$. Summation of these two terms yields the identity

$$\mathrm{I} := \int_{\mathbb{R}^3 \setminus \Gamma} \bar{s} \left| \widehat{\boldsymbol{E}} \right|^2 + s \left| \widehat{\boldsymbol{H}} \right|^2 \mathrm{d}\boldsymbol{x} = \left[\gamma_T^+ \widehat{\boldsymbol{H}}, \gamma_T^+ \widehat{\boldsymbol{E}} \right]_\Gamma - \left[\gamma_T^- \widehat{\boldsymbol{H}}, \gamma_T^- \widehat{\boldsymbol{E}} \right]_\Gamma. \tag{3.26}$$

Any part of the time-harmonic electromagnetic fields can always be rewritten in terms of each others **curl**, by inserting (3.20) and (3.21) respectively. Using the separation $\mathrm{I} = (1-\theta)\mathrm{I} + \theta\mathrm{I}$ and inserting the time-harmonic Maxwell problem in the second summand reformulates the left-hand side to the expression

$$\begin{aligned} \mathrm{I} = \int_{\mathbb{R}^3 \setminus \Gamma} \Big(&(1-\theta) \bar{s} \left| \widehat{\boldsymbol{E}} \right|^2 + \theta s \left| s^{-1} \mathbf{curl}\, \widehat{\boldsymbol{E}} \right|^2 \\ &+ (1-\theta) s \left| \widehat{\boldsymbol{H}} \right|^2 + \theta \bar{s} \left| s^{-1} \mathbf{curl}\, \widehat{\boldsymbol{H}} \right|^2 \Big) \mathrm{d}\boldsymbol{x}. \end{aligned}$$

Taking the real part on both sides slightly simplifies the right-hand side to

$$\begin{aligned} \operatorname{Re} \mathrm{I} = \operatorname{Re} s \int_{\mathbb{R}^3 \setminus \Gamma} \Big(&(1-\theta) \left| \widehat{\boldsymbol{E}} \right|^2 + \theta \left| s \right|^{-2} \left| \mathbf{curl}\, \widehat{\boldsymbol{E}} \right|^2 \\ &+ (1-\theta) \left| \widehat{\boldsymbol{H}} \right|^2 + \theta \left| s \right|^{-2} \left| \mathbf{curl}\, \widehat{\boldsymbol{H}} \right|^2 \Big) \mathrm{d}\boldsymbol{x}. \end{aligned}$$

The parameter θ is free and chosen in such a way that the preceding factors of the summands agree, which is achieved by setting $1 - \theta = \theta |s|^{-2}$. Rearranging this requirements leads to the choice of $\theta = 1/(1 + |s|^{-2})$. Inserting this particular choice of θ, yields the identity

$$\operatorname{Re} \mathrm{I} = \frac{\operatorname{Re} s}{|s^2| + 1} \left(\|\widehat{\boldsymbol{E}}\|^2_{\boldsymbol{H}(\mathbf{curl}, \mathbb{R}^3 \setminus \Gamma)} + \|\widehat{\boldsymbol{H}}\|^2_{\boldsymbol{H}(\mathbf{curl}, \mathbb{R}^3 \setminus \Gamma)} \right). \tag{3.27}$$

In other words, the real part of the term I constitutes, up to a preceding factor, the left-hand side of the stated bound (3.24). The real part of I is, due to the right-hand side of (3.26), also characterized by

$$\operatorname{Re} \mathrm{I} = \operatorname{Re}\Big(\Big[\gamma_T^+ \widehat{\boldsymbol{H}}, \gamma_T^+ \widehat{\boldsymbol{E}} \Big]_\Gamma - \Big[\gamma_T^- \widehat{\boldsymbol{H}}, \gamma_T^- \widehat{\boldsymbol{E}} \Big]_\Gamma \Big).$$

Rewriting the right-hand side in terms of jumps and averages by summing several mixed terms and using the transmission conditions (3.22)–(3.23) yields

$$\begin{aligned} \operatorname{Re} \mathrm{I} &= \operatorname{Re}\Big(\Big[[\gamma_T] \widehat{\boldsymbol{H}}, \{\gamma_T\} \widehat{\boldsymbol{E}} \Big]_\Gamma + \Big[-[\gamma_T] \widehat{\boldsymbol{E}}, \{\gamma_T\} \widehat{\boldsymbol{H}} \Big]_\Gamma \Big) \\ &= \operatorname{Re}\Big(\Big[\widehat{\boldsymbol{\varphi}}, \{\gamma_T\} \widehat{\boldsymbol{E}} \Big]_\Gamma + \Big[\widehat{\boldsymbol{\psi}}, \{\gamma_T\} \widehat{\boldsymbol{H}} \Big]_\Gamma \Big). \end{aligned} \tag{3.28}$$

The self-duality of $\boldsymbol{X}_\Gamma$ implies a Cauchy–Schwarz type inequality with the corresponding norm and the duality pairing $[\cdot,\cdot]_\Gamma$. Combined with the Cauchy–Schwarz inequality on $\mathbb{R}^2$, this yields

$$\begin{aligned} \operatorname{Re} \mathrm{I} &\leq \|\widehat{\boldsymbol{\varphi}}\|_{\boldsymbol{X}_\Gamma} \|\{\gamma_T\} \widehat{\boldsymbol{E}}\|_{\boldsymbol{X}_\Gamma} + \|\widehat{\boldsymbol{\psi}}\|_{\boldsymbol{X}_\Gamma} \|\{\gamma_T\} \widehat{\boldsymbol{H}}\|_{\boldsymbol{X}_\Gamma} = \begin{pmatrix} \|\widehat{\boldsymbol{\varphi}}\|_{\boldsymbol{X}_\Gamma} \\ \|\widehat{\boldsymbol{\psi}}\|_{\boldsymbol{X}_\Gamma} \end{pmatrix} \cdot \begin{pmatrix} \|\{\gamma_T\} \widehat{\boldsymbol{E}}\|_{\boldsymbol{X}_\Gamma} \\ \|\{\gamma_T\} \widehat{\boldsymbol{H}}\|_{\boldsymbol{X}_\Gamma} \end{pmatrix} \\ &\leq \Big(\|\widehat{\boldsymbol{\varphi}}\|_{\boldsymbol{X}_\Gamma}^2 + \|\widehat{\boldsymbol{\psi}}\|_{\boldsymbol{X}_\Gamma}^2 \Big)^{1/2} \Big(\|\{\gamma_T\} \widehat{\boldsymbol{E}}\|_{\boldsymbol{X}_\Gamma}^2 + \|\{\gamma_T\} \widehat{\boldsymbol{H}}\|_{\boldsymbol{X}_\Gamma}^2 \Big)^{1/2}. \end{aligned}$$

To estimate the second factor of the above expression, we intend to use the bound of the tangential trace $\{\gamma_T\} : \boldsymbol{H}(\mathbf{curl}, \mathbb{R}^3 \setminus \Gamma) \to \boldsymbol{X}_\Gamma$. The time-harmonic electromagnetic fields $\widehat{\boldsymbol{E}}$ and $\widehat{\boldsymbol{H}}$ are in the local Sobolev space $\boldsymbol{H}_{\mathrm{loc}}(\mathbf{curl}, \mathbb{R}^3 \setminus \Gamma)$ (cf. [26]). Moreover, the tangential trace $\{\gamma_T\}$ extends to a bounded operator from $\boldsymbol{H}(\mathbf{curl}, \Omega_\Gamma)$ to $\boldsymbol{X}_\Gamma$, where Ω_Γ is a bounded domain large enough to contain the boundary Γ. Hence, the left-hand side $\operatorname{Re} \mathrm{I}$ is bounded and the electromagnetic fields are in the global Sobolev space $\boldsymbol{H}(\mathbf{curl}, \mathbb{R}^3 \setminus \Gamma)$. With the operator norm of the tangential average $C_\Gamma = \|\{\gamma_T\}\|_{\boldsymbol{X}_\Gamma \leftarrow \boldsymbol{H}(\mathbf{curl}, \mathbb{R}^3 \setminus \Gamma)}$, the right-hand side is therefore bounded via

$$\operatorname{Re} \mathrm{I} \leq C_\Gamma \Big(\|\widehat{\boldsymbol{\varphi}}\|_{\boldsymbol{X}_\Gamma}^2 + \|\widehat{\boldsymbol{\psi}}\|_{\boldsymbol{X}_\Gamma}^2 \Big)^{1/2} \Big(\|\widehat{\boldsymbol{E}}\|_{\boldsymbol{H}(\mathbf{curl}, \mathbb{R}^3 \setminus \Gamma)}^2 + \|\widehat{\boldsymbol{H}}\|_{\boldsymbol{H}(\mathbf{curl}, \mathbb{R}^3 \setminus \Gamma)}^2 \Big)^{1/2}.$$

Inserting (3.27) on the left-hand side and dividing through the second factor on the right-hand side yields the stated bound. □

Setting the boundary densities in Lemma 3.3 successively to zero yields the following result.

Lemma 3.4. *For s with positive real part, the electromagnetic layer potential operators extend by density to a family of bounded linear operators from $\boldsymbol{X}_\Gamma$ to $\boldsymbol{H}(\mathbf{curl}, \mathbb{R}^3 \setminus \Gamma)$. The operator norms fulfill the bounds*

$$\begin{aligned} \|\boldsymbol{\mathcal{S}}(s)\|_{\boldsymbol{H}(\mathbf{curl}, \mathbb{R}^3 \setminus \Gamma) \leftarrow \boldsymbol{X}_\Gamma} &\leq C_\Gamma \frac{|s|^2 + 1}{\operatorname{Re} s}, \\ \|\boldsymbol{\mathcal{D}}(s)\|_{\boldsymbol{H}(\mathbf{curl}, \mathbb{R}^3 \setminus \Gamma) \leftarrow \boldsymbol{X}_\Gamma} &\leq C_\Gamma \frac{|s|^2 + 1}{\operatorname{Re} s}, \end{aligned}$$

where again $C_\Gamma = \|\{\gamma_T\}\|_{\boldsymbol{X}_\Gamma \leftarrow \boldsymbol{H}(\mathbf{curl}, \mathbb{R}^3 \setminus \Gamma)}$.

Consider the transmission problem (3.20)–(3.23), which is fulfilled by any fields defined through the representation formulas. The unknown electromagnetic scattered fields $\widehat{\boldsymbol{E}}, \widehat{\boldsymbol{H}}$ are naturally only defined in the exterior domain $\Omega = \Omega^+$, but can be understood as the solution to a transmission problem by extending the fields by zero into the interior domain Ω^-. Then, their tangential jumps reduce to the exterior tangential traces. Inserting the boundary data of the scattered fields into the representation formulas therefore recovers the scattered fields at any point, namely it holds that

$$\widehat{\boldsymbol{E}} = -\boldsymbol{\mathcal{S}}(s)\big(\gamma_T \widehat{\boldsymbol{H}}\big) + \boldsymbol{\mathcal{D}}(s)\big(-\gamma_T \widehat{\boldsymbol{E}}\big) \quad \text{in } \Omega, \tag{3.29}$$

$$\widehat{\boldsymbol{H}} = -\boldsymbol{\mathcal{D}}(s)\big(\gamma_T \widehat{\boldsymbol{H}}\big) - \boldsymbol{\mathcal{S}}(s)\big(-\gamma_T \widehat{\boldsymbol{E}}\big) \quad \text{in } \Omega. \tag{3.30}$$

Our approach will therefore be, as before, to first determine the tangential traces of interest from the boundary integral equations, and then draw conclusions on the electromagnetic fields in the domain through the representation formulas. This approach accompanies us throughout this thesis, in the context of time-harmonic, time-dependent and time-discrete representation formulas.

The time-harmonic bounds of Lemma 3.3 can be improved when the solution to the transmission problem is zero in one of the domains, a fact that is shown in the next lemma.

Lemma 3.5. *Consider the setting of Lemma 3.3 and assume further that the interior tangential traces of $\widehat{\boldsymbol{E}}$ and $\widehat{\boldsymbol{H}}$ vanish. The jumps then reduce to the boundary data, i.e. $\gamma_T \widehat{\boldsymbol{H}} = \widehat{\boldsymbol{\varphi}}$ and $-\gamma_T \widehat{\boldsymbol{E}} = \widehat{\boldsymbol{\psi}}$. Under these assumptions, the bound of Lemma 3.3 is enhanced to*

$$\left\| \begin{pmatrix} \widehat{\boldsymbol{E}} \\ \widehat{\boldsymbol{H}} \end{pmatrix} \right\|_{\boldsymbol{H}(\mathbf{curl},\Omega)^2} \leq \left(\frac{|s|^2 + 1}{2 \operatorname{Re} s} \right)^{1/2} \left\| \begin{pmatrix} \widehat{\boldsymbol{\varphi}} \\ \widehat{\boldsymbol{\psi}} \end{pmatrix} \right\|_{\boldsymbol{X}_\Gamma{}^2}.$$

Additionally, in terms of the weaker $\boldsymbol{L}^2$-norm we have the bound

$$\left\| \begin{pmatrix} \widehat{\boldsymbol{E}} \\ \widehat{\boldsymbol{H}} \end{pmatrix} \right\|_{\boldsymbol{L}^2(\Omega)^2} \leq \left(\frac{1}{2 \operatorname{Re} s} \right)^{1/2} \left\| \begin{pmatrix} \widehat{\boldsymbol{\varphi}} \\ \widehat{\boldsymbol{\psi}} \end{pmatrix} \right\|_{\boldsymbol{X}_\Gamma{}^2}.$$

Proof. The proof is strictly simpler than the proof of Lemma 3.3, but some of the necessary steps are repeated here for the convenience of the reader. Green's formula implies

$$\int_\Omega \bar{s} \big|\widehat{\boldsymbol{E}}\big|^2 + s \big|\widehat{\boldsymbol{H}}\big|^2 \mathrm{d}\boldsymbol{x} = \left[\gamma_T^+ \widehat{\boldsymbol{H}}, \gamma_T^+ \widehat{\boldsymbol{E}} \right]_\Gamma \leq \|\widehat{\boldsymbol{\varphi}}\|_{\boldsymbol{X}_\Gamma} \|\widehat{\boldsymbol{\psi}}\|_{\boldsymbol{X}_\Gamma}. \tag{3.31}$$

The $\boldsymbol{L}^2$-result is then given by taking the real part, dividing through the constant dependent on s and applying Young's inequality on the right-hand side. The bound for the $\boldsymbol{H}(\mathbf{curl},\Omega)$ norm is obtained by repeating the arguments from (3.26) to (3.27), which yields

$$\frac{\operatorname{Re} s}{|s^2| + 1} \left(\|\widehat{\boldsymbol{E}}\|^2_{\boldsymbol{H}(\mathbf{curl},\Omega)} + \|\widehat{\boldsymbol{H}}\|^2_{\boldsymbol{H}(\mathbf{curl},\Omega)} \right) = \operatorname{Re} s \int_\Omega \big|\widehat{\boldsymbol{E}}\big|^2 + \big|\widehat{\boldsymbol{H}}\big|^2 \mathrm{d}\boldsymbol{x}.$$

□

3.3.3. Time-harmonic boundary operators and the Calderón operator

The composition of the tangential averages with the potential operators defines the electromagnetic *single and double layer boundary operators*, which operate on the trace space $\boldsymbol{X}_\Gamma$ and are defined as

$$\boldsymbol{V}(s) = \{\gamma_T\} \circ \boldsymbol{\mathcal{S}}(s), \qquad \boldsymbol{K}(s) = \{\gamma_T\} \circ \boldsymbol{\mathcal{D}}(s).$$

The *Calderón operator* is a block operator consisting of these boundary operators and has been introduced in the present setting by [46] (note the sign correction from [58]):

$$\boldsymbol{C}(s) = \begin{pmatrix} -\boldsymbol{V}(s) & \boldsymbol{K}(s) \\ -\boldsymbol{K}(s) & -\boldsymbol{V}(s) \end{pmatrix} = \{\gamma_T\} \circ \begin{pmatrix} -\boldsymbol{\mathcal{S}}(s) & \boldsymbol{\mathcal{D}}(s) \\ -\boldsymbol{\mathcal{D}}(s) & -\boldsymbol{\mathcal{S}}(s) \end{pmatrix}, \tag{3.32}$$

where the potential block operator on the right is the representation formula (3.18)–(3.19). Consider outgoing solutions of the time-harmonic Maxwell's equations $\widehat{\boldsymbol{E}}, \widehat{\boldsymbol{H}}$, thus characterized by the representation formulas. The composition of the tangential averages with the representation formulas reveals the jump relations of the Calderón operator (see (3.20)–(3.23)):

$$\boldsymbol{C}(s) \begin{pmatrix} [\gamma_T]\widehat{\boldsymbol{H}} \\ -[\gamma_T]\widehat{\boldsymbol{E}} \end{pmatrix} = \begin{pmatrix} \{\gamma_T\}\widehat{\boldsymbol{E}} \\ \{\gamma_T\}\widehat{\boldsymbol{H}} \end{pmatrix}. \tag{3.33}$$

Since the application of the Calderón operator can be understood as the transition from jumps to averages, we can immediately draw conclusions on the operator through Lemma 3.3 and even more directly through Lemma 3.4.

The following bound on the operator norm improves on previously existing time-harmonic s-explicit bounds of the boundary operators; we refer the reader to [7, Theorem 4.4] and [46, Lemma 2.3] for bounds of the order $O(|s|^2)$.

Lemma 3.6. *For s with positive real part, the Calderón operator is a linear operator family on the trace space $\boldsymbol{C}(s) : {\boldsymbol{X}_\Gamma}^2 \to {\boldsymbol{X}_\Gamma}^2$ and fulfills the bound*

$$\|\boldsymbol{C}(s)\|_{{\boldsymbol{X}_\Gamma}^2 \leftarrow {\boldsymbol{X}_\Gamma}^2} \leq C_\Gamma^2 \frac{|s|^2 + 1}{\operatorname{Re} s}, \tag{3.34}$$

where the constant is the norm of the tangential average $C_\Gamma = \|\{\gamma_T\}\|_{\boldsymbol{X}_\Gamma \leftarrow \boldsymbol{H}(\mathbf{curl}, \mathbb{R}^3 \setminus \Gamma)}$. The identical bound holds for the electromagnetic single and double layer boundary operators, i.e. on the expression $\|\boldsymbol{V}(s)\|_{\boldsymbol{X}_\Gamma \leftarrow \boldsymbol{X}_\Gamma} + \|\boldsymbol{K}(s)\|_{\boldsymbol{X}_\Gamma \leftarrow \boldsymbol{X}_\Gamma}$.

The skew-hermitian pairing $[\cdot, \cdot]_\Gamma$ is notationally extended from $\boldsymbol{X}_\Gamma \times \boldsymbol{X}_\Gamma$ to ${\boldsymbol{X}_\Gamma}^2 \times {\boldsymbol{X}_\Gamma}^2$ in the natural way:

$$\left[\begin{pmatrix} \boldsymbol{\varphi} \\ \boldsymbol{\psi} \end{pmatrix}, \begin{pmatrix} \boldsymbol{v} \\ \boldsymbol{\xi} \end{pmatrix} \right]_\Gamma = [\boldsymbol{\varphi}, \boldsymbol{v}]_\Gamma + [\boldsymbol{\psi}, \boldsymbol{\xi}]_\Gamma.$$

As was shown in [46, Lemma 3.1], the Calderón operator $\boldsymbol{C}(s)$ is positive with respect to this extended skew-symmetric pairing $[\cdot, \cdot]_\Gamma$. The following lemma repeats this key property and

gives a slightly improved formulation, with a simplified s-explicit bound and a restructured proof.

Lemma 3.7 (essentially [46, Lemma 3.1]). *The Calderón operator is of positive type, namely for* $\operatorname{Re} s > 0$, *the following bound holds*

$$\operatorname{Re}\left[\begin{pmatrix}\boldsymbol{\varphi}\\ \boldsymbol{\psi}\end{pmatrix}, \boldsymbol{C}(s)\begin{pmatrix}\boldsymbol{\varphi}\\ \boldsymbol{\psi}\end{pmatrix}\right]_\Gamma \geq \frac{1}{c_\Gamma^2}\frac{\operatorname{Re} s}{|s|^2+1}\left(\|\boldsymbol{\varphi}\|_{\boldsymbol{X}_\Gamma}^2 + \|\boldsymbol{\psi}\|_{\boldsymbol{X}_\Gamma}^2\right) \tag{3.35}$$

for all $(\boldsymbol{\varphi}, \boldsymbol{\psi}) \in {\boldsymbol{X}_\Gamma}^2$. *The constant is the norm of the jump operator associated to the tangential trace, namely* $c_\Gamma = \|[\boldsymbol{\gamma}_T]\|_{\boldsymbol{X}_\Gamma \leftarrow \boldsymbol{H}(\mathbf{curl}, \mathbb{R}^3\setminus\Gamma)}$.

Proof. Consider $(\widehat{\boldsymbol{\varphi}}, \widehat{\boldsymbol{\psi}}) \in {\boldsymbol{X}_\Gamma}^2$ and let the time-harmonic fields $\widehat{\boldsymbol{E}}, \widehat{\boldsymbol{H}} \in \boldsymbol{H}(\mathbf{curl}, \mathbb{R}^3 \setminus \Gamma)$ be given through the representation formula, therefore solving the associated transmission problem of Lemma 3.3. The result is then given by the following chain of inequalities, taken from the proof of [59, Lemma 3.5]

$$\begin{aligned}
&\left\|\begin{pmatrix}\widehat{\boldsymbol{\varphi}}\\ \widehat{\boldsymbol{\psi}}\end{pmatrix}\right\|_{\boldsymbol{X}_\Gamma\times\boldsymbol{X}_\Gamma}^2 = \left\|\begin{pmatrix}[\boldsymbol{\gamma}_T]\widehat{\boldsymbol{H}}\\ -[\boldsymbol{\gamma}_T]\widehat{\boldsymbol{E}}\end{pmatrix}\right\|_{\boldsymbol{X}_\Gamma\times\boldsymbol{X}_\Gamma}^2 && \text{by (3.22)–(3.23)}\\
&\leq c_\Gamma^2\left(\|\widehat{\boldsymbol{H}}\|_{\boldsymbol{H}(\mathbf{curl},\mathbb{R}^3\setminus\Gamma)}^2 + \|\widehat{\boldsymbol{E}}\|_{\boldsymbol{H}(\mathbf{curl},\mathbb{R}^3\setminus\Gamma)}^2\right) && \text{by def. of } c_\Gamma\\
&= c_\Gamma^2\frac{|s|^2+1}{\operatorname{Re} s}\operatorname{Re}\left[\begin{pmatrix}[\boldsymbol{\gamma}_T]\widehat{\boldsymbol{H}}\\ -[\boldsymbol{\gamma}_T]\widehat{\boldsymbol{E}}\end{pmatrix}, \begin{pmatrix}\{\boldsymbol{\gamma}_T\}\widehat{\boldsymbol{E}}\\ \{\boldsymbol{\gamma}_T\}\widehat{\boldsymbol{H}}\end{pmatrix}\right]_\Gamma && \text{by (3.27)–(3.28)}\\
&= c_\Gamma^2\frac{|s|^2+1}{\operatorname{Re} s}\operatorname{Re}\left[\begin{pmatrix}[\boldsymbol{\gamma}_T]\widehat{\boldsymbol{H}}\\ -[\boldsymbol{\gamma}_T]\widehat{\boldsymbol{E}}\end{pmatrix}, \boldsymbol{C}(s)\begin{pmatrix}[\boldsymbol{\gamma}_T]\widehat{\boldsymbol{H}}\\ -[\boldsymbol{\gamma}_T]\widehat{\boldsymbol{E}}\end{pmatrix}\right]_\Gamma && \text{by (3.33)}\\
&= c_\Gamma^2\frac{|s|^2+1}{\operatorname{Re} s}\operatorname{Re}\left[\begin{pmatrix}\widehat{\boldsymbol{\varphi}}\\ \widehat{\boldsymbol{\psi}}\end{pmatrix}, \boldsymbol{C}(s)\begin{pmatrix}\widehat{\boldsymbol{\varphi}}\\ \widehat{\boldsymbol{\psi}}\end{pmatrix}\right]_\Gamma && \text{by (3.22)–(3.23).}
\end{aligned}$$

□

3.4. Boundary integral equation for tangential traces under time-harmonic generalized impedance boundary conditions

The previous results provide a path towards the development of well-posed and stable boundary integral equations for the time-harmonic Maxwell's equations (3.14)–(3.15) for $\operatorname{Re} s > 0$. This section is devoted to the derivation of such equations whose solutions fulfill the weak formulation of the generalized impedance boundary condition (3.13),

$$[\boldsymbol{v}, \boldsymbol{\gamma}_T\widehat{\boldsymbol{E}}]_\Gamma + \langle \boldsymbol{v}, \boldsymbol{Z}(s)\boldsymbol{\gamma}_T\widehat{\boldsymbol{H}}\rangle_\Gamma = \langle \boldsymbol{v}, \widehat{\boldsymbol{g}}^{\mathrm{inc}}\rangle_\Gamma \qquad \text{for all } \boldsymbol{v} \in \boldsymbol{V}_\Gamma, \tag{3.36}$$

where the electromagnetic impedance $\boldsymbol{Z}(s)$ satisfies the described framework (3.8)–(3.9), and the data $\widehat{\boldsymbol{g}}^{\mathrm{inc}}$ on the right-hand side is at least in ${\boldsymbol{V}_\Gamma}'$.

Any solution of the time-harmonic Maxwell's equations formulated on the exterior domain $\Omega = \Omega^+$ is trivially extended to the full space $\mathbb{R}^3 \setminus \Gamma$ by extending the fields by zero inside of the scatterer Ω^-. In that sense, such solutions solve an associated transmission problem in the form of Lemma 3.3. By construction, the inner traces of the extended fields vanish and consequently the jumps and averages reduce to the outer boundary data.

The representation formulas then only depend on the boundary data, as in (3.29)–(3.30). As a consequence, the jump conditions of the Calderón operator (3.33) then reduce to

$$\boldsymbol{C}(s) \begin{pmatrix} \gamma_T \widehat{\boldsymbol{H}} \\ -\gamma_T \widehat{\boldsymbol{E}} \end{pmatrix} = \frac{1}{2} \begin{pmatrix} \gamma_T \widehat{\boldsymbol{E}} \\ \gamma_T \widehat{\boldsymbol{H}} \end{pmatrix}. \tag{3.37}$$

At this point in the previous chapter, the corresponding identity was modified by a skew-symmetric block operator, to eliminate one of the traces on the right-hand side. Analogous to this procedure, we rewrite the above identity by adding a *symmetric* block operator and arrive at

$$\boldsymbol{C}_{\mathrm{imp}}(s) \begin{pmatrix} \gamma_T \widehat{\boldsymbol{H}} \\ -\gamma_T \widehat{\boldsymbol{E}} \end{pmatrix} = \begin{pmatrix} \gamma_T \widehat{\boldsymbol{E}} \\ 0 \end{pmatrix}, \qquad \boldsymbol{C}_{\mathrm{imp}}(s) = \boldsymbol{C}(s) + \begin{pmatrix} 0 & -\frac{1}{2}\mathbf{Id} \\ -\frac{1}{2}\mathbf{Id} & 0 \end{pmatrix}. \tag{3.38}$$

The following notation for the boundary densities is used in the subsequent sections

$$\widehat{\boldsymbol{\varphi}} = \gamma_T \widehat{\boldsymbol{H}}, \qquad \widehat{\boldsymbol{\psi}} = -\gamma_T \widehat{\boldsymbol{E}}. \tag{3.39}$$

Testing both sides with test functions $(\boldsymbol{v}, \boldsymbol{\xi}) \in \boldsymbol{V}_\Gamma \times \boldsymbol{X}_\Gamma$ yields

$$\left[\begin{pmatrix} \boldsymbol{v} \\ \boldsymbol{\xi} \end{pmatrix}, \boldsymbol{C}_{\mathrm{imp}}(s) \begin{pmatrix} \widehat{\boldsymbol{\varphi}} \\ \widehat{\boldsymbol{\psi}} \end{pmatrix} \right]_\Gamma = \left[\boldsymbol{v}, \gamma_T \widehat{\boldsymbol{E}} \right]_\Gamma.$$

The weak formulation of the boundary integral equation is now given by inserting the boundary condition (3.36) on the right-hand side and rearranging the impedance operator to the left-hand side.

Time-harmonic boundary integral equation: *Let* $\operatorname{Re} s > 0$ *and furthermore consider* $\widehat{\boldsymbol{g}}^{\mathrm{inc}} \in \boldsymbol{V}_\Gamma{}'$. *The boundary data* $(\widehat{\boldsymbol{\varphi}}, \widehat{\boldsymbol{\psi}}) \in \boldsymbol{V}_\Gamma \times \boldsymbol{X}_\Gamma$ *weakly solves the time-harmonic boundary integral equations if for all* $(\boldsymbol{v}, \boldsymbol{\xi}) \in \boldsymbol{V}_\Gamma \times \boldsymbol{X}_\Gamma$ *it holds that*

$$\left[\begin{pmatrix} \boldsymbol{v} \\ \boldsymbol{\xi} \end{pmatrix}, \boldsymbol{C}_{\mathrm{imp}}(s) \begin{pmatrix} \widehat{\boldsymbol{\varphi}} \\ \widehat{\boldsymbol{\psi}} \end{pmatrix} \right]_\Gamma + \langle \boldsymbol{v}, \boldsymbol{Z}(s) \widehat{\boldsymbol{\varphi}} \rangle_\Gamma = \langle \boldsymbol{v}, \widehat{\boldsymbol{g}}^{\mathrm{inc}} \rangle_\Gamma. \tag{3.40}$$

The left-hand side of the boundary integral equation is notationally compressed by the analytic operator family $\boldsymbol{A}(s) : \boldsymbol{V}_\Gamma \times \boldsymbol{X}_\Gamma \to \boldsymbol{V}_\Gamma{}' \times \boldsymbol{X}_\Gamma{}'$, namely for all $(\boldsymbol{\varphi}, \boldsymbol{\psi})$ and $(\boldsymbol{v}, \boldsymbol{\xi}) \in \boldsymbol{V}_\Gamma \times \boldsymbol{X}_\Gamma$, we define the evaluation of $\boldsymbol{A}(s)$ via

$$\left\langle \begin{pmatrix} \boldsymbol{v} \\ \boldsymbol{\xi} \end{pmatrix}, \boldsymbol{A}(s) \begin{pmatrix} \boldsymbol{\varphi} \\ \boldsymbol{\psi} \end{pmatrix} \right\rangle_\Gamma = \left[\begin{pmatrix} \boldsymbol{v} \\ \boldsymbol{\xi} \end{pmatrix}, \boldsymbol{C}_{\mathrm{imp}}(s) \begin{pmatrix} \boldsymbol{\varphi} \\ \boldsymbol{\psi} \end{pmatrix} \right]_\Gamma + \langle \boldsymbol{v}, \boldsymbol{Z}(s) \boldsymbol{\varphi} \rangle_\Gamma, \tag{3.41}$$

where the anti-duality between $\boldsymbol{V}_\Gamma \times \boldsymbol{X}_\Gamma$ and $\boldsymbol{V}_\Gamma' \times \boldsymbol{X}_\Gamma'$ on the left-hand side is denoted by $\langle \cdot, \cdot \rangle_\Gamma$.

With this operator family, the boundary integral equation (3.40) condenses to the following formulation: find $(\widehat{\boldsymbol{\varphi}}, \widehat{\boldsymbol{\psi}}) \in \boldsymbol{V}_\Gamma \times \boldsymbol{X}_\Gamma$ such that

$$\left\langle \begin{pmatrix} \boldsymbol{v} \\ \boldsymbol{\xi} \end{pmatrix}, \boldsymbol{A}(s) \begin{pmatrix} \widehat{\boldsymbol{\varphi}} \\ \widehat{\boldsymbol{\psi}} \end{pmatrix} \right\rangle_\Gamma = \langle \boldsymbol{v}, \widehat{\boldsymbol{g}}^{\mathrm{inc}} \rangle_\Gamma \qquad \text{for all } (\boldsymbol{v}, \boldsymbol{\xi}) \in \boldsymbol{V}_\Gamma \times \boldsymbol{X}_\Gamma. \tag{3.42}$$

Even more compactly, the above expression is rewritten as

$$\boldsymbol{A}(s) \begin{pmatrix} \widehat{\boldsymbol{\varphi}} \\ \widehat{\boldsymbol{\psi}} \end{pmatrix} = \begin{pmatrix} \widehat{\boldsymbol{g}}^{\mathrm{inc}} \\ 0 \end{pmatrix}. \tag{3.43}$$

The operator family $\boldsymbol{A}(s)$ associated to the boundary integral equations defined by (3.41) inherits crucial properties of the Calderón operator $\boldsymbol{C}(s)$ and the impedance operator $\boldsymbol{Z}(s)$ respectively. In particular, the boundedness and positivity from Lemma 3.6–3.7 and (3.8)–(3.9) is preserved, as described in the following two lemmas.

Lemma 3.8. *For $\operatorname{Re} s \geq \sigma > 0$, the operator family $\boldsymbol{A}(s) : \boldsymbol{V}_\Gamma \times \boldsymbol{X}_\Gamma \to \boldsymbol{V}_\Gamma' \times \boldsymbol{X}_\Gamma'$ defined by (3.41) satisfies the bound*

$$\|\boldsymbol{A}(s)\|_{\boldsymbol{V}_\Gamma' \times \boldsymbol{X}_\Gamma' \leftarrow \boldsymbol{V}_\Gamma \times \boldsymbol{X}_\Gamma} \leq C_\sigma \frac{|s|^2}{\operatorname{Re} s}.$$

The bounding constant C_σ only depends polynomially on σ^{-1} and on the boundary Γ via the norm of the tangential trace operator, as well as the bounding constant of the transfer operator $\boldsymbol{Z}(s)$.

Proof. The stated bound is a direct consequence of the triangle inequality for operator norms, applied to summands of the boundary integral operator family $\boldsymbol{A}(s)$.

The bound for the Calderón operator $\boldsymbol{C}(s)$ is provided in Lemma 3.6. The required bound is assumed, with some $\kappa \leq 1$, for the transfer operator in (3.8), which leaves only the identity operators $\mathbf{Id}_{\boldsymbol{V}_\Gamma' \leftarrow \boldsymbol{X}_\Gamma}$ and $\mathbf{Id}_{\boldsymbol{X}_\Gamma' \leftarrow \boldsymbol{V}_\Gamma}$ occurring in $\boldsymbol{C}_{\mathrm{imp}}$. These operators are bounded due to the continuous embeddings $\boldsymbol{V}_\Gamma \subset \boldsymbol{X}_\Gamma = \boldsymbol{X}_\Gamma' \subset \boldsymbol{V}_\Gamma'$. □

Lemma 3.9. *The operator family $\boldsymbol{A}(s)$ fulfills the following coercivity property: for $\sigma_0 \geq 0$, the constant of (3.9), and for any $\sigma > \sigma_0$ there exists a constant $c_\sigma > 0$ such that for all $\operatorname{Re} s \geq \sigma$ we have the bound*

$$\operatorname{Re} \left\langle \begin{pmatrix} \boldsymbol{\varphi} \\ \boldsymbol{\psi} \end{pmatrix}, \boldsymbol{A}(s) \begin{pmatrix} \boldsymbol{\varphi} \\ \boldsymbol{\psi} \end{pmatrix} \right\rangle_\Gamma \geq c_\sigma \frac{\operatorname{Re} s}{|s|^2} \left(\|\boldsymbol{\varphi}\|_{\boldsymbol{V}_\Gamma}^2 + \|\boldsymbol{\psi}\|_{\boldsymbol{X}_\Gamma}^2 \right)$$

for all $(\boldsymbol{\varphi}, \boldsymbol{\psi}) \in \boldsymbol{V}_\Gamma \times \boldsymbol{X}_\Gamma$. The constant c_σ is explicitly given by $c_\sigma = \min\left(c_\Gamma^{-2}, c_\sigma^{(\boldsymbol{Z})}\right)$, where c_Γ denotes the operator norm of the tangential trace operator and $c_\sigma^{(\boldsymbol{Z})}$ is the constant from the positivity of the Calderón operator. Consequently, the constant c_σ only depends polynomially on σ^{-1} and on the boundary Γ.

Proof. The shifted Calderón operator $\boldsymbol{C}_{\mathrm{imp}}(s)$ inherits the coercivity property from $\boldsymbol{C}(s)$, since the skew-hermitian bilinear form associated with the shift fulfills

$$\operatorname{Re}\left[\begin{pmatrix}\boldsymbol{\varphi}\\ \boldsymbol{\psi}\end{pmatrix}, \begin{pmatrix}0 & \mathbf{Id}\\ \mathbf{Id} & 0\end{pmatrix}\begin{pmatrix}\boldsymbol{\varphi}\\ \boldsymbol{\psi}\end{pmatrix}\right]_\Gamma = \operatorname{Re}\big([\boldsymbol{\varphi},\boldsymbol{\psi}]_\Gamma + [\boldsymbol{\psi},\boldsymbol{\varphi}]_\Gamma\big) = 0.$$

The coercivity of the Calderón operator from Lemma 3.7 and the corresponding property (3.9) of the transfer operator $\boldsymbol{Z}(s)$ then imply the stated result via

$$\begin{aligned}\operatorname{Re}\left\langle\begin{pmatrix}\boldsymbol{\varphi}\\ \boldsymbol{\psi}\end{pmatrix}, \boldsymbol{A}(s)\begin{pmatrix}\boldsymbol{\varphi}\\ \boldsymbol{\psi}\end{pmatrix}\right\rangle_\Gamma &= \operatorname{Re}\left[\begin{pmatrix}\boldsymbol{\varphi}\\ \boldsymbol{\psi}\end{pmatrix}, \boldsymbol{C}(s)\begin{pmatrix}\boldsymbol{\varphi}\\ \boldsymbol{\psi}\end{pmatrix}\right]_\Gamma + \operatorname{Re}\langle\boldsymbol{\varphi}, \boldsymbol{Z}(s)\boldsymbol{\varphi}\rangle_\Gamma\\ &\geq \frac{1}{c_\Gamma^2}\frac{\operatorname{Re} s}{|s|^2+1}\left(\|\boldsymbol{\varphi}\|_{X_\Gamma}^2 + \|\boldsymbol{\psi}\|_{X_\Gamma}^2\right) + c_\sigma^{(\boldsymbol{Z})}\frac{\operatorname{Re} s}{|s|^2}\,|\boldsymbol{\varphi}|_{V_\Gamma}^2\\ &\geq c_\sigma\frac{\operatorname{Re} s}{|s|^2}\left(\|\boldsymbol{\varphi}\|_{V_\Gamma}^2 + \|\boldsymbol{\psi}\|_{X_\Gamma}^2\right).\end{aligned}$$

□

Applying the previous lemmas to the boundary integral equation yields the following result.

Theorem 3.1 (Well-posedness of the time-harmonic boundary integral equation)**.** *Consider the boundary integral equation (3.42) for some fixed Laplace parameter with* $\operatorname{Re} s \geq \sigma > \sigma_0 \geq 0$*. The boundary integral equation has a unique solution* $(\widehat{\boldsymbol{\varphi}}, \widehat{\boldsymbol{\psi}}) \in \boldsymbol{V}_\Gamma \times \boldsymbol{X}_\Gamma$*, which fulfills*

$$\left\|\begin{pmatrix}\widehat{\boldsymbol{\varphi}}\\ \widehat{\boldsymbol{\psi}}\end{pmatrix}\right\|_{\boldsymbol{V}_\Gamma\times\boldsymbol{X}_\Gamma} \leq C_\sigma\frac{|s|^2}{\operatorname{Re} s}\left\|\widehat{\boldsymbol{g}}^{\mathrm{inc}}\right\|_{\boldsymbol{V}_{\Gamma'}}. \tag{3.44}$$

The constant C_σ *is the reciprocal of the constant from Lemma 3.9 and as such, only depends polynomially on the inverse of* σ *and on the boundary* Γ *through the norm of the tangential trace operator.*

Proof. The bounds of the Lemmas 3.8 and 3.9 provide the conditions for the Lax–Milgram theorem, which show that $\boldsymbol{A}(s)$ is invertible and its well-posed inverse fulfills, for $\operatorname{Re} s \geq \sigma > \sigma_0$, the bound

$$\left\|\boldsymbol{A}(s)^{-1}\right\|_{\boldsymbol{V}_\Gamma\times\boldsymbol{X}_\Gamma\leftarrow\boldsymbol{V}_{\Gamma'}\times\boldsymbol{X}_{\Gamma'}} \leq C_\sigma\frac{|s|^2}{\operatorname{Re} s}. \tag{3.45}$$

Applying this bound to the boundary integral equation yields the stated result. □

Remark 3.1. *In order to give a more concrete bound in terms of the incident wave, whose dependency is described in terms of the rather abstract space* $\boldsymbol{V}_\Gamma{}'$*, we remark the following alternatives.*

The norms chosen in Lemma 3.1 and Lemma 3.2 fulfill the property $\delta^{1/2}\|\boldsymbol{\phi}\|_{\boldsymbol{L}^2(\Gamma)} \leq \|\boldsymbol{\phi}\|_{\boldsymbol{V}_\Gamma}$ *for all*

$\boldsymbol{\phi} \in \boldsymbol{V}_\Gamma$. *Applying this property yields for any tangential vector field* $\widehat{\boldsymbol{g}}^{\mathrm{inc}} \in \boldsymbol{L}^2(\Gamma)$ *the estimate*

$$\begin{aligned}\left\|\widehat{\boldsymbol{g}}^{\mathrm{inc}}\right\|_{\boldsymbol{V}_\Gamma'} &= \sup_{\|\boldsymbol{\phi}\|_{\boldsymbol{V}_\Gamma}=1} \langle \boldsymbol{\phi}, \widehat{\boldsymbol{g}}^{\mathrm{inc}} \rangle_\Gamma = \sup_{\|\boldsymbol{\phi}\|_{\boldsymbol{V}_\Gamma}=1} (\boldsymbol{\phi}, \widehat{\boldsymbol{g}}^{\mathrm{inc}})_\Gamma \\ &\leq \sup_{\|\boldsymbol{\phi}\|_{\boldsymbol{L}^2(\Gamma)} \leq \delta^{-1/2}} (\boldsymbol{\phi}, \widehat{\boldsymbol{g}}^{\mathrm{inc}})_\Gamma = \delta^{-1/2} \left\|\widehat{\boldsymbol{g}}^{\mathrm{inc}}\right\|_{\boldsymbol{L}^2(\Gamma)}.\end{aligned}$$

Since $\|\boldsymbol{\phi}\|_{\boldsymbol{X}_\Gamma} \leq \|\boldsymbol{\phi}\|_{\boldsymbol{V}_\Gamma}$ *for all* $\boldsymbol{\phi} \in \boldsymbol{V}_\Gamma$ *we further have, provided that* $\widehat{\boldsymbol{g}}^{\mathrm{inc}}$ *is in* $\boldsymbol{X}_\Gamma$*, the direct bound*

$$\left\|\widehat{\boldsymbol{g}}^{\mathrm{inc}}\right\|_{\boldsymbol{V}_\Gamma'} \leq \left\|\widehat{\boldsymbol{g}}^{\mathrm{inc}}\right\|_{\boldsymbol{X}_\Gamma}$$

without any dependence on the small parameter δ*. The assumed property* $\widehat{\boldsymbol{g}}^{\mathrm{inc}} \in \boldsymbol{X}_\Gamma$*, where* $\widehat{\boldsymbol{g}}^{\mathrm{inc}}$ *is the expression* $\widehat{\boldsymbol{g}}^{\mathrm{inc}} = -\widehat{\boldsymbol{E}}_T^{\mathrm{inc}} - \boldsymbol{Z}(s)\gamma_T \widehat{\boldsymbol{H}}^{\mathrm{inc}}$*, holds for sufficiently regular fields* $\widehat{\boldsymbol{E}}^{\mathrm{inc}}$ *and* $\widehat{\boldsymbol{H}}^{\mathrm{inc}}$*, for a sufficiently smooth boundary* Γ *and for transfer operators* $\boldsymbol{Z}(s)$ *in the situations of Lemmas 3.1 and 3.2.*

3.4.1. Well-posedness of time-harmonic scattering with generalized impedance boundary conditions

Combining the above properties yields the following result.

Theorem 3.2 (Well-posedness of the time-harmonic scattering problem)**.** *Consider the time-harmonic scattering problem (3.14)–(3.15) completed with the generalized impedance boundary condition (3.36) for* $\operatorname{Re} s \geq \sigma > \sigma_0 \geq 0$*. Let* $\boldsymbol{Z}(s)$ *satisfy the conditions (3.8)–(3.9) and further let* $\widehat{\boldsymbol{g}}^{\mathrm{inc}} \in \boldsymbol{V}_\Gamma'$*.*

(a) The time-harmonic electromagnetic scattering problem has a unique solution $(\widehat{\boldsymbol{E}}, \widehat{\boldsymbol{H}}) \in \boldsymbol{H}(\mathbf{curl}, \Omega)^2$ *characterized by the representation formulas (3.29)–(3.30). The corresponding boundary data is identified by the unique solution to the system of boundary integral equations of Theorem 3.1, through the identity*

$$(\widehat{\boldsymbol{\varphi}}, \widehat{\boldsymbol{\psi}}) = (\gamma_T \widehat{\boldsymbol{H}}, -\gamma_T \widehat{\boldsymbol{E}}) \in \boldsymbol{V}_\Gamma \times \boldsymbol{X}_\Gamma.$$

(b) The time-harmonic electromagnetic fields fulfill

$$\|\widehat{\boldsymbol{E}}\|_{\boldsymbol{H}(\mathbf{curl},\Omega)} + \|\widehat{\boldsymbol{H}}\|_{\boldsymbol{H}(\mathbf{curl},\Omega)} \leq C_\sigma \frac{|s|^3}{(\operatorname{Re} s)^{3/2}} \left\|\widehat{\boldsymbol{g}}^{\mathrm{inc}}\right\|_{\boldsymbol{V}_\Gamma'},$$

where the constant C_σ *only depends polynomially on* σ^{-1} *and on* Γ *through norms of tangential trace operator. In the case of the impedance operators (1.13)–(1.16), the constant is in particular independent of the small parameter* δ *(note Remark 3.1).*

Proof. Theorem 3.1 implies the existence of a unique solution $(\widehat{\boldsymbol{\varphi}}, \widehat{\boldsymbol{\psi}}) \in \boldsymbol{V}_\Gamma \times \boldsymbol{X}_\Gamma$ of the boundary integral equation (3.43), which is bounded by (3.44). Employing the representation formulas (3.18)–(3.19) yields time-harmonic fields $\widehat{\boldsymbol{E}}, \widehat{\boldsymbol{H}} \in \boldsymbol{H}(\mathbf{curl}, \mathbb{R}^3 \setminus \Gamma)$, which by Lemma 3.3 solve the transmission problem (3.20)–(3.23). Furthermore, applying (3.22)–(3.23), which relates $(\widehat{\boldsymbol{\varphi}}, \widehat{\boldsymbol{\psi}})$

by the fields $(\widehat{\boldsymbol{E}}, \widehat{\boldsymbol{H}})$, yields

$$\boldsymbol{C}_{\mathrm{imp}}(s)\begin{pmatrix}\widehat{\boldsymbol{\varphi}}\\ \widehat{\boldsymbol{\psi}}\end{pmatrix} = \boldsymbol{C}(s)\begin{pmatrix}\widehat{\boldsymbol{\varphi}}\\ \widehat{\boldsymbol{\psi}}\end{pmatrix} - \frac{1}{2}\begin{pmatrix}\widehat{\boldsymbol{\psi}}\\ \widehat{\boldsymbol{\varphi}}\end{pmatrix} = \begin{pmatrix}\{\gamma_T\widehat{\boldsymbol{E}}\}\\ \{\gamma_T\widehat{\boldsymbol{H}}\}\end{pmatrix} - \frac{1}{2}\begin{pmatrix}-[\gamma_T\widehat{\boldsymbol{E}}]\\ [\gamma_T\widehat{\boldsymbol{H}}]\end{pmatrix} = \begin{pmatrix}\gamma_T^+\widehat{\boldsymbol{E}}\\ \gamma_T^-\widehat{\boldsymbol{H}}\end{pmatrix}. \tag{3.46}$$

Applying the above identity to the weak formulation of the boundary integral equation (3.40) and setting the test functions successively to zero yields

$$\big[\boldsymbol{v}, \gamma_T^+\widehat{\boldsymbol{E}}\big]_\Gamma + \big\langle \boldsymbol{v}, \boldsymbol{Z}(s)\widehat{\boldsymbol{\varphi}}\big\rangle_\Gamma = \big(\boldsymbol{v}, \widehat{\boldsymbol{g}}^{\mathrm{inc}}\big)_\Gamma \qquad \text{for all } \boldsymbol{v} \in \boldsymbol{V}_\Gamma, \tag{3.47}$$

$$\big[\boldsymbol{\xi}, \gamma_T^-\widehat{\boldsymbol{H}}\big]_\Gamma = 0 \qquad \text{for all } \boldsymbol{\xi} \in \boldsymbol{X}_\Gamma. \tag{3.48}$$

Moreover, the inner magnetic trace $\gamma_T^-\widehat{\boldsymbol{H}}$ vanishes, since the trace space $\boldsymbol{X}_\Gamma$ coincides with its own dual. Consequently, the boundary density reduces to $\widehat{\boldsymbol{\varphi}} = \gamma_T^+\widehat{\boldsymbol{H}}$, implying by (3.47) that the pair $(\widehat{\boldsymbol{E}}, \widehat{\boldsymbol{H}})|_{\Omega^+}$ satisfies the generalized impedance boundary condition (3.36). Applying Green's formula (3.5) in the interior domain Ω^- for the solutions of (3.14)–(3.15) yields

$$\int_{\Omega^-} \bar{s}\big|\widehat{\boldsymbol{E}}\big|^2 + s\big|\widehat{\boldsymbol{H}}\big|^2 \,\mathrm{d}\boldsymbol{x} = -\int_\Gamma (\gamma_T^-\widehat{\boldsymbol{H}} \times \boldsymbol{\nu}) \cdot \gamma_T^-\widehat{\boldsymbol{E}} \,\mathrm{d}\boldsymbol{x} = 0.$$

Taking the real part on both sides gives $\widehat{\boldsymbol{E}}|_{\Omega^-} = \widehat{\boldsymbol{H}}|_{\Omega^-} = 0$ and consequently $\gamma_T^-\widehat{\boldsymbol{E}} = 0$ and $\widehat{\boldsymbol{\psi}} = -\gamma_T^+\widehat{\boldsymbol{E}}$. This completes the proof of part (a).

As the inner traces have been shown to vanish, we have arrived in the situation of Lemma 3.5, which yields the stated bound of (b) in combination with the bound of Theorem 3.1.

□

Remark 3.2. *Applying the $\boldsymbol{L}^2$-bound of Lemma 3.5 yields the alternative $\boldsymbol{L}^2$-bound*

$$\|\widehat{\boldsymbol{E}}\|_{\boldsymbol{L}^2(\Omega)} + \|\widehat{\boldsymbol{H}}\|_{\boldsymbol{L}^2(\Omega)} \leq C_\sigma \frac{|s|^2}{(\operatorname{Re} s)^{3/2}} \left\|\widehat{\boldsymbol{g}}^{\mathrm{inc}}\right\|_{\boldsymbol{V}_\Gamma'}. \tag{3.49}$$

3.4.2. Bounds for the time-harmonic potential operators away from the boundary

As before, point evaluations fulfill a more favourable dependence on s for large real parts of the Laplace parameter s than the established bounds of Lemma 3.4.

The following lemma from [59] gives such a result in the electromagnetic context by generalizing earlier ideas from [7, Theorem 4.4 (c)], which provide similar estimates for smooth domains. The proof of the following lemma addresses the additional technicalities of Lipschitz domains.

Lemma 3.10. *Consider the electromagnetic single and double layer potential operators $\boldsymbol{\mathcal{S}}(s), \boldsymbol{\mathcal{D}}(s)$, evaluated at a point $\boldsymbol{x} \in \mathbb{R}^3 \setminus \Gamma$, away from the boundary with distance $d = \operatorname{dist}(\boldsymbol{x}, \Gamma) > 0$. For all $\sigma > 0$, there exists a constant C_σ depending only on $\sigma, \boldsymbol{x}$ and Γ such that for all $\operatorname{Re} s \geq \sigma$ the following*

bounds hold

$$|(\boldsymbol{\mathcal{S}}(s)\boldsymbol{\varphi})(\boldsymbol{x})| \leq C_\sigma |s|^2 e^{-d\,\mathrm{Re}\,s} \|\boldsymbol{\varphi}\|_{\boldsymbol{X}_\Gamma},$$
$$|(\boldsymbol{\mathcal{D}}(s)\boldsymbol{\varphi})(\boldsymbol{x})| \leq C_\sigma |s|^2 e^{-d\,\mathrm{Re}\,s} \|\boldsymbol{\varphi}\|_{\boldsymbol{X}_\Gamma},$$

for any $\boldsymbol{\varphi} \in \boldsymbol{X}_\Gamma$.

Proof. The j-th unit vector in $\mathbb{R}^3$ is denoted by $\boldsymbol{e}_j$. Furthermore, consider some point away from the boundary $\boldsymbol{x} \in \Omega$ with the distance $d = \mathrm{dist}(\boldsymbol{x}, \Gamma) > 0$. Rewriting and estimating the integral yields

$$\begin{aligned}
\left| \boldsymbol{e}_j \cdot \int_\Gamma G(s, \boldsymbol{x}-\boldsymbol{y}) \boldsymbol{\varphi}(\boldsymbol{y}) \mathrm{d}\boldsymbol{y} \right| &= \left| \int_\Gamma G(s, \boldsymbol{x}-\boldsymbol{y}) \boldsymbol{e}_j \cdot \boldsymbol{\varphi}(\boldsymbol{y}) \mathrm{d}\boldsymbol{y} \right| \\
&= \left| \int_\Gamma G(s, \boldsymbol{x}-\boldsymbol{y}) \left(\boldsymbol{e}_j \times \boldsymbol{\nu}\right) \cdot \left(\boldsymbol{\varphi}(\boldsymbol{y}) \times \boldsymbol{\nu}\right) \mathrm{d}\boldsymbol{y} \right| \\
&\leq C \left\| \gamma_T \left(G(s, \boldsymbol{x}-\cdot) \boldsymbol{e}_j \right) \right\|_{\boldsymbol{X}_\Gamma} \|\boldsymbol{\varphi}\|_{\boldsymbol{X}_\Gamma} \\
&\leq C \left\| G(s, \boldsymbol{x}-\cdot) \boldsymbol{e}_j \right\|_{\boldsymbol{H}(\mathbf{curl}, \mathbb{R}^3 \setminus \Omega)} \|\boldsymbol{\varphi}\|_{\boldsymbol{X}_\Gamma} \\
&\leq C \left\| G(s, \boldsymbol{x}-\cdot) \right\|_{H^1(\mathbb{R}^3 \setminus \Omega)} \|\boldsymbol{\varphi}\|_{\boldsymbol{X}_\Gamma},
\end{aligned}$$

where the bound on the tangential trace is the trace theorem from [25, Theorem 4.1]. The estimation of the second summand is straightforward, as

$$\begin{aligned}
\left| \nabla \int_\Gamma G(s, \boldsymbol{x}-\boldsymbol{y}) \,\mathrm{div}_\Gamma\, \boldsymbol{\varphi}(\boldsymbol{y}) \mathrm{d}\boldsymbol{y} \right| &\leq \left\| \nabla G(s, \boldsymbol{x}-\cdot) \right\|_{\boldsymbol{H}^{1/2}(\Gamma)} \left\| \mathrm{div}_\Gamma\, \boldsymbol{\varphi}(\boldsymbol{y}) \right\|_{H^{-1/2}(\Gamma)} \\
&\leq \left\| G(s, \boldsymbol{x}-\cdot) \right\|_{H^2(\mathbb{R}^3 \setminus \Omega)} \|\boldsymbol{\varphi}\|_{\boldsymbol{X}_\Gamma}.
\end{aligned}$$

Applying a partial derivative with respect to a coordinate x_i to the first summand of the single layer operator is bounded by the same argument structure as before, namely it holds that

$$\begin{aligned}
\left| \partial_{x_i} \boldsymbol{e}_j \cdot \int_\Gamma G(s, \boldsymbol{x}-\boldsymbol{y}) \boldsymbol{\varphi}(\boldsymbol{y}) \mathrm{d}\boldsymbol{y} \right| &= \left| \boldsymbol{e}_j \cdot \int_\Gamma \partial_{x_i} G(s, \boldsymbol{x}-\boldsymbol{y}) \boldsymbol{\varphi}(\boldsymbol{y}) \mathrm{d}\boldsymbol{y} \right| \\
&\leq \left\| \partial_{x_i} G(s, \boldsymbol{x}-\cdot) \right\|_{H^1(\mathbb{R}^3 \setminus \Omega)} \|\boldsymbol{\varphi}\|_{\boldsymbol{X}_\Gamma}.
\end{aligned}$$

Any linear combination of partial derivatives is therefore bounded by an estimate of the same structure, which includes the **curl** operator. Consequently, the double layer potential operator fulfills the stated bound.

□

The final part of the above proof immediately generalizes to the following extension for spatial differential operators. A particularly interesting implication of the following lemma is that the corresponding (time-harmonic) solution field $\widehat{\boldsymbol{E}} = -\boldsymbol{\mathcal{S}}(s)\widehat{\boldsymbol{\varphi}} + \boldsymbol{\mathcal{D}}(s)\widehat{\boldsymbol{\psi}}$ to given traces $\widehat{\boldsymbol{\varphi}}, \widehat{\boldsymbol{\psi}} \in \boldsymbol{X}_\Gamma$, is smooth at every point $\boldsymbol{x} \in \Omega \setminus \Gamma$.

Lemma 3.11. *For every positive integer order of differentiation k and for all partial derivatives, namely for all $j = 1, 2, 3$, the following bounds hold for $\boldsymbol{x} \in \mathbb{R}^3 \setminus \Gamma$ with $d = \operatorname{dist}(\boldsymbol{x}, \Gamma) > 0$ and $\operatorname{Re} s \geq \sigma > 0$:*

$$\begin{aligned} \left| \left(\partial_{x_j}^k \boldsymbol{\mathcal{S}}(s) \boldsymbol{\varphi} \right)(\boldsymbol{x}) \right| &\leq C_\sigma \, |s|^{2+k} \, e^{-d \operatorname{Re} s} \, \|\boldsymbol{\varphi}\|_{\boldsymbol{X}_\Gamma}, \\ \left| \left(\partial_{x_j}^k \boldsymbol{\mathcal{D}}(s) \boldsymbol{\varphi} \right)(\boldsymbol{x}) \right| &\leq C_\sigma \, |s|^{2+k} \, e^{-d \operatorname{Re} s} \, \|\boldsymbol{\varphi}\|_{\boldsymbol{X}_\Gamma}, \end{aligned} \qquad \text{for all } \boldsymbol{\varphi} \in \boldsymbol{X}_\Gamma.$$

The constant C_σ only depends on $k, \sigma, \boldsymbol{x}$ and Γ. Any combination of partial derivatives in mixed directions fulfill a similar bound, where k then denotes the overall order of the spatial differential operator.

Taking the above estimates and integrating over all points $\Omega_d \subset \Omega$ with at least a given distance d away from the boundary Γ, gives a structurally similar result to Lemma 3.4. In exchange for restricting the domain to Ω_d, the s-dependence in the estimates becomes more favourable for large real parts.

Lemma 3.12. *Consider the domain away from the boundary by at least some fixed distance $d > 0$, namely $\Omega_d = \{\boldsymbol{x} \in \Omega \mid \operatorname{dist}(\boldsymbol{x}, \Gamma) > d\}$. Restricted to this domain, the electromagnetic single and double layer potential operators $\boldsymbol{\mathcal{S}}(s), \boldsymbol{\mathcal{D}}(s)$ satisfy the following bounds:*

$$\begin{aligned} \|\boldsymbol{\mathcal{S}}(s)\|_{\boldsymbol{H}(\mathbf{curl}, \Omega_d) \leftarrow \boldsymbol{X}_\Gamma} &\leq C_\sigma e^{-d \operatorname{Re} s} \, |s|^3, \\ \|\boldsymbol{\mathcal{D}}(s)\|_{\boldsymbol{H}(\mathbf{curl}, \Omega_d) \leftarrow \boldsymbol{X}_\Gamma} &\leq C_\sigma e^{-d \operatorname{Re} s} \, |s|^3, \end{aligned}$$

for $\operatorname{Re} s \geq \sigma > 0$. The constant C_σ only depends on d, Γ and σ.

Proof. Let $\boldsymbol{\varphi} \in \boldsymbol{X}_\Gamma$ be an arbitrary boundary function of the tangential trace space. Consider now the square of the $\boldsymbol{H}(\mathbf{curl}, \Omega)$-norm of the single layer potential applied to this arbitrary function

$$\begin{aligned} \|(\boldsymbol{\mathcal{S}}(s)\boldsymbol{\varphi})\|^2_{\boldsymbol{H}(\mathbf{curl}, \Omega_d)} &= \int_{\Omega_d} |(\boldsymbol{\mathcal{S}}(s)\boldsymbol{\varphi})(\boldsymbol{x})|^2 + |(\mathbf{curl}\, \boldsymbol{\mathcal{S}}(s)\boldsymbol{\varphi})(\boldsymbol{x})|^2 \, \mathrm{d}\boldsymbol{x} \\ &\leq C_\sigma \, \|\boldsymbol{\varphi}\|^2_{\boldsymbol{X}_\Gamma} \, |s|^6 \int_{\Omega_d} e^{-2 \operatorname{dist}(x, \Gamma) \operatorname{Re} s} \mathrm{d}\boldsymbol{x}, \end{aligned}$$

where the final estimate holds due to the bounds from Lemma 3.11. The integral is bounded in the proof of Lemma 2.13.

Repeating the arguments for the double layer potential operator yields the analogous result for $\boldsymbol{\mathcal{D}}(s)$.

□

Finally, we give a result in terms of the $\boldsymbol{L}^p(\Gamma)$ norm on the surface, which will be crucial in the final chapter due to its favourable dependence on s.

Lemma 3.13. *Let Γ be smooth and consider $\boldsymbol{x} \in \Omega$, some arbitrary point away from the boundary with at least the distance $d = \operatorname{dist}(\boldsymbol{x}, \Gamma) > 0$. Then, for all $p \geq 1$ and $\boldsymbol{\varphi} \in \boldsymbol{X}_\Gamma \cap \boldsymbol{L}^p(\Gamma)$, we have*

$$\begin{aligned} |(\boldsymbol{\mathcal{S}}(s)\boldsymbol{\varphi})(\boldsymbol{x})| &\leq C \, |s| \, e^{-d \operatorname{Re} s} \, \|\boldsymbol{\varphi}\|_{\boldsymbol{L}^p(\Gamma)}, \\ |(\boldsymbol{\mathcal{D}}(s)\boldsymbol{\varphi})(\boldsymbol{x})| &\leq C \, |s| \, e^{-d \operatorname{Re} s} \, \|\boldsymbol{\varphi}\|_{\boldsymbol{L}^p(\Gamma)}, \end{aligned}$$

where the constant C only depends on the boundary Γ. Point evaluations of the potential operators then extend by density to continuous linear operators $\boldsymbol{\mathcal{S}}_{\boldsymbol{x}}(s) : \boldsymbol{L}^p(\Gamma) \to \mathbb{C}^3$ and $\boldsymbol{\mathcal{D}}_{\boldsymbol{x}}(s) : \boldsymbol{L}^p(\Gamma) \to \mathbb{C}^3$.

Proof. The bounds are a direct consequence of Hölder's inequality. To show the bound for the second integral of the single layer potential operator, we additionally use partial integration on the surface to rewrite

$$\int_\Gamma G(s, \boldsymbol{x} - \boldsymbol{y}) \operatorname{div}_\Gamma \boldsymbol{\varphi}(\boldsymbol{y}) \, \mathrm{d}\boldsymbol{y} = - \int_\Gamma (\nabla_\Gamma G(s, \boldsymbol{x} - \boldsymbol{y})) \, \boldsymbol{\varphi}(\boldsymbol{y}) \, \mathrm{d}\boldsymbol{y}.$$

□

3.5. Time-dependent Maxwell's equations with generalized impedance boundary conditions

The frequency-explicit estimates of Section 3.3 have direct implications for their time-dependent counterparts. Important properties, such as the stability and well-posedness of the problem formulations, naturally carry over via the procedure described in Section 3.1.1, (following [52]). Employing the inverse Laplace transform on both sides leads to the time-dependent version of the time-harmonic boundary integral equation (3.38), which forms the starting point of this section.

The formulation of the time-dependent boundary integral equation is obtained by formally replacing the Laplace transform variable s by the time differentiation operator ∂_t.

Time-dependent boundary integral equation: *The time-dependent boundary functions, denoted by $(\boldsymbol{\varphi}, \boldsymbol{\psi}) \colon [0, T] \to \boldsymbol{V}_\Gamma \times \boldsymbol{X}_\Gamma$ with sufficient temporal regularity (to be specified in the subsequent sections) are said to be solutions of the time-dependent boundary integral equations, if for almost every $t \in [0, T]$ and for all $(\boldsymbol{v}, \boldsymbol{\xi}) \in \boldsymbol{V}_\Gamma \times \boldsymbol{X}_\Gamma$, it holds that*

$$\left[\begin{pmatrix} \boldsymbol{v} \\ \boldsymbol{\xi} \end{pmatrix}, \boldsymbol{C}_{\mathrm{imp}}(\partial_t) \begin{pmatrix} \boldsymbol{\varphi} \\ \boldsymbol{\psi} \end{pmatrix} \right]_\Gamma + \langle \boldsymbol{v}, \boldsymbol{Z}(\partial_t) \boldsymbol{\varphi} \rangle_\Gamma = \langle \boldsymbol{v}, \boldsymbol{g}^{\mathrm{inc}} \rangle_\Gamma. \tag{3.50}$$

The time-dependent right-hand side $\boldsymbol{g}^{\mathrm{inc}} : [0, T] \to \boldsymbol{V}_\Gamma{}'$ encodes the properties of the time-dependent incident waves via (3.4), and is assumed to be of the regularity $\boldsymbol{g}^{\mathrm{inc}} \in \boldsymbol{H}_0^k(0, T; \boldsymbol{V}_\Gamma{}')$ for k appropriately large. The definition of this spatio-temporal Hilbert space is provided in Appendix A and the specific order of k is discussed in the following sections.

This boundary integral equation is notationally compressed as in (3.43) by employing the time-harmonic operator family $\boldsymbol{A}(s) : \boldsymbol{V}_\Gamma \times \boldsymbol{X}_\Gamma \to \boldsymbol{V}_\Gamma{}' \times \boldsymbol{X}_\Gamma{}'$, which collects the appropriate terms of the boundary integral equations and has been formally defined by (3.41). In view of this operator family, the time-dependent boundary integral equation thus reduces to

$$\boldsymbol{A}(\partial_t) \begin{pmatrix} \boldsymbol{\varphi} \\ \boldsymbol{\psi} \end{pmatrix} = \begin{pmatrix} \boldsymbol{g}^{\mathrm{inc}} \\ 0 \end{pmatrix}. \tag{3.51}$$

As the inverse of $\boldsymbol{A}(s)$ is, for $\operatorname{Re} s > \sigma_0$, well-defined and bounded via (3.45), the temporal

convolution operator $\boldsymbol{A}^{-1}(\partial_t)$ is well-defined by (A.3). Moreover, the composition rule implies that

$$\boldsymbol{A}^{-1}(\partial_t)\boldsymbol{A}(\partial_t) = \mathbf{Id}_{\boldsymbol{V}_\Gamma \times \boldsymbol{X}_\Gamma} \quad \text{and} \quad \boldsymbol{A}(\partial_t)\boldsymbol{A}^{-1}(\partial_t) = \mathbf{Id}_{\boldsymbol{V}_\Gamma{}' \times \boldsymbol{X}_\Gamma{}'}.$$

Consequently, the time-dependent unique solution of (3.51) is directly characterized by the application of a temporal convolution operator through

$$\begin{pmatrix} \boldsymbol{\varphi} \\ \boldsymbol{\psi} \end{pmatrix} = \boldsymbol{A}^{-1}(\partial_t) \begin{pmatrix} \boldsymbol{g}^{\text{inc}} \\ 0 \end{pmatrix}. \tag{3.52}$$

Furthermore, the time-harmonic bounds imply the regularity properties of the temporal convolution operator above, namely applying (A.3) (i.e. [52, Lemma 2.1]) to $A^{-1}(\partial_t)$ with the exponent $\kappa = 2$, yields the following result.

Theorem 3.3 (Well-posedness of the time-dependent boundary integral equation)**.** *Let $r \geq 0$ and further consider an incident time-dependent wave such that $\boldsymbol{g}^{\text{inc}} \in \boldsymbol{H}_0^{r+3}(0,T;\boldsymbol{V}_\Gamma{}')$. Then, the temporal boundary integral equation (3.50) has a unique solution $(\boldsymbol{\varphi},\boldsymbol{\psi}) \in \boldsymbol{H}_0^{r+1}(0,T;\boldsymbol{V}_\Gamma \times \boldsymbol{X}_\Gamma)$, and*

$$\left\| \begin{pmatrix} \boldsymbol{\varphi} \\ \boldsymbol{\psi} \end{pmatrix} \right\|_{\boldsymbol{H}_0^{r+1}(0,T;\boldsymbol{V}_\Gamma \times \boldsymbol{X}_\Gamma)} \leq C_T \left\| \boldsymbol{g}^{\text{inc}} \right\|_{\boldsymbol{H}_0^{r+3}(0,T;\boldsymbol{V}_\Gamma{}')}. \tag{3.53}$$

The constant C_T depends on the final time T (polynomially if $\sigma_0 = 0$ in (3.9)) and, through norms of tangential trace operators, on the boundary Γ.

Time-dependent boundary data $\boldsymbol{\varphi}, \boldsymbol{\psi}$, in particular the solution of the boundary integral equation from Theorem 3.3, are related to electromagnetic fields in the domain through the time-dependent representation formulas

$$\boldsymbol{E} = -\boldsymbol{\mathcal{S}}(\partial_t)\boldsymbol{\varphi} + \boldsymbol{\mathcal{D}}(\partial_t)\boldsymbol{\psi}, \tag{3.54}$$
$$\boldsymbol{H} = -\boldsymbol{\mathcal{D}}(\partial_t)\boldsymbol{\varphi} - \boldsymbol{\mathcal{S}}(\partial_t)\boldsymbol{\psi}. \tag{3.55}$$

We turn our attention towards the well-posedness of the time-dependent scattering problem under the generalized impedance boundary condition, specifically an analogous time-dependent result to Theorem 3.2. The following theorem gives precisely such a result, by combining the time-harmonic preparations with classical techniques surrounding the Laplace transform already used in the acoustic setting.

Theorem 3.4 (Well-posedness of the time-dependent scattering problem)**.** *Consider the time-dependent Maxwell's equations (3.1)–(3.2) completed with the generalized impedance boundary condition (3.13), where the transfer operator $\boldsymbol{Z}(s)$ satisfies the conditions (3.8)–(3.9) with $\kappa \leq 1$ and with $\boldsymbol{g}^{\text{inc}} \in \boldsymbol{H}_0^{r+3}(0,T;\boldsymbol{V}_\Gamma{}')$ for some arbitrary $r \geq 0$.*

(a) The time-dependent scattering problem has a unique solution

$$(\boldsymbol{E},\boldsymbol{H}) \in \boldsymbol{H}_0^r(0,T;\boldsymbol{H}(\mathbf{curl},\Omega)^2) \cap \boldsymbol{H}_0^{r+1}(0,T;(\boldsymbol{L}^2(\Omega))^2),$$

which is characterized by the representation formulas (3.54)–(3.55). The corresponding time-dependent tangential traces are identified by the unique solution of the system of boundary integral equations (3.50)

through the identity

$$(\boldsymbol{\varphi}, \boldsymbol{\psi}) = (\gamma_T \boldsymbol{H}, -\gamma_T \boldsymbol{E}) \in \boldsymbol{H}_0^{r+1}(0, T; \boldsymbol{V}_\Gamma \times \boldsymbol{X}_\Gamma).$$

(b) The time-dependent electromagnetic solution fields are bounded by the incident wave via

$$\|\boldsymbol{E}\|_{\boldsymbol{H}_0^r(0,T;\boldsymbol{H}(\mathbf{curl},\Omega))} + \|\boldsymbol{H}\|_{\boldsymbol{H}_0^r(0,T;\boldsymbol{H}(\mathbf{curl},\Omega))} \leq C_T \|\boldsymbol{g}^{\mathrm{inc}}\|_{\boldsymbol{H}_0^{r+3}(0,T;\boldsymbol{V}_\Gamma{}')}.$$

The right-hand side of the above expression further bounds the $\boldsymbol{H}_0^{r+1}(0, T; (\boldsymbol{L}^2(\Omega))^2)$ *norms of the scattered fields. As before, the constant* C_T *depends on* T *(polynomially if* $\sigma_0 = 0$ *in* (3.9)*) and, through norms of tangential trace operators, on the boundary* Γ*. In particular, for the impedance operators* (1.13)–(1.16)*, the constant is independent of the small parameter* δ*.*

Proof. This proof was essentially formulated in [59, Theorem 4.2].

We start by extending the boundary data $\boldsymbol{g}^{\mathrm{inc}} \in \boldsymbol{H}_0^r(0, T; \boldsymbol{V}_\Gamma{}')$ from the finite interval $(0, T)$ to a function in $\boldsymbol{H}^r(\mathbb{R}; \boldsymbol{V}_\Gamma{}')$ on the whole real line, with finite support on $[0, 2T]$. Now, consider the fields $(\boldsymbol{E}, \boldsymbol{H})$ defined by the time-dependent boundary integral equation (3.51) and the time-dependent representation formulas (3.54)–(3.55). These fields are of the stated regularity, as the time-harmonic bounds of Theorem 3.2 provide the necessary conditions for (A.3) with the exponent $\kappa = 3$. Moreover, these fields satisfy the stated bounds for all finite time intervals $(0, \bar{T})$ with constants growing at most exponentially with a fixed exponent σ_0. Therefore, the Laplace transform $(\widehat{\boldsymbol{E}}(s), \widehat{\boldsymbol{H}}(s))$ exists for $\operatorname{Re} s > \sigma_0$, and is the unique solution to the time-harmonic boundary integral equation (3.43) and the time-harmonic representation formulas (3.29)–(3.30). The equivalence of the time-harmonic system of boundary integral equations and the time-harmonic scattering problem described by Theorem 3.2 therefore implies that $(\widehat{\boldsymbol{E}}(s), \widehat{\boldsymbol{H}}(s))$ is the unique solution to the time-harmonic scattering problem under the time-harmonic generalized impedance boundary condition. Applying the inverse Laplace transform then shows that $(\boldsymbol{E}, \boldsymbol{H})$ are solutions of the time-dependent Maxwell's equations (3.1)–(3.2) with the time-dependent generalized impedance boundary condition (3.13).

Finally, the uniqueness of the time-dependent solution $(\boldsymbol{E}, \boldsymbol{H})$ is a direct consequence of the uniqueness result for the time-harmonic scattering problem.

□

3.6. Semi-discretization in time by Runge–Kutta convolution quadrature

3.6.1. Convolution quadrature for the scattering problem

Employing the convolution quadrature discretization to the time-dependent boundary integral equation (3.51) is notationally straightforward and leads to the discrete convolution equation

$$\boldsymbol{A}(\partial_t^\tau) \begin{pmatrix} \boldsymbol{\varphi}^\tau \\ \boldsymbol{\psi}^\tau \end{pmatrix} = \begin{pmatrix} \boldsymbol{g}^{\mathrm{inc}} \\ 0 \end{pmatrix}. \tag{3.56}$$

Analogous to the analytic treatment of this boundary integral equation, we apply the discrete composition rule (B.9) to obtain a direct representation of the semi-discrete solution. This repre-

sentation is the convolution quadrature semi-discretization of the convolution (3.52) and reads

$$\begin{pmatrix} \boldsymbol{\varphi}^\tau \\ \boldsymbol{\psi}^\tau \end{pmatrix} = \boldsymbol{A}^{-1}(\partial_t^\tau) \begin{pmatrix} \boldsymbol{g}^{\mathrm{inc}} \\ 0 \end{pmatrix}.$$

This identity is extremely useful for the convergence analysis and practical computations, since it interprets the solution of the discretized boundary integral equation as a mere convolution quadrature with some analytic operator family. General convolution quadrature approximation results such as Lemma B.1, are directly applicable for such schemes and yield error bounds. This argument structure originates from [52]. A particular advantage of this time discretization is the absence of stability issues.

Time-discrete electromagnetic fields on the whole domain Ω are then computationally accessible by applying the convolution quadrature time discretization to the representation formulas (3.54)–(3.55):

$$\boldsymbol{E}^\tau = -\boldsymbol{\mathcal{S}}(\partial_t^\tau)\boldsymbol{\varphi}^\tau + \boldsymbol{\mathcal{D}}(\partial_t^\tau)\boldsymbol{\psi}^\tau, \tag{3.57}$$

$$\boldsymbol{H}^\tau = -\boldsymbol{\mathcal{D}}(\partial_t^\tau)\boldsymbol{\varphi}^\tau - \boldsymbol{\mathcal{S}}(\partial_t^\tau)\boldsymbol{\psi}^\tau. \tag{3.58}$$

These fields are characterized directly in terms of the boundary data $\boldsymbol{g}^{\mathrm{inc}}$ by again applying the composition rule, which gives the semi-discrete fields as the convolution quadrature discretization of the complete operator $\boldsymbol{\mathcal{U}}(\partial_t)$. Specifically, we have

$$\begin{pmatrix} \boldsymbol{E}^\tau \\ \boldsymbol{H}^\tau \end{pmatrix} = \boldsymbol{\mathcal{U}}(\partial_t^\tau)\boldsymbol{g}^{\mathrm{inc}} \qquad \text{of} \qquad \begin{pmatrix} \boldsymbol{E} \\ \boldsymbol{H} \end{pmatrix} = \boldsymbol{\mathcal{U}}(\partial_t)\boldsymbol{g}^{\mathrm{inc}}, \tag{3.59}$$

where the complete operator is explicitly given by Theorem 3.4 through the composition

$$\boldsymbol{\mathcal{U}}(s) = \begin{pmatrix} -\boldsymbol{\mathcal{S}}(s) & \boldsymbol{\mathcal{D}}(s) \\ -\boldsymbol{\mathcal{D}}(s) & -\boldsymbol{\mathcal{S}}(s) \end{pmatrix} \boldsymbol{A}(s)^{-1} \begin{pmatrix} \mathbf{Id} \\ 0 \end{pmatrix} : \boldsymbol{V}_\Gamma{}' \to \boldsymbol{H}(\mathbf{curl}, \Omega)^2.$$

This operator is bounded by Theorem 3.2, namely for any $\sigma > \sigma_0 \geq 0$ there exists a constant C_σ such that for all $\operatorname{Re} s \geq \sigma$ it holds that

$$\|\boldsymbol{\mathcal{U}}(s)\|_{\boldsymbol{H}(\mathbf{curl},\Omega)^2 \leftarrow \boldsymbol{V}_\Gamma{}'} \leq C_\sigma \frac{|s|^3}{(\operatorname{Re} s)^{3/2}}.$$

Furthermore, for point evaluations and domains away from the boundary by some fixed distance d, we obtain alternative bounds. Combining the bounds on the potential operators from Lemmas 3.10–3.12 with Theorem 3.1 implies for $\operatorname{Re} s \geq \sigma > \sigma_0 \geq 0$

$$\|\boldsymbol{\mathcal{U}}(s)\|_{(\boldsymbol{C}^1(\overline{\Omega}_d)^3)^2 \leftarrow \boldsymbol{V}_\Gamma{}'} + \|\boldsymbol{\mathcal{U}}(s)\|_{\boldsymbol{H}(\mathbf{curl},\Omega_d)^2 \leftarrow \boldsymbol{V}_\Gamma{}'} \leq C_\sigma |s|^5 e^{-d \operatorname{Re} s},$$

where Ω_d denotes again all points in the domain with at least a fixed distance $d > 0$ away from the boundary. The first summand is the $\boldsymbol{C}^1(\overline{\Omega}_d)$-norm, i.e. the maximum norm on continuously differentiable functions and their first derivatives on $\overline{\Omega}_d$, the closure of Ω_d.

Remark 3.3. *Any discrete fields* $(\boldsymbol{E}^\tau, \boldsymbol{H}^\tau)$ *fulfilling the discretized representation formulas* (3.57)–(3.58) *are, just as their continuous counterparts, divergence-free. This is a consequence of the fact that the generating functions* $\sum_{n\geq 0} \boldsymbol{E}^n \zeta^n, \sum_{n\geq 0} \boldsymbol{H}^n \zeta^n$ *are themselves characterized by time-harmonic representation formulas for* $|\zeta| < 1$.

These bounds are the requirements for Lemma B.1 to give an approximation property of the convolution quadrature method. Applying this lemma to the operator family $\boldsymbol{\mathcal{U}}(s)$ with its various time-harmonic bounds yields the following result.

Proposition 3.1 (Error bound of the semi-discretization in time)**.** *Consider the setting of Theorem 3.4, and further the semi-discretization in time* (3.56)*, discretized by Runge–Kutta convolution quadrature based on the Radau IIA method with* m *stages. Let* $\boldsymbol{E}^\tau$ *and* $\boldsymbol{H}^\tau$ *further denote the fields obtained by the discrete representation formulas* (3.57)–(3.58)*. Let* $r > 2m+3$ *and assume that the regularity of the incident wave implies* $\boldsymbol{g}^{\mathrm{inc}} \in \boldsymbol{C}^r([0,T], \boldsymbol{V}_\Gamma{}')$*, with* $\boldsymbol{g}^{\mathrm{inc}}$ *vanishing initially together with its first* $r-1$ *time derivatives.*

Under these conditions, the resulting approximations of the semi-discrete electromagnetic fields $\boldsymbol{E}^n = \left[(\boldsymbol{E}^\tau)^{n-1}\right]_m$ *and* $\boldsymbol{H}^n = \left[(\boldsymbol{H}^\tau)^{n-1}\right]_m$ *fulfill the following error bounds at the time* $t_n = n\tau \in [0,T]$*:*

$$\left\| \begin{pmatrix} \boldsymbol{E}^n - \boldsymbol{E}(t_n) \\ \boldsymbol{H}^n - \boldsymbol{H}(t_n) \end{pmatrix} \right\|_{\boldsymbol{H}(\mathbf{curl},\Omega)^2} \leq C\, \tau^{m-1/2}\, M(\boldsymbol{g}^{\mathrm{inc}}, t_n).$$

For points away from the boundary, specifically for $\Omega_d = \{\boldsymbol{x} \in \Omega : \operatorname{dist}(\boldsymbol{x}, \Gamma) > d\}$ *with* $d > 0$*, a corresponding bound with the full classical order* $2m-1$ *holds:*

$$\left\| \begin{pmatrix} \boldsymbol{E}^n - \boldsymbol{E}(t_n) \\ \boldsymbol{H}^n - \boldsymbol{H}(t_n) \end{pmatrix} \right\|_{\left(\boldsymbol{H}(\mathbf{curl},\Omega_d)\cap \mathbf{C}^1(\overline{\Omega}_d)^3\right)^2} \leq C_d\, \tau^{2m-1}\, M(\boldsymbol{g}^{\mathrm{inc}}, t_n).$$

An equivalent bound holds for point evaluations at any point $\boldsymbol{x} \in \Omega$*. The constant originates from Lemma B.1 and has the explicit form*

$$M(\boldsymbol{g}, t) = \|\boldsymbol{g}^{(r)}(0)\|_{\boldsymbol{V}_\Gamma{}'} + \int_0^t \|\boldsymbol{g}^{(r+1)}(t')\|_{\boldsymbol{V}_\Gamma{}'}\, \mathrm{d}t'.$$

The constants C *and* C_d *in the error bounds depend on the final time* T *and on the boundary* Γ*, but are crucially independent of* n*,* τ *and* $\boldsymbol{g}^{\mathrm{inc}}$*. As indicated by the index,* C_d *additionally depends on the distance* d*. In particular, for the impedance operators* (1.13)–(1.16)*, both* C *and* C_d *are independent of the small parameter* δ*.*

The above described full-order convergence away from the boundary for the Runge–Kutta convolution quadrature time discretization was originally observed and proved in the context of acoustic scattering from a sound-soft obstacle [14]. In view of this fact, Proposition 3.1 (particularly through Lemmas 3.10–3.12) transports these favourable error bounds to the electromagnetic scattering with generalized impedance boundary conditions.

3.7. Full discretization

To derive fully-discrete schemes, we employ a Galerkin approximation of the boundary integral equation (3.56) with finite dimensional boundary element spaces $\boldsymbol{V}_h \subset \boldsymbol{V}_\Gamma$ and $\boldsymbol{X}_h \subset \boldsymbol{X}_\Gamma$. These subspaces consist of a set of piecewise polynomials operating on a family of triangulations with arbitrary small mesh width h.

Both boundary element spaces $\boldsymbol{V}_h$ and $\boldsymbol{X}_h$ are chosen to be the Raviart–Thomas boundary element space of order $k \geq 0$, a polynomial space whose restriction to the unit triangle $\widehat{K}$ as a reference element reads

$$\mathrm{RT}_k(\widehat{K}) = \left\{ \boldsymbol{x} \mapsto \boldsymbol{p}_1(\boldsymbol{x}) + p_2(\boldsymbol{x})\boldsymbol{x} \,:\, \boldsymbol{p}_1 \in P_k(\widehat{K})^2,\ p_2 \in P_k(\widehat{K}) \right\},$$

where $P_k(\widehat{K})$ is the polynomial space of degree k on $\widehat{K}$. Details can be found in the original paper [60]. This definition of Raviart–Thomas elements extends to arbitrary grids by a piecewise pullback to the reference element.

For $h \to 0$, boundary element spaces are expected to approximate smooth enough functions arbitrary well, by means of a rate-specific best-approximation result. Such an estimate is crucial for our error analysis and provided by Lemma 15 and Theorem 14 of [26], which themselves originate from the original references [22, Section III.3.3] and [23].

To formulate this result, we use the original notation from [26] and define the trace space $\boldsymbol{H}^p_\times(\Gamma) = \gamma_T \boldsymbol{H}^{p+1/2}(\Omega)$.

Lemma 3.14. *Let the subspaces $\boldsymbol{X}_h \subset \boldsymbol{X}_\Gamma$ and $\boldsymbol{V}_h \subset \boldsymbol{V}_\Gamma$ both be chosen as the Raviart–Thomas elements of order k, where $\boldsymbol{V}_\Gamma$ denotes the space of Lemma 3.1 or Lemma 3.2. Consider arbitrary boundary functions of the regularity $\boldsymbol{\xi} \in \boldsymbol{X}_\Gamma \cap \boldsymbol{H}^{k+1}_\times(\Gamma)$ and $\boldsymbol{v} \in \boldsymbol{V}_\Gamma \cap \boldsymbol{H}^{k+1}_\times(\Gamma)$. The best-approximation error of the Raviart–Thomas space of order k is then bounded by*

$$\inf_{\boldsymbol{\xi}_h \in \boldsymbol{X}_h} \|\boldsymbol{\xi}_h - \boldsymbol{\xi}\|_{\boldsymbol{X}_\Gamma} \leq C h^{k+3/2} \|\boldsymbol{\xi}\|_{\boldsymbol{H}^{k+1}_\times(\Gamma)},$$
$$\inf_{\boldsymbol{v}_h \in \boldsymbol{V}_h} \|\boldsymbol{v}_h - \boldsymbol{v}\|_{\boldsymbol{V}_\Gamma} \leq C h^{k+1} \|\boldsymbol{v}\|_{\boldsymbol{H}^{k+1}_\times(\Gamma)}.$$

Remark 3.4. *In view of the situation for acoustic generalized impedance boundary conditions (compare e.g. Theorem 2.5), a more natural estimate for the best-approximation property of $\boldsymbol{V}_\Gamma$-norm would be the order $\mathcal{O}(h^{k+3/2} + \delta^{1/2} h^{k+1})$. Proving error bounds of this order with the presented techniques requires the $\boldsymbol{V}_\Gamma$-norm stability of the projection from $\boldsymbol{X}_\Gamma$ to $\boldsymbol{X}_h$, which was used to derive the best-approximation estimate in $\boldsymbol{X}_\Gamma$. Whether such a result holds is unclear, however to prove such a result is beyond the scope of the thesis. More details on the projection operators can be found in [23] and the references therein.*

Applying the boundary element discretization to the time-discrete boundary integral equation (3.56) by restricting the weak formulation to $\boldsymbol{V}_h \times \boldsymbol{X}_h$ then reads

$$\left\langle \begin{pmatrix} \boldsymbol{v}_h \\ \boldsymbol{\xi}_h \end{pmatrix}, \boldsymbol{A}(\partial_t^\tau) \begin{pmatrix} \boldsymbol{\varphi}_h^\tau \\ \boldsymbol{\psi}_h^\tau \end{pmatrix} \right\rangle_\Gamma = \langle \boldsymbol{v}_h, \boldsymbol{g}^{\mathrm{inc}} \rangle_\Gamma \qquad \forall\, (\boldsymbol{v}_h, \boldsymbol{\xi}_h) \in (\boldsymbol{V}_h \times \boldsymbol{X}_h)^m. \tag{3.60}$$

This fully discrete scheme is solved by the approximate boundary densities

$$\boldsymbol{\varphi}_h^\tau = \big((\boldsymbol{\varphi}_h^\tau)^n\big)_{n\geq 0} \quad \text{with} \quad (\boldsymbol{\varphi}_h^\tau)^n = \big((\boldsymbol{\varphi}_h^\tau)_i^n\big)_{i=1}^m \in \boldsymbol{V}_h^m,$$
$$\boldsymbol{\psi}_h^\tau = \big((\boldsymbol{\psi}_h^\tau)^n\big)_{n\geq 0} \quad \text{with} \quad (\boldsymbol{\varphi}_h^\tau)^n = \big((\boldsymbol{\psi}_h^\tau)_i^n\big)_{i=1}^m \in \boldsymbol{X}_h^m.$$

These fully discrete densities yield approximations to the electromagnetic fields away from the boundary through the time-discrete representation formulas

$$\boldsymbol{E}_h^\tau = -\boldsymbol{\mathcal{S}}(\partial_t^\tau)\boldsymbol{\varphi}_h^\tau + \boldsymbol{\mathcal{D}}(\partial_t^\tau)\boldsymbol{\psi}_h^\tau, \tag{3.61}$$
$$\boldsymbol{H}_h^\tau = -\boldsymbol{\mathcal{D}}(\partial_t^\tau)\boldsymbol{\varphi}_h^\tau - \boldsymbol{\mathcal{S}}(\partial_t^\tau)\boldsymbol{\psi}_h^\tau. \tag{3.62}$$

Error bounds for the fully discrete solutions are described in the following theorem, under regularity assumptions on the exact solution of the boundary integral equation. The assumptions taken are presumably stricter than necessary, but are required for the present techniques.

Theorem 3.5 (Error bound of the full discretization)**.** *Consider the solutions of the time-dependent boundary integral equation whose existence and regularity is guaranteed by Theorem 3.4 under the conditions stated there. In this setting, consider the approximations with the following discretizations:*

- *Convolution quadrature time discretization based on the Radau IIA Runge–Kutta method with $m \geq 2$ stages employed for the boundary integral equation (3.56) and the discrete representation formulas (3.57)–(3.58) and*
- *boundary element space discretization based on Raviart–Thomas elements of order k, applied to the boundary integral equation (3.51).*

Let $\boldsymbol{g}^{\mathrm{inc}} \in \boldsymbol{C}^r([0,T], \boldsymbol{V}_\Gamma{}')$ for some $r > 2m+3$, and further let $\boldsymbol{g}^{\mathrm{inc}}$ vanish at $t=0$ together with its first $r-1$ time derivatives. Moreover, the exact solution $(\boldsymbol{\varphi}, \boldsymbol{\psi})$ of the boundary integral equation (3.51) is assumed to be in $\boldsymbol{C}^{10}([0,T], \boldsymbol{H}_\times^{k+1}(\Gamma)^2)$, vanishing at $t=0$ together with its time derivatives.
Under these conditions, the following error bounds hold for the approximations to the electromagnetic fields $\boldsymbol{E}_h^n = \big[(\boldsymbol{E}_h^\tau)^{n-1}\big]_m$ and $\boldsymbol{H}_h^n = \big[(\boldsymbol{H}_h^\tau)^{n-1}\big]_m$ in time and space at $t_n = n\tau \in [0,T]$:

$$\left\| \begin{pmatrix} \boldsymbol{E}_h^n - \boldsymbol{E}(t_n) \\ \boldsymbol{H}_h^n - \boldsymbol{H}(t_n) \end{pmatrix} \right\|_{\boldsymbol{H}(\mathbf{curl},\Omega)^2} \leq C\big(\tau^{m-1/2} + h^{k+1}\big).$$

For points away from the boundary, specifically for $\Omega_d = \{\boldsymbol{x} \in \Omega : \operatorname{dist}(\boldsymbol{x}, \Gamma) > d\}$ with $d > 0$, a corresponding bound with the full classical order $2m-1$ holds:

$$\left\| \begin{pmatrix} \boldsymbol{E}_h^n - \boldsymbol{E}(t_n) \\ \boldsymbol{H}_h^n - \boldsymbol{H}(t_n) \end{pmatrix} \right\|_{\left(\boldsymbol{H}(\mathbf{curl},\Omega_d)\cap \boldsymbol{C}^1(\overline{\Omega}_d)^3\right)^2} \leq C_d\big(\tau^{2m-1} + h^{k+1}\big).$$

The constants C and C_d in the error bounds depend on the final time T, on the boundary Γ, on the incident waves through $\boldsymbol{g}^{\mathrm{inc}}$ and on higher Sobolev norms of the exact solution $(\boldsymbol{\varphi}, \boldsymbol{\psi})$, but are crucially independent of h,n and τ. As indicated by the index, C_d additionally depends on the distance d. In particular, for the impedance operators (1.13)–(1.16), both C and C_d are independent of the small parameter δ.

Proof. The proof is separated into three parts (a)–(c), starting from analyzing the time-harmonic space discretization, extending these results to the time-dependent space discretization and finally showing the stated bounds for the time-dependent full discretization.

(a) *(Discretized time-harmonic boundary integral equation).* Consider the time-harmonic boundary integral equation (3.42), for $\operatorname{Re} s \geq \sigma > \sigma_0 \geq 0$. The spatially discrete solution operator of the time-harmonic boundary integral equation, which maps $\widehat{g} \mapsto (\widehat{\varphi}_h, \widehat{\psi}_h)$, is denoted by $\boldsymbol{L}_h(s) : \boldsymbol{V}_\Gamma{}' \to \boldsymbol{V}_h \times \boldsymbol{X}_h$ and defined by the Galerkin approximation in $\boldsymbol{V}_h \times \boldsymbol{X}_h$

$$\left\langle \begin{pmatrix} v_h \\ \xi_h \end{pmatrix}, \boldsymbol{A}(s) \begin{pmatrix} \widehat{\varphi}_h \\ \widehat{\psi}_h \end{pmatrix} \right\rangle_\Gamma = \langle v_h, \widehat{g} \rangle_\Gamma \qquad \forall\, (v_h, \xi_h) \in \boldsymbol{V}_h \times \boldsymbol{X}_h. \tag{3.63}$$

By the bound of $\boldsymbol{A}(s)$ in Lemma 3.8, the coercivity estimate of Lemma 3.9 and the Lax–Milgram Lemma, we obtain the bound

$$\|\boldsymbol{L}_h(s)\|_{\boldsymbol{V}_h \times \boldsymbol{X}_h \leftarrow \boldsymbol{V}_\Gamma{}'} \leq \frac{1}{c_\sigma} \frac{|s|^2}{\operatorname{Re} s}. \tag{3.64}$$

Additionally, consider the Ritz projection associated to the bilinear form on the left-hand side, denoted by $\boldsymbol{R}_h(s) : \boldsymbol{V}_\Gamma \times \boldsymbol{X}_\Gamma \to \boldsymbol{V}_h \times \boldsymbol{X}_h$. This operator projects $(\widehat{\varphi}, \widehat{\psi}) \in \boldsymbol{V}_\Gamma \times \boldsymbol{X}_\Gamma$ on the boundary element functions $(\widehat{\varphi}_h, \widehat{\psi}_h) \in \boldsymbol{V}_h \times \boldsymbol{X}_h$, which fulfill

$$\left\langle \begin{pmatrix} v_h \\ \xi_h \end{pmatrix}, \boldsymbol{A}(s) \begin{pmatrix} \widehat{\varphi}_h \\ \widehat{\psi}_h \end{pmatrix} \right\rangle_\Gamma = \left\langle \begin{pmatrix} v_h \\ \xi_h \end{pmatrix}, \boldsymbol{A}(s) \begin{pmatrix} \widehat{\varphi} \\ \widehat{\psi} \end{pmatrix} \right\rangle_\Gamma \qquad \forall\, (v_h, \xi_h) \in \boldsymbol{V}_h \times \boldsymbol{X}_h.$$

The Lax–Milgram Lemma shows that this problem is well-posed, namely the above system is uniquely solved by the pair of discrete boundary densities $(\widehat{\varphi}_h, \widehat{\psi}_h) \in \boldsymbol{V}_h \times \boldsymbol{X}_h$. Applying Céa's Lemma further yields an estimate of the projection error in terms of the approximation properties of the underlying boundary element space

$$\left\| \begin{pmatrix} \widehat{\varphi}_h \\ \widehat{\psi}_h \end{pmatrix} - \begin{pmatrix} \widehat{\varphi} \\ \widehat{\psi} \end{pmatrix} \right\|_{\boldsymbol{V}_\Gamma \times \boldsymbol{X}_\Gamma} \leq \frac{C_\sigma}{c_\sigma} \left(\frac{|s|^2}{\operatorname{Re} s} \right)^2 \inf_{(v_h, \xi_h) \in \boldsymbol{V}_h \times \boldsymbol{X}_h} \left\| \begin{pmatrix} v_h \\ \xi_h \end{pmatrix} - \begin{pmatrix} \widehat{\varphi} \\ \widehat{\psi} \end{pmatrix} \right\|_{\boldsymbol{V}_\Gamma \times \boldsymbol{X}_\Gamma}.$$

The best-approximation on the right-hand side is the subject of Lemma 3.14 and applying the bounds therein shows that the associated error operator

$$\boldsymbol{\mathcal{E}}_h(s) = \boldsymbol{R}_h(s) - \mathbf{Id}$$

is a bounded operator from $\boldsymbol{H}_\times^{k+1}(\Gamma)^2$ to $\boldsymbol{V}_\Gamma \times \boldsymbol{X}_\Gamma$ with the bound, for $\operatorname{Re} s \geq \sigma > \sigma_0 \geq 0$,

$$\|\boldsymbol{\mathcal{E}}_h(s)\|_{\boldsymbol{V}_\Gamma \times \boldsymbol{X}_\Gamma \leftarrow \boldsymbol{H}_\times^{k+1}(\Gamma)^2} \leq \widetilde{C}_\sigma \frac{|s|^4}{(\operatorname{Re} s)^2} h^{k+1}. \tag{3.65}$$

(b) *(Error of the spatial semi-discretization).* We turn our attention towards the spatial semi-

discretization of the time-dependent boundary integral equation (3.51), which reads

$$\left\langle \begin{pmatrix} v_h \\ \xi_h \end{pmatrix}, \boldsymbol{A}(\partial_t) \begin{pmatrix} \varphi_h \\ \psi_h \end{pmatrix} \right\rangle_\Gamma = \langle v_h, g^{\mathrm{inc}} \rangle_\Gamma \qquad \forall\, (v_h, \xi_h) \in \boldsymbol{V}_h \times \boldsymbol{X}_h. \tag{3.66}$$

The unique solution of the above system is characterized directly by the above discussed operators transferred to the time domain. The time-dependent spatial semi-discretization of the solution is therefore given by

$$\begin{pmatrix} \varphi_h \\ \psi_h \end{pmatrix} = \boldsymbol{L}_h(\partial_t) g^{\mathrm{inc}} = \boldsymbol{R}_h(\partial_t) \begin{pmatrix} \varphi \\ \psi \end{pmatrix},$$

where $(\varphi, \psi)^\top = \boldsymbol{A}^{-1}(\partial_t)(g^{\mathrm{inc}}, 0)^\top$ is the solution of the fully continuous boundary integral equation (3.51). We collect the potential operators and their sign structure from the representation formulas in a block operator, which is denoted by

$$\boldsymbol{\mathcal{W}}(s) = \begin{pmatrix} -\boldsymbol{\mathcal{S}}(s) & \boldsymbol{\mathcal{D}}(s) \\ -\boldsymbol{\mathcal{D}}(s) & -\boldsymbol{\mathcal{S}}(s), \end{pmatrix}$$

and set

$$\boldsymbol{\mathcal{U}}_h(s) = \boldsymbol{\mathcal{W}}(s) \boldsymbol{L}_h(s) : \boldsymbol{V}_\Gamma{}' \to \boldsymbol{H}(\mathbf{curl}, \Omega)^2. \tag{3.67}$$

Employing the established bounds of the operators $\boldsymbol{\mathcal{W}}(s)$ and $\boldsymbol{L}_h(s)$, specifically the bounds from Lemma 3.4 and (3.64), implies the bound

$$\|\boldsymbol{\mathcal{U}}_h(s)\|_{\boldsymbol{H}(\mathbf{curl},\Omega)^2 \leftarrow \boldsymbol{V}_\Gamma{}'} \leq \bar{C}_\sigma \frac{|s|^4}{(\operatorname{Re} s)^2}. \tag{3.68}$$

The temporal convolution operator $\boldsymbol{\mathcal{U}}_h(\partial_t)$ is therefore well-defined and extends to a bounded operator via (A.3). Consequently, the spatial semi-discretization of the scattering problem is characterized by the evaluation of this operator on the right-hand side, namely

$$\begin{pmatrix} \boldsymbol{E}_h \\ \boldsymbol{H}_h \end{pmatrix} = \boldsymbol{\mathcal{U}}_h(\partial_t) g^{\mathrm{inc}}.$$

By employing the analogous identity for the fully continuous densities (3.59), its error is rewritten as

$$\begin{aligned} \begin{pmatrix} \boldsymbol{E}_h \\ \boldsymbol{H}_h \end{pmatrix} - \begin{pmatrix} \boldsymbol{E} \\ \boldsymbol{H} \end{pmatrix} &= \boldsymbol{\mathcal{U}}_h(\partial_t) g^{\mathrm{inc}} - \boldsymbol{\mathcal{U}}(\partial_t) g^{\mathrm{inc}} = \boldsymbol{\mathcal{W}}(\partial_t) \begin{pmatrix} \varphi_h \\ \psi_h \end{pmatrix} - \boldsymbol{\mathcal{W}}(\partial_t) \begin{pmatrix} \varphi \\ \psi \end{pmatrix} \\ &= \boldsymbol{\mathcal{W}}(\partial_t)(\boldsymbol{R}_h - \mathbf{Id}) \begin{pmatrix} \varphi \\ \psi \end{pmatrix} = \boldsymbol{\mathcal{W}}(\partial_t)\, \boldsymbol{\mathcal{E}}_h(\partial_t) \begin{pmatrix} \varphi \\ \psi \end{pmatrix}. \end{aligned}$$

Using the bounds of Lemma 3.4 for the complete potential operator $\boldsymbol{\mathcal{W}}(s)$ and the bound (3.65) for the error operator $\boldsymbol{\mathcal{E}}_h(s)$ in combination with (A.3) (with $\kappa = 2$ and $\kappa = 4$ respectively) yields that their time-dependent counterparts extend to well-posed bounded operators on the

spaces stated there. Further using the embedding $\boldsymbol{H}^1(0,T;\boldsymbol{H}) \subset \boldsymbol{C}([0,T],\boldsymbol{H})$, which holds for any Hilbert space $\boldsymbol{H}$, we obtain the following error bound for the spatial semi-discretization

$$\begin{aligned}\max_{0\le t\le T}\left\|\begin{pmatrix}\boldsymbol{E}_h(t)\\ \boldsymbol{H}_h(t)\end{pmatrix}-\begin{pmatrix}\boldsymbol{E}(t)\\ \boldsymbol{H}(t)\end{pmatrix}\right\|_{\boldsymbol{H}(\mathbf{curl},\Omega)^2} &\le C\left\|\begin{pmatrix}\boldsymbol{E}_h\\ \boldsymbol{H}_h\end{pmatrix}-\begin{pmatrix}\boldsymbol{E}\\ \boldsymbol{H}\end{pmatrix}\right\|_{\boldsymbol{H}^1_0(0,T;\boldsymbol{H}(\mathbf{curl},\Omega)^2)}\\ \le c_T\left\|\boldsymbol{\mathcal{E}}_h(\partial_t)\begin{pmatrix}\boldsymbol{\varphi}\\ \boldsymbol{\psi}\end{pmatrix}\right\|_{\boldsymbol{H}^3_0(0,T;\boldsymbol{V}_\Gamma\times\boldsymbol{X}_\Gamma)} &\le C_T\,h^{k+1}\left\|\begin{pmatrix}\boldsymbol{\varphi}\\ \boldsymbol{\psi}\end{pmatrix}\right\|_{\boldsymbol{H}^7_0(0,T;\boldsymbol{H}^{k+1}_\times(\Gamma)^2)}.\end{aligned} \tag{3.69}$$

Repeating the argument with the pointwise bounds away from the boundary given by Lemmas 3.10 and 3.11 instead of Lemma 3.4 yields the analogous result

$$\max_{0\le t\le T}\left\|\begin{pmatrix}\boldsymbol{E}_h(t)\\ \boldsymbol{H}_h(t)\end{pmatrix}-\begin{pmatrix}\boldsymbol{E}(t)\\ \boldsymbol{H}(t)\end{pmatrix}\right\|_{\boldsymbol{C}^1(\overline{\Omega}_d)^2} \le C_T\,h^{k+1}\left\|\begin{pmatrix}\boldsymbol{\varphi}\\ \boldsymbol{\psi}\end{pmatrix}\right\|_{\boldsymbol{H}^8_0(0,T;\boldsymbol{H}^{k+1}_\times(\Gamma)^2)}. \tag{3.70}$$

An identical bound holds for any point evaluation $\boldsymbol{x}\in\Omega$.

(c) *(Error of the full discretization).* We decompose the total error into the differences

$$\begin{pmatrix}\boldsymbol{E}_h^n\\ \boldsymbol{H}_h^n\end{pmatrix}-\begin{pmatrix}\boldsymbol{E}^n\\ \boldsymbol{H}^n\end{pmatrix} \quad+\quad \begin{pmatrix}\boldsymbol{E}^n\\ \boldsymbol{H}^n\end{pmatrix}-\begin{pmatrix}\boldsymbol{E}(t_n)\\ \boldsymbol{H}(t_n)\end{pmatrix}.$$

The second summand of the above expression is the error of the temporal semi-discretization, bounded by the stated orders in their respective norms in Proposition 3.1. Our focus is therefore on the first difference, which is rewritten by the operators introduced in the first part of this proof via

$$\begin{aligned}\boldsymbol{\mathcal{W}}(\partial_t^\tau)\boldsymbol{\mathcal{E}}_h(\partial_t^\tau)\begin{pmatrix}\boldsymbol{\varphi}\\ \boldsymbol{\psi}\end{pmatrix} = &\left(\boldsymbol{\mathcal{W}}(\partial_t^\tau)\boldsymbol{\mathcal{E}}_h(\partial_t^\tau)\begin{pmatrix}\boldsymbol{\varphi}\\ \boldsymbol{\psi}\end{pmatrix}-\boldsymbol{\mathcal{W}}(\partial_t)\boldsymbol{\mathcal{E}}_h(\partial_t)\begin{pmatrix}\boldsymbol{\varphi}\\ \boldsymbol{\psi}\end{pmatrix}\right)\\ &+\ \boldsymbol{\mathcal{W}}(\partial_t)\boldsymbol{\mathcal{E}}_h(\partial_t)\begin{pmatrix}\boldsymbol{\varphi}\\ \boldsymbol{\psi}\end{pmatrix}.\end{aligned}$$

The summand in the last row is the error of the spatial semi-discretization and therefore bounded in the part (b) by (3.69).

The remaining difference written on the right-hand side is a defect due to the convolution quadrature method, which is accessible by the general approximation result of Lemma B.1. The established bounds on $\boldsymbol{\mathcal{W}}(s)\boldsymbol{\mathcal{E}}_h(s)$ ensure that the approximation property of Lemma B.1 holds with the constants $M_\sigma \le C_\sigma h^{k+1}$, $\kappa = 6$ and $\nu = 3$.

Choosing $q = 2$ and $r = 10 > 2q - 1 + \kappa$, gives a convergence in time of order $\min(2q-1, q+1-\kappa+\nu) = q - 2 = 0$. The error term is therefore shown to be of the overall order $\mathcal{O}(h^{k+1})$ in the $\boldsymbol{H}(\mathbf{curl},\Omega)^2$-norm. Combining the defects yields overall the stated $\mathcal{O}(\tau^{m-1/2}+h^{k+1})$ error bound in the $\boldsymbol{H}(\mathbf{curl},\Omega)^2$ norm.

We turn our attention towards the full-order error bound away from the boundary. To derive

full-order error bounds for points away from the boundary, we rewrite the total error by

$$\begin{pmatrix} \boldsymbol{E}_h^n \\ \boldsymbol{H}_h^n \end{pmatrix} - \begin{pmatrix} \boldsymbol{E}_h(t_n) \\ \boldsymbol{H}_h(t_n) \end{pmatrix} \quad + \quad \begin{pmatrix} \boldsymbol{E}_h(t_n) \\ \boldsymbol{H}_h(t_n) \end{pmatrix} - \begin{pmatrix} \boldsymbol{E}(t_n) \\ \boldsymbol{H}(t_n) \end{pmatrix}.$$

Contrasting the argument structure before, the second difference is now the error of the spatial semi-discretization studied in part (b). The remaining first difference is a convolution quadrature defect for the transfer operator $\boldsymbol{\mathcal{U}}_h(s)$ of (3.67). For points away from the boundary, this operator decays exponentially in terms of the real part of s, which leads to favourable convergence properties of the convolution quadrature scheme. In particular, stronger convergence bounds are obtained by rewriting the remaining error as

$$\begin{pmatrix} \boldsymbol{E}_h^n \\ \boldsymbol{H}_h^n \end{pmatrix} - \begin{pmatrix} \boldsymbol{E}_h(t_n) \\ \boldsymbol{H}_h(t_n) \end{pmatrix} = \left[\left(\boldsymbol{\mathcal{U}}_h(\partial_t^\tau) \boldsymbol{g}^{\mathrm{inc}} \right)^{n-1} \right]_m - \boldsymbol{\mathcal{U}}_h(\partial_t) \boldsymbol{g}^{\mathrm{inc}}(t_n),$$

which is bounded with regards to the full classical order through Lemma B.1, by employing the exponentially decaying bounds from Lemmas 3.10–3.12.

□

Remark 3.5. *Pursuing the second approach for the $\boldsymbol{H}(\mathbf{curl}, \Omega)^2$ norm and applying Lemma B.1 results in error bounds with the reduced temporal order $O(\tau^{m-1})$.*

The proof of the above theorem further implies the following corollary, in which a convergence result is formulated for the boundary densities, namely the boundary data of the numerical solution. The concrete result is given by following the arguments of the previous proof, where the complete operator (3.67) simplifies to $\boldsymbol{L}_h(s)$.

Corollary 3.1. *Consider the setting and assumptions of Theorem 3.5. Then, the following error bounds hold for the approximations $\boldsymbol{\varphi}_h^n = \left[(\boldsymbol{\varphi}_h^\tau)^{n-1} \right]_m$ and $\boldsymbol{\psi}_h^n = \left[(\boldsymbol{\psi}_h^\tau)^{n-1} \right]_m$ in time and space at $t_n = n\tau \in [0, T]$*

$$\left\| \begin{pmatrix} \boldsymbol{\varphi}_h^n - \boldsymbol{\varphi}(t_n) \\ \boldsymbol{\psi}_h^n - \boldsymbol{\psi}(t_n) \end{pmatrix} \right\|_{H^{-1/2}(\Gamma) \times V} \leq C \left(\tau^m + h^{k+1} \right).$$

The constant C in the error bounds depend on the final time T, on the boundary Γ, on the incident waves through g^{inc} and on higher Sobolev norms of the exact solution $(\boldsymbol{\varphi}, \boldsymbol{\psi})$, but are crucially independent of h,n and τ. In particular, for the impedance operators (1.13)–(1.16), C is independent of the small parameter δ.

Remark 3.6 (Similarities to acoustic scattering)**.** *Many key results in the electromagnetic analysis are reminiscent of the previous acoustic analysis, starting from the settings of the respective transfer operators (2.8)–(2.9) and (3.8)–(3.9). The well-posedness of the transmission problem for the Helmholtz problem in Lemma 2.4 is analogous to the corresponding result for the time-harmonic Maxwell's equations in Lemma 3.3. Whereas the representation formulas differ in their specific form and their functional analytic setting, the bounds of the time-harmonic potential operators coincide. As a consequence, the well-posedness results for the acoustic scattering problems in Theorems 2.2 & 2.4 are structurally analogous to their electromagnetic counterparts in Theorem 3.2 and Theorem 3.4. The structural similarities*

of the boundary integral equations and the time-harmonic bounds of the associated boundary integral operator families leads to the similarities of the convergence result, which is seen by the analogous proofs of Theorem 2.5 and Theorem 3.5 respectively.

3.8. Numerical experiments

The numerical experiments and figures presented here are taken from the original paper [59]. The implementation that has been used for these experiments is available under [56]. As before in the acoustic experiments, we set our first numerical experiment in the exterior of the unit sphere centered around the origin. Consider the following incoming electric planar wave, a solution to Maxwell's equations on $\mathbb{R}^3$, which reads

$$\boldsymbol{E}^{\text{inc}}(t, \boldsymbol{x}) = e^{-c(t-x_3-t_0)^2}\boldsymbol{e}_1, \tag{3.71}$$

where $c = 50$, $\boldsymbol{e_1} = (1,0,0)^T$ and $t_0 = -2$. On the surface of the sphere, the strongly absorbing generalized impedance boundary condition (1.15) is employed, identified by the transfer operator $\boldsymbol{Z}(\partial_t) = \delta\partial_t^{1/2}$, with $\delta = 10^{-1}, 10$ respectively. The 0-th order Raviart–Thomas element space is employed as the boundary element space and the convolution quadrature method based on the Radau IIA Runge–Kutta method with 2 and 3 stages is used as the time discretization. To estimate the error of the scheme, a reference solution was computed with a space discretization with 23871 degrees of freedoms and the 3-stage Radau IIA time discretization with $N = 2^{10}$ time steps. The convergence plots are then obtained by mutually fixing various mesh sizes for the 0-th order Raviart–Thomas element space and time step sizes for the convolution quadrature method based on the 2-stage Radau IIA Runge–Kutta method, which was conducted for both values of δ to obtain the convergence plots.

Figure 3.2 and 3.3 illustrate the error bounds of Theorem 3.5. To obtain an estimate of the error, numerical approximations are computed at a simple point $\boldsymbol{P} = (2,0,0)$ and compared with the reference solution $\boldsymbol{E}_{ref}(\boldsymbol{P}, t_n)$.

Figure 3.2 is the temporal convergence plot, where the error for multiple grids corresponding to decreasing mesh width h is shown with varying time step sizes τ. For large τ we observe that the temporal error is dominating, where for small τ the error curves flatten out due to the dominating space convergence error. When the step size is large enough for the temporal error to dominate, we observe that the slope of the error curves approach the order of convergence of the theoretical result, as indicated by the reference lines.

Analogously, Figure 3.3 depicts two similar plots, corresponding to the parameters $\delta = 10^{-1}$ (left) and $\delta = 10$ (right), but reversing the roles of the mesh width h and the time step size τ, thus revealing the spatial convergence properties of the scheme. Even though the predicted convergence rates of Theorem 3.5 are independent of the small parameter δ, we expect in view of the acoustic result of Theorem 2.5 the stronger δ-explicit error bound $O(h^{k+3/2} + \delta^{1/2}h^{k+1})$ to hold. The numerical results indicate that the dependence on the small δ is favourable for the presented example, though for h small enough the observed error behaviour is very similar. This behaviour is predicted by the theory, but might also be explained by the fact that the exact solution depends on δ.

We conclude this section by computing the $3D$-scattering arising from a torus with a revolving circle of radius $r = 0.2$, where the outer centers lie on a circle of radius $R = 0.8$, which is illuminated by the planar wave (3.71) with $t_0 = -1$. On the surface of the scatterer, strongly absorbing boundary conditions corresponding to the impedance operator $\boldsymbol{Z}(\partial_t) = \delta \partial_t^{1/2}$ with $\delta = 0.1$ are employed.

A 0-th order Raviart–Thomas element space with 2688 degrees of freedom is employed and combined with the convolution quadrature based on the 3-stage Radau IIA method with $N = 100$ time steps. Two types of figures are generated from this computation, starting from Figure 3.1, which visualizes the frequencies s_k for $k = 1, \ldots, mL$ (L being the amount of Laplace transform evaluations used in the underlying trapezoidal quadrature rule), at which the Laplace domain operator $\boldsymbol{\mathcal{U}}_h(s_k)$ is evaluated during the computation. On the right-hand side, the condition number of the arising systems $\boldsymbol{A}_h(s)$ is visualized, as the reader follows the contour depicted on the left plot. Several markers relate the position of the complex frequencies in the Laplace domain and the condition numbers. Throughout the contour, the condition numbers remain mild and enable the effective use of iterative solvers to solve the arising resulting linear systems. The resulting numerical approximation is then visualized in Figures 3.4–3.5, which show the absolute value of the approximated total wave $\boldsymbol{E}^{\text{tot}}$ on the $x_2 = 0$ plane at different times.

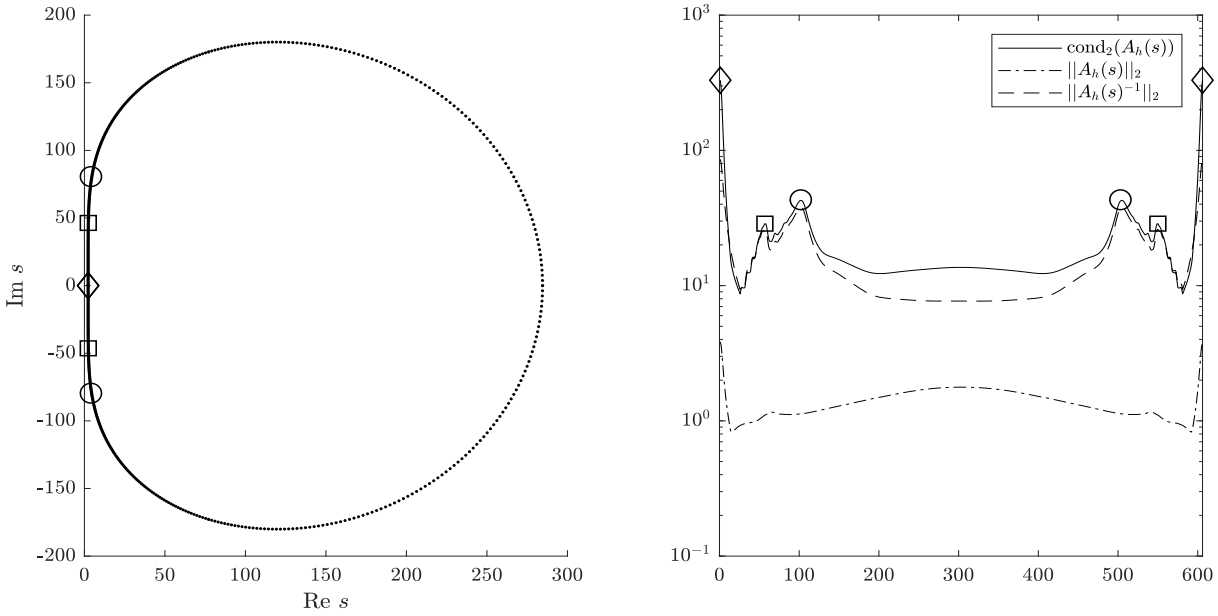

Figure 3.1.: The left-hand side plot shows a plot of the occurring frequencies for the 3-stage Radau IIA method for $N = 100$ and $T = 4$. On the right-hand side, the condition numbers and the euclidean norms of the occurring matrices are shown, as they appear when following the integral contour on the left-hand side. The markers on both plots localize the corresponding spikes of the condition numbers on the integral contour. The figure and its description are taken from [59, Figure 7.3].

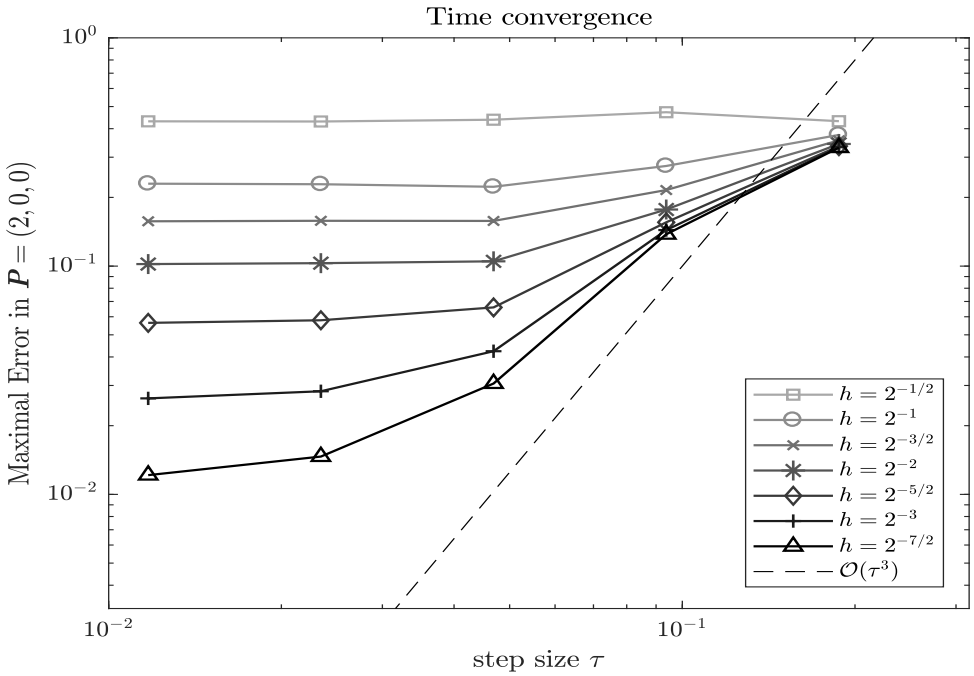

Figure 3.2.: Convergence plot in time for the fully discrete problem, with $\delta = 0.1$, taken from [59, Figure 7.1].

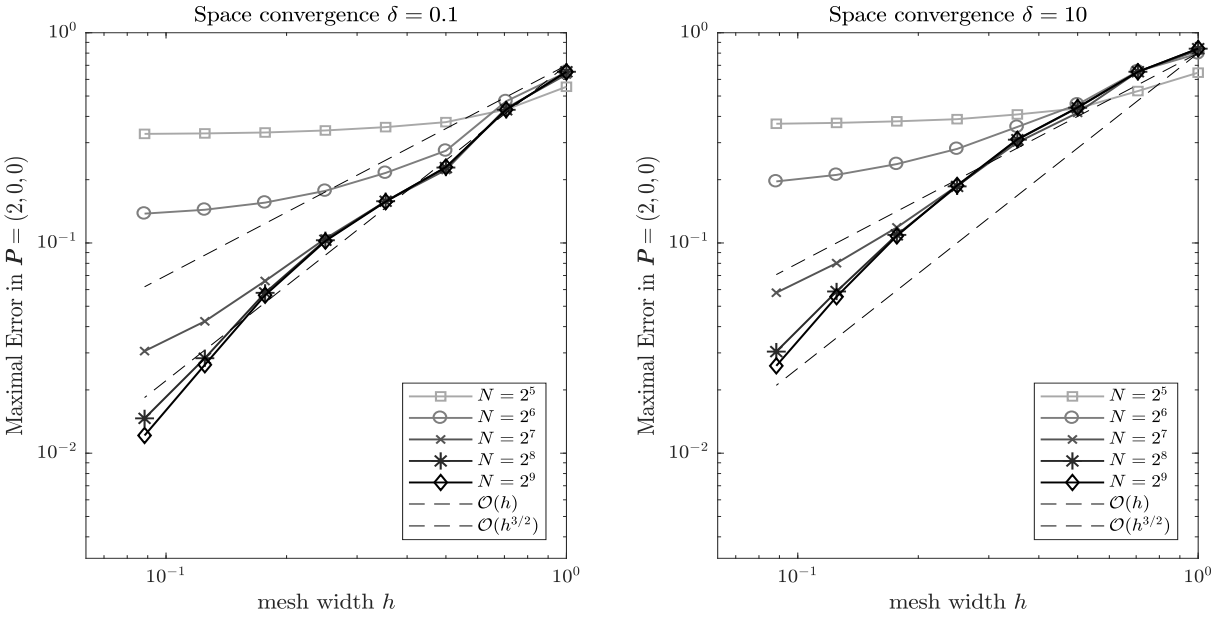

Figure 3.3.: Space convergence plot of the fully discrete system, with varying layer thickness $\delta = 10^{-2}$ (left), and $\delta = 10$ (right), taken from [59, Figure 7.2].

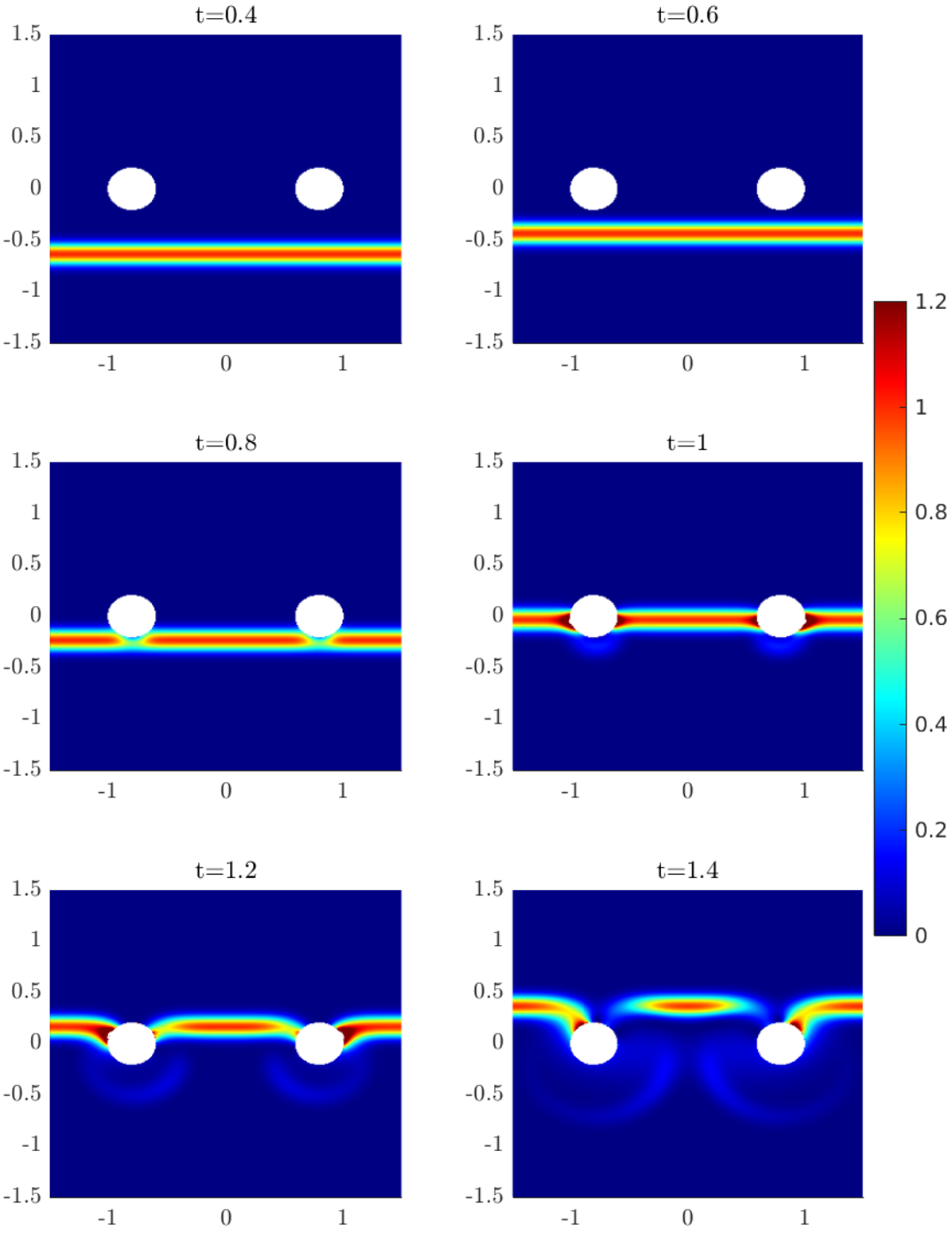

Figure 3.4.: 3D-scattering arising from the boundary condition (1.15) with $\delta = 0.1$, employed at a torus. Shown is the $x_2 = 0$ plane, through the middle of the scatterer at several times t in the time interval $[0.4, 1.4]$. The data was originally generated for [59, Figure 7.4].

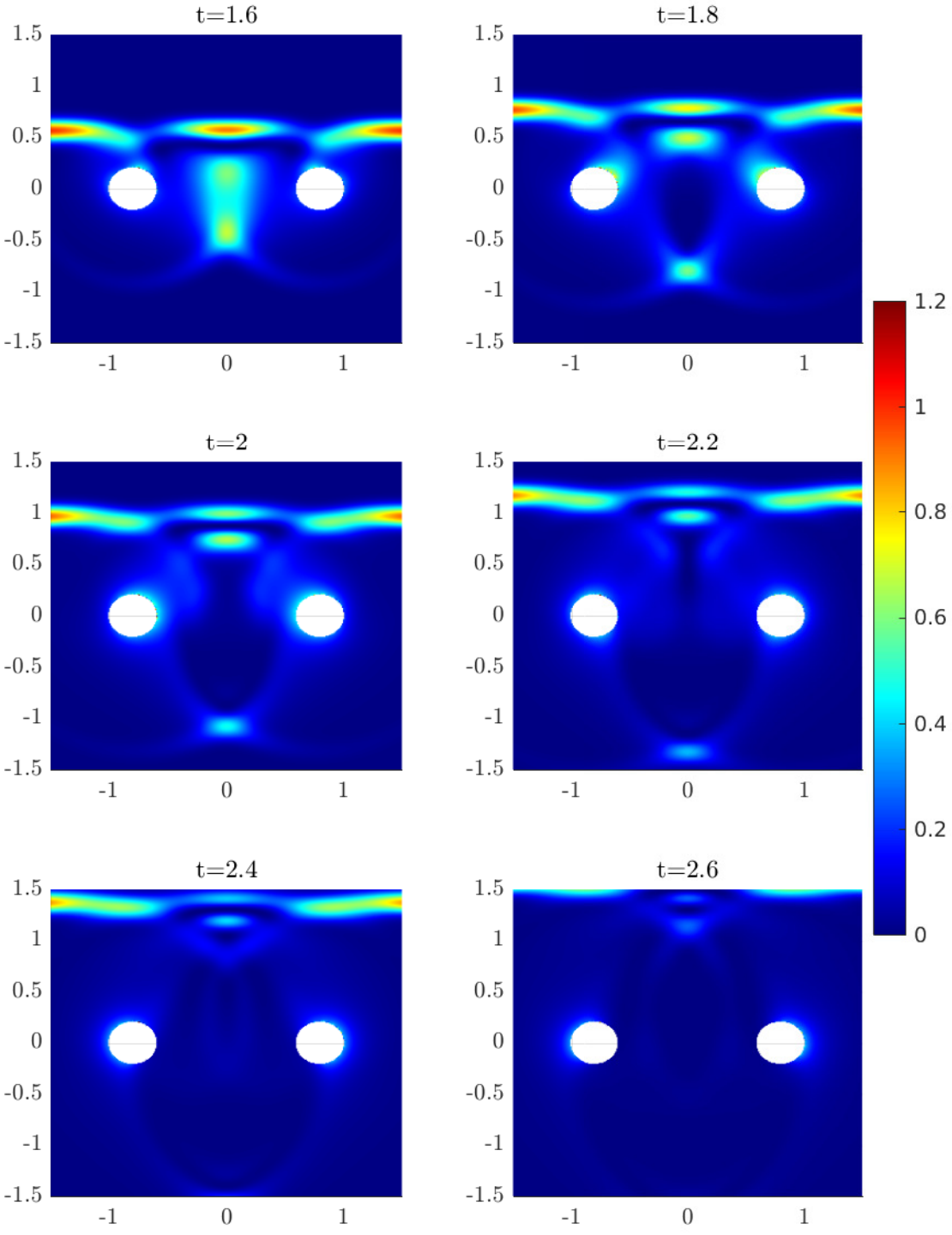

Figure 3.5.: 3D-scattering arising from the boundary condition (1.15) with $\delta = 0.1$, employed at a torus. Shown is the $x_2 = 0$ plane, through the middle of the scatterer at several times t in the time interval $[1.6, 2.6]$. The data was originally generated for [59, Figure 7.4].

4. Nonlinear electromagnetic scattering

The final class of boundary conditions studied in this thesis is a nonlinear extension of the previous boundary conditions, where the impedance operator is nonlinear, but fulfills a crucial monotonicity condition. The traces of the electric and magnetic fields are said to fulfill the nonlinear boundary condition if

$$\boldsymbol{E}^{\text{tot}} \times \boldsymbol{\nu} + \boldsymbol{a}(\boldsymbol{H}^{\text{tot}} \times \boldsymbol{\nu}) \times \boldsymbol{\nu} = 0 \quad \text{on } \Gamma = \partial\Omega, \tag{4.1}$$

where $\boldsymbol{\nu}$ denotes again the outer unit normal vector. Note that the rescaling of $\boldsymbol{H}$ with regards to the physical constant μ is, in this formulation of the boundary condition, assumed to be incorporated into the nonlinearity $\boldsymbol{a}$.

The formulation of this boundary condition is very close to the previously covered boundary condition, yet serious novel challenges arise, in particular in the error analysis of the subsequent sections. Throughout this chapter, we restrict the range of nonlinearities to the following type of power-law

$$\boldsymbol{a}(\boldsymbol{x}) = |\boldsymbol{x}|^{\alpha-1}\boldsymbol{x} \quad \text{for all } \boldsymbol{x} \in \mathbb{R}^3, \tag{4.2}$$

for some $\alpha \in (0,1]$. The above formulation is found in the literature (e.g. [66, 67, 70]) and is the natural nonlinear extension of the previous boundary condition. In the original paper of the author [57], this formulation is used to give a complete numerical analysis. This chapter transports the treatment there to the following (equivalent) inverted formulation

$$\boldsymbol{H}^{\text{tot}} \times \boldsymbol{\nu} + \boldsymbol{b}(-\boldsymbol{E}^{\text{tot}} \times \boldsymbol{\nu}) \times \boldsymbol{\nu} = 0 \quad \text{on } \Gamma = \partial\Omega, \tag{4.3}$$

where $\boldsymbol{b}$ denotes the inverse of $\boldsymbol{a}$, which has the closed form

$$\boldsymbol{b}(\boldsymbol{x}) = \boldsymbol{a}^{-1}(\boldsymbol{x}) = |\boldsymbol{x}|^{\frac{1-\alpha}{\alpha}}\boldsymbol{x} \quad \text{for all } \boldsymbol{x} \in \mathbb{R}^3. \tag{4.4}$$

It should be noted that the above transformation only holds for nonlinearities which commute with a rotation around the normal vector, namely the nonlinearity is required to fulfill $\boldsymbol{b}(\boldsymbol{\nu} \times \boldsymbol{x}) = \boldsymbol{\nu} \times \boldsymbol{b}(\boldsymbol{x})$ for all $\boldsymbol{x}, \boldsymbol{\nu} \in \mathbb{R}^3$. Without such a property, the inverted boundary condition is generally of a more convoluted form. The derivation of boundary integral equations for this formulation slightly differs in comparison to the previous chapter.

4.1. Problem setting

We reformulate the electromagnetic nonlinear scattering problem in terms of the scattered fields $\boldsymbol{E}$ and $\boldsymbol{H}$. The incident waves are again denoted by $(\boldsymbol{E}^{\text{inc}}, \boldsymbol{H}^{\text{inc}})$ and fulfill the same

conditions as in the previous chapter. As such, they are assumed to be solutions to the time-dependent Maxwell's equations on the whole free space $\mathbb{R}^3$, with initial support away from the boundary Γ.

The scattered fields $\boldsymbol{E} = \boldsymbol{E}^{\text{tot}} - \boldsymbol{E}^{\text{inc}}$ and $\boldsymbol{H} = \boldsymbol{H}^{\text{tot}} - \boldsymbol{H}^{\text{inc}}$, which arise due to the nonlinear boundary condition employed at the surface of the scatterer, then solve the following initial–boundary value problem of Maxwell's equations:

$$\partial_t \boldsymbol{E} - \mathbf{curl}\, \boldsymbol{H} = 0 \qquad \text{in} \quad \Omega, \tag{4.5}$$

$$\partial_t \boldsymbol{H} + \mathbf{curl}\, \boldsymbol{E} = 0 \qquad \text{in} \quad \Omega, \tag{4.6}$$

$$\boldsymbol{H} \times \boldsymbol{\nu} + \boldsymbol{\nu} \times \boldsymbol{b}(-\boldsymbol{E} \times \boldsymbol{\nu} - \boldsymbol{E}^{\text{inc}} \times \boldsymbol{\nu}) = -\boldsymbol{H}^{\text{inc}} \times \boldsymbol{\nu} \quad \text{on} \quad \Gamma. \tag{4.7}$$

The boundary value problem is completed by vanishing initial conditions.

In order to derive a weak formulation of the boundary condition and subsequently boundary integral equations, an appropriate functional analytic framework is necessary. Such a setting of the nonlinear scattering problem must reconcile the properties of the nonlinearity $\boldsymbol{b}$ with the previously discussed setting of Maxwell's equations. The following section investigates the nonlinearity and provides fundamental results for the subsequent analysis.

4.1.1. Functional analytical setting of the nonlinear function b

For $\alpha \in (0, 1]$, we repeat the power-law type nonlinearity from the boundary condition originally discussed in [66] and occuring in the nonlinear evolution equation described in [70], whose inverse reads

$$\boldsymbol{b}(\boldsymbol{x}) = |\boldsymbol{x}|^{\frac{1-\alpha}{\alpha}} \boldsymbol{x}, \quad \text{for } \boldsymbol{x} \in \mathbb{R}^3. \tag{4.8}$$

Several positivity conditions apply to this boundary condition, in particular for arbitrary $\boldsymbol{x} \in \mathbb{R}^3$, we trivially obtain

$$\boldsymbol{x} \cdot \boldsymbol{b}(\boldsymbol{x}) = |\boldsymbol{x}|^{\frac{1+\alpha}{\alpha}}. \tag{4.9}$$

This identity, completed by a bound from above, provides the necessary foundation for a stability estimate of the continuous problem. The error analysis in the subsequent sections requires stronger pointwise properties, specifically a strong monotonicity condition.

The following lemma gives such bounds, estimating the differences of $\boldsymbol{b}$ from above and below.

Lemma 4.1 (Pointwise bounds on $\boldsymbol{b}$). *Consider the nonlinearity $\boldsymbol{b}(\boldsymbol{x}) = |\boldsymbol{x}|^{\frac{\alpha-1}{\alpha}} \boldsymbol{x}$ for some $\alpha \in (0, 1]$. There exists a constant c_α, depending only on α, such that for all $\boldsymbol{u}, \boldsymbol{v} \in \mathbb{R}^3$, it holds that*

$$(\boldsymbol{u} - \boldsymbol{v}) \cdot (\boldsymbol{b}(\boldsymbol{u}) - \boldsymbol{b}(\boldsymbol{v})) \geq c_\alpha \, |\boldsymbol{u} - \boldsymbol{v}|^{\frac{1+\alpha}{\alpha}}. \tag{4.10}$$

Additionally, there exists a positive constant C_α , depending only on α, such that the following bound

$$|\boldsymbol{b}(\boldsymbol{u}) - \boldsymbol{b}(\boldsymbol{v})| \leq C_\alpha \left(|\boldsymbol{u}| + |\boldsymbol{v}|\right)^{\frac{1-\alpha}{\alpha}} |\boldsymbol{u} - \boldsymbol{v}|\,, \tag{4.11}$$

holds for all $\boldsymbol{u}, \boldsymbol{v} \in \mathbb{R}^3$.

Proof. The strong monotonicity result is found in [69][Lemma 2.3.16]. We continue with the bound on the difference from above. The Jacobian of the nonlinearity $\boldsymbol{b}$, in the following denoted by $\boldsymbol{Db} : \mathbb{R}^3 \to \mathbb{R}^{3\times 3}$, is derived from standard integration rules and has the explicit form

$$\mathcal{D}\boldsymbol{b}_{\boldsymbol{x}} = \frac{1-\alpha}{\alpha} |\boldsymbol{x}|^{\frac{1-\alpha}{\alpha}-2} \boldsymbol{x}\boldsymbol{x}^t + |\boldsymbol{x}|^{\frac{1-\alpha}{\alpha}} \boldsymbol{I}_3 \quad \text{for } \boldsymbol{x} \in \mathbb{R}^3 \setminus \{0\},$$

where $\boldsymbol{I}_3 \in \mathbb{R}^{3\times 3}$ denotes the identity matrix. The second bound is then given by applying the fundamental theorem of calculus, which yields

$$\begin{aligned} |\boldsymbol{b}(\boldsymbol{u}) - \boldsymbol{b}(\boldsymbol{v})| &= \left| \int_0^1 \frac{\mathrm{d}}{\mathrm{d}\theta} \boldsymbol{b}(\boldsymbol{v} + \theta(\boldsymbol{u} - \boldsymbol{v}))\, \mathrm{d}\theta \right| = \left| \int_0^1 \boldsymbol{Db}_{\boldsymbol{v}+\theta(\boldsymbol{u}-\boldsymbol{v})}(\boldsymbol{u} - \boldsymbol{v})\, \mathrm{d}\theta \right| \\ &\leq C_\alpha |\boldsymbol{u} - \boldsymbol{v}| \int_0^1 |\boldsymbol{v} + \theta(\boldsymbol{u} - \boldsymbol{v})|^{\frac{1-\alpha}{\alpha}}\, \mathrm{d}\theta \\ &\leq C_\alpha |\boldsymbol{u} - \boldsymbol{v}| \left(|\boldsymbol{u}| + |\boldsymbol{v}|\right)^{\frac{1-\alpha}{\alpha}}. \end{aligned} \tag{4.12}$$

□

An alternative inequality to (4.11) is seen by repeating the steps from (4.12) and estimating

$$\begin{aligned} |\boldsymbol{b}(\boldsymbol{u}) - \boldsymbol{b}(\boldsymbol{v})| &\leq C_\alpha |\boldsymbol{u} - \boldsymbol{v}| \int_0^1 |\boldsymbol{v} + \theta(\boldsymbol{u} - \boldsymbol{v})|^{\frac{1-\alpha}{\alpha}}\, \mathrm{d}\theta \\ &\leq C_\alpha \left(|\boldsymbol{v}|^{\frac{1-\alpha}{\alpha}} |\boldsymbol{u} - \boldsymbol{v}| + |\boldsymbol{u} - \boldsymbol{v}|^{\frac{1}{\alpha}} \right). \end{aligned} \tag{4.13}$$

In addition to the pointwise bounds, we interpret the function $\boldsymbol{b}$ as a nonlinear operator acting on appropriate Banach spaces. More precisely, we give function spaces on which the nonlinear operator defined by the composition with $\boldsymbol{b}$ acts, namely the operator $\boldsymbol{u} \mapsto \boldsymbol{b} \circ \boldsymbol{u}$ for appropriate vector fields on the boundary $\boldsymbol{u} \colon \Gamma \to \mathbb{R}^3$.

Due to the power-law structure of the nonlinearity, the natural spaces are the $\boldsymbol{L}^p$ space for $p > 1$ on the boundary Γ, which are defined by

$$\boldsymbol{L}^p_T(\Gamma) = \{\boldsymbol{u} \in \boldsymbol{L}^p(\Gamma) \mid \boldsymbol{u} \cdot \boldsymbol{\nu} = 0\}.$$

The spaces are completed with the associated norm inherited from the full space $\boldsymbol{L}^p(\Gamma)$ defined by

$$\|\boldsymbol{u}\|_{\boldsymbol{L}^p(\Gamma)} = \left(\int_\Gamma |\boldsymbol{u}|^p \right)^{\frac{1}{p}}.$$

Lemma 4.2 (Setting of $\boldsymbol{b}$). *Consider the nonlinear operator defined by the composition with the nonlinearity $\boldsymbol{b}(\boldsymbol{x}) = |\boldsymbol{x}|^{\frac{1-\alpha}{\alpha}}\,\boldsymbol{x}$ for $\alpha \in (0,1]$. This operator is well-posed and bijective on the spaces*

$$\boldsymbol{b} : \boldsymbol{L}_T^{\frac{1+\alpha}{\alpha}}(\Gamma) \to \boldsymbol{L}_T^{1+\alpha}(\Gamma). \tag{4.14}$$

Proof. Inserting the closed form of $\boldsymbol{b}$ yields

$$\|\boldsymbol{b}(\boldsymbol{u})\|_{\boldsymbol{L}^{1+\alpha}(\Gamma)} = \left\| |\boldsymbol{u}|^{\frac{1-\alpha}{\alpha}}\,\boldsymbol{u} \right\|_{\boldsymbol{L}^{1+\alpha}(\Gamma)} = \left\| |\boldsymbol{u}|^{\frac{1}{\alpha}} \right\|_{L^{1+\alpha}(\Gamma)} = \|\boldsymbol{u}\|^{\frac{1}{\alpha}}_{\boldsymbol{L}^{\frac{1+\alpha}{\alpha}}(\Gamma)}, \tag{4.15}$$

which in particular shows that the left-hand side is bounded for arbitrary $\boldsymbol{u} \in \boldsymbol{L}_T^{\frac{1+\alpha}{\alpha}}(\Gamma)$. The well-posedness of the inverse is seen analogously by repeating the argument for the function

$$\boldsymbol{b}^{-1}(\boldsymbol{x}) = |\boldsymbol{x}|^{\alpha-1}\,\boldsymbol{x},$$

which shows that $\boldsymbol{b}$ is a bijection. □

As the boundary $\Gamma = \partial\Omega$ of the scatterer is a bounded surface, we have the following chain of dense inclusions

$$\boldsymbol{L}_T^{\frac{1+\alpha}{\alpha}}(\Gamma) \subset \boldsymbol{L}_T^{2}(\Gamma) \subset \boldsymbol{L}_T^{1+\alpha}(\Gamma). \tag{4.16}$$

The pivot space $\boldsymbol{L}_T^2$ makes the above spaces their respective duals, as the sum of the reciprocal of their exponents is one. More precisely, the $\boldsymbol{L}^2$-scalar product is a continuous hermitian bilinear form on $\boldsymbol{L}_T^{\frac{1+\alpha}{\alpha}}(\Gamma) \times \boldsymbol{L}_T^{1+\alpha}(\Gamma)$ and makes these spaces their respective dual. This property is ensured by Hölder's inequality, which reads for boundary functions $\boldsymbol{u}$ and $\boldsymbol{v}$ in the respective spaces

$$(\boldsymbol{u}, \boldsymbol{v})_\Gamma \leq \|\boldsymbol{u}\|_{\boldsymbol{L}^{1+\alpha}(\Gamma)}\, \|\boldsymbol{v}\|_{\boldsymbol{L}^{\frac{1+\alpha}{\alpha}}(\Gamma)}. \tag{4.17}$$

The nonlinear operator $\boldsymbol{b}$, understood on these spaces, therefore maps into the dual of its domain, where the anti-duality between both spaces takes the explicit form of an extended $\boldsymbol{L}^2$-pairing.

We combine the proper trace space in the context of Maxwell's equations discussed in the previous section with the setting of the nonlinearity $\boldsymbol{b}$, which yields a suitable setting for the boundary integral equation corresponding to the nonlinear scattering problem (4.5)–(4.7). For this purpose, we introduce the dense subspace

$$\boldsymbol{V}_\Gamma = \boldsymbol{X}_\Gamma \cap \boldsymbol{L}_T^{\frac{1+\alpha}{\alpha}}(\Gamma) \subset \boldsymbol{X}_\Gamma,$$

equipped with the associated norm

$$\|\boldsymbol{\phi}\|_{\boldsymbol{V}_\Gamma} = \|\boldsymbol{\phi}\|_{\boldsymbol{X}_\Gamma} + \|\boldsymbol{\phi}\|_{\boldsymbol{L}^{\frac{1+\alpha}{\alpha}}(\Gamma)}.$$

4.1.2. Weak formulation of the nonlinear boundary condition

Consider some time-independent continuous tangential vector field $\boldsymbol{\phi}$ on the boundary Γ. Testing the strong formulation of the boundary condition (4.7) by means of the anti-symmetric product $[\cdot,\cdot]_\Gamma$ with $\boldsymbol{\phi}$ yields

$$[\boldsymbol{\phi}, \gamma_T \boldsymbol{H}]_\Gamma + [\boldsymbol{\phi}, \boldsymbol{b}(-\gamma_T \boldsymbol{E} - \gamma_T \boldsymbol{E}^{\text{inc}}) \times \boldsymbol{\nu}]_\Gamma = -[\boldsymbol{\phi}, \gamma_T \boldsymbol{H}^{\text{inc}}]_\Gamma. \tag{4.18}$$

The tested nonlinearity reduces to the $\boldsymbol{L}^2(\Gamma)$ inner product, which reveals the *weak formulation of the nonlinear boundary condition* (4.3): find $\boldsymbol{E}, \boldsymbol{H} \in \boldsymbol{L}^2(0,T;\boldsymbol{H}(\mathbf{curl},\Omega)) \cap \boldsymbol{H}^1(0,T;\boldsymbol{L}^2(\Omega)^3)$, solutions to the time-dependent Maxwell's equations with vanishing initial conditions, such that their tangential traces $(\gamma_T \boldsymbol{H}, \gamma_T \boldsymbol{E}) \in \boldsymbol{L}^2(0,T;\boldsymbol{X}_\Gamma \times \boldsymbol{V}_\Gamma)$ fulfill for almost every $t \in (0,T)$

$$[\boldsymbol{\phi}, \gamma_T \boldsymbol{H}]_\Gamma + (\boldsymbol{\phi}, \boldsymbol{b}(-\gamma_T \boldsymbol{E} - \gamma_T \boldsymbol{E}^{\text{inc}}))_\Gamma = [\gamma_T \boldsymbol{H}^{\text{inc}}, \boldsymbol{\phi}]_\Gamma \qquad \text{for all } \boldsymbol{\phi} \in \boldsymbol{V}_\Gamma. \tag{4.19}$$

The above expressions are well-defined under the stated regularity assumptions.

4.1.3. Time-dependent representation formulas and a time-dependent transmission problem

Analogously to the time-harmonic analysis of the previous chapters, we introduce a time-dependent transmission problem, which is the starting point for the subsequent stability analysis. This result rigorously associates electromagnetic fields on the domain to any pair of time-dependent boundary densities in $\boldsymbol{X}_\Gamma$ with sufficient temporal regularity.

Let $k \geq 2$ and consider boundary densities $(\boldsymbol{\varphi}, \boldsymbol{\psi}) \in \boldsymbol{H}_0^k(0,T;\boldsymbol{X}_\Gamma \times \boldsymbol{X}_\Gamma)$, which are generally not the tangential traces of solutions to the time-dependent Maxwell's equations. Associated temporal electromagnetic fields $\boldsymbol{E}, \boldsymbol{H} \in \boldsymbol{H}_0^{k-2}(0,T;\boldsymbol{H}(\mathbf{curl},\mathbb{R}^3 \setminus \Gamma))$ are then obtained by the time-dependent representation formulas (already formulated in (3.54)–(3.55), but repeated here due to their central role in this chapter)

$$\boldsymbol{E} = -\boldsymbol{\mathcal{S}}(\partial_t)\boldsymbol{\varphi} + \boldsymbol{\mathcal{D}}(\partial_t)\boldsymbol{\psi}, \tag{4.20}$$

$$\boldsymbol{H} = -\boldsymbol{\mathcal{D}}(\partial_t)\boldsymbol{\varphi} - \boldsymbol{\mathcal{S}}(\partial_t)\boldsymbol{\psi}. \tag{4.21}$$

The temporal convolution operators are again defined via the Heaviside notation of operational calculus (1.2) and the time-harmonic potential operators. With these fields $(\boldsymbol{E}, \boldsymbol{H})$, the following time-dependent transmission problem holds

$$\partial_t \boldsymbol{E} - \mathbf{curl}\, \boldsymbol{H} = 0 \qquad \text{in} \quad \mathbb{R}^3 \setminus \Gamma, \tag{4.22}$$

$$\partial_t \boldsymbol{H} + \mathbf{curl}\, \boldsymbol{E} = 0 \qquad \text{in} \quad \mathbb{R}^3 \setminus \Gamma, \tag{4.23}$$

$$[\gamma_T]\boldsymbol{H} = \boldsymbol{\varphi}, \tag{4.24}$$

$$-[\gamma_T]\boldsymbol{E} = \boldsymbol{\psi}. \tag{4.25}$$

The fields $\boldsymbol{E}$ and $\boldsymbol{H}$ solve the time-dependent Maxwell's equations(4.22)–(4.23) away from the boundary, by construction of the potential operators. The relations on the boundary (4.24)–

(4.25) follow from the jump conditions of the potential operators. Moreover, the complete transmission problem is a consequence of applying the inverse Laplace transform to the analogous time-harmonic transmission problem (3.20)–(3.23).

The time-dependent Calderón operator fulfills temporal jump conditions, which are analogous to the time-harmonic jump conditions (3.33), which read in the setting of the above transmission problem

$$\boldsymbol{C}(\partial_t)\begin{pmatrix}[\gamma_T \boldsymbol{H}]\\ -[\gamma_T \boldsymbol{E}]\end{pmatrix} = \begin{pmatrix}\{\gamma_T \boldsymbol{E}\}\\ \{\gamma_T \boldsymbol{H}\}\end{pmatrix}. \tag{4.26}$$

The time-harmonic coercivity result for the Calderón operator in Lemma 3.7 implies a time domain coercivity result via the operator-valued Herglotz theorem [16, Lemma 2.2]. With this result, we obtain a constant c_T, only depending polynomially on the inverse of T and Γ, such that

$$\int_0^T e^{-t/T}\left[\begin{pmatrix}\boldsymbol{\varphi}\\ \boldsymbol{\psi}\end{pmatrix}, \boldsymbol{C}(\partial_t)\begin{pmatrix}\boldsymbol{\varphi}\\ \boldsymbol{\psi}\end{pmatrix}\right]_\Gamma \mathrm{d}t \geq c_T \int_0^T e^{-t/T}\left(\left\|\partial_t^{-1}\boldsymbol{\varphi}\right\|^2_{\boldsymbol{X}_\Gamma} + \left\|\partial_t^{-1}\boldsymbol{\psi}\right\|^2_{\boldsymbol{X}_\Gamma}\right)\mathrm{d}t, \tag{4.27}$$

for $(\boldsymbol{\varphi}, \boldsymbol{\psi}) \in \boldsymbol{H}^5_0(0,T;{\boldsymbol{X}_\Gamma}^2)$. Details are found in [16, Lemma 4.1]. A positivity result of this type is crucial for the stability analysis of boundary integral equations derived from the time-dependent Calderón operator.

Consider now the time-dependent electromagnetic fields $\boldsymbol{E}, \boldsymbol{H} \in \boldsymbol{L}^2(0,T;\boldsymbol{H}(\mathbf{curl},\Omega))$, solutions to the time-dependent Maxwell's equations with vanishing initial conditions in the exterior domain Ω. Together with the tangential traces

$$\boldsymbol{\varphi} = \gamma_T \boldsymbol{H}, \qquad \boldsymbol{\psi} = -\gamma_T \boldsymbol{E}, \tag{4.28}$$

the representation formulas (4.20)–(4.21) and the time-dependent transmission problem (4.22)–(4.25) holds, when the $\boldsymbol{E}$ and $\boldsymbol{H}$ are completed by zero in the interior domain Ω^-.

Under these assumptions, the temporal jump conditions of the time-dependent Calderón operator (4.26) reduce to

$$\boldsymbol{C}(\partial_t)\begin{pmatrix}\gamma_T \boldsymbol{H}\\ -\gamma_T \boldsymbol{E}\end{pmatrix} = \frac{1}{2}\begin{pmatrix}\gamma_T \boldsymbol{E}\\ \gamma_T \boldsymbol{H}\end{pmatrix}. \tag{4.29}$$

These jump conditions are the familiar starting point of the previous chapters (in the time-harmonic setting) and originally of [13, 18]. Green's formula for the electromagnetic fields on the interior and exterior domains respectively gives, upon inserting (4.22)–(4.23), the crucial identities

$$\begin{aligned}[\gamma_T \boldsymbol{H}, \gamma_T \boldsymbol{E}]_\Gamma &= \pm\int_{\Omega^\pm} \mathbf{curl}\,\boldsymbol{H}\cdot\boldsymbol{E} - \boldsymbol{H}\cdot\mathbf{curl}\,\boldsymbol{E}\,\mathrm{d}\boldsymbol{x} \\ &= \pm\frac{1}{2}\partial_t \int_{\Omega^\pm} |\boldsymbol{E}|^2 + |\boldsymbol{H}|^2\,\mathrm{d}\boldsymbol{x}.\end{aligned} \tag{4.30}$$

4.2. Maxwell's equations with the nonlinear boundary condition

In contrast to the treatment in the previous chapter, we subtract a symmetric block operator to obtain the following alternative shifted Calderón operator

$$\boldsymbol{C}^{-}_{\mathrm{imp}}(\partial_t)\begin{pmatrix}\gamma_T\boldsymbol{H}\\ -\gamma_T\boldsymbol{E}\end{pmatrix}=\begin{pmatrix}0\\ \gamma_T\boldsymbol{H}\end{pmatrix},\qquad \boldsymbol{C}^{-}_{\mathrm{imp}}(\partial_t)=\boldsymbol{C}(\partial_t)-\begin{pmatrix}0 & -\frac{1}{2}\boldsymbol{I}\\ -\frac{1}{2}\boldsymbol{I} & 0\end{pmatrix}. \tag{4.31}$$

The jump conditions are weakly formulated by testing with $(\boldsymbol{\eta},\boldsymbol{\xi})\in\boldsymbol{X}_\Gamma\times\boldsymbol{V}_\Gamma$, which yields

$$\left[\begin{pmatrix}\boldsymbol{\eta}\\ \boldsymbol{\xi}\end{pmatrix},\boldsymbol{C}^{-}_{\mathrm{imp}}(\partial_t)\begin{pmatrix}\boldsymbol{\varphi}\\ \boldsymbol{\psi}\end{pmatrix}\right]_\Gamma=[\boldsymbol{\eta},\gamma_T\boldsymbol{H}]_\Gamma\,.$$

Inserting the weak formulation of the nonlinear boundary condition (4.19) into the right-hand side and rearranging all terms depending on the unknown scattered wave to the left-hand side reveals the weak formulation of the boundary integral equation.

Nonlinear boundary integral equation: *Find $(\boldsymbol{\varphi},\boldsymbol{\psi})\in\boldsymbol{L}^2_0(0,T;\boldsymbol{X}_\Gamma\times\boldsymbol{V}_\Gamma)$, the temporal boundary densities, such that for all $(\boldsymbol{\eta},\boldsymbol{\xi})\in\boldsymbol{X}_\Gamma\times\boldsymbol{V}_\Gamma$ it holds that*

$$\left[\begin{pmatrix}\boldsymbol{\eta}\\ \boldsymbol{\xi}\end{pmatrix},\boldsymbol{C}^{-}_{\mathrm{imp}}(\partial_t)\begin{pmatrix}\boldsymbol{\varphi}\\ \boldsymbol{\psi}\end{pmatrix}\right]_\Gamma+(\boldsymbol{\xi},\boldsymbol{b}(\boldsymbol{\psi}-\gamma_T\boldsymbol{E}^{\mathrm{inc}}))_\Gamma=[\gamma_T\boldsymbol{H}^{\mathrm{inc}},\boldsymbol{\xi}]_\Gamma. \tag{4.32}$$

By construction, the boundary data of a solution to the time-dependent nonlinear electromagnetic scattering problem (4.5)–(4.7) solves the above boundary integral equation. The converse statement is also true but not as easily seen from the construction. In the subsequent section, such an equivalence result of the scattering problem and the boundary integral equation is established, which leads to a stability result of the boundary integral equation.

Remark 4.1. *For any $\sigma>0$, we find an equivalent boundary integral equation, which has been shifted in the frequency domain, in the following sense. We denote the (in the Laplace domain) shifted Calderón operator with $\widetilde{\boldsymbol{C}_{imp}}^{-}(s)=\boldsymbol{C}^{-}_{imp}(s+\sigma)$. The boundary integral equation (4.32) is then equivalent to the boundary integral equation*

$$\left[\begin{pmatrix}\boldsymbol{\eta}\\ \boldsymbol{\xi}\end{pmatrix},\widetilde{\boldsymbol{C}_{imp}}^{-}(\partial_t)\begin{pmatrix}\widetilde{\boldsymbol{\varphi}}\\ \widetilde{\boldsymbol{\psi}}\end{pmatrix}\right]_\Gamma+e^{-\sigma t}(\boldsymbol{\xi},\boldsymbol{b}(e^{\sigma t}\widetilde{\boldsymbol{\psi}}-\gamma_T\boldsymbol{E}^{\mathrm{inc}}))_\Gamma=e^{-\sigma t}[\gamma_T\boldsymbol{H}^{inc},\boldsymbol{\xi}]_\Gamma, \tag{4.33}$$

where solutions of the above system of equations are related to the previous boundary densities via $\widetilde{\boldsymbol{\varphi}}=e^{-\sigma t}\boldsymbol{\varphi}$ and $\widetilde{\boldsymbol{\psi}}=e^{-\sigma t}\boldsymbol{\psi}$. In that sense, this boundary integral equation is equivalent to (4.32) and their solutions coincide up to this factor. Numerical discretizations of this system of boundary integral equations generally differ and lead to slightly different schemes. Moreover, large parts of the subsequent error analysis (more precisely, the error analysis for multistage methods with more than 2 stages) require such a positive shift, though numerical experiments indicate that such a shift is not necessary for practical computations.

4.2.1. Bounds on the solution of the boundary integral equation

The following result clarifies the connection of the boundary integral equation and the associated scattering problem, and concludes with a bound on the exact solution in terms of the incident waves. Additionally, the uniqueness of solutions to the boundary integral equation is shown. An existence result for solutions of the boundary integral equation is beyond the scope of this thesis, but can be deduced from the well-posedness of the scattering problem, which can be proven by employing the theory of monotone operators (see [31, Corollary 2.6]).

Proposition 4.1 (Bounds on the exact solution)**.** *Consider the time-dependent boundary densities $(\boldsymbol{\varphi}, \boldsymbol{\psi}) \in \boldsymbol{L}_0^2(0,T;\boldsymbol{X}_\Gamma \times \boldsymbol{V}_\Gamma)$, solutions of the nonlinear boundary integral equation (4.32). Then, there exist electromagnetic fields, solutions to the time-dependent Maxwell's equations of regularity*

$$(\boldsymbol{E},\boldsymbol{H}) \in \boldsymbol{C}\left(0,T;\boldsymbol{L}^2(\Omega)^2\right) \cap \boldsymbol{H}_0^{-1}\left(0,T;\boldsymbol{H}(\mathbf{curl},\Omega)^2\right),$$

which fulfill the weak formulation of the nonlinear boundary condition (4.19). Furthermore, $(\boldsymbol{\varphi}, \boldsymbol{\psi})$ coincide with the tangential traces of the electromagnetic fields $(\boldsymbol{E},\boldsymbol{H})$ via (4.28). Finally, there exists no other solution to the boundary integral equation, $(\boldsymbol{\varphi}, \boldsymbol{\psi})$ is therefore unique.

The above quantities are further bounded by the following estimates. There exists a positive constant $C_\alpha > 0$, only depending on the parameter α, such that

$$\int_0^T \|\boldsymbol{\varphi}\|_{\boldsymbol{L}^{1+\alpha}(\Gamma)}^{1+\alpha} + \|\boldsymbol{\psi}\|_{\boldsymbol{L}^{\frac{1+\alpha}{\alpha}}(\Gamma)}^{\frac{1+\alpha}{\alpha}} \,\mathrm{d}t \leq C_\alpha \int_0^T \left\|\gamma_T \boldsymbol{H}^{\mathrm{inc}}\right\|_{\boldsymbol{L}^{1+\alpha}(\Gamma)}^{1+\alpha} + \left\|\gamma_T \boldsymbol{E}^{\mathrm{inc}}\right\|_{\boldsymbol{L}^{\frac{1+\alpha}{\alpha}}(\Gamma)}^{\frac{1+\alpha}{\alpha}} \mathrm{d}t,$$

holds, under the assumption that the right-hand side is well-defined. The electromagnetic fields are bounded by an estimate of the same structure, namely there exists a constant $C_\alpha > 0$, again only depending on α, such that for all $t \in [0,T]$, it holds that

$$\|\boldsymbol{E}(t)\|_{\boldsymbol{L}^2(\Omega)}^2 + \|\boldsymbol{H}(t)\|_{\boldsymbol{L}^2(\Omega)}^2 \leq C_\alpha \int_0^t \left\|\gamma_T \boldsymbol{H}^{\mathrm{inc}}\right\|_{\boldsymbol{L}^{1+\alpha}(\Gamma)}^{1+\alpha} + \left\|\gamma_T \boldsymbol{E}^{\mathrm{inc}}\right\|_{\boldsymbol{L}^{\frac{1+\alpha}{\alpha}}(\Gamma)}^{\frac{1+\alpha}{\alpha}} \mathrm{d}t'.$$

Proof. The monotonicity (4.10) of $\boldsymbol{b}$ and the positivity condition (4.27) of the time domain Calderón operator $\boldsymbol{C}(\partial_t)$ yield the uniqueness of the solution.

Let $(\boldsymbol{\varphi}, \boldsymbol{\psi}) \in \boldsymbol{L}_0^2(0,T;\boldsymbol{V}_\Gamma \times \boldsymbol{X}_\Gamma)$ be solutions of the boundary integral equation (4.32) and let $\boldsymbol{E},\boldsymbol{H} \in \boldsymbol{H}_0^{-2}(0,T;\boldsymbol{H}(\mathbf{curl},\mathbb{R}^3 \setminus \Gamma))$ be defined by the time-dependent representation formulas. Consequently, the associated transmission problem (4.22)–(4.25) holds. Furthermore, the jump conditions of the temporal Calderón operator (4.26) imply for the shifted Calderón operator

$$\boldsymbol{C}_{\mathrm{imp}}^-(\partial_t)\begin{pmatrix}\boldsymbol{\varphi}\\ \boldsymbol{\psi}\end{pmatrix} = \boldsymbol{C}(\partial_t)\begin{pmatrix}\boldsymbol{\varphi}\\ \boldsymbol{\psi}\end{pmatrix} + \frac{1}{2}\begin{pmatrix}\boldsymbol{\psi}\\ \boldsymbol{\varphi}\end{pmatrix} = \begin{pmatrix}\{\gamma_T \boldsymbol{E}\}\\ \{\gamma_T \boldsymbol{H}\}\end{pmatrix} + \frac{1}{2}\begin{pmatrix}-[\gamma_T \boldsymbol{E}]\\ [\gamma_T \boldsymbol{H}]\end{pmatrix} = \begin{pmatrix}\gamma_T^- \boldsymbol{E}\\ \gamma_T^+ \boldsymbol{H}\end{pmatrix}. \tag{4.34}$$

Applying the time-harmonic bounds of the Calderón operator in combination with [52, Lemma 2.1] yields that the tangential traces $\gamma_T^- \widehat{\boldsymbol{E}}$ and $\gamma_T^+ \widehat{\boldsymbol{H}}$ are at least of the regularity $\boldsymbol{H}_0^{-2}(0,T;\boldsymbol{X}_\Gamma)$.

Setting the test functions $\boldsymbol{\eta}$ and $\boldsymbol{\xi}$ mutually to zero reduces the weak formulation (4.32) to

$$\left[\boldsymbol{\eta}, \gamma_T^- \boldsymbol{E}\right]_\Gamma = 0, \qquad \text{for all } \boldsymbol{\eta} \in \boldsymbol{X}_\Gamma, \tag{4.35}$$

$$[\boldsymbol{\xi}, \gamma_T^+ \boldsymbol{H}]_\Gamma + \left(\boldsymbol{\xi}\,,\, \boldsymbol{b}\left(\boldsymbol{\psi} - \gamma_T \boldsymbol{E}^{\mathrm{inc}}\right)\right)_\Gamma = [\gamma_T \boldsymbol{H}^{\mathrm{inc}}, \boldsymbol{\xi}]_\Gamma, \qquad \text{for all } \boldsymbol{\xi} \in \boldsymbol{V}_\Gamma. \tag{4.36}$$

By (4.35), we obtain $\gamma_T^- \boldsymbol{E} = 0$, which in particular shows that the electromagnetic fields vanish in the inner domain, since Green's formula (4.30) implies, after integration in time, the identity

$$\frac{1}{2}\int_{\Omega^-} |\boldsymbol{E}|^2 + |\boldsymbol{H}|^2 \,\mathrm{d}\boldsymbol{x} = -\partial_t^{-1}\left[\gamma_T^- \boldsymbol{H}, \gamma_T^- \boldsymbol{E}\right]_\Gamma = 0.$$

The electromagnetic waves $\boldsymbol{E}$ and $\boldsymbol{H}$ therefore vanish in the interior domain Ω^-, which shows that the boundary densities are the boundary data of the outer fields, i.e. (4.24)–(4.25) imply $\boldsymbol{\varphi} = \gamma_T^+ \boldsymbol{H}$ and $\boldsymbol{\psi} = -\gamma_T^+ \boldsymbol{E}$. Inserting these identites into (4.36) reveals that $\boldsymbol{E}$ and $\boldsymbol{H}$, understood as fields restricted to the outer domain Ω^+, are the scattered fields which fulfill the nonlinear boundary condition (4.19). Applying Green's formula on the exterior domain Ω^+ and integration on both sides gives

$$\frac{1}{2}\int_{\Omega^+} |\boldsymbol{E}|^2 + |\boldsymbol{H}|^2 \,\mathrm{d}\boldsymbol{x} = \partial_t^{-1}\left[\gamma_T^+ \boldsymbol{H}, \gamma_T^+ \boldsymbol{E}\right]_\Gamma = \partial_t^{-1}\left[\boldsymbol{\psi}, \gamma_T^+ \boldsymbol{H}\right]_\Gamma.$$

Testing the reduced boundary integral equation (4.36) with $\boldsymbol{\psi}$, integration in time and inserting this identity on the left-hand side shows

$$\frac{1}{2}\left(\|\boldsymbol{E}\|^2_{L^2(\Omega^+)} + \|\boldsymbol{H}\|^2_{L^2(\Omega^+)}\right) + \int_0^t \left(\boldsymbol{\psi}, \boldsymbol{b}\left(\boldsymbol{\psi} - \gamma_T \boldsymbol{E}^{\mathrm{inc}}\right)\right)_\Gamma \,\mathrm{d}t' = \int_0^t [\gamma_T \boldsymbol{H}^{\mathrm{inc}}, \boldsymbol{\psi}]_\Gamma \,\mathrm{d}t'.$$

The nonlinear term is bounded from below by employing an intermediate term in combination with the positivity result (4.9). Further using Hölder's inequality with the exponents from (4.17) and the bound (4.15) on $\boldsymbol{b}$ shows

$$\begin{aligned}
\left(\boldsymbol{\psi},\, \boldsymbol{b}\left(\boldsymbol{\psi} - \gamma_T \boldsymbol{E}^{\mathrm{inc}}\right)\right)_\Gamma &= \left\|\boldsymbol{\psi} - \gamma_T \boldsymbol{E}^{\mathrm{inc}}\right\|^{\frac{1+\alpha}{\alpha}}_{\boldsymbol{L}^{\frac{1+\alpha}{\alpha}}(\Gamma)} + \left(\gamma_T \boldsymbol{E}^{\mathrm{inc}},\, \boldsymbol{b}\left(\boldsymbol{\psi} - \gamma_T \boldsymbol{E}^{\mathrm{inc}}\right)\right)_\Gamma \\
&\geq \left\|\boldsymbol{\psi} - \gamma_T \boldsymbol{E}^{\mathrm{inc}}\right\|^{\frac{1+\alpha}{\alpha}}_{\boldsymbol{L}^{\frac{1+\alpha}{\alpha}}(\Gamma)} - \left(\left\|\gamma_T \boldsymbol{E}^{\mathrm{inc}}\right\|_{\boldsymbol{L}^{\frac{1+\alpha}{\alpha}}(\Gamma)} \left\|\boldsymbol{\psi} - \gamma_T \boldsymbol{E}^{\mathrm{inc}}\right\|^{\frac{1}{\alpha}}_{\boldsymbol{L}^{\frac{1+\alpha}{\alpha}}(\Gamma)}\right) \\
&\geq \left\|\boldsymbol{\psi} - \gamma_T \boldsymbol{E}^{\mathrm{inc}}\right\|^{\frac{1+\alpha}{\alpha}}_{\boldsymbol{L}^{\frac{1+\alpha}{\alpha}}(\Gamma)} - \left(C\left\|\gamma_T \boldsymbol{E}^{\mathrm{inc}}\right\|^{\frac{1+\alpha}{\alpha}}_{\boldsymbol{L}^{\frac{1+\alpha}{\alpha}}(\Gamma)} + \frac{1}{2}\left\|\boldsymbol{\psi} - \gamma_T \boldsymbol{E}^{\mathrm{inc}}\right\|^{\frac{1+\alpha}{\alpha}}_{\boldsymbol{L}^{\frac{1+\alpha}{\alpha}}(\Gamma)}\right),
\end{aligned}$$

where the last inequality is the consequence of the Young inequality. The remaining term on the right-hand side is estimated analogously by employing Hölder's and Young's inequality, which yields for every $\epsilon > 0$ an inversely proportional C such that

$$[\gamma_T \boldsymbol{H}^{\mathrm{inc}}, \boldsymbol{\psi}]_\Gamma \leq \left\|\gamma_T \boldsymbol{H}^{\mathrm{inc}}\right\|_{\boldsymbol{L}^{1+\alpha}(\Gamma)} \|\boldsymbol{\psi}\|_{\boldsymbol{L}^{\frac{1+\alpha}{\alpha}}} \leq C\left\|\gamma_T \boldsymbol{H}^{\mathrm{inc}}\right\|^{1+\alpha}_{\boldsymbol{L}^{1+\alpha}(\Gamma)} + \epsilon\|\boldsymbol{\psi}\|^{\frac{1+\alpha}{\alpha}}_{\boldsymbol{L}^{\frac{1+\alpha}{\alpha}}}.$$

The term depending on $\boldsymbol{\psi}$ is absorbed to the left-hand side, which gives the estimate

$$\begin{aligned}\left(\|\boldsymbol{E}\|^2_{\boldsymbol{L}^2(\Omega^+)} + \|\boldsymbol{H}\|^2_{\boldsymbol{L}^2(\Omega^+)}\right) + \int_0^t \|\boldsymbol{\psi}\|^{\frac{1+\alpha}{\alpha}}_{\boldsymbol{L}^{\frac{1+\alpha}{\alpha}}(\Gamma)} \,\mathrm{d}t' \\ \leq C_\alpha \int_0^t \left\|\gamma_T \boldsymbol{E}^{\mathrm{inc}}\right\|^{\frac{1+\alpha}{\alpha}}_{\boldsymbol{L}^{\frac{1+\alpha}{\alpha}}(\Gamma)} + \left\|\gamma_T \boldsymbol{H}^{\mathrm{inc}}\right\|^{1+\alpha}_{\boldsymbol{L}^{1+\alpha}(\Gamma)} \mathrm{d}t'.\end{aligned}$$

We turn our attention to the remaining estimate on $\boldsymbol{\varphi}$. Rearranging (4.36) and using Hölder's inequality yields, for arbitrary $\boldsymbol{\eta} \in \boldsymbol{V}_\Gamma$, the estimate

$$\begin{aligned}[\boldsymbol{\eta}, \boldsymbol{\varphi}]_\Gamma &= [\gamma_T \boldsymbol{H}^{\mathrm{inc}}, \boldsymbol{\eta}]_\Gamma - \left(\boldsymbol{\eta},\, \boldsymbol{b}\left(\boldsymbol{\psi} - \gamma_T \boldsymbol{E}^{\mathrm{inc}}\right)\right)_\Gamma \\ &\leq \|\boldsymbol{\eta}\|_{\boldsymbol{L}^{\frac{1+\alpha}{\alpha}}(\Gamma)} \left(\left\|\gamma_T \boldsymbol{H}^{\mathrm{inc}}\right\|_{\boldsymbol{L}^{1+\alpha}(\Gamma)} + \left\|\boldsymbol{\psi} - \gamma_T \boldsymbol{E}^{\mathrm{inc}}\right\|^{\frac{1}{\alpha}}_{\boldsymbol{L}^{\frac{1+\alpha}{\alpha}}(\Gamma)}\right).\end{aligned}$$

Since the embedding $\boldsymbol{V}_\Gamma \subset \boldsymbol{L}^{\frac{1+\alpha}{\alpha}}(\Gamma)$ is dense, we finally obtain the estimate

$$\|\boldsymbol{\varphi}\|_{\boldsymbol{L}^{1+\alpha}(\Gamma)} = \sup_{\boldsymbol{\eta} \in \boldsymbol{V}_\Gamma} \frac{[\boldsymbol{\eta}, \boldsymbol{\psi}]_\Gamma}{\|\boldsymbol{\eta}\|_{\boldsymbol{L}^{\frac{1+\alpha}{\alpha}}(\Gamma)}} \leq \left\|\gamma_T \boldsymbol{H}^{\mathrm{inc}}\right\|_{\boldsymbol{L}^{1+\alpha}(\Gamma)} + \left\|\boldsymbol{\psi} - \gamma_T \boldsymbol{E}^{\mathrm{inc}}\right\|^{\frac{1}{\alpha}}_{\boldsymbol{L}^{\frac{1+\alpha}{\alpha}}(\Gamma)}.$$

Taking both sides to the power of $1+\alpha$ yields that the corresponding terms on $\boldsymbol{\varphi}$ are bounded in terms of the previously bounded norms of $\boldsymbol{\psi}$, thus providing the stated result. □

4.3. Semi-discretization in time by Runge–Kutta convolution quadrature

4.3.1. Runge–Kutta convolution quadrature

We refer the reader to Appendix B for the used notation regarding the convolution quadrature method. A key technique in this section is the use of generating functions. Consider a sequence $\Phi_n \in V^m$ for all $n \in \mathbb{N}$, thus a sequence of elements with m components in the Banach space V. Let $\sigma > 0$ be a real value and $\rho = e^{-\sigma\tau}$ a weight approaching 1 for $N \to \infty$. The generating function $\widehat{\Phi}$ operates on the complex disk with radius ρ and is defined by the power series

$$\widehat{\Phi}^\tau : \zeta \mapsto \sum_{n=0}^{\infty} \zeta^n \Phi_n \quad |\zeta| \leq \rho.$$

Bilinear forms defined on a Banach space $V \times V$ are extended to $V^m \times V^m$ with the weight matrix $\mathscr{B} = \mathrm{diag}(\boldsymbol{b}_1, ..., \boldsymbol{b}_m)$ through the following expression

$$\boldsymbol{u} \cdot \boldsymbol{v} = (\boldsymbol{u}, \boldsymbol{v})_{\boldsymbol{b}} = \overline{\boldsymbol{u}}^T \mathscr{B} \boldsymbol{v} = \sum_{i=1}^{m} \boldsymbol{b}_i \boldsymbol{u}_i \cdot \boldsymbol{v}_i \qquad \boldsymbol{u}, \boldsymbol{v} \in V^m,$$

where the dot product $\cdot$ here is to be understood as the bilinear form on the underlying Banach space V. This definition generalizes the $\boldsymbol{L}^2$-pairing and the anti-symmetric pairing to functions

evaluated at multiple stages. When the dot product denotes the standard dot product, or more generally some bilinear form that fulfills a Cauchy–Schwarz type estimate with an associated norm $|\cdot|$, we have the following discrete partial integration inequality.

Lemma 4.3 (Discrete partial integration inequality)**.** *Let $(\boldsymbol{u}_n)_{i=1}^m$ and $(\boldsymbol{v}_n)_{i=1}^m$ be sequences with finitely many non-zero entries, elementwise in $\mathbb{R}^m$. Consider the Runge–Kutta convolution quadrature differentiation operator ∂_t^τ, based on the $m-$stage Radau IIA method. Let the parameter $\rho = e^{-\tau/T}$ be defined as before. For any $\epsilon > 0$, there exists an inversely proportional constant C independent of τ,$\boldsymbol{u}$ and $\boldsymbol{v}$ such that*

$$\sum_{n=0}^{\infty} \rho^n (\partial_t^\tau \boldsymbol{u})_n \cdot \boldsymbol{v}_n \leq \sum_{n=0}^{\infty} \epsilon \rho^n \left|\boldsymbol{u}_n\right|^2 + C\rho^n \left|(\partial_t^\tau \boldsymbol{v})_n\right|^2.$$

Proof. Parseval's theorem applied to the left-hand side of the stated bound rewrites the series with a complex integral over the contour $\mathbb{S}_\rho = \{\zeta \in \mathbb{C} : \ |\zeta| = \rho\}$, which reads

$$\begin{aligned}\sum_{n=0}^{\infty} \rho^n \left((\partial_t^\tau \boldsymbol{u})_n, \boldsymbol{v}_n\right)_{\boldsymbol{b}} &= \int_{\mathbb{S}_\rho} \left(\frac{\Delta(\zeta)}{\tau}\widehat{\boldsymbol{u}}, \widehat{\boldsymbol{v}}\right)_{\boldsymbol{b}} \mathrm{d}\zeta \\ &= \frac{1}{\tau}\int_{\mathbb{S}_\rho} \left(\overline{\Delta(\zeta)\widehat{\boldsymbol{u}}}\right)^T \mathscr{B}\left(\Delta(\zeta)^{-1}\Delta(\zeta)\widehat{\boldsymbol{v}}\right) \mathrm{d}\zeta.\end{aligned}$$

The integrand is rewritten by the associativity of the matrix multiplication to the Cauchy–Schwarz inequality combined with Young's inequality to give the estimate

$$\begin{aligned}&\frac{1}{\tau}\left|\int_{\mathbb{S}_\rho} \overline{(\widehat{\boldsymbol{u}})}^T \left(\Delta(\overline{\zeta})^T \mathscr{B}\Delta(\zeta)^{-1}\Delta(\zeta)\widehat{\boldsymbol{v}}\right) \mathrm{d}\zeta\right| \\ &\leq \int_{\mathbb{S}_\rho} \left|\Delta(\overline{\zeta})^T \mathscr{B}\Delta(\zeta)^{-1}\right| \left|\widehat{\boldsymbol{u}}\right| \left|\frac{\Delta(\zeta)}{\tau}\widehat{\boldsymbol{v}}\right| \mathrm{d}\zeta \\ &\leq \int_{\mathbb{S}_\rho} \left|\Delta(\overline{\zeta})^T \mathscr{B}\Delta(\zeta)^{-1}\right| \left(\frac{\widetilde{\epsilon}}{2}\left|\widehat{\boldsymbol{u}}\right|^2 + \frac{1}{2\widetilde{\epsilon}}\left|\frac{\Delta(\zeta)}{\tau}\widehat{\boldsymbol{v}}\right|^2\right) \mathrm{d}\zeta,\end{aligned}$$

where the last inequality holds for all $\widetilde{\epsilon} > 0$. The absolute value of the first factor in the integrand denotes the Euclidian matrix norm. It remains to show that this term is bounded independently of τ. Inserting the explicit form of the Runge–Kutta differentiation symbol (B.5) and its inverse (seen from (B.4)), and applying the triangle inequality yields

$$\begin{aligned}\left|\Delta(\overline{\zeta})^T \mathscr{B}\Delta(\zeta)^{-1}\right| &= \left|\left(\boldsymbol{I}_m - \overline{\zeta}\,\boldsymbol{e}_m\,\mathbb{1}^T\right)\mathscr{A}^{-T}\mathscr{B}\left(\mathscr{A} + \frac{\zeta}{1-\zeta}\mathbb{1}\boldsymbol{b}^T\right)\right| \\ &\leq (1+m^{1/2})\left|\mathscr{A}^{-T}\mathscr{B}\mathscr{A}\right| + \frac{\left|\left(\boldsymbol{I}_m - \overline{\zeta}\,\boldsymbol{e}_m\,\mathbb{1}^T\right)\mathscr{A}^{-T}\boldsymbol{b}\boldsymbol{b}^T\right|}{|1-\zeta|}.\end{aligned}$$

The first summand is constant and therefore bounded. To bound the remaining term, we use

that $\boldsymbol{c}_m = 1$ implies the identity $\mathscr{A}^{-T}\boldsymbol{b} = \boldsymbol{e}_m$, which yields

$$\frac{\left|\left(\boldsymbol{I}_m - \overline{\zeta}\,\boldsymbol{e}_m\,\mathbb{1}^T\right)\mathscr{A}^{-T}\boldsymbol{b}\boldsymbol{b}^T\right|}{|1-\zeta|} = \frac{\left|\left(\boldsymbol{e}_m - \overline{\zeta}\,\boldsymbol{e}_m\,\mathbb{1}^T\boldsymbol{e}_m\right)\boldsymbol{b}^T\right|}{|1-\zeta|} = \frac{\left|\left(\boldsymbol{e}_m - \overline{\zeta}\,\boldsymbol{e}_m\right)\boldsymbol{b}^T\right|}{|1-\zeta|}$$
$$= \frac{|1-\overline{\zeta}|}{|1-\zeta|}\left|\boldsymbol{e}_m\boldsymbol{b}^T\right| = \left|\boldsymbol{e}_m\boldsymbol{b}^T\right|.$$

The stated result is now given by applying the above estimation of the matrix norm to the integrand from Parseval's formula, which yields for any ϵ a constant $C > 0$, only depending on the coefficients of the Runge–Kutta methods and inversely proportional to ϵ, such that

$$\sum_{n=0}^{\infty}\rho^n\left(\left(\partial_t^\tau\boldsymbol{u}\right)_n,\boldsymbol{v}_n\right)_{\boldsymbol{b}} \le \int_{\mathsf{S}_\rho}\epsilon\,|\widehat{\boldsymbol{u}}|^2 + C\left|\tau^{-1}\Delta(\zeta)\widehat{\boldsymbol{v}}\right|^2\mathrm{d}\theta$$
$$= \sum_{n=0}^{\infty}\epsilon\rho^n\,|\boldsymbol{u}_n|^2 + C\rho^n\,|(\partial_t^\tau\boldsymbol{v})_n|^2,$$

where $\epsilon > 0$ is arbitrary and C is inversely proportional to ϵ. □

Runge–Kutta convolution quadrature methods based on the Radau IIA methods preserve the positivity of continuous operators, a result which in particular holds for the discrete differentiation operator ∂_t^τ. The following positivity property is the direct consequence of the general result from the dedicated paper [13, Theorem 3.1] (by setting the parameters in the reference to $\sigma = 1/(4T)$, $c = 1/2$ and $\alpha = \sigma$).

Lemma 4.4. *Consider the convolution quadrature discretization based on the m-stage Radau IIA method, with $m \le 2$. Let $\langle\cdot,\cdot\rangle$ denote the anti-duality on V, which is extended to V^m with the weight matrix $\mathscr{B}$. Then, with $\rho = e^{-\tau/T}$, it holds that*

$$\tau\sum_{n=0}^{\infty}\rho^n\,\langle f_n,(\partial_t^\tau f)_n\rangle \ge \frac{\tau}{4T}\sum_{n=0}^{\infty}\rho^n\,\|f_n\|_V^2,$$

for every sequence $(f_n)_{n\ge0}$ in V^2 with finitely many non-zero entries. For $m > 2$, such an estimate is not known, however, the left-hand side remains positive:

$$\sum_{n=0}^{\infty}\rho^n\,\langle f_n,(\partial_t^\tau f)_n\rangle \ge 0.$$

The inverse of the discrete differentiation operator $(\partial_t^\tau)^{-1}$ is a bounded operator. More precisely, in the setting of Lemma 4.4 with $m = 2$, we have

$$\frac{\tau}{(4T)^2}\sum_{n=0}^{\infty}\rho^n\left\|\left((\partial_t^\tau)^{-1}f\right)_n\right\|_V^2 \le \tau\sum_{n=0}^{\infty}\rho^n\,\|f_n\|_V^2, \tag{4.37}$$

which will turn out to be a useful inequality in the subsequent sections. The estimate is a

special case of the Runge–Kutta convolution quadrature coercivity [13, Theorem 3.1] (obtained for $L(s) = 1$, $R(s) = s^{-1}$, with the parameters $\sigma = 1/(4T)$, $c = 1/2$ and $\alpha = \sigma^2$). For general $m > 2$, an analogous result still holds when the discrete integration operator $(\partial_t^\tau)^{-1}$ is shifted appropriately in the Laplace domain, as described in the Remarks 4.1–4.2.

4.3.2. Auxiliary result: Time discrete transmission problem

The following lemma is a discrete variant of the continuous time-dependent transmission problem (4.22)–(4.25) and relates sequences in the trace space $\boldsymbol{X}_\Gamma{}^2$ with discrete fields away from the boundary through a time-discrete transmission problem.

Lemma 4.5. *Let $\boldsymbol{\varphi}_n \in \boldsymbol{X}_\Gamma{}^m$ and $\boldsymbol{\psi}_n \in \boldsymbol{X}_\Gamma{}^m$ for $n \in \mathbb{N}$ denote some sequences with finitely many non-zero entries in the trace space. Discrete fields $\boldsymbol{E}_n^\tau, \boldsymbol{H}_n^\tau \in \boldsymbol{H}(\mathbf{curl}, \mathbb{R}^3 \setminus \Gamma)^m$ for all $n \in \mathbb{N}$ are defined by the discrete representation formula based on the m-stage Radau IIA method:*

$$\boldsymbol{E}^\tau = -\boldsymbol{\mathcal{S}}(\partial_t^\tau)\boldsymbol{\varphi} + \boldsymbol{\mathcal{D}}(\partial_t^\tau)\boldsymbol{\psi}, \tag{4.38}$$
$$\boldsymbol{H}^\tau = -\boldsymbol{\mathcal{D}}(\partial_t^\tau)\boldsymbol{\varphi} - \boldsymbol{\mathcal{S}}(\partial_t^\tau)\boldsymbol{\psi}. \tag{4.39}$$

Then, the following time-discrete transmission problem holds:

$$\partial_t^\tau \boldsymbol{E}^\tau - \mathbf{curl}\, \boldsymbol{H}^\tau = 0 \quad \text{in} \quad \mathbb{R}^3 \setminus \Gamma, \tag{4.40}$$
$$\partial_t^\tau \boldsymbol{H}^\tau + \mathbf{curl}\, \boldsymbol{E}^\tau = 0 \quad \text{in} \quad \mathbb{R}^3 \setminus \Gamma, \tag{4.41}$$
$$[\gamma_T]\boldsymbol{H}^\tau = \boldsymbol{\varphi}, \tag{4.42}$$
$$-[\gamma_T]\boldsymbol{E}^\tau = \boldsymbol{\psi}. \tag{4.43}$$

Proof. Taking the generating function on both sides of the discrete representation formulas (4.38)–(4.39) shows that the generating function of the scattered waves $\widehat{\boldsymbol{E}}^\tau(\zeta)$ and $\widehat{\boldsymbol{H}}^\tau(\zeta)$ fulfill the time-harmonic representation formula

$$\widehat{\boldsymbol{E}}^\tau(\zeta) = -\boldsymbol{\mathcal{S}}\left(\frac{\Delta(\zeta)}{\tau}\right)\widehat{\boldsymbol{\varphi}}(\zeta) + \boldsymbol{\mathcal{D}}\left(\frac{\Delta(\zeta)}{\tau}\right)\widehat{\boldsymbol{\psi}}(\zeta).$$

An analogous formula holds for the generating function $\widehat{\boldsymbol{H}}^\tau$ associated to the discrete magnetic field. The time-harmonic representation formulas (3.29)–(3.30) and the jump conditions (3.17) of the potential operators $\boldsymbol{\mathcal{S}}(s)$ and $\boldsymbol{\mathcal{D}}(s)$ consequently yield the following time-harmonic transmission problem for the generating functions

$$\frac{\Delta(\zeta)}{\tau}\widehat{\boldsymbol{E}}^\tau(\zeta) - \mathbf{curl}\, \widehat{\boldsymbol{H}}^\tau(\zeta) = 0 \qquad \text{in} \quad \mathbb{R}^3 \setminus \Gamma,$$
$$\frac{\Delta(\zeta)}{\tau}\widehat{\boldsymbol{H}}^\tau(\zeta) + \mathbf{curl}\, \widehat{\boldsymbol{E}}^\tau(\zeta) = 0 \qquad \text{in} \quad \mathbb{R}^3 \setminus \Gamma,$$
$$[\gamma_T]\widehat{\boldsymbol{H}}^\tau(\zeta) = \widehat{\boldsymbol{\varphi}}(\zeta) \quad \text{on} \quad \Gamma,$$
$$-[\gamma_T]\widehat{\boldsymbol{E}}^\tau(\zeta) = \widehat{\boldsymbol{\psi}}(\zeta) \quad \text{on} \quad \Gamma.$$

The stated time-discrete transmission problem then follows by coefficient comparison. □

The stability analysis for the time-continuous scattering problem in Proposition 4.1 was enabled through the jump conditions of $\boldsymbol{C}(\partial_t)$. In the following lemma, we transport these jump conditions to the time-discrete Calderón operator $\boldsymbol{C}(\partial_t^\tau)$ and show a related identity with respect to the skew-symmetric pairing on the boundary.

Lemma 4.6. *Let $\boldsymbol{C}(\partial_t^\tau)$ denote the convolution quadrature approximation based on the m-stage Radau IIA method applied to the time-dependent Calderón operator $\boldsymbol{C}(\partial_t)$. Let further $\boldsymbol{\varphi}_n \in \boldsymbol{X}_\Gamma{}^m$ and $\boldsymbol{\psi}_n \in \boldsymbol{X}_\Gamma{}^m$ for $n \in \mathbb{N}$ denote arbitrary sequences with finitely many non-zero entries, with associated discrete fields $\boldsymbol{E}^\tau$ and $\boldsymbol{H}^\tau$ with support on $\mathbb{R}^3 \setminus \Gamma$, defined via the time-discrete representation formulas (4.38)–(4.39), such that the time-discrete transmission problem of Lemma 4.5 holds. For these fields, the Calderón operator fulfills the identity*

$$\boldsymbol{C}(\partial_t^\tau) \begin{pmatrix} \boldsymbol{\varphi} \\ \boldsymbol{\psi} \end{pmatrix} = \begin{pmatrix} \{\gamma_T \boldsymbol{E}^\tau\} \\ \{\gamma_T \boldsymbol{H}^\tau\} \end{pmatrix}. \tag{4.44}$$

Moreover, for all $n \in \mathbb{N}$, the following identity holds

$$\left[\begin{pmatrix} \boldsymbol{\varphi}_n \\ \boldsymbol{\psi}_n \end{pmatrix}, \left(\boldsymbol{C}(\partial_t^\tau) \begin{pmatrix} \boldsymbol{\varphi} \\ \boldsymbol{\psi} \end{pmatrix} \right)^n \right]_\Gamma = \int_{\mathbb{R}^3 \setminus \Gamma} \boldsymbol{E}_n^\tau \cdot (\partial_t^\tau \boldsymbol{E}^\tau)_n + \boldsymbol{H}_n^\tau \cdot (\partial_t^\tau \boldsymbol{H}^\tau)_n \, \mathrm{d}\boldsymbol{x}.$$

Proof. Applying the time-harmonic jump conditions (3.33) to the generating function of the time-discrete Calderón operator applied to the sequence $(\boldsymbol{\varphi}, \boldsymbol{\psi})^T$ yields

$$\widehat{\boldsymbol{C}(\partial_t^\tau) \begin{pmatrix} \boldsymbol{\varphi} \\ \boldsymbol{\psi} \end{pmatrix}} = \boldsymbol{C}\left(\frac{\Delta(\zeta)}{\tau} \right) \begin{pmatrix} \widehat{\boldsymbol{\varphi}}(\zeta) \\ \widehat{\boldsymbol{\psi}}(\zeta) \end{pmatrix} = \begin{pmatrix} \{\gamma_T \widehat{\boldsymbol{E}}^\tau\} \\ \{\gamma_T \widehat{\boldsymbol{H}}^\tau\} \end{pmatrix}.$$

The first stated identity therefore follows by coefficient comparison. Inserting these time-discrete jump conditions into the left-hand side of the second stated identity yields

$$\begin{aligned} \left[\begin{pmatrix} \boldsymbol{\varphi}_n \\ \boldsymbol{\psi}_n \end{pmatrix}, \left(\boldsymbol{C}(\partial_t^\tau) \begin{pmatrix} \boldsymbol{\varphi}^\tau \\ \boldsymbol{\psi}^\tau \end{pmatrix} \right)^n \right]_\Gamma &= \left[\begin{pmatrix} [\gamma_T] \boldsymbol{H}_n^\tau \\ -[\gamma_T] \boldsymbol{E}_n^\tau \end{pmatrix}, \begin{pmatrix} \{\gamma_T\} \widehat{\boldsymbol{E}}_n^\tau \\ \{\gamma_T\} \widehat{\boldsymbol{H}}_n^\tau \end{pmatrix} \right]_\Gamma \\ &= [\gamma_T^+ \boldsymbol{H}_n^\tau, \gamma_T^+ \boldsymbol{E}_n^\tau]_\Gamma - [\gamma_T^- \boldsymbol{H}_n^\tau, \gamma_T^- \boldsymbol{E}_n^\tau]_\Gamma, \end{aligned}$$

where the necessary intermediate summands for the final identity are analogous to the time-harmonic identity (3.28). The statement follows from Green's formula (4.30) on the interior and exterior domain by inserting the time-discrete Maxwell's equations (4.40)–(4.41), which yields

$$\begin{aligned} [\gamma_T^+ \boldsymbol{H}_n^\tau, \gamma_T^+ \boldsymbol{E}_n^\tau]_\Gamma - [\gamma_T^- \boldsymbol{H}_n^\tau, \gamma_T^- \boldsymbol{E}_n^\tau]_\Gamma &= \int_{\mathbb{R}^3 \setminus \Gamma} \mathbf{curl}\, \boldsymbol{H}_n^\tau \cdot \boldsymbol{E}_n^\tau - \boldsymbol{H}_n^\tau \cdot \mathbf{curl}\, \boldsymbol{E}_n^\tau \, \mathrm{d}\boldsymbol{x} \\ &= \int_{\mathbb{R}^3 \setminus \Gamma} (\partial_t^\tau \boldsymbol{E}^\tau)_n \cdot \boldsymbol{E}_n^\tau + \boldsymbol{H}_n^\tau \cdot (\partial_t^\tau \boldsymbol{H}^\tau)_n \, \mathrm{d}\boldsymbol{x}. \end{aligned}$$

□

Remark 4.2. *Combining this result with Lemma 4.4 yields a positivity result in terms of the discrete fields away from the boundary for $m \leq 2$. For $m > 2$, a positivity result of this type is not achievable (cf. [13, Lemma 3.2 (b)]), however, shifting the formulation in the frequency domain by some $\sigma > 0$ through $\widetilde{\boldsymbol{C}}(s) = \boldsymbol{C}(s + \sigma)$, as described in the shifted boundary integral equation (4.33), gives*

$$\left[\begin{pmatrix}\boldsymbol{\varphi}_n\\ \boldsymbol{\psi}_n\end{pmatrix}, \left(\widetilde{\boldsymbol{C}}(\partial_t^\tau)\begin{pmatrix}\boldsymbol{\varphi}\\ \boldsymbol{\psi}\end{pmatrix}\right)^n\right]_\Gamma = \int_{\mathbb{R}^3\setminus\Gamma} \boldsymbol{E}_n^\tau \cdot (\partial_t^\tau \boldsymbol{E}^\tau)_n + \sigma\,|\boldsymbol{E}_n^\tau|^2 + \boldsymbol{H}_n^\tau \cdot (\partial_t^\tau \boldsymbol{H}^\tau)_n + \sigma\,|\boldsymbol{H}_n^\tau|^2 \,\mathrm{d}\boldsymbol{x}.$$

Crucially, employing the second inequality of Lemma 4.4 on the right-hand side gives a coercivity result for the time-discrete Calderón operator. The subsequent error analysis relies on a positivity result of this type, though numerical computations indicate that the implementation of such a shift is not necessary in practice.

4.3.3. Convolution quadrature for the nonlinear boundary integral equation

The application of the Runge–Kutta convolution quadrature method to the temporal Calderón operator in the boundary integral equation (4.32) yields the following time-discrete boundary integral equation.

Time-discrete boundary integral equation: *Find, for all $n \leq N$, the sequence of boundary densities $(\boldsymbol{\varphi}^n, \boldsymbol{\psi}^n) = (\boldsymbol{\varphi}_i^n, \boldsymbol{\psi}_i^n)_{i=1}^m \in \boldsymbol{V}_\Gamma{}^m \times \boldsymbol{X}_\Gamma{}^m$ such that for all $(\boldsymbol{\eta}, \boldsymbol{\xi}) \in \boldsymbol{V}_\Gamma \times \boldsymbol{X}_\Gamma$ and $n \leq N$ it holds that*

$$\left[\begin{pmatrix}\boldsymbol{\eta}\\ \boldsymbol{\xi}\end{pmatrix}, \left(\boldsymbol{C}_{\mathrm{imp}}(\partial_t^\tau)\begin{pmatrix}\boldsymbol{\varphi}^\tau\\ \boldsymbol{\psi}^\tau\end{pmatrix}\right)^n\right]_\Gamma + \left(\boldsymbol{\xi},\, \boldsymbol{b}\left(\boldsymbol{\psi}_n^\tau - \gamma_T \boldsymbol{E}_n^{\mathrm{inc}}\right)\right)_\Gamma = [\gamma_T \boldsymbol{H}_n^{\mathrm{inc}}, \boldsymbol{\xi}]_\Gamma. \tag{4.45}$$

In the above semi-discretization and in the following sections, we use the shorthand notation $\boldsymbol{E}_n^{\mathrm{inc}} = \boldsymbol{E}^{\mathrm{inc}}(\underline{t_n})$, where we denoted $\boldsymbol{E}^{\mathrm{inc}}(\underline{t_n}) = \left(\boldsymbol{E}^{\mathrm{inc}}(t_n + c_i\tau)\right)_{i=1}^m$. The semi-discrete numerical solution is then recovered at any point in the domain away from the boundary through the time-discrete representation formula, discretized by the convolution quadrature method based on the m-stage Radau IIA method.

With the time-discrete boundary densities $\boldsymbol{\varphi}^\tau$ and $\boldsymbol{\psi}^\tau$, we therefore obtain the following numerical approximations in the domain

$$\boldsymbol{E}^\tau = -\boldsymbol{\mathcal{S}}(\partial_t^\tau)\boldsymbol{\varphi}^\tau + \boldsymbol{\mathcal{D}}(\partial_t^\tau)\boldsymbol{\psi}^\tau, \tag{4.46}$$

$$\boldsymbol{H}^\tau = -\boldsymbol{\mathcal{D}}(\partial_t^\tau)\boldsymbol{\varphi}^\tau - \boldsymbol{\mathcal{S}}(\partial_t^\tau)\boldsymbol{\psi}^\tau. \tag{4.47}$$

The time-discrete electromagnetic fields $\boldsymbol{E}^\tau$ and $\boldsymbol{H}^\tau$ obtained via the discrete boundary integral equation and the representation formulas are equivalent to applying the Runge–Kutta discretization to the exterior Maxwell's equations under the nonlinear boundary condition, which is described in the following proposition. Connections of this type are well-established in the literature, for example in [52, Theorem 5.2].

Proposition 4.2. *Let $\boldsymbol{E}^\tau$ and $\boldsymbol{H}^\tau$ be the discrete electromagnetic fields obtained via the representation formulas (4.46)–(4.47) with the corresponding boundary densities $\boldsymbol{\varphi}^\tau$ and $\boldsymbol{\psi}^\tau$, solutions of the discrete boundary integral equations (4.45), discretized via the 2-stage Radau IIA method. These fields are then the solution to the following discrete scattering problem:*

$$\partial_t^\tau \boldsymbol{E}^\tau - \mathbf{curl}\, \boldsymbol{H}^\tau = 0 \qquad \text{in} \quad \Omega, \tag{4.48}$$

$$\partial_t^\tau \boldsymbol{H}^\tau + \mathbf{curl}\, \boldsymbol{E}^\tau = 0 \qquad \text{in} \quad \Omega, \tag{4.49}$$

$$[\boldsymbol{\phi}, \gamma_T \boldsymbol{H}^\tau]_\Gamma + (\boldsymbol{\phi}, \boldsymbol{b}(-\gamma_T \boldsymbol{E}^\tau - \gamma_T \boldsymbol{E}^{\text{inc}}))_\Gamma = [\gamma_T \boldsymbol{H}^{inc}, \boldsymbol{\phi}]_\Gamma \qquad \text{for all } \boldsymbol{\phi} \in \boldsymbol{V}_\Gamma{}'. \tag{4.50}$$

The discrete solutions of the boundary integral equation are related to the fields via

$$\boldsymbol{\varphi}^\tau = \gamma_T \boldsymbol{H}^\tau, \qquad \boldsymbol{\psi}^\tau = -\gamma_T \boldsymbol{E}^\tau. \tag{4.51}$$

Proof. Any fields defined through the time-discrete representation formulas fulfill, as a consequence of Lemma 4.5, the first identities (4.48)–(4.49) in Ω. Furthermore, the boundary densities are, as described in Lemma 4.5, the jumps of the evaluated fields. It remains to show that the numerical approximation vanishes in the domain Ω^-, inside of the scatterer.
Applying the jump conditions of the Calderón operator yields

$$\boldsymbol{C}_{\text{imp}}^-(\partial_t^\tau) \begin{pmatrix} \boldsymbol{\varphi}^\tau \\ \boldsymbol{\psi}^\tau \end{pmatrix} = \boldsymbol{C}_{\text{imp}}(\partial_t^\tau) \begin{pmatrix} \boldsymbol{\varphi}^\tau \\ \boldsymbol{\psi}^\tau \end{pmatrix} + \frac{1}{2} \begin{pmatrix} \boldsymbol{\psi}^\tau \\ \boldsymbol{\varphi}^\tau \end{pmatrix} = \begin{pmatrix} \{\gamma_T \boldsymbol{E}^\tau\} \\ \{\gamma_T \boldsymbol{H}^\tau\} \end{pmatrix} + \frac{1}{2} \begin{pmatrix} -[\gamma_T \boldsymbol{E}^\tau] \\ [\gamma_T \boldsymbol{H}^\tau] \end{pmatrix} = \begin{pmatrix} \gamma_T^- \boldsymbol{E}^\tau \\ \gamma_T^+ \boldsymbol{H}^\tau \end{pmatrix},$$

which is the time-discrete analogue of (4.34). Inserting this identity into the original discrete boundary integral equation (4.45) yields discrete versions of (4.35)–(4.36)

$$\left[\boldsymbol{\eta}, \gamma_T^- \boldsymbol{E}_n^\tau\right]_\Gamma = 0, \qquad \text{for all } \boldsymbol{\eta} \in \boldsymbol{X}_\Gamma, \tag{4.52}$$

$$[\boldsymbol{\xi}, \gamma_T^+ \boldsymbol{H}_n^\tau]_\Gamma + \left(\boldsymbol{\xi}\,,\, \boldsymbol{b}\left(\boldsymbol{\psi}_n^\tau - \gamma_T \boldsymbol{E}_n^{\text{inc}}\right)\right)_\Gamma = [\gamma_T \boldsymbol{H}_n^{\text{inc}}, \boldsymbol{\xi}]_\Gamma, \qquad \text{for all } \boldsymbol{\xi} \in \boldsymbol{V}_\Gamma. \tag{4.53}$$

The first identity implies $\gamma_T^- \boldsymbol{E}_n^\tau = 0$. Inserting the discretized Maxwell's equations in (4.48)–(4.49) into Green's formula (4.30) for the interior domain yields for all n

$$\int_{\Omega^-} \boldsymbol{E}_n^\tau \cdot (\partial_t^\tau \boldsymbol{E}^\tau)_n + \boldsymbol{H}_n^\tau \cdot (\partial_t^\tau \boldsymbol{H}^\tau)_n \, \mathrm{d}\boldsymbol{x} = -\left[\gamma_T^- \boldsymbol{E}^n, \gamma_T^- \boldsymbol{H}^\tau\right]_\Gamma = 0.$$

Applying the coercivity of Lemma 4.4 shows $\boldsymbol{E}_{|\Omega^-}^\tau = \boldsymbol{H}_{|\Omega^-}^\tau = 0$, hence the boundary densities coincide with the exterior tangential traces as stated. □

Remark 4.3. *By shifting the boundary integral equation (4.32), as described in Remark 4.1, an analogous result to Proposition 4.2 can be derived for $m > 2$.*

4.3.4. Error bounds for the semi-discretization in time

This section is devoted to the derivation of error bounds for the solutions of the semi-discrete boundary integral equation (4.45). The error analysis builds on the preceding auxiliary results and is mainly conducted in the exterior domain $\Omega = \Omega^+$.

In the following theorem, error bounds with specific convergence rates for the semi-discrete numerical solution are provided, under assumptions on the regularity of the exact solution of the boundary integral equation (4.32). The only requirement for the nonlinearity $\boldsymbol{b}$ is the monotonicity implied through pointwise bounds of Lemma 4.1.

Theorem 4.1. *Let $(\boldsymbol{\varphi}, \boldsymbol{\psi}) \in \boldsymbol{H}_0^{m+5}(0,T;\boldsymbol{V}_\Gamma \times \boldsymbol{X}_\Gamma)$ be the solution of the boundary integral equation (4.32). Consider the semi-discrete boundary densities $(\boldsymbol{\varphi}_n^\tau, \boldsymbol{\psi}_n^\tau) \in {\boldsymbol{V}_\Gamma}^m \times {\boldsymbol{X}_\Gamma}^m$ for all $n \leq N$, solution to the m-stage Radau IIA Runge–Kutta based convolution quadrature semi-discretization of the boundary integral equation*

- *(4.32), in the case of $m \leq 2$;*
- *(4.33) with $\sigma = 1/T$, in the case of $m > 2$.*

The errors of the m-stage Radau IIA semi-discretization are denoted by $\boldsymbol{e}_{\boldsymbol{\varphi}} = \boldsymbol{\varphi}^\tau - \boldsymbol{\varphi}$ and $\boldsymbol{e}_{\boldsymbol{\psi}} = \boldsymbol{\psi}^\tau - \boldsymbol{\psi}$. These quantities are understood as the sequences whose elements are given by the error of the approximations in the stages, i.e. $\boldsymbol{e}_{\boldsymbol{\varphi}}^n = \left(\boldsymbol{\varphi}_i^n\right)_{i=1}^m - \boldsymbol{\varphi}(\underline{t_n})$, where the evaluations at the stages $\boldsymbol{c}$ are denoted by $\boldsymbol{\varphi}(\underline{t_n}) = (\boldsymbol{\varphi}(t_n + c_i\tau))_{i=1}^m$. With this notation, the following error bound holds

$$\left(\tau \sum_{n=0}^{N} \left\| \left(\left(\partial_t^\tau\right)^{-1} \boldsymbol{e}_{\boldsymbol{\varphi}} \right)_n \right\|_{\boldsymbol{X}_\Gamma}^2 + \left\| \left(\left(\partial_t^\tau\right)^{-1} \boldsymbol{e}_{\boldsymbol{\psi}} \right)_n \right\|_{\boldsymbol{X}_\Gamma}^2 \right)^{1/2} \leq C\tau^m.$$

The constant C depends on higher Sobolev norms of the exact solution $(\boldsymbol{\varphi}, \boldsymbol{\psi})$, the boundary Γ and polynomially on the final time T.

Proof. We restrict our attention to the analysis of the non-shifted scheme (4.45), which therefore only holds for $m \leq 2$. Repeating the argument structure for the corresponding semi-discretization of the shifted boundary integral equation (4.33) shows the stated result for $m > 2$.

Subtracting the boundary integral equation (4.32) from the time-discrete scheme (4.45) yields

$$\begin{aligned} &\left[\begin{pmatrix} \boldsymbol{\eta} \\ \boldsymbol{\xi} \end{pmatrix}, \boldsymbol{C}_{\mathrm{imp}}^-(\partial_t^\tau) \begin{pmatrix} \boldsymbol{\varphi}^\tau \\ \boldsymbol{\psi}^\tau \end{pmatrix} - \boldsymbol{C}_{\mathrm{imp}}^-(\partial_t) \begin{pmatrix} \boldsymbol{\varphi} \\ \boldsymbol{\psi} \end{pmatrix} \right]_\Gamma \\ &+ \left(\boldsymbol{\xi}, \boldsymbol{b}\left(\boldsymbol{\psi}^\tau - \gamma_T \boldsymbol{E}^{\mathrm{inc}}\right) - \boldsymbol{b}\left(\boldsymbol{\psi} - \gamma_T \boldsymbol{E}^{\mathrm{inc}}\right)\right)_\Gamma = 0. \end{aligned}$$

Testing the above equation with the errors $\boldsymbol{e}_{\boldsymbol{\varphi}} = \boldsymbol{\varphi}^\tau - \boldsymbol{\varphi}$ and $\boldsymbol{e}_{\boldsymbol{\psi}} = \boldsymbol{\psi}^\tau - \boldsymbol{\psi}$ yields, upon inserting the monotonicity of $\boldsymbol{b}$ as stated by (4.10), the estimate

$$\left[\begin{pmatrix} \boldsymbol{e}_{\boldsymbol{\varphi}} \\ \boldsymbol{e}_{\boldsymbol{\psi}} \end{pmatrix}, \boldsymbol{C}_{\mathrm{imp}}^-(\partial_t^\tau) \begin{pmatrix} \boldsymbol{\varphi}^\tau \\ \boldsymbol{\psi}^\tau \end{pmatrix} - \boldsymbol{C}_{\mathrm{imp}}^-(\partial_t) \begin{pmatrix} \boldsymbol{\varphi} \\ \boldsymbol{\psi} \end{pmatrix} \right]_\Gamma \leq 0.$$

The summand depending on the nonlinearity has therefore been eliminated. Rearranging and subtracting the appropriate intermediate term yields the following inequality

$$\left[\begin{pmatrix} \boldsymbol{e}_{\boldsymbol{\varphi}} \\ \boldsymbol{e}_{\boldsymbol{\psi}} \end{pmatrix}, \boldsymbol{C}_{\mathrm{imp}}^-(\partial_t^\tau) \begin{pmatrix} \boldsymbol{e}_{\boldsymbol{\varphi}} \\ \boldsymbol{e}_{\boldsymbol{\psi}} \end{pmatrix} \right]_\Gamma \leq \left[\begin{pmatrix} \boldsymbol{e}_{\boldsymbol{\varphi}} \\ \boldsymbol{e}_{\boldsymbol{\psi}} \end{pmatrix}, \left(\boldsymbol{C}_{\mathrm{imp}}^-(\partial_t) - \boldsymbol{C}_{\mathrm{imp}}^-(\partial_t^\tau) \right) \begin{pmatrix} \boldsymbol{\varphi} \\ \boldsymbol{\psi} \end{pmatrix} \right]_\Gamma. \tag{4.54}$$

To employ the discrete jump conditions of the time-discrete Calderón operator, we introduce the following discrete fields

$$\boldsymbol{E}_*^\tau = -\boldsymbol{\mathcal{S}}(\partial_t^\tau)\boldsymbol{\varphi} + \boldsymbol{\mathcal{D}}(\partial_t^\tau)\boldsymbol{\psi}, \tag{4.55}$$
$$\boldsymbol{H}_*^\tau = -\boldsymbol{\mathcal{D}}(\partial_t^\tau)\boldsymbol{\varphi} - \boldsymbol{\mathcal{S}}(\partial_t^\tau)\boldsymbol{\psi}. \tag{4.56}$$

The application of the convolution quadrature approximation result in Lemma B.1 with $\kappa = 2$ and $\nu = 1$, where the necessary time-harmonic bounds on the potential operators are provided by Lemma 3.4, gives a positive constant $C > 0$ such that

$$\left\|(\boldsymbol{E}_*^\tau)_n - \boldsymbol{E}(\underline{t_n})\right\|_{\boldsymbol{H}(\mathbf{curl},\Omega)} + \left\|(\boldsymbol{H}_*^\tau)_n - \boldsymbol{H}(\underline{t_n})\right\|_{\boldsymbol{H}(\mathbf{curl},\Omega)} \leq C\tau^m \left\| \begin{pmatrix} \boldsymbol{\varphi} \\ \boldsymbol{\psi} \end{pmatrix} \right\|_{H_0^{m+5}\left(0,T;X_\Gamma{}^2\right)}. \tag{4.57}$$

Applying the second identity of Lemma 4.6 to the left-hand side of the transformed error equation (4.54) gives the identity

$$\begin{aligned}\left[\begin{pmatrix} \boldsymbol{e}_{\boldsymbol{\varphi}}^n \\ \boldsymbol{e}_{\boldsymbol{\psi}}^n \end{pmatrix}, \left(\boldsymbol{C}_{\mathrm{imp}}^-(\partial_t^\tau) \begin{pmatrix} \boldsymbol{e}_{\boldsymbol{\varphi}} \\ \boldsymbol{e}_{\boldsymbol{\psi}} \end{pmatrix} \right)^n \right]_\Gamma &= \int_{\mathbb{R}^3\setminus\Gamma} (\boldsymbol{E}^\tau - \boldsymbol{E}_*^\tau)_n \cdot (\partial_t^\tau(\boldsymbol{E}^\tau - \boldsymbol{E}_*^\tau))_n \\ &\quad + (\boldsymbol{H}^\tau - \boldsymbol{H}_*^\tau)_n \cdot (\partial_t^\tau(\boldsymbol{H}^\tau - \boldsymbol{H}_*^\tau))_n \,\mathrm{d}\boldsymbol{x}.\end{aligned}$$

Summation on both sides and the coercivity of the operator ∂_t^τ, which is provided by Lemma 4.4, implies the following coercivity bound purely in terms of the discrete fields away from the boundary

$$\begin{aligned}\sum_{n=0}^\infty \rho^n \left[\begin{pmatrix} \boldsymbol{e}_{\boldsymbol{\varphi}}^n \\ \boldsymbol{e}_{\boldsymbol{\psi}}^n \end{pmatrix}, \left(\boldsymbol{C}_{\mathrm{imp}}^-(\partial_t^\tau) \begin{pmatrix} \boldsymbol{e}_{\boldsymbol{\varphi}} \\ \boldsymbol{e}_{\boldsymbol{\psi}} \end{pmatrix} \right)^n \right]_\Gamma &\geq c \sum_{n=0}^\infty \rho^n \left\|(\boldsymbol{E}^\tau - \boldsymbol{E}_*^\tau)_n\right\|_{\boldsymbol{L}^2(\mathbb{R}^3\setminus\Gamma)}^2 \\ &\quad + c \sum_{n=0}^\infty \rho^n \left\|(\boldsymbol{H}^\tau - \boldsymbol{H}_*^\tau)_n\right\|_{\boldsymbol{L}^2(\mathbb{R}^3\setminus\Gamma)}^2,\end{aligned} \tag{4.58}$$

where $\rho^n = e^{-n\tau/T}$. In the following, we rewrite the defect terms on the right-hand side of (4.54), with the intention to absorb the terms depending on the numerical solution on the right-hand side with the lower bound (4.58) above.

The exact solution of the boundary integral equation is, due to Proposition 4.1, the solution of the time-dependent scattering problem and, by Lemma 4.5, the jumps of the discrete transmission problem (4.48)–(4.43) with $(\boldsymbol{E}_*^\tau, \boldsymbol{H}_*^\tau)$. Consequently, the jumps of the discrete transmission problem and the boundary data of the continuous problem coincide, namely

$$\gamma_T^+ \boldsymbol{H} = \boldsymbol{\varphi} = (\gamma_T^+ \boldsymbol{H}_*^\tau - \gamma_T^- \boldsymbol{H}_*^\tau), \tag{4.59}$$
$$-\gamma_T^+ \boldsymbol{E} = \boldsymbol{\psi} = -(\gamma_T^+ \boldsymbol{E}_*^\tau - \gamma_T^- \boldsymbol{E}_*^\tau). \tag{4.60}$$

The jump conditions of the temporal and time-discrete Calderón operators (namely (4.34) and

(4.44) respectively) imply, together with (4.60), the identity

$$\begin{aligned}\left[\begin{pmatrix}\boldsymbol{e}_{\boldsymbol{\varphi}}\\ \boldsymbol{e}_{\boldsymbol{\psi}}\end{pmatrix}, \left(\boldsymbol{C}^{-}_{\mathrm{imp}}(\partial_t) - \boldsymbol{C}^{-}_{\mathrm{imp}}(\partial_t^\tau)\right)\begin{pmatrix}\boldsymbol{\varphi}\\ \boldsymbol{\psi}\end{pmatrix}\right]_\Gamma &= \left[\begin{pmatrix}\boldsymbol{e}_{\boldsymbol{\varphi}}\\ \boldsymbol{e}_{\boldsymbol{\psi}}\end{pmatrix}, \begin{pmatrix}0\\ \gamma_T^+\boldsymbol{H}\end{pmatrix} - \begin{pmatrix}\gamma_T^-\boldsymbol{E}_*^\tau\\ \gamma_T^+\boldsymbol{H}_*^\tau\end{pmatrix}\right]_\Gamma\\ &= \left[\begin{pmatrix}\boldsymbol{e}_{\boldsymbol{\varphi}}\\ \boldsymbol{e}_{\boldsymbol{\psi}}\end{pmatrix}, \begin{pmatrix}\gamma_T^+(\boldsymbol{E}-\boldsymbol{E}_*^\tau)\\ \gamma_T^+(\boldsymbol{H}-\boldsymbol{H}_*^\tau)\end{pmatrix}\right]_\Gamma.\end{aligned} \tag{4.61}$$

We continue with the first component on the right-hand side. Rewriting the boundary densities in terms of the fields through Proposition 4.1 and Proposition 4.2 implies, with an additional intermediate term

$$\begin{aligned}\left[\boldsymbol{\varphi}^\tau - \boldsymbol{\varphi}, \gamma_T^+(\boldsymbol{E}-\boldsymbol{E}_*^\tau)\right]_\Gamma &= \left[\gamma_T^+(\boldsymbol{H}^\tau - \boldsymbol{H}), \gamma_T^+(\boldsymbol{E}-\boldsymbol{E}_*^\tau)\right]_\Gamma\\ &= \left[\gamma_T^+(\boldsymbol{H}^\tau - \boldsymbol{H}_*^\tau), \gamma_T^+(\boldsymbol{E}-\boldsymbol{E}_*^\tau)\right]_\Gamma\\ &\quad + \left[\gamma_T^+(\boldsymbol{H}_*^\tau - \boldsymbol{H}), \gamma_T^+(\boldsymbol{E}-\boldsymbol{E}_*^\tau)\right].\end{aligned}$$

The above summands are structurally simpler, since the first summand consists of the tangential traces corresponding to the fields appearing in (4.58) and the second summand is independent of the numerical solution and directly bounded via

$$\begin{aligned}\left[\gamma_T^+(\boldsymbol{H}_*^\tau - \boldsymbol{H}), \gamma_T^+(\boldsymbol{E}-\boldsymbol{E}_*^\tau)\right] &\leq \left\|\gamma_T^+(\boldsymbol{H}_*^\tau - \boldsymbol{H})\right\|_{\boldsymbol{X}_\Gamma} \left\|\gamma_T^+(\boldsymbol{E}_*^\tau - \boldsymbol{E})\right\|_{\boldsymbol{X}_\Gamma}\\ &\leq \left\|\boldsymbol{H}_*^\tau - \boldsymbol{H}\right\|_{\boldsymbol{H}(\mathbf{curl},\Omega^+)} \left\|\boldsymbol{E}_*^\tau - \boldsymbol{E}\right\|_{\boldsymbol{H}(\mathbf{curl},\Omega^+)}\\ &\leq C\tau^{2m} \left\|\begin{pmatrix}\boldsymbol{\varphi}\\ \boldsymbol{\psi}\end{pmatrix}\right\|^2_{\boldsymbol{H}_0^{m+5}\left(0,T;\boldsymbol{X}_\Gamma{}^2\right)}.\end{aligned}$$

The remaining first summand is rewritten by combining Green's formula and the time-discrete Maxwell's equations (4.48), which yields

$$\begin{aligned}&\left[\gamma_T^+(\boldsymbol{H}^\tau - \boldsymbol{H}_*^\tau), \gamma_T^+(\boldsymbol{E}-\boldsymbol{E}_*^\tau)\right]_\Gamma\\ &= \int_{\Omega^+} \mathbf{curl}(\boldsymbol{H}^\tau - \boldsymbol{H}_*^\tau)\cdot(\boldsymbol{E}-\boldsymbol{E}_*^\tau) - (\boldsymbol{H}^\tau - \boldsymbol{H}_*^\tau)\cdot\mathbf{curl}(\boldsymbol{E}-\boldsymbol{E}_*^\tau)\,\mathrm{d}\boldsymbol{x}\\ &\leq \int_{\Omega^+} (\partial_t^\tau\boldsymbol{E}^\tau - \partial_t^\tau\boldsymbol{E}_*^\tau)\cdot(\boldsymbol{E}-\boldsymbol{E}_*^\tau)\,\mathrm{d}\boldsymbol{x} + \left\|\boldsymbol{H}^\tau - \boldsymbol{H}_*^\tau\right\|_{\boldsymbol{L}^2(\Omega^+)} \left\|\boldsymbol{E}-\boldsymbol{E}_*^n\right\|_{\boldsymbol{H}(\mathbf{curl},\Omega^+)}\\ &\leq \int_{\Omega^+} (\partial_t^\tau\boldsymbol{E}^\tau - \partial_t^\tau\boldsymbol{E}_*^\tau)\cdot(\boldsymbol{E}-\boldsymbol{E}_*^\tau)\,\mathrm{d}\boldsymbol{x} + C\tau^m \left\|\boldsymbol{H}^\tau - \boldsymbol{H}_*^\tau\right\|_{\boldsymbol{L}^2(\Omega^+)},\end{aligned}$$

where the inequalities are given by the Cauchy–Schwarz inequality on the domain Ω and (4.57). The second summand above is then bounded by applying Young's inequality and absorbing the remaining term depending on the numerical solution with (4.58).

We continue with the remaining first summand, where a discrete derivative of the numerical solution has arisen. Applying the discrete partial integration formula of Lemma 4.3 yields for

any $\epsilon > 0$ a positive constant C such that

$$\begin{aligned}&\sum_{n=0}^{\infty} \rho^n \int_{\Omega^+} \left(\partial_t^\tau (\boldsymbol{E}^\tau - \boldsymbol{E}_*^\tau)\right)_n \cdot (\boldsymbol{E} - \boldsymbol{E}_*^\tau)_n \,\mathrm{d}\boldsymbol{x} \\ &\qquad \leq \sum_{n=0}^{\infty} \rho^n \left(\epsilon \left\|(\boldsymbol{E}^\tau - \boldsymbol{E}_*^\tau)_n\right\|^2_{\boldsymbol{L}^2(\Omega^+)} + C \left\|\left(\partial_t^\tau (\boldsymbol{E} - \boldsymbol{E}_*^\tau)\right)_n\right\|^2_{\boldsymbol{L}^2(\Omega^+)}\right),\end{aligned}$$

where we choose ϵ small enough to absorb the term with (4.58).

To bound the remaining term, we apply the discretized Maxwell's equation for $\boldsymbol{E}_*^\tau$ to obtain

$$\begin{aligned}\left\|\partial_t^\tau (\boldsymbol{E} - \boldsymbol{E}_*^\tau)\right\|_{\boldsymbol{L}^2(\Omega^+)} &\leq \left\|\partial_t^\tau \boldsymbol{E} - \partial_t \boldsymbol{E}\right\|_{\boldsymbol{L}^2(\Omega^+)} + \left\|\mathbf{curl}(\boldsymbol{H} - \boldsymbol{H}_*^\tau)\right\|_{\boldsymbol{L}^2(\Omega^+)} \\ &\leq C\tau^m \left\|\begin{pmatrix}\boldsymbol{\varphi} \\ \boldsymbol{\psi}\end{pmatrix}\right\|_{\boldsymbol{H}_0^{m+5}\left(0,T;\boldsymbol{X}_\Gamma{}^2\right)}.\end{aligned}$$

This bound completes the estimation of the first component of (4.61).

The remaining component of (4.61) is estimated by repeating the same arguments, starting from inserting (4.60), which yields

$$\begin{aligned}\left[\boldsymbol{e}_{\boldsymbol{\psi}}, \gamma_T^+(\boldsymbol{H} - \boldsymbol{H}_*^\tau)\right]_\Gamma &= \left[-\gamma_T^+ (\boldsymbol{E}^\tau - \boldsymbol{E}), \gamma_T^+(\boldsymbol{H} - \boldsymbol{H}_*^\tau)\right]_\Gamma \\ &= \left[-\gamma_T^+ (\boldsymbol{E}^\tau - \boldsymbol{E}_*^\tau), \gamma_T^+(\boldsymbol{H} - \boldsymbol{H}_*^\tau)\right]_\Gamma \\ &\quad + \left[-\gamma_T^+ (\boldsymbol{E}_*^\tau - \boldsymbol{E}), \gamma_T^+(\boldsymbol{H} - \boldsymbol{H}_*^\tau)\right]_\Gamma.\end{aligned}$$

The second summand is again independent of the numerical solution and bounded from above via

$$\begin{aligned}\left[\gamma_T^+ (\boldsymbol{E}_*^\tau - \boldsymbol{E}), \gamma_T^+(\boldsymbol{H} - \boldsymbol{H}_*^\tau)\right]_\Gamma &\leq \left\|\boldsymbol{E} - \boldsymbol{E}_*^\tau\right\|_{\boldsymbol{H}(\mathbf{curl},\Omega^+)} \left\|\boldsymbol{H} - \boldsymbol{H}_*^\tau\right\|_{\boldsymbol{H}(\mathbf{curl},\Omega^+)} \\ &\leq C\tau^{2m} \left\|\begin{pmatrix}\boldsymbol{\varphi} \\ \boldsymbol{\psi}\end{pmatrix}\right\|^2_{\boldsymbol{H}_0^{m+5}\left(0,T;\boldsymbol{X}_\Gamma{}^2\right)}.\end{aligned}$$

Applying Green's formula (4.30) to the first summand and inserting (4.41) yields

$$\begin{aligned}&\left[\gamma_T^+ (\boldsymbol{E}_*^\tau - \boldsymbol{E}^\tau), \gamma_T^+(\boldsymbol{H} - \boldsymbol{H}_*^\tau)\right]_\Gamma \\ &= \int_{\Omega^+} \mathbf{curl}(\boldsymbol{E}_*^\tau - \boldsymbol{E}^\tau) \cdot (\boldsymbol{H} - \boldsymbol{H}_*^\tau) - (\boldsymbol{E}_*^\tau - \boldsymbol{E}^\tau) \cdot \mathbf{curl}(\boldsymbol{H} - \boldsymbol{H}_*^\tau) \mathrm{d}\boldsymbol{x} \\ &\leq \int_{\Omega^+} (\partial_t^\tau \boldsymbol{H}^\tau - \partial_t^\tau \boldsymbol{H}_*^\tau) \cdot (\boldsymbol{H} - \boldsymbol{H}_*^\tau) \,\mathrm{d}\boldsymbol{x} + \left\|\boldsymbol{E}_*^\tau - \boldsymbol{E}^\tau\right\|_{\boldsymbol{L}(\Omega^+)} \left\|\boldsymbol{H} - \boldsymbol{H}_*^\tau\right\|_{\boldsymbol{H}(\mathbf{curl},\Omega^+)}.\end{aligned}$$

The second summand is again bounded from above by employing Young's inequality, (4.57) and absorbing the remaining term. Applying the discrete partial integration formula of Lemma 4.3

shows the estimate

$$\sum_{n=0}^{\infty} \rho^n \int_{\Omega^+} (\partial_t^\tau \boldsymbol{H}^\tau - \partial_t^\tau \boldsymbol{H}_*^\tau)_n \cdot (\boldsymbol{H} - \boldsymbol{H}_*^\tau)_n \,\mathrm{d}\boldsymbol{x} \\ \leq \sum_{n=0}^{\infty} \rho^n \left(\epsilon \, \|(\boldsymbol{H}^\tau - \boldsymbol{H}_*^\tau)_n\|^2_{\boldsymbol{L}^2(\Omega^+)} + C \, \|(\partial_t^\tau (\boldsymbol{H} - \boldsymbol{H}_*^\tau))_n\|^2_{\boldsymbol{L}^2(\Omega^+)} \right).$$

As before, the constant ϵ is arbitrary small and is chosen small enough such that the corresponding summand can be absorbed to the left-hand side with (4.58). Inserting the time-discrete Maxwell's equation once more into the first summand completes the proof by

$$\|\partial_t^\tau (\boldsymbol{H} - \boldsymbol{H}_*^\tau)\|_{\boldsymbol{L}^2(\Omega^+)} \leq \|\partial_t^\tau \boldsymbol{H} - \partial_t \boldsymbol{H}\|_{\boldsymbol{L}^2(\Omega^+)} + \|\mathbf{curl}(\boldsymbol{E} - \boldsymbol{E}_*^\tau)\|_{\boldsymbol{L}^2(\Omega^+)} \\ \leq C\tau^m \left\| \begin{pmatrix} \boldsymbol{\varphi} \\ \boldsymbol{\psi} \end{pmatrix} \right\|_{\boldsymbol{H}_0^{m+5}\left(0,T;\boldsymbol{X}_\Gamma{}^2\right)}.$$

□

4.4. Semi-discretization in space by the boundary element method

We turn our attention towards the semi-discretization in space, which restricts the weak formulation to a finite dimensional subspace. As in the previous chapter, we make use of the Raviart–Thomas boundary element space, whose favourable approximation properties are discussed in Section 3.7.

In contrast to the previous chapter, we begin with the time-continuous formulation, which is a suitable setting to present the error analysis for the spatial defects. The time-continuous spatial semi-discretization reads:
Find $\boldsymbol{\varphi}_h, \boldsymbol{\psi}_h \in \boldsymbol{L}_0^2(\boldsymbol{X}_h \times \boldsymbol{V}_h)$ such that for all $(\boldsymbol{\eta}_h, \boldsymbol{\xi}_h) \in \boldsymbol{X}_h \times \boldsymbol{V}_h$, it holds that

$$\left[\begin{pmatrix} \boldsymbol{\eta}_h \\ \boldsymbol{\xi}_h \end{pmatrix}, \boldsymbol{C}_{\mathrm{imp}}^-(\partial_t) \begin{pmatrix} \boldsymbol{\varphi}_h \\ \boldsymbol{\psi}_h \end{pmatrix} \right]_\Gamma + \left(\boldsymbol{\xi}_h, \boldsymbol{b}\left(\boldsymbol{\psi}_h - \gamma_T \boldsymbol{E}^{\mathrm{inc}}\right)\right)_\Gamma = [\gamma_T \boldsymbol{H}^{\mathrm{inc}}, \boldsymbol{\xi}_h]_\Gamma. \tag{4.62}$$

Let $\boldsymbol{I}_h : \boldsymbol{V}_\Gamma \to \boldsymbol{V}_h$ (or $\boldsymbol{I}_h : \boldsymbol{X}_\Gamma \to \boldsymbol{X}_h$ respectively) denote the interpolation operator of the underlying boundary element space. The following proposition gives a stability estimate of the error arising from the spatial semi-discretization, bounding it purely by interpolation errors of the exact solution.

Remark 4.4. *In contrast to Chapter 2, both boundary element spaces $\boldsymbol{V}_h$ and $\boldsymbol{X}_h$ coincide in practice, since we choose Raviart–Thomas boundary elements of order k to approximate both traces. Consequently, we abstain from notationally differentiating between the interpolation operators associated to the boundary element spaces $\boldsymbol{V}_h$ and $\boldsymbol{X}_h$ respectively.*

4.4.1. Spatial semi-discretization: Quasi-optimality

Proposition 4.3. *Let $(\boldsymbol{\varphi}, \boldsymbol{\psi}) \in \boldsymbol{H}^3_0(0,T;\boldsymbol{V}_\Gamma \times \boldsymbol{X}_\Gamma)$ be the solution of the boundary integral equation (4.32) and $\boldsymbol{\varphi}_h, \boldsymbol{\psi}_h \in \boldsymbol{L}^2_0(\boldsymbol{V}_h \times \boldsymbol{X}_h)$ be solutions of the spatially discrete formulation (4.62). For brevity of notation, we introduce a nonlinear defect, which we set to be*

$$\boldsymbol{d}_{\boldsymbol{b}} \coloneqq \boldsymbol{b}\left(\boldsymbol{I}_h\boldsymbol{\psi} - \gamma_T \boldsymbol{E}^{inc}\right) - \boldsymbol{b}\left(\boldsymbol{\psi} - \gamma_T \boldsymbol{E}^{inc}\right).$$

The spatial semi-discretization errors are denoted by $\boldsymbol{e}^h_{\boldsymbol{\varphi}} = \boldsymbol{\varphi}_h - \boldsymbol{I}_h\boldsymbol{\varphi}$ and $\boldsymbol{e}^h_{\boldsymbol{\psi}} = \boldsymbol{\psi}_h - \boldsymbol{I}_h\boldsymbol{\psi}$. Then, we have the following stability estimate

$$\int_0^T \left\| \partial_t^{-1} \begin{pmatrix} \boldsymbol{e}^h_{\boldsymbol{\varphi}} \\ \boldsymbol{e}^h_{\boldsymbol{\psi}} \end{pmatrix} \right\|^2_{\boldsymbol{X}_\Gamma{}^2} + \left\| \boldsymbol{e}^h_{\boldsymbol{\psi}} \right\|^{\frac{1+\alpha}{\alpha}}_{\boldsymbol{L}^{\frac{1+\alpha}{\alpha}}(\Gamma)} \mathrm{d}t \leq C \left\| \begin{pmatrix} \boldsymbol{I}_h\boldsymbol{\varphi} - \boldsymbol{\varphi} \\ \boldsymbol{I}_h\boldsymbol{\psi} - \boldsymbol{\psi} \end{pmatrix} \right\|^2_{\boldsymbol{H}^3_0\left(0,T;\boldsymbol{X}_\Gamma{}^2\right)} + C \int_0^\infty e^{-t/T} \left\| \boldsymbol{d}_{\boldsymbol{b}} \right\|^{1+\alpha}_{\boldsymbol{L}^{1+\alpha}(\Gamma)} \mathrm{d}t. \tag{4.63}$$

The constant C only depends on the boundary and polynomially on the final time T.

Proof. Inserting the interpolation into the exact formulation and rearranging yields

$$\begin{aligned} &\left[\begin{pmatrix} \boldsymbol{\eta} \\ \boldsymbol{\xi} \end{pmatrix}, \boldsymbol{C}^-_{\mathrm{imp}}(\partial_t) \begin{pmatrix} \boldsymbol{I}_h\boldsymbol{\varphi} \\ \boldsymbol{I}_h\boldsymbol{\psi} \end{pmatrix} \right]_\Gamma + \left(\boldsymbol{\xi}, \boldsymbol{b}\left(\boldsymbol{I}_h\boldsymbol{\psi} - \gamma_T \boldsymbol{E}^{\mathrm{inc}}\right)\right)_\Gamma \\ &\qquad = \left[\gamma_T \boldsymbol{H}^{\mathrm{inc}}, \boldsymbol{\xi}\right]_\Gamma + \left[\begin{pmatrix} \boldsymbol{\eta} \\ \boldsymbol{\xi} \end{pmatrix}, \boldsymbol{C}^-_{\mathrm{imp}}(\partial_t) \begin{pmatrix} \boldsymbol{I}_h\boldsymbol{\varphi} - \boldsymbol{\varphi} \\ \boldsymbol{I}_h\boldsymbol{\psi} - \boldsymbol{\psi} \end{pmatrix} \right]_\Gamma + \left(\boldsymbol{\xi}, \mathbf{d}_{\boldsymbol{b}}\right)_\Gamma. \end{aligned}$$

Subtraction from the spatial semi-discretization and testing with the defect equation above with $\boldsymbol{\eta}_h = \boldsymbol{e}^h_{\boldsymbol{\varphi}}$ and $\boldsymbol{\xi}_h = \boldsymbol{e}^h_{\boldsymbol{\psi}}$ provides the error equation

$$\left[\begin{pmatrix} \boldsymbol{e}^h_{\boldsymbol{\varphi}} \\ \boldsymbol{e}^h_{\boldsymbol{\psi}} \end{pmatrix}, \boldsymbol{C}^-_{\mathrm{imp}}(\partial_t) \begin{pmatrix} \boldsymbol{e}^h_{\boldsymbol{\varphi}} \\ \boldsymbol{e}^h_{\boldsymbol{\psi}} \end{pmatrix} \right]_\Gamma + \left(\boldsymbol{e}^h_{\boldsymbol{\psi}}, \boldsymbol{b}\left(\boldsymbol{\psi}_h - \gamma_T \boldsymbol{E}^{\mathrm{inc}}\right) - \boldsymbol{b}\left(\boldsymbol{I}_h\,\boldsymbol{\psi} - \gamma_T \boldsymbol{E}^{\mathrm{inc}}\right)\right)_\Gamma \tag{4.64}$$

$$= \left[\begin{pmatrix} \boldsymbol{e}^h_{\boldsymbol{\varphi}} \\ \boldsymbol{e}^h_{\boldsymbol{\psi}} \end{pmatrix}, \boldsymbol{C}^-_{\mathrm{imp}}(\partial_t) \begin{pmatrix} \boldsymbol{I}_h\boldsymbol{\varphi} - \boldsymbol{\varphi} \\ \boldsymbol{I}_h\boldsymbol{\psi} - \boldsymbol{\psi} \end{pmatrix} \right]_\Gamma + \left(\boldsymbol{e}^h_{\boldsymbol{\psi}}, \mathbf{d}_{\boldsymbol{b}}\right)_\Gamma. \tag{4.65}$$

Both the terms occuring on the left-hand side above can be estimated from below. The coercivity of the time domain Calderón operator (4.27) yields a positive constant $c > 0$, depending only polynomially on the inverse of T and on the boundary Γ, such that

$$c \int_0^\infty e^{-t/T} \left\| \partial_t^{-1} \begin{pmatrix} \boldsymbol{e}^h_{\boldsymbol{\varphi}} \\ \boldsymbol{e}^h_{\boldsymbol{\psi}} \end{pmatrix} \right\|^2_{\boldsymbol{X}_\Gamma{}^2} \mathrm{d}t \leq \int_0^\infty e^{-t/T} \left[\begin{pmatrix} \boldsymbol{e}^h_{\boldsymbol{\varphi}} \\ \boldsymbol{e}^h_{\boldsymbol{\psi}} \end{pmatrix}, \boldsymbol{C}_{\mathrm{imp}}(\partial_t) \begin{pmatrix} \boldsymbol{e}^h_{\boldsymbol{\varphi}} \\ \boldsymbol{e}^h_{\boldsymbol{\psi}} \end{pmatrix} \right]_\Gamma \mathrm{d}t.$$

Applying the positivity of the nonlinearity (4.10) to the second summand occuring in the error

equation yields

$$\left(e_{\psi}^{h},\, \boldsymbol{b}\left(\psi_h - \gamma_T \boldsymbol{E}^{\mathrm{inc}}\right) - \boldsymbol{b}\left(\boldsymbol{I}_h \psi - \gamma_T \boldsymbol{E}^{\mathrm{inc}}\right)\right)_{\Gamma} \geq c_{\alpha} \left\| e_{\psi}^{h} \right\|_{\boldsymbol{L}^{\frac{1+\alpha}{\alpha}}(\Gamma)}^{\frac{1+\alpha}{\alpha}}.$$

These positivity estimates provide, in combination with the error equation (4.64), the bound

$$\begin{aligned} & c \int_0^{\infty} e^{-t/T} \left\| \partial_t^{-1} \begin{pmatrix} e_{\varphi}^{h} \\ e_{\psi}^{h} \end{pmatrix} \right\|_{\boldsymbol{X}_{\Gamma}^{2}}^{2} + e^{-t/T} \left\| e_{\psi}^{h} \right\|_{\boldsymbol{L}^{\frac{1+\alpha}{\alpha}}(\Gamma)}^{\frac{1+\alpha}{\alpha}} \mathrm{d}t \\ & \leq \int_0^{\infty} e^{-t/T} \left[\begin{pmatrix} e_{\varphi}^{h} \\ e_{\psi}^{h} \end{pmatrix}, \boldsymbol{C}_{\mathrm{imp}}^{-}(\partial_t) \begin{pmatrix} \boldsymbol{I}_h \varphi - \varphi \\ \boldsymbol{I}_h \psi - \psi \end{pmatrix} \right]_{\Gamma} + e^{-t/T} \left(e_{\psi}^{h}, \mathbf{d}_b \right)_{\Gamma} \mathrm{d}t. \end{aligned} \tag{4.66}$$

The first summand is bounded through partial integration and Young's inequality, which yields for any $\epsilon > 0$ a constant C such that

$$\begin{aligned} & \int_0^{\infty} e^{-t/T} \left[\begin{pmatrix} e_{\varphi}^{h} \\ e_{\psi}^{h} \end{pmatrix}, \boldsymbol{C}_{\mathrm{imp}}^{-}(\partial_t) \begin{pmatrix} \boldsymbol{I}_h \varphi - \varphi \\ \boldsymbol{I}_h \psi - \psi \end{pmatrix} \right]_{\Gamma} \mathrm{d}t \\ & \leq \epsilon \int_0^{\infty} e^{-t/T} \left\| \partial_t^{-1} \begin{pmatrix} e_{\varphi}^{h} \\ e_{\psi}^{h} \end{pmatrix} \right\|_{\boldsymbol{X}_{\Gamma}^{2}}^{2} \mathrm{d}t + C \int_0^{\infty} e^{-t/T} \left\| \partial_t \boldsymbol{C}_{\mathrm{imp}}^{-}(\partial_t) \begin{pmatrix} \boldsymbol{I}_h \varphi - \varphi \\ \boldsymbol{I}_h \psi - \psi \end{pmatrix} \right\|_{\boldsymbol{X}_{\Gamma}^{2}}^{2} \mathrm{d}t. \end{aligned}$$

Absorbing the first summand by choosing ϵ small enough and applying (A.3) to the remaining term yields

$$\int_0^{\infty} e^{-t/T} \left\| \partial_t \boldsymbol{C}_{\mathrm{imp}}^{-}(\partial_t) \begin{pmatrix} \boldsymbol{I}_h \varphi - \varphi \\ \boldsymbol{I}_h \psi - \psi \end{pmatrix} \right\|_{\boldsymbol{X}_{\Gamma}^{2}}^{2} \mathrm{d}t \leq C \int_0^{\infty} e^{-t/T} \left\| \partial_t^{3} \begin{pmatrix} \boldsymbol{I}_h \varphi - \varphi \\ \boldsymbol{I}_h \psi - \psi \end{pmatrix} \right\|_{\boldsymbol{X}_{\Gamma}^{2}}^{2} \mathrm{d}t.$$

Choosing ϵ small enough allows the first summand to be absorbed. Applying Hölder's inequality and Young's inequality successively to the nonlinear term in (4.66) finally yields

$$\left(e_{\psi}^{h}, \mathbf{d}_b\right)_{\Gamma} \leq \left\| e_{\psi}^{h} \right\|_{\boldsymbol{L}^{\frac{1+\alpha}{\alpha}}(\Gamma)} \left\| \mathbf{d}_b \right\|_{\boldsymbol{L}^{1+\alpha}(\Gamma)} \leq \epsilon \left\| e_{\psi}^{h} \right\|_{\boldsymbol{L}^{\frac{1+\alpha}{\alpha}}(\Gamma)}^{\frac{1+\alpha}{\alpha}} + C \left\| \mathbf{d}_b \right\|_{\boldsymbol{L}^{1+\alpha}(\Gamma)}^{1+\alpha}.$$

The constant $C > 0$ is only dependent on ϵ, which is set small enough such that the first summand can be absorbed on the second summand on the left-hand side of (4.66). □

Remark 4.5. *We note that the previous stability estimate readily extends to a more general class of projection operators. However, since the approximation properties of the interpolation operators $\boldsymbol{I}_h$ associated to the Raviart–Thomas boundary element spaces are sufficient in the confines of this chapter, we restrict the presentation to these interpolation operators.*

4.4.2. Spatial semi-discretization: Error rates

The $\boldsymbol{L}^{1+\alpha}(\Gamma)$-norm is bounded by the $\boldsymbol{L}^2(\Gamma)$- norm, which follows from Hölder's inequality with $q = \frac{2}{1+\alpha}$ and $p = \frac{2}{1-\alpha}$, which implies

$$\|\boldsymbol{u}\|^{1+\alpha}_{\boldsymbol{L}^{1+\alpha}(\Gamma)} = \int_\Gamma |\boldsymbol{u}|^{1+\alpha} \,\mathrm{d}\boldsymbol{x} \leq \|\mathbf{1}\|_{\boldsymbol{L}^{\frac{2}{1-\alpha}}(\Gamma)} \left\| |\boldsymbol{u}|^{1+\alpha} \right\|_{\boldsymbol{L}^{\frac{2}{1+\alpha}}(\Gamma)} = C_{\alpha,\Gamma} \|\boldsymbol{u}\|^{1+\alpha}_{\boldsymbol{L}^2(\Gamma)} . \tag{4.67}$$

For Raviart–Thomas elements of order k and $\boldsymbol{\varphi} \in \boldsymbol{H}^{k+1}_\times(\Gamma)$, we therefore have, from [26, Lemma 15], the interpolation estimate

$$\|\boldsymbol{I}_h\boldsymbol{\varphi} - \boldsymbol{\varphi}\|_{\boldsymbol{L}^{1+\alpha}(\Gamma)} \leq \|\boldsymbol{I}_h\boldsymbol{\varphi} - \boldsymbol{\varphi}\|_{\boldsymbol{L}^2(\Gamma)} \leq Ch^{k+1} \|\boldsymbol{\varphi}\|_{\boldsymbol{H}^{k+1}_\times(\Gamma)} . \tag{4.68}$$

Moreover, an additional interpolation approximation result from [26, Lemma 15] shows

$$\|\boldsymbol{I}_h\boldsymbol{\varphi} - \boldsymbol{\varphi}\|_{\boldsymbol{X}_\Gamma} \leq Ch^{k+1} \|\boldsymbol{\varphi}\|_{\boldsymbol{H}^{k+1}_\times(\Gamma)} . \tag{4.69}$$

These interpolation estimates are sufficient approximation properties of the underlying boundary element space for the error analysis in this chapter. Inserting the approximation properties of the Raviart–Thomas boundary element space on the right-hand side of the stability result gives the following convergence result.

Theorem 4.2. *Let $(\boldsymbol{\varphi}, \boldsymbol{\psi})$ be the solution of the boundary integral equation (4.32), assumed to be of regularity*

$$(\boldsymbol{\varphi}, \boldsymbol{\psi}) \in \boldsymbol{H}^3_0\left(0, T; \boldsymbol{H}^{k+1}_\times(\Gamma)^2\right).$$

Moreover, let $\boldsymbol{\psi}(t), \gamma_T \boldsymbol{E}^{\mathrm{inc}} \in \boldsymbol{L}^\infty(\Gamma)$ for all $t \in [0, T]$. Consider the spatially discrete boundary densities $(\boldsymbol{\varphi}_h(t), \boldsymbol{\psi}_h(t)) \in \boldsymbol{V}^m_h \times \boldsymbol{X}^m_h$ for all $t \geq 0$, solutions to the semi-discrete boundary integral equation (4.62), discretized by Raviart–Thomas boundary elements of order k. These approximations fulfill the error bounds

$$\left\| \partial_t^{-1} \begin{pmatrix} \boldsymbol{\varphi}_h - \boldsymbol{\varphi} \\ \boldsymbol{\psi}_h - \boldsymbol{\psi} \end{pmatrix} \right\|_{\boldsymbol{L}^2_0(0,T;\boldsymbol{X}_\Gamma{}^2)} \leq Ch^{\frac{1+\alpha}{2}(k+1)}.$$

The constant C depends on the incident waves, higher Sobolev norms of the exact solution $(\boldsymbol{\varphi}, \boldsymbol{\psi})$, the boundary Γ, polynomially on the final time T and on α.

Proof. The stability analysis of Proposition 4.3 implies bounds for the complete error, a fact that is seen by using the interpolation as an intermediate term and employing the approximation result (4.69), which yields

$$\left\| \partial_t^{-1} \begin{pmatrix} \boldsymbol{\varphi}_h - \boldsymbol{\varphi} \\ \boldsymbol{\psi}_h - \boldsymbol{\psi} \end{pmatrix} \right\|_{\boldsymbol{L}^2_0(0,T;\boldsymbol{X}_\Gamma{}^2)} \leq \left\| \partial_t^{-1} \begin{pmatrix} \boldsymbol{\varphi}_h - \boldsymbol{I}_h\boldsymbol{\varphi} \\ \boldsymbol{\psi}_h - \boldsymbol{I}_h\boldsymbol{\psi} \end{pmatrix} \right\|_{\boldsymbol{L}^2_0(0,T;\boldsymbol{X}_\Gamma{}^2)} + Ch^{k+1}.$$

Consequently, we restrict our attention for the rest of the proof on the remaining summand, which was estimated in Proposition 4.3. The right-hand side of the stability estimate (4.63) consists of two spatial defects, which are connected to the Calderón operator and the nonlinearity

$\boldsymbol{b}$ respectively. The first spatial defect is directly bounded via the interpolation error estimate (4.69) through

$$\left\| \begin{pmatrix} \boldsymbol{I}_h \boldsymbol{\varphi} - \boldsymbol{\varphi} \\ \boldsymbol{I}_h \boldsymbol{\psi} - \boldsymbol{\psi} \end{pmatrix} \right\|_{\boldsymbol{H}_0^3(0,T;\boldsymbol{X}_\Gamma \times \boldsymbol{X}_\Gamma)} \leq C h^{k+1} \left\| \begin{pmatrix} \partial_t^3 \boldsymbol{\varphi} \\ \partial_t^3 \boldsymbol{\psi} \end{pmatrix} \right\|_{\boldsymbol{L}_0^2\left(0,T;\boldsymbol{H}_\times^{k+1}(\Gamma)^2\right)}.$$

The nonlinear defect term is pointwise bounded by (4.11), which yields the existence of a constant C, depending on α and the incident electric wave, such that

$$\begin{aligned} \|\mathbf{d}_{\boldsymbol{b}}\|_{\boldsymbol{L}^{1+\alpha}(\Gamma)}^{1+\alpha} &= \left\| \boldsymbol{b}\left(\boldsymbol{I}_h \boldsymbol{\psi} - \gamma_T \boldsymbol{E}^{\mathrm{inc}}\right) - \boldsymbol{b}\left(\boldsymbol{\psi} - \gamma_T \boldsymbol{E}^{\mathrm{inc}}\right) \right\|_{\boldsymbol{L}^{1+\alpha}(\Gamma)}^{1+\alpha} \\ &\leq C \int_\Gamma \left(|\boldsymbol{I}_h \boldsymbol{\psi}| + |\boldsymbol{\psi}| \right)^{\frac{1-\alpha^2}{\alpha}} |\boldsymbol{I}_h \boldsymbol{\psi} - \boldsymbol{\psi}|^{1+\alpha} \, \mathrm{d}\boldsymbol{x} \\ &\leq C \left(\|\boldsymbol{I}_h \boldsymbol{\psi}\|_{\boldsymbol{L}^\infty(\Gamma)} + \|\boldsymbol{\psi}\|_{\boldsymbol{L}^\infty(\Gamma)} \right)^{\frac{1-\alpha^2}{\alpha}} \|\boldsymbol{I}_h \boldsymbol{\psi} - \boldsymbol{\psi}\|_{\boldsymbol{L}^{1+\alpha}(\Gamma)}^{1+\alpha}. \end{aligned}$$

Applying the approximation result (4.68) for the interpolation operator of the Raviart–Thomas element space finally implies

$$\|\mathbf{d}_{\boldsymbol{b}}\|_{\boldsymbol{L}^{1+\alpha}(\Gamma)}^{1+\alpha} \leq C h^{(1+\alpha)(k+1)} \left(1 + \|\boldsymbol{\psi}\|_{\boldsymbol{L}^\infty(\Gamma)}\right)^{\frac{1-\alpha^2}{\alpha}} \|\boldsymbol{\psi}\|_{\boldsymbol{H}_\times^{k+1}(\Gamma)}^{1+\alpha}.$$

Combining the stability result (4.63) with these bounds completes the proof. □

4.5. Full discretization

Combining the m-stage Radau IIA Runge–Kutta convolution quadrature time discretization with the k-th order Raviart–Thomas boundary element space discretization yields the following fully discrete scheme.

Full discretization of the boundary integral equation: *Find the sequence of fully discrete boundary densities* $(\boldsymbol{\varphi}_n^{\tau,h}, \boldsymbol{\psi}_n^{\tau,h}) \in \boldsymbol{V}_h^m \times \boldsymbol{X}_h^m$ *for* $n \leq N$ *such that for all* $(\boldsymbol{\eta}_h, \boldsymbol{\xi}_h) \in \boldsymbol{V}_h \times \boldsymbol{X}_h$, *it holds that*

$$\left[\begin{pmatrix} \boldsymbol{\eta}_h \\ \boldsymbol{\xi}_h \end{pmatrix}, \left(\boldsymbol{C}_{\mathrm{imp}}^-(\partial_t^\tau) \begin{pmatrix} \boldsymbol{\varphi}^{\tau,h} \\ \boldsymbol{\psi}^{\tau,h} \end{pmatrix} \right)^n \right]_\Gamma + \left(\boldsymbol{\xi}_h, \boldsymbol{b}\left(\boldsymbol{\psi}_n^{\tau,h} - \gamma_T \boldsymbol{E}_n^{\mathrm{inc}} \right) \right)_\Gamma = [\gamma_T \boldsymbol{H}_n^{\mathrm{inc}}, \boldsymbol{\xi}_h]_\Gamma. \tag{4.70}$$

At every time step, this scheme requires the solution of the nonlinear system

$$\left[\begin{pmatrix} \boldsymbol{\eta}_h \\ \boldsymbol{\xi}_h \end{pmatrix}, \boldsymbol{C}_{\mathrm{imp}}^- \left(\frac{\Delta(0)}{\tau} \right) \begin{pmatrix} \boldsymbol{\varphi}_n^{\tau,h} \\ \boldsymbol{\psi}_n^{\tau,h} \end{pmatrix} \right]_\Gamma + \left(\boldsymbol{\xi}_h, \boldsymbol{b}\left(\boldsymbol{\psi}_n^{\tau,h} - \gamma_T \boldsymbol{E}_n^{\mathrm{inc}} \right) \right)_\Gamma = \left[f_n, \begin{pmatrix} \boldsymbol{\eta}_h \\ \boldsymbol{\xi}_h \end{pmatrix} \right]_\Gamma,$$

where the right-hand side f_n is determined by the incident waves and the history of the solution, as described in (C.12).

The above system has, for every $n \geq 0$, a unique solution. This result is provided by the Browder–Minty theorem, where the crucial monotonicity is given by Lemma 3.7 (note that the

eigenvalues of $\Delta(0) = \mathscr{A}^{-1}$ have positive real part, see e.g. [14, Lemma 3]) for the Calderón operator and by (4.10) for the nonlinearity $\boldsymbol{b}$ respectively. More details are found in [18, Theorem 4.4], which gives a proof in the acoustic setting for multistep-based convolution quadrature methods.

4.5.1. Error bounds for the full discretization

This section is devoted to the derivation of error bounds for the full discretization, by combining the key ideas used to derive error bounds for the semi-discretizations. In contrast to the error analysis of the semi-discretization in time, the temporal defects are estimated with terms that also act on the interior domain Ω^-.

Theorem 4.3. *The solution of the boundary integral equation (4.32) is assumed to be at least of the regularity*

$$(\boldsymbol{\varphi}, \boldsymbol{\psi}) \in \boldsymbol{H}_0^{m+5}\left(0, T; \boldsymbol{H}_\times^1(\Gamma)^2\right) \cap \boldsymbol{H}_0^3\left(0, T; \boldsymbol{H}_\times^{k+1}(\Gamma)^2\right).$$

Moreover, let $\boldsymbol{\psi}(t), \gamma_T \boldsymbol{E}^{\mathrm{inc}} \in \boldsymbol{L}^\infty(\Gamma)$ for all $t \geq 0$. Consider the fully discrete boundary densities $(\boldsymbol{\varphi}_n^{\tau,h}, \boldsymbol{\psi}_n^{\tau,h}) \in \boldsymbol{V}_h^m \times \boldsymbol{X}_h^m$ for all $n \leq N$, solution to the full discretization of the boundary integral equation (4.70), discretized by

- *Runge–Kutta convolution quadrature based on the m-stage Radau IIA method and*
- *Raviart–Thomas boundary elements of order k in space.*

For $m > 2$, we assume the full discretization to be applied to the shifted boundary integral equation (4.33), with $\sigma = 1/T$. The errors $\boldsymbol{e}_{\boldsymbol{\varphi}} = \boldsymbol{\varphi}_h^\tau - \boldsymbol{I}_h \boldsymbol{\varphi}$ and $\boldsymbol{e}_{\boldsymbol{\psi}} = \boldsymbol{\psi}_h^\tau - \boldsymbol{I}_h \boldsymbol{\psi}$ then fulfill the bounds

$$\left(\tau \sum_{n=0}^{N} \left\| \left((\partial_t^\tau)^{-1} \boldsymbol{e}_{\boldsymbol{\varphi}}\right)_n \right\|_{\boldsymbol{X}_\Gamma}^2 + \left\| \left((\partial_t^\tau)^{-1} \boldsymbol{e}_{\boldsymbol{\psi}}\right)_n \right\|_{\boldsymbol{X}_\Gamma}^2 \right)^{1/2} \leq C\left(\tau^m + h^{\frac{1+\alpha}{2}(k+1)}\right).$$

The electromagnetic fields, defined through the discrete representation formulas (4.46)–(4.47), further fulfill the error bounds

$$\left(\tau \sum_{n=0}^{N} \left\| \boldsymbol{E}_n^{\tau,h} - \boldsymbol{E}(\underline{t_n}) \right\|_{\boldsymbol{L}^2(\Omega)}^2 + \left\| \boldsymbol{H}_n^{\tau,h} - \boldsymbol{H}(\underline{t_n}) \right\|_{\boldsymbol{L}^2(\Omega)}^2 \right)^{1/2} \leq C\left(\tau^m + h^{\frac{1+\alpha}{2}(k+1)}\right),$$

where $\boldsymbol{E}(\underline{t_n}) = (\boldsymbol{E}(t_n + c_i\tau))_{i=1}^m$ denotes the evaluations at the stages $\boldsymbol{c}$ of the Radau IIA Runge–Kutta method. The constants depend on the incident waves, higher Sobolev norms of the exact solution $(\boldsymbol{\varphi}, \boldsymbol{\psi})$, the boundary Γ and polynomially on the final time T.

Proof. Whenever clear from the context, we omit the index $n \in \mathbb{N}$ or respectively the time point t_n, to simplify the notation. The proof here is presented for $m \leq 2$, which enables the use of the direct application of the coercivity property from Lemma 4.4. For $m > 2$, the proof is then generalized by recovering the positivity through a shift as described in Remark 4.2 and repeating the arguments precisely as they appear in the following proof.

Inserting a projection of the exact solution yields a sequence of defects $\mathbf{d} = (\mathbf{d}_n)_{n\geq 0}$, which are elementwise boundary element functions $\mathbf{d}_n \in \boldsymbol{X}_h^m \times \boldsymbol{V}_h^m$ for all $n \geq 0$, and ensure the perturbed boundary integral equation

$$\begin{aligned}\left[\begin{pmatrix}\boldsymbol{\eta}_h\\ \boldsymbol{\xi}_h\end{pmatrix}, \boldsymbol{C}_{\mathrm{imp}}^{-}(\partial_t^\tau)\begin{pmatrix}\boldsymbol{I}_h\boldsymbol{\varphi}\\ \boldsymbol{I}_h\boldsymbol{\psi}\end{pmatrix}\right]_\Gamma + \left(\boldsymbol{\xi}_h, \boldsymbol{b}\left(\boldsymbol{I}_h\boldsymbol{\psi} - \gamma_T\boldsymbol{E}^{\mathrm{inc}}\right)\right)_\Gamma \\ = \left[\gamma_T\boldsymbol{H}^{\mathrm{inc}}, \boldsymbol{\xi}_h\right]_\Gamma + \left[\begin{pmatrix}\boldsymbol{\eta}_h\\ \boldsymbol{\xi}_h\end{pmatrix}, \mathbf{d}\right]_\Gamma.\end{aligned} \tag{4.71}$$

Similarly to the error analysis for the semi-discretization in time, we define fields associated with the projected exact solutions through the discrete representation formulas via

$$\begin{pmatrix}\boldsymbol{E}_\Pi^{\tau,h}\\ \boldsymbol{H}_\Pi^{\tau,h}\end{pmatrix} = \begin{pmatrix}-\boldsymbol{\mathcal{S}}(\partial_t^\tau)\boldsymbol{I}_h\boldsymbol{\varphi} + \boldsymbol{\mathcal{D}}(\partial_t^\tau)\boldsymbol{I}_h\boldsymbol{\psi}\\ -\boldsymbol{\mathcal{D}}(\partial_t^\tau)\boldsymbol{I}_h\boldsymbol{\varphi} - \boldsymbol{\mathcal{S}}(\partial_t^\tau)\boldsymbol{I}_h\boldsymbol{\psi}\end{pmatrix} = \boldsymbol{\mathcal{W}}(\partial_t^\tau)\begin{pmatrix}\boldsymbol{I}_h\boldsymbol{\varphi}\\ \boldsymbol{I}_h\boldsymbol{\psi}\end{pmatrix}. \tag{4.72}$$

For brevity of notation, we use the notational short hand $\boldsymbol{E}_\Pi^{n,h} = (\boldsymbol{E}_\Pi^{\tau,h})_n$, for the sequence element approximating $\boldsymbol{E}$ at the stages $(t_n + c_i\tau)_{i=1}^m$. The discrete transmission problem of Lemma 4.5 shows

$$\begin{pmatrix}\boldsymbol{I}_h\boldsymbol{\varphi}\\ \boldsymbol{I}_h\boldsymbol{\psi}\end{pmatrix} = \begin{pmatrix}\gamma_T^+\boldsymbol{H}_\Pi^{\tau,h}\\ -\gamma_T^+\boldsymbol{E}_\Pi^{\tau,h}\end{pmatrix} - \begin{pmatrix}\gamma_T^-\boldsymbol{H}_\Pi^{\tau,h}\\ -\gamma_T^-\boldsymbol{E}_\Pi^{\tau,h}\end{pmatrix}. \tag{4.73}$$

These fields are approximations of the exact fields $\boldsymbol{E}$ and $\boldsymbol{H}$ and approximate these fields with a higher order than the stated error bounds since

$$\begin{pmatrix}\boldsymbol{E}_\Pi^{\tau,h} - \boldsymbol{E}\\ \boldsymbol{H}_\Pi^{\tau,h} - \boldsymbol{H}\end{pmatrix} = \left(\boldsymbol{\mathcal{W}}(\partial_t^\tau) - \boldsymbol{\mathcal{W}}(\partial_t)\right)\begin{pmatrix}\boldsymbol{I}_h\boldsymbol{\varphi}\\ \boldsymbol{I}_h\boldsymbol{\psi}\end{pmatrix} + \boldsymbol{\mathcal{W}}(\partial_t)\begin{pmatrix}\boldsymbol{I}_h\boldsymbol{\varphi} - \boldsymbol{\varphi}\\ \boldsymbol{I}_h\boldsymbol{\psi} - \boldsymbol{\psi}\end{pmatrix}.$$

Error bounds for these fields are then ensured by the error bound (4.69) of the interpolation operator and the convolution quadrature method approximation result of Lemma B.2. Using this result with $\kappa = 2$ and $\nu = 1$, where the time-harmonic bounds are provided by Lemma 3.10, then implies the existence of a constant C such that

$$\begin{aligned}&\left\|\boldsymbol{E}_\Pi^{n,h} - \boldsymbol{E}(\underline{t_n})\right\|_{\boldsymbol{H}(\mathbf{curl},\Omega)} + \left\|\boldsymbol{H}_\Pi^{n,h} - \boldsymbol{H}(\underline{t_n})\right\|_{\boldsymbol{H}(\mathbf{curl},\Omega)} \\ &\quad\leq C\left(\tau^m\left\|\begin{pmatrix}\boldsymbol{\varphi}\\ \boldsymbol{\psi}\end{pmatrix}\right\|_{\boldsymbol{H}_0^{m+5}(0,T;\boldsymbol{X}_\Gamma{}^2)} + h^{k+1}\left\|\begin{pmatrix}\boldsymbol{\varphi}\\ \boldsymbol{\psi}\end{pmatrix}\right\|_{\boldsymbol{H}_0^3(0,T;\boldsymbol{H}_\times^{k+1}(\Gamma)^2)}\right),\end{aligned} \tag{4.74}$$

where the constant only depends on the surface Γ and polynomially on the final time T. Subtracting the perturbed scheme from the full discretization and testing with the errors $\boldsymbol{e}_{\boldsymbol{\varphi}}^n$ and $\boldsymbol{e}_{\boldsymbol{\psi}}^n$

yields the following error equation

$$\begin{aligned}&\left[\begin{pmatrix} e_{\varphi}^n \\ e_{\psi}^n \end{pmatrix}, \left(\boldsymbol{C}_{\mathrm{imp}}^{-}(\partial_t^\tau) \begin{pmatrix} e_{\varphi} \\ e_{\psi} \end{pmatrix} \right)^n \right]_\Gamma \\ &+ \left(e_{\psi}^n, \boldsymbol{b}\left(\boldsymbol{\psi}_n^{\tau,h} - \gamma_T \boldsymbol{E}_n^{\mathrm{inc}} \right) - \boldsymbol{b}\left(\boldsymbol{I}_h \boldsymbol{\psi}(\underline{t_n}) - \gamma_T \boldsymbol{E}_n^{\mathrm{inc}} \right) \right)_\Gamma = \left[\begin{pmatrix} e_{\varphi}^n \\ e_{\psi}^n \end{pmatrix}, \mathbf{d}^n \right]_\Gamma .\end{aligned} \tag{4.75}$$

The second summand with the nonlinearity $\boldsymbol{b}$ is bounded from below through the pointwise monotonicity estimate of $\boldsymbol{b}$ from Lemma 4.10, which yields

$$\left(e_{\psi}^n, \boldsymbol{b}\left(\boldsymbol{\psi}_n^{\tau,h} - \gamma_T \boldsymbol{E}_n^{\mathrm{inc}} \right) - \boldsymbol{b}\left(\boldsymbol{I}_h \boldsymbol{\psi}(\underline{t_n}) - \gamma_T \boldsymbol{E}_n^{\mathrm{inc}} \right) \right)_\Gamma \geq c_\alpha \left\| e_{\psi}^n \right\|_{\boldsymbol{L}^{\frac{1+\alpha}{\alpha}}(\Gamma)}^{\frac{1+\alpha}{\alpha}} .$$

In order to estimate the tested time-discrete Calderón operator from below, we apply the second identity of Lemma 4.6, which reads for the present fields

$$\begin{aligned}\left[\begin{pmatrix} e_{\varphi}^n \\ e_{\psi}^n \end{pmatrix}, \left(\boldsymbol{C}_{\mathrm{imp}}^{-}(\partial_t^\tau) \begin{pmatrix} e_{\varphi} \\ e_{\psi} \end{pmatrix} \right)^n \right]_\Gamma &= \int_{\mathbb{R}^3 \setminus \Gamma} (\boldsymbol{E}^{\tau,h} - \boldsymbol{E}_{\Pi}^{\tau,h})_n \cdot \left(\partial_t^\tau \left(\boldsymbol{E}^{\tau,h} - \boldsymbol{E}_{\Pi}^{\tau,h} \right) \right)_n \\ &\quad + \left(\boldsymbol{H}^{\tau,h} - \boldsymbol{H}_{\Pi}^{\tau,h} \right)_n \cdot \left(\partial_t^\tau \left(\boldsymbol{H}^{\tau,h} - \boldsymbol{H}_{\Pi}^{\tau,h} \right) \right)_n \mathrm{d}\boldsymbol{x}.\end{aligned}$$

Employing the coercivity of the discrete operator ∂_t^τ, given by Lemma 4.4, now yields an estimate from below.

Taking the weighted sum over the error equation (4.75), where the term corresponding to the time point t_n is weighted by $\rho^n = e^{-n\tau/T}$, inserting this identity into the left-hand side and applying Lemma 4.4 yields a positive constant C such that

$$\begin{aligned}&\sum_{n=0}^{N} \rho^n \left(\left\| \boldsymbol{E}_n^{\tau,h} - \boldsymbol{E}_{\Pi}^{n,h} \right\|_{\boldsymbol{L}^2(\mathbb{R}^3 \setminus \Gamma)}^2 + \left\| \boldsymbol{H}_n^{\tau,h} - \boldsymbol{H}_{\Pi}^{n,h} \right\|_{\boldsymbol{L}^2(\mathbb{R}^3 \setminus \Gamma)}^2 + \left\| e_{\psi}^n \right\|_{\boldsymbol{L}^{\frac{1+\alpha}{\alpha}}(\Gamma)}^{\frac{1+\alpha}{\alpha}} \right) \\ &\quad \leq C \sum_{n=0}^{N} \rho^n \left[\begin{pmatrix} e_{\varphi}^n \\ e_{\psi}^n \end{pmatrix}, \mathbf{d}^n \right]_\Gamma .\end{aligned} \tag{4.76}$$

The term depending on the defect is rewritten by subtracting the exact boundary integral equation (4.32) from the perturbed equation (4.71), which yields the following decomposition

$$\begin{aligned}\left[\begin{pmatrix} e_{\varphi}^n \\ e_{\psi}^n \end{pmatrix}, \mathbf{d}^n \right]_\Gamma &= \left[\begin{pmatrix} e_{\varphi}^n \\ e_{\psi}^n \end{pmatrix}, \left(\boldsymbol{C}_{\mathrm{imp}}^{-}(\partial_t^\tau) \begin{pmatrix} \boldsymbol{I}_h \boldsymbol{\varphi} \\ \boldsymbol{I}_h \boldsymbol{\psi} \end{pmatrix} - \boldsymbol{C}_{\mathrm{imp}}^{-}(\partial_t) \begin{pmatrix} \boldsymbol{\varphi} \\ \boldsymbol{\psi} \end{pmatrix} \right)^n \right]_\Gamma \qquad \text{(A)} \\ &\quad + \left(e_{\psi}^n, \boldsymbol{b}\left(\boldsymbol{I}_h \boldsymbol{\psi}(\underline{t_n}) - \gamma_T \boldsymbol{E}_n^{\mathrm{inc}} \right) - \boldsymbol{b}\left(\boldsymbol{\psi}(\underline{t_n}) - \gamma_T \boldsymbol{E}_n^{\mathrm{inc}} \right) \right)_\Gamma \qquad \text{(B)}.\end{aligned}$$

The defect naturally consists of a temporal defect, depending on the approximation of the time-dependent Calderón operator, and a defect depending on the nonlinearity $\boldsymbol{b}$. These terms are subsequently estimated successively.

(A) We begin our investigations with the temporal defect, for which inserting the jump conditions of the discrete Calderón operator (4.44) and the continuous time-dependent Calderón operator (4.29) imply

$$\left[\begin{pmatrix} \boldsymbol{e}_{\boldsymbol{\varphi}} \\ \boldsymbol{e}_{\boldsymbol{\psi}} \end{pmatrix}, \boldsymbol{C}_{\mathrm{imp}}^{-}(\partial_t^{\tau}) \begin{pmatrix} \boldsymbol{I}_h\boldsymbol{\varphi} \\ \boldsymbol{I}_h\boldsymbol{\psi} \end{pmatrix} - \boldsymbol{C}_{\mathrm{imp}}^{-}(\partial_t) \begin{pmatrix} \boldsymbol{\varphi} \\ \boldsymbol{\psi} \end{pmatrix}\right]_{\Gamma} = \left[\begin{pmatrix} \boldsymbol{e}_{\boldsymbol{\varphi}} \\ \boldsymbol{e}_{\boldsymbol{\psi}} \end{pmatrix}, \begin{pmatrix} \gamma_T^{-}\boldsymbol{E}_{\Pi}^{\tau,h} \\ \gamma_T^{+}\boldsymbol{H}_{\Pi}^{\tau,h} - \gamma_T^{+}\boldsymbol{H} \end{pmatrix}\right]_{\Gamma}.$$

The left argument of the anti-symmetric pairing is split by rewriting the numerical approximation and the projected exact solution in terms of the jumps of their respective fields via (4.42)–(4.43) and (4.73) respectively, which yields

$$\begin{aligned} &\left[\begin{pmatrix} \boldsymbol{\varphi}^{\tau,h} - \boldsymbol{I}_h\boldsymbol{\varphi} \\ \boldsymbol{\psi}^{\tau,h} - \boldsymbol{I}_h\boldsymbol{\psi} \end{pmatrix}, \begin{pmatrix} \gamma_T^{-}\boldsymbol{E}_{\Pi}^{\tau,h} \\ \gamma_T^{+}\boldsymbol{H}_{\Pi}^{\tau,h} - \gamma_T^{+}\boldsymbol{H} \end{pmatrix}\right]_{\Gamma} \\ &= \left[\begin{pmatrix} \gamma_T^{+}(\boldsymbol{H}^{\tau,h} - \boldsymbol{H}_{\Pi}^{\tau,h}) \\ -\gamma_T^{+}(\boldsymbol{E}^{\tau,h} - \boldsymbol{E}_{\Pi}^{\tau,h}) \end{pmatrix}, \begin{pmatrix} \gamma_T^{-}\boldsymbol{E}_{\Pi}^{\tau,h} \\ \gamma_T^{+}\boldsymbol{H}_{\Pi}^{\tau,h} - \gamma_T^{+}\boldsymbol{H} \end{pmatrix}\right]_{\Gamma} \qquad (4.77) \\ &- \left[\begin{pmatrix} \gamma_T^{-}(\boldsymbol{H}^{\tau,h} - \boldsymbol{H}_{\Pi}^{n,h}) \\ -\gamma_T^{-}(\boldsymbol{E}^{\tau,h} - \boldsymbol{E}_{\Pi}^{\tau,h}) \end{pmatrix}, \begin{pmatrix} \gamma_T^{-}\boldsymbol{E}_{\Pi}^{\tau,h} \\ \gamma_T^{+}\boldsymbol{H}_{\Pi}^{\tau,h} - \gamma_T^{+}\boldsymbol{H} \end{pmatrix}\right]_{\Gamma}. \qquad (4.78) \end{aligned}$$

In the following, we estimate these terms corresponding to errors in the interior and exterior domains. The only inner trace appearing in the first summand is the inner tangential trace of the electric field, which is rewritten via the jump condition (4.73) of the discrete transmission problem, which implies

$$\gamma_T^{-}\boldsymbol{E}_{\Pi}^{\tau,h} = \gamma_T^{+}\boldsymbol{E}_{\Pi}^{\tau,h} + \boldsymbol{I}_h\boldsymbol{\psi} = \left(\gamma_T^{+}\boldsymbol{E}_{\Pi}^{\tau,h} - \gamma_T^{+}\boldsymbol{E}\right) - (\boldsymbol{\psi} - \boldsymbol{I}_h\boldsymbol{\psi}).$$

Inserting this identity into the first summand (4.77) gives

$$\begin{aligned} &\left[\begin{pmatrix} \gamma_T^{+}(\boldsymbol{H}^{\tau,h} - \boldsymbol{H}_{\Pi}^{\tau,h}) \\ -\gamma_T^{+}(\boldsymbol{E}^{\tau,h} - \boldsymbol{E}_{\Pi}^{\tau,h}) \end{pmatrix}, \begin{pmatrix} \gamma_T^{-}\boldsymbol{E}_{\Pi}^{\tau,h} \\ \gamma_T^{+}\boldsymbol{H}_{\Pi}^{\tau,h} - \gamma_T^{+}\boldsymbol{H} \end{pmatrix}\right]_{\Gamma} \\ &= \left[\gamma_T^{+}(\boldsymbol{H}^{\tau,h} - \boldsymbol{H}_{\Pi}^{\tau,h}), \gamma_T^{+}(\boldsymbol{E}_{\Pi}^{\tau,h} - \boldsymbol{E})\right]_{\Gamma} \qquad \text{(i)} \\ &- \left[\gamma_T^{+}(\boldsymbol{H}^{\tau,h} - \boldsymbol{H}_{\Pi}^{\tau,h}), \boldsymbol{\psi} - \boldsymbol{I}_h\boldsymbol{\psi}\right]_{\Gamma} \qquad \text{(ii)} \\ &- \left[\gamma_T^{+}(\boldsymbol{E}^{\tau,h} - \boldsymbol{E}_{\Pi}^{\tau,h}), \gamma_T^{+}\left(\boldsymbol{H}_{\Pi}^{\tau,h} - \boldsymbol{H}\right)\right]_{\Gamma}. \qquad \text{(iii)} \end{aligned}$$

The following paragraphs are dedicated to the successive estimation of the terms (i)–(iii).

(i) Green's formula (4.30), in combination with inserting the time-discrete Maxwell's equa-

tions (4.40) and the Cauchy–Schwarz inequality, yields

$$\begin{aligned}
&\left[\gamma_T^+(\boldsymbol{H}^{\tau,h} - \boldsymbol{H}_\Pi^{\tau,h}),\, \gamma_T^+(\boldsymbol{E}_\Pi^{\tau,h} - \boldsymbol{E})\right]_\Gamma \\
&= \int_{\Omega^+} \mathbf{curl}(\boldsymbol{H}^{\tau,h} - \boldsymbol{H}_\Pi^{\tau,h}) \cdot (\boldsymbol{E}_\Pi^{\tau,h} - \boldsymbol{E}) - (\boldsymbol{H}^{\tau,h} - \boldsymbol{H}_\Pi^{\tau,h}) \cdot \mathbf{curl}(\boldsymbol{E}_\Pi^{\tau,h} - \boldsymbol{E})\,\mathrm{d}\boldsymbol{x} \qquad (4.79)\\
&\leq \int_{\Omega^+} \left(\partial_t^\tau \boldsymbol{E}^{\tau,h} - \partial_t^\tau \boldsymbol{E}_\Pi^{\tau,h}\right) \cdot \left(\boldsymbol{E}_\Pi^{\tau,h} - \boldsymbol{E}\right)\,\mathrm{d}\boldsymbol{x} \\
&+ \left\|\boldsymbol{H}^{\tau,h} - \boldsymbol{H}_\Pi^{\tau,h}\right\|_{\boldsymbol{L}^2(\Omega+)} \left\|\mathbf{curl}\,\boldsymbol{E}_\Pi^{\tau,h} - \mathbf{curl}\,\boldsymbol{E}\right\|_{\boldsymbol{L}^2(\Omega+)}.
\end{aligned}$$

Summation on both sides, applying the discrete integration bound of Lemma 4.3 to the first summand and Young's inequality to the second summand consequently gives for any $\epsilon > 0$ a constant C such that

$$\begin{aligned}
&\sum_{n=0}^{N} \rho^n \left[\gamma_T^+(\boldsymbol{H}_n^{\tau,h} - \boldsymbol{H}_\Pi^{n,h}),\, \gamma_T^+(\boldsymbol{E}_\Pi^{n,h} - \boldsymbol{E}(\underline{t_n}))\right]_\Gamma \\
&\leq \sum_{n=0}^{N} \rho^n \left(\epsilon \left\|\left(\boldsymbol{E}^{\tau,h} - \boldsymbol{E}_\Pi^{\tau,h}\right)_n\right\|_{\boldsymbol{L}^2(\Omega)}^2 + C \left\|\left(\partial_t^\tau \boldsymbol{E}_\Pi^{\tau,h} - \partial_t^\tau \boldsymbol{E}\right)_n\right\|_{\boldsymbol{L}^2(\Omega)}^2\right) \\
&+ \sum_{n=0}^{N} \rho^n \left(\epsilon \left\|\left(\boldsymbol{H}^{\tau,h} - \boldsymbol{H}_\Pi^{\tau,h}\right)_n\right\|_{\boldsymbol{L}^2(\Omega)}^2 + C \left\|\left(\boldsymbol{E}_\Pi^{\tau,h} - \boldsymbol{E}\right)_n\right\|_{\boldsymbol{H}(\mathbf{curl},\Omega)}^2\right).
\end{aligned}$$

By choosing $\epsilon > 0$ small enough, the terms depending on the numerical solution are absorbed to the left-hand side (4.76). The error of the intermediate field $\boldsymbol{E}_\Pi^{\tau,h}$ in the $\boldsymbol{H}(\mathbf{curl},\Omega)$ norm is bounded by (4.74). This leaves the second summand, consisting of the temporal discrete differentiation, which is bounded from above through

$$\begin{aligned}
\left\|\left(\partial_t^\tau \boldsymbol{E}_\Pi^{\tau,h} - \partial_t^\tau \boldsymbol{E}\right)_n\right\|_{\boldsymbol{L}^2(\Omega^+)} &\leq \left\|\left(\mathbf{curl}\,\boldsymbol{H}_\Pi^{\tau,h} - \mathbf{curl}\,\boldsymbol{H}\right)_n\right\|_{\boldsymbol{L}^2(\Omega^+)} + \|(\partial_t \boldsymbol{E} - \partial_t^\tau \boldsymbol{E})_n\|_{\boldsymbol{L}^2(\Omega^+)} \\
&\leq C(\tau^m + h^{k+1}),
\end{aligned}$$

where the bound is obtained by (4.74) and Lemma B.2 (with $\kappa = 1$ and $\nu = 0$) respectively.

(ii) The discrete partial integration inequality of Lemma 4.3 yields, in combination with $\partial_t^\tau\,(\partial_t^\tau)^{-1} = \mathbf{Id}$ (which holds due to (B.9)), the estimate

$$\begin{aligned}
&\sum_{n=0}^{N} \rho^n \left[\gamma_T^+(\boldsymbol{H}_n^{\tau,h} - \boldsymbol{H}_\Pi^{n,h}), \boldsymbol{\psi}(\underline{t_n}) - \boldsymbol{I}_h \boldsymbol{\psi}(\underline{t_n})\right]_\Gamma \\
&\leq \sum_{n=0}^{N} \rho^n \left(\epsilon \left\|\left((\partial_t^\tau)^{-1}\,\gamma_T^+(\boldsymbol{H}^{\tau,h} - \boldsymbol{H}_\Pi^{\tau,h})\right)_n\right\|_{\boldsymbol{X}_\Gamma}^2 + C\,\|(\partial_t^\tau\,(\boldsymbol{\psi} - \boldsymbol{I}_h \boldsymbol{\psi}))_n\|_{X_\Gamma}^2\right). \qquad (4.80)
\end{aligned}$$

Applying the trace theorem to the first summand, which depends on the numerical solution,

yields

$$\begin{aligned}&\left\|\left((\partial_t^\tau)^{-1}\gamma_T^+(\boldsymbol{H}^{\tau,h}-\boldsymbol{H}_\Pi^{\tau,h})\right)_n\right\|_{\boldsymbol{X}_\Gamma}^2 \le \left\|\left((\partial_t^\tau)^{-1}\boldsymbol{H}^{\tau,h}-(\partial_t^\tau)^{-1}\boldsymbol{H}_\Pi^{\tau,h}\right)_n\right\|_{\boldsymbol{H}(\mathbf{curl},\Omega^+)}^2\\&=\int_{\Omega^+}\left|\left((\partial_t^\tau)^{-1}\boldsymbol{H}^{\tau,h}-(\partial_t^\tau)^{-1}\boldsymbol{H}_\Pi^{\tau,h}\right)_n\right|^2+\left|\boldsymbol{E}_h^n-\boldsymbol{E}_\Pi^{n,h}\right|^2\,\mathrm{d}\boldsymbol{x}.\end{aligned}$$

The first summand is bounded by (4.37), which yields a constant C such that

$$\sum_{n=0}^{\infty}\rho^n\int_{\Omega^+}\left|\left((\partial_t^\tau)^{-1}\boldsymbol{H}^{\tau,h}-(\partial_t^\tau)^{-1}\boldsymbol{H}_\Pi^{\tau,h}\right)_n\right|^2\mathrm{d}\boldsymbol{x}\le C\sum_{n=0}^{\infty}\rho^n\left\|\boldsymbol{H}_n^{\tau,h}-\boldsymbol{H}_\Pi^{n,h}\right\|_{\boldsymbol{L}^2(\Omega^+)}^2,$$

where the constant C depends only polynomially on the final time T. Consequently, the first summand of (4.80) can be absorbed to the left-hand side of (4.76) by choosing ϵ small enough.

The remaining second summand of (4.80) is rewritten by splitting the temporal discrete differentiation operator into $\partial_t^\tau = \partial_t - (\partial_t - \partial_t^\tau)$, for which the first resulting term is directly bounded through the approximation result of the interpolation operator. Applying Lemma B.2 to the remaining summand then gives, for all n, the chain of inequalities

$$\begin{aligned}\left\|\left(\partial_t^\tau\left(\boldsymbol{\psi}-\boldsymbol{I}_h\boldsymbol{\psi}\right)\right)_n\right\|_{\boldsymbol{X}_\Gamma}&\le C\left\|\partial_t\left(\boldsymbol{\psi}-\boldsymbol{I}_h\boldsymbol{\psi}\right)\right\|_{\boldsymbol{X}_\Gamma}^2+C\left\|\left(\left(\partial_t-\partial_t^\tau\right)\left(\boldsymbol{\psi}-\boldsymbol{I}_h\boldsymbol{\psi}\right)\right)_n\right\|_{\boldsymbol{X}_\Gamma}\\&\le Ch^{(k+1)}\left\|\boldsymbol{\psi}\right\|_{\boldsymbol{H}_0^2(0,T;\boldsymbol{H}_\times^{k+1})}+C\tau^m\left\|\partial_t^{m+3}\boldsymbol{\psi}-\boldsymbol{I}_h\partial_t^{m+3}\boldsymbol{\psi}\right\|_{\boldsymbol{L}_0^2(0,T;\boldsymbol{X}_\Gamma)}^2\\&\le Ch^{(k+1)}\left\|\boldsymbol{\psi}\right\|_{\boldsymbol{H}_0^2(0,T;\boldsymbol{H}_\times^{k+1})}+C\tau^m h\left\|\boldsymbol{\psi}\right\|_{\boldsymbol{L}_0^2(0,T;\boldsymbol{H}_\times^1(\Gamma))}^2.\end{aligned}\tag{4.81}$$

In order to estimate the first summand, we further used the continuous embedding $\boldsymbol{H}^1(0,T)\subset\boldsymbol{C}(0,T)$. The final bound on the interpolation in the second summand is provided by [26, Lemma 15] with $s=1$.

(iii) We repeat the argument structure of (i) for the final term, starting from Green's formula and the Cauchy–Schwarz inequality, which yields

$$\begin{aligned}&\left[\gamma_T^+\left(\boldsymbol{E}^{\tau,h}-\boldsymbol{E}_\Pi^{\tau,h}\right),\gamma_T^+\left(\boldsymbol{H}_\Pi^{\tau,h}-\boldsymbol{H}\right)\right]_\Gamma\\&=\int_{\Omega^+}\mathbf{curl}\left(\boldsymbol{E}^{\tau,h}-\boldsymbol{E}_\Pi^{\tau,h}\right)\cdot\left(\boldsymbol{H}_\Pi^{\tau,h}-\boldsymbol{H}\right)-\left(\boldsymbol{E}^{\tau,h}-\boldsymbol{E}_\Pi^{\tau,h}\right)\cdot\mathbf{curl}\left(\boldsymbol{H}_\Pi^{\tau,h}-\boldsymbol{H}\right)\mathrm{d}\boldsymbol{x}\\&\le\int_{\Omega^+}-\left(\partial_t^\tau\boldsymbol{H}^{\tau,h}-\partial_t^\tau\boldsymbol{H}_\Pi^{\tau,h}\right)\cdot\left(\boldsymbol{H}_\Pi^{\tau,h}-\boldsymbol{H}\right)\mathrm{d}\boldsymbol{x}\\&+\left\|\boldsymbol{E}^{\tau,h}-\boldsymbol{E}_\Pi^{\tau,h}\right\|_{\boldsymbol{L}^2(\Omega^+)}\left\|\mathbf{curl}\,\boldsymbol{H}_\Pi^{\tau,h}-\mathbf{curl}\,\boldsymbol{H}\right\|_{\boldsymbol{L}^2(\Omega^+)}.\end{aligned}\tag{4.82}$$

The discrete integration inequality of Lemma 4.3, applied to the first summand, in combination

with Young's inequality applied to the second summand yields

$$\begin{aligned}
&\sum_{n=0}^{N} \rho^n \left[\gamma_T^+ \left(\boldsymbol{E}_n^{\tau,h} - \boldsymbol{E}_\Pi^{n,h} \right), \gamma_T^+ \left(\boldsymbol{H}_\Pi^{n,h} - \boldsymbol{H}(\underline{t_n}) \right) \right]_\Gamma \\
&\leq \sum_{n=0}^{N} \rho^n \left(\epsilon \left\| \boldsymbol{H}_n^{\tau,h} - \boldsymbol{H}_\Pi^{n,h} \right\|_{\boldsymbol{L}^2(\Omega^+)}^2 + C \left\| \left(\partial_t^\tau \boldsymbol{H}_\Pi^{\tau,h} - \partial_t^\tau \boldsymbol{H} \right)_n \right\|_{\boldsymbol{L}^2(\Omega^+)}^2 \right) \\
&\quad + \rho^n \left(\epsilon \left\| \boldsymbol{E}_n^{\tau,h} - \boldsymbol{E}_\Pi^{n,h} \right\|_{\boldsymbol{L}^2(\Omega^+)}^2 + C \left\| \boldsymbol{H}_\Pi^{n,h} - \boldsymbol{H}(\underline{t_n}) \right\|_{\boldsymbol{H}(\mathbf{curl},\Omega^+)}^2 \right),
\end{aligned}$$

where only the terms multiplied by $\epsilon > 0$ depend on the numerical solution, which are absorbed to the left-hand side (4.76). The second summand in the final line is directly estimated by (4.74). Again, the only remaining term is the discretely differentiated temporal defect, which is rewritten by (4.41) and consequently bounded from above through

$$\begin{aligned}
\left\| \left(\partial_t^\tau \boldsymbol{H}_\Pi^{\tau,h} - \partial_t^\tau \boldsymbol{H} \right)_n \right\|_{\boldsymbol{L}^2(\Omega^+)} &\leq \left\| \mathbf{curl}\, \boldsymbol{E}_\Pi^{n,h} - \mathbf{curl}\, \boldsymbol{E}(\underline{t_n}) \right\|_{\boldsymbol{L}^2(\Omega^+)} + \left\| (\partial_t \boldsymbol{H} - \partial_t^\tau \boldsymbol{H})_n \right\|_{\boldsymbol{L}^2(\Omega^+)} \\
&\leq C(\tau^m + h^{k+1}).
\end{aligned}$$

This completes the estimation of the terms collecting the outer traces from (4.77).

Consequently, we turn our attention to the second summand (4.78), mostly associated to tangential traces of the inner domain Ω^-. The only remaining term depending on outer traces is rewritten in view of $\gamma_T^- \boldsymbol{H} = 0$, which implies

$$\gamma_T^+ \boldsymbol{H}_\Pi^{\tau,h} - \gamma_T^+ \boldsymbol{H} = \gamma_T^- \boldsymbol{H}_\Pi^{\tau,h} + \boldsymbol{I}_h \boldsymbol{\varphi} - \boldsymbol{\varphi} = \left(\gamma_T^- \boldsymbol{H}_\Pi^{\tau,h} - \gamma_T^- \boldsymbol{H} \right) - (\boldsymbol{\varphi} - \boldsymbol{I}_h \boldsymbol{\varphi}).$$

Analogously to before, we insert this identity into the right-hand side of (4.78), which gives with $\gamma_T^- \boldsymbol{E} = 0$, the decomposition

$$\begin{aligned}
&\left[\begin{pmatrix} \gamma_T^- (\boldsymbol{H}^{\tau,h} - \boldsymbol{H}_\Pi^{\tau,h}) \\ -\gamma_T^- (\boldsymbol{E}^{\tau,h} - \boldsymbol{E}_\Pi^{\tau,h}) \end{pmatrix}, \begin{pmatrix} \gamma_T^- \boldsymbol{E}_\Pi^{\tau,h} \\ \gamma_T^+ \boldsymbol{H}_\Pi^{\tau,h} - \gamma_T^+ \boldsymbol{H} \end{pmatrix} \right]_\Gamma \\
&\quad = \left[\gamma_T^- (\boldsymbol{H}^{\tau,h} - \boldsymbol{H}_\Pi^{\tau,h}), \gamma_T^- \left(\boldsymbol{E}_\Pi^{\tau,h} - \boldsymbol{E} \right) \right]_\Gamma && \text{(iv)} \\
&\quad + \left[\gamma_T^- (\boldsymbol{E}^{\tau,h} - \boldsymbol{E}_\Pi^{\tau,h}), \gamma_T^- \left(\boldsymbol{H}_\Pi^{\tau,h} - \boldsymbol{H} \right) \right]_\Gamma && \text{(v)} \\
&\quad + \left[\gamma_T^- (\boldsymbol{E}^{\tau,h} - \boldsymbol{E}_\Pi^{\tau,h}), \boldsymbol{\varphi} - \boldsymbol{I}_h \boldsymbol{\varphi} \right]_\Gamma. && \text{(vi)}
\end{aligned}$$

These terms are structurally identical to (i)–(iii) and are therefore bounded with the stated bound by repeating the arguments from above. We shortly sketch connections between these terms.

(iv) This term is analogous to the term (i), since Green's formula implies

$$\begin{aligned}&\left[\gamma_T^-(\boldsymbol{H}^{\tau,h}-\boldsymbol{H}_\Pi^{n,h}),\gamma_T^-\left(\boldsymbol{E}_\Pi^{\tau,h}-\boldsymbol{E}\right)\right]_\Gamma\\&=-\int_{\Omega^-}\mathbf{curl}(\boldsymbol{H}^{\tau,h}-\boldsymbol{H}_\Pi^{\tau,h})\cdot(\boldsymbol{E}_\Pi^{\tau,h}-\boldsymbol{E})-(\boldsymbol{H}^{\tau,h}-\boldsymbol{H}_\Pi^{\tau,h})\cdot\mathbf{curl}(\boldsymbol{E}_\Pi^{\tau,h}-\boldsymbol{E})\,\mathrm{d}\boldsymbol{x}.\end{aligned}$$

The integrand on the right-hand side is identical to the integrand in (4.79). Repeating the exact same arguments as before therefore gives an appropriate estimate for the above term.

(v) The connection of this term to (iii) is readily apparent and using Green's formula gives

$$\begin{aligned}&\left[\gamma_T^-(\boldsymbol{E}^{\tau,h}-\boldsymbol{E}_\Pi^{\tau,h}),\gamma_T^-\left(\boldsymbol{H}_\Pi^{\tau,h}-\boldsymbol{H}\right)\right]_\Gamma\\&=-\int_{\Omega^-}\mathbf{curl}\left(\boldsymbol{E}^{\tau,h}-\boldsymbol{E}_\Pi^{\tau,h}\right)\cdot\left(\boldsymbol{H}_\Pi^{\tau,h}-\boldsymbol{H}\right)-\left(\boldsymbol{E}^{\tau,h}-\boldsymbol{E}_\Pi^{\tau,h}\right)\cdot\mathbf{curl}\left(\boldsymbol{H}_\Pi^{\tau,h}-\boldsymbol{H}\right)\mathrm{d}\boldsymbol{x}.\end{aligned}$$

This integral is, aside from the domain, identical to (4.82). Employing the same arguments as before consequently shows the required estimate.

(vi) The estimation of this term is analogous to (ii), but we repeat some of the steps taken there for the completeness of the proof. Applying the discrete partial integration inequality of Lemma 4.3 yields again

$$\begin{aligned}&\sum_{n=0}^{N}\rho^n\left[\gamma_T^-(\boldsymbol{E}_n^{\tau,h}-\boldsymbol{E}_\Pi^{n,h}),\boldsymbol{\varphi}(\underline{t_n})-\boldsymbol{I}_h\boldsymbol{\varphi}(\underline{t_n})\right]_\Gamma\\&\leq\sum_{n=0}^{N}\rho^n\left(\epsilon\left\|\left(\left(\partial_t^\tau\right)^{-1}\gamma_T^-(\boldsymbol{E}^{\tau,h}-\boldsymbol{E}_\Pi^{\tau,h})\right)_n\right\|_{\boldsymbol{X}_\Gamma}^2+C\left\|\left(\partial_t^\tau\left(\boldsymbol{\varphi}-\boldsymbol{I}_h\boldsymbol{\varphi}\right)\right)_n\right\|_{X_\Gamma}^2\right).\end{aligned}\tag{4.83}$$

The chain of inequalities from (4.81) directly bounds the second summand.
Applying the trace theorem to the first summand of (4.83), implies

$$\begin{aligned}&\left\|\left(\left(\partial_t^\tau\right)^{-1}\gamma_T^+(\boldsymbol{E}^{\tau,h}-\boldsymbol{E}_\Pi^{\tau,h})\right)_n\right\|_{\boldsymbol{X}_\Gamma}^2\leq\left\|\left(\left(\partial_t^\tau\right)^{-1}\boldsymbol{E}^{\tau,h}-\left(\partial_t^\tau\right)^{-1}\boldsymbol{E}_\Pi^{\tau,h}\right)_n\right\|_{\boldsymbol{H}(\mathbf{curl},\Omega^+)}^2\\&=\int_{\Omega^+}\left|\left(\left(\partial_t^\tau\right)^{-1}\boldsymbol{E}^{\tau,h}-\left(\partial_t^\tau\right)^{-1}\boldsymbol{E}_\Pi^{\tau,h}\right)_n\right|^2+\left|\boldsymbol{H}_h^n-\boldsymbol{H}_\Pi^{n,h}\right|^2\mathrm{d}\boldsymbol{x}.\end{aligned}$$

Moreover, applying (4.37) gives the estimate

$$\sum_{n=0}^{\infty}\rho^n\int_{\Omega^+}\left|\left(\left(\partial_t^\tau\right)^{-1}\boldsymbol{E}^{\tau,h}-\left(\partial_t^\tau\right)^{-1}\boldsymbol{E}_\Pi^{\tau,h}\right)_n\right|^2\mathrm{d}\boldsymbol{x}\leq C\sum_{n=0}^{\infty}\rho^n\left\|\boldsymbol{E}_n^{\tau,h}-\boldsymbol{E}_\Pi^{n,h}\right\|_{\boldsymbol{L}^2(\Omega^+)}^2,$$

where the constant C only depends polynomially on the final time T. This term is then absorbed to the left-hand side of (4.76) by choosing ϵ in (4.80) small enough.

(B) For an efficient notation, we introduce the following shorthand notation for the defect associated to the nonlinearity

$$\mathbf{d}_{\boldsymbol{b}} = \boldsymbol{b}\left(\boldsymbol{I}_h\boldsymbol{\psi} - \gamma_T\boldsymbol{E}^{\mathrm{inc}}\right) - \boldsymbol{b}\left(\boldsymbol{\psi} - \gamma_T\boldsymbol{E}^{\mathrm{inc}}\right).$$

We continue by repeating the arguments presented in the context of the error analysis for the spatial semi-discretization, starting from applying Hölder's inequality and Young's inequality, which yields for any $\epsilon > 0$ a constant C such that

$$\begin{aligned}\left(\boldsymbol{\psi}^{\tau,h} - \boldsymbol{I}_h\boldsymbol{\psi}, \mathbf{d}_{\boldsymbol{b}}\right)_\Gamma &\leq \left\|\boldsymbol{\psi}^{\tau,h} - \boldsymbol{I}_h\boldsymbol{\psi}\right\|_{\boldsymbol{L}^{\frac{1+\alpha}{\alpha}}(\Gamma)} \|\mathbf{d}_{\boldsymbol{b}}\|_{\boldsymbol{L}^{1+\alpha}(\Gamma)} \\ &\leq \epsilon \left\|\boldsymbol{\psi}^{\tau,h} - \boldsymbol{I}_h\boldsymbol{\psi}\right\|^{\frac{1+\alpha}{\alpha}}_{\boldsymbol{L}^{\frac{1+\alpha}{\alpha}}(\Gamma)} + C\,\|\mathbf{d}_{\boldsymbol{b}}\|^{1+\alpha}_{\boldsymbol{L}^{1+\alpha}(\Gamma)}.\end{aligned}$$

The first term is the error in the numerical solution and pointwise absorbed by the left-hand side of (4.76). By employing the pointwise estimate on the nonlinearity (4.11), the remaining defect yields a constant C, depending on α and the incident electric wave, such that

$$\begin{aligned}\|\mathbf{d}_{\boldsymbol{b}}\|^{1+\alpha}_{\boldsymbol{L}^{1+\alpha}(\Gamma)} &= \left\|\boldsymbol{b}\left(\boldsymbol{I}_h\boldsymbol{\psi} - \gamma_T\boldsymbol{E}^{\mathrm{inc}}\right) - \boldsymbol{b}\left(\boldsymbol{\psi} - \gamma_T\boldsymbol{E}^{\mathrm{inc}}\right)\right\|^{1+\alpha}_{\boldsymbol{L}^{1+\alpha}(\Gamma)} \\ &\leq C\int_\Gamma \left(|\boldsymbol{I}_h\boldsymbol{\psi}| + |\boldsymbol{\psi}|\right)^{\frac{1-\alpha^2}{\alpha}} |\boldsymbol{I}_h\boldsymbol{\psi} - \boldsymbol{\psi}|^{1+\alpha}\,\mathrm{d}\boldsymbol{x} \\ &\leq C\left(\|\boldsymbol{I}_h\boldsymbol{\psi}\|_{\boldsymbol{L}^\infty(\Gamma)} + \|\boldsymbol{\psi}\|_{\boldsymbol{L}^\infty(\Gamma)}\right)^{\frac{1-\alpha^2}{\alpha}} \|\boldsymbol{I}_h\boldsymbol{\psi} - \boldsymbol{\psi}\|^{1+\alpha}_{\boldsymbol{L}^{1+\alpha}(\Gamma)}.\end{aligned}$$

Finally applying the approximation properties of the interpolation operator based on Raviart–Thomas elements yields

$$\|\mathbf{d}_{\boldsymbol{b}}\|^{1+\alpha}_{\boldsymbol{L}^{1+\alpha}(\Gamma)} \leq Ch^{(1+\alpha)(k+1)}\left(1 + \|\boldsymbol{\psi}\|_{\boldsymbol{L}^\infty(\Gamma)}\right)^{\frac{1-\alpha^2}{\alpha}} \|\boldsymbol{\psi}\|^{1+\alpha}_{\boldsymbol{H}^{k+1}_\times(\Gamma)}.$$

All defects have now been estimated in the stated order, which gives the presented error bounds. □

4.5.2. Pointwise error bounds

In view of the pointwise error bounds of previous chapters, we expect the evaluation of the approximation to the scattered wave at any fixed point $\boldsymbol{x} \in \Omega$ to converge to the exact solution. Due to the nonlinear component of the boundary integral equation, the previously used techniques are not directly applicable.

To give such a result for point evaluations in the nonlinear setting, we derive additional error bounds for the magnetic trace $\boldsymbol{\psi}^{\tau,h}$ and a slightly transformed electric trace $\widetilde{\boldsymbol{\varphi}}^{\tau,h}$, in terms of the norms corresponding to the spaces $\boldsymbol{L}^{\frac{1+\alpha}{\alpha}}(\Gamma)$ and $\boldsymbol{L}^{1+\alpha}(\Gamma)$. Pointwise error estimates are then obtained by employing the corresponding time-harmonic bounds of Lemma 3.13.

Theorem 4.4. *Let Γ be smooth and further let the assumptions of Theorem 4.3 hold. Consider the boundary densities $(\widetilde{\boldsymbol{\varphi}}^{\tau,h}, \widetilde{\boldsymbol{\psi}}^{\tau,h})$, derived from the solutions of the full discretization of the boundary integral equation (4.70), through the expressions*

$$\widetilde{\boldsymbol{\varphi}}^{\tau,h} = \boldsymbol{b}(\boldsymbol{\psi}^{\tau,h} - \gamma_T \boldsymbol{E}^{\mathrm{inc}}) \times \boldsymbol{\nu} + \gamma_T \boldsymbol{H}^{\mathrm{inc}}, \qquad \widetilde{\boldsymbol{\psi}}^{\tau,h} = \boldsymbol{\psi}^{\tau,h}.$$

These fully discrete approximations fulfill, under the stated conditions, the following error bound

$$\left(\tau \sum_{n=0}^{N} \left\| \widetilde{\boldsymbol{\varphi}}_n^{\tau,h} - \boldsymbol{\varphi}(\underline{t}_n) \right\|^2_{\boldsymbol{L}^{1+\alpha}(\Gamma)} + \left\| \widetilde{\boldsymbol{\psi}}_n^{\tau,h} - \boldsymbol{\psi}(\underline{t}_n) \right\|^2_{\boldsymbol{L}^{\frac{1+\alpha}{\alpha}}(\Gamma)} \right)^{\frac{1}{2}} \leq C \left(\tau^{m \frac{2\alpha}{1+\alpha}} + h^{\alpha(k+1)} \right).$$

Electromagnetic fields associated to the boundary densities $(\widetilde{\boldsymbol{\varphi}}^{\tau,h}, \widetilde{\boldsymbol{\psi}}^{\tau,h})$, defined through the discrete representation formulas (4.46)–(4.47), are denoted again by $\boldsymbol{E}^{\tau,h}$ and $\boldsymbol{H}^{\tau,h}$.

The error of the approximation to the scattered fields at the point $\boldsymbol{x} \in \Omega$ is, under the stated conditions, bounded by

$$\left(\tau \sum_{n=0}^{N} \left| \boldsymbol{E}_n^{\tau,h}(\boldsymbol{x}) - \boldsymbol{E}(\boldsymbol{x}, \underline{t}_n) \right|^2 + \left| \boldsymbol{H}_n^{\tau,h}(\boldsymbol{x}) - \boldsymbol{H}(\boldsymbol{x}, \underline{t}_n) \right|^2 \right)^{1/2} \leq \frac{C}{\tau} \left(\tau^{m \frac{2\alpha}{1+\alpha}} + h^{\alpha(k+1)} \right),$$

where the constant C depends in both cases on the exact solution and its derivatives, on $\Gamma, \boldsymbol{x}, \alpha$ and polynomially on the final time T. The specific expression on the right-hand side of the error bound requires the mild mesh size restriction $h^{2(1+\alpha)(k+1)} \leq C\tau$, though more convoluted error rates can be derived without such an assumption.

Proof. The stated error bound for $\widetilde{\boldsymbol{\psi}}_n^{\tau,h}$ with regards to the $\boldsymbol{L}^{\frac{1+\alpha}{\alpha}}(\Gamma)$- norm is directly implied by Theorem 4.3, which yields in combination with Hölder's inequality

$$\begin{aligned} \left(\tau \sum_{n=0}^{N} \left\| \widetilde{\boldsymbol{\psi}}_n^{\tau,h} - \boldsymbol{\psi}(\underline{t}_n) \right\|^2_{\boldsymbol{L}^{\frac{1+\alpha}{\alpha}}(\Gamma)} \right)^{\frac{1}{2}} &\leq T^{\frac{1-\alpha}{1+\alpha}} \left(\tau \sum_{n=0}^{N} \left\| \boldsymbol{\psi}_n^{\tau,h} - \boldsymbol{\psi}(\underline{t}_n) \right\|^{\frac{1+\alpha}{\alpha}}_{\boldsymbol{L}^{\frac{1+\alpha}{\alpha}}(\Gamma)} \right)^{\frac{\alpha}{1+\alpha}} \\ &\leq C \left(\tau^{2m} + h^{(1+\alpha)(k+1)} \right)^{\frac{\alpha}{1+\alpha}}. \end{aligned} \tag{4.84}$$

We turn our attention towards the stated error bounds of $\widetilde{\boldsymbol{\varphi}}^{\tau,h}$. Using the pointwise estimate (4.13) then yields

$$\begin{aligned} \left| \widetilde{\boldsymbol{\varphi}}^{\tau,h} - \boldsymbol{\varphi} \right| &= \left| \boldsymbol{b}(\boldsymbol{\psi}^{\tau,h} - \gamma_T \boldsymbol{E}^{\mathrm{inc}}) - \boldsymbol{b}(\boldsymbol{\psi} - \gamma_T \boldsymbol{E}^{\mathrm{inc}}) \right| \\ &\leq C \left| \boldsymbol{\psi}^{\tau,h} - \boldsymbol{\psi} \right| \left| \boldsymbol{\psi} - \gamma_T \boldsymbol{E}^{\mathrm{inc}} \right|^{\frac{1-\alpha}{\alpha}} + C \left| \boldsymbol{\psi}^{\tau,h} - \boldsymbol{\psi} \right|^{\frac{1}{\alpha}}, \end{aligned}$$

where the above estimate is understood pointwise in time and space. Inserting this inequality

in the $\boldsymbol{L}^{1+\alpha}$-norm of the corresponding error term yields

$$\begin{aligned}\left\|\widetilde{\boldsymbol{\varphi}}^{\tau,h}-\boldsymbol{\varphi}\right\|^{1+\alpha}_{\boldsymbol{L}^{1+\alpha}(\Gamma)} &\leq C\left\|\boldsymbol{\psi}^{\tau,h}-\boldsymbol{\psi}\right\|^{1+\alpha}_{\boldsymbol{L}^{1+\alpha}(\Gamma)}\left\|\boldsymbol{\psi}-\gamma_T\boldsymbol{E}^{\mathrm{inc}}\right\|^{\frac{1-\alpha}{\alpha}}_{\boldsymbol{L}^{\infty}(\Gamma)}\\ &\quad + C\left\|\boldsymbol{\psi}^{\tau,h}-\boldsymbol{\psi}\right\|^{\frac{1+\alpha}{\alpha}}_{\boldsymbol{L}^{\frac{1+\alpha}{\alpha}}(\Gamma)}.\end{aligned}$$

The $\boldsymbol{L}^{\infty}$-norm of the exact solution is independent of h and τ and assumed to be finite. Therefore, we obtain the estimate

$$\begin{aligned}\left(\tau\sum_{n=0}^{N}\left\|\widetilde{\boldsymbol{\varphi}}_n^{\tau,h}-\boldsymbol{\varphi}(\underline{t_n})\right\|^2_{\boldsymbol{L}^{1+\alpha}(\Gamma)}\right)^{\frac{1}{2}} &\leq C\left(\tau\sum_{n=0}^{N}\left\|\boldsymbol{\psi}_n^{\tau,h}-\boldsymbol{\psi}(\underline{t_n})\right\|^2_{\boldsymbol{L}^{1+\alpha}(\Gamma)}\right)^{\frac{1}{2}}\\ &\quad + C\left(\tau\sum_{n=0}^{N}\left\|\boldsymbol{\psi}_n^{\tau,h}-\boldsymbol{\psi}(\underline{t_n})\right\|^{\frac{2}{\alpha}}_{\boldsymbol{L}^{\frac{1+\alpha}{\alpha}}(\Gamma)}\right)^{\frac{1}{2}}.\end{aligned}\tag{4.85}$$

The first sum on the right-hand side is bounded by (4.84). We note the basic inequality

$$x^{\frac{2}{1+\alpha}}+y^{\frac{2}{1+\alpha}}\leq(x+y)^{\frac{2}{1+\alpha}}\quad\text{for all}\quad x,y\geq 0,$$

which is seen for example by Minkowski's inequality with $p=\frac{1+\alpha}{2}<1$. Using this estimate repeatedly shows

$$\begin{aligned}\tau^{\frac{2}{1+\alpha}}\sum_{n=0}^{N}\left\|\boldsymbol{\psi}_n^{\tau,h}-\boldsymbol{\psi}(\underline{t_n})\right\|^{\frac{2}{\alpha}}_{\boldsymbol{L}^{\frac{1+\alpha}{\alpha}}(\Gamma)} &\leq \left(\tau\sum_{n=0}^{N}\left\|\boldsymbol{\psi}_n^{\tau,h}-\boldsymbol{\psi}(\underline{t_n})\right\|^{\frac{1+\alpha}{\alpha}}_{\boldsymbol{L}^{\frac{1+\alpha}{\alpha}}(\Gamma)}\right)^{\frac{2}{1+\alpha}}\\ &\leq C\left(\tau^{\frac{4}{1+\alpha}}m+h^{2(k+1)}\right).\end{aligned}$$

Dividing through the additional powers of τ on the left-hand side and taking the square root on both sides yields

$$\begin{aligned}\left(\tau\sum_{n=0}^{N}\left\|\boldsymbol{\psi}_n^{\tau,h}-\boldsymbol{\psi}(\underline{t_n})\right\|^{\frac{2}{\alpha}}_{\boldsymbol{L}^{\frac{1+\alpha}{\alpha}}(\Gamma)}\right)^{\frac{1}{2}} &\leq C\tau^{\frac{\alpha-1}{2(1+\alpha)}}\left(\tau^{\frac{2}{1+\alpha}}m+h^{(k+1)}\right)\\ &\leq C\left(\tau^{\frac{2\alpha}{1+\alpha}}m+h^{\alpha(k+1)}\right),\end{aligned}$$

where the final estimate holds due to $h^{2(1+\alpha)(k+1)}\leq C\tau$, the stated mild mesh width restriction, since then

$$\tau^{\frac{\alpha-1}{2(1+\alpha)}}\left(\tau^{\frac{2-2\alpha}{1+\alpha}}m+h^{(1-\alpha)(k+1)}\right)\leq\left(\tau^{3/2}\right)^{\frac{1-\alpha}{1+\alpha}}+\tau^{\frac{\alpha-1}{2(1+\alpha)}}h^{(1-\alpha)(k+1)}\leq C.$$

Overall, we obtain the following additional combined error bounds for the boundary densities:

$$\left(\tau\sum_{n=0}^{N}\left\|\boldsymbol{\psi}_n^{\tau,h}-\boldsymbol{\psi}(\underline{t}_n)\right\|^2_{\boldsymbol{L}^{\frac{1+\alpha}{\alpha}}(\Gamma)}+\left\|\widetilde{\boldsymbol{\varphi}}_n^{\tau,h}-\boldsymbol{\varphi}(\underline{t}_n)\right\|^2_{\boldsymbol{L}^{1+\alpha}(\Gamma)}\right)^{\frac{1}{2}}\leq C\left(\tau^{m\frac{2\alpha}{1+\alpha}}+h^{\alpha(k+1)}\right). \tag{4.86}$$

We turn our attention towards pointwise error bounds, which are consequence of the time-harmonic bounds of Lemma 3.13 for the potential operators. Formulated for the combined block potential operator (4.72) in the present setting, this bound reads

$$\|\boldsymbol{\mathcal{W}}_{\boldsymbol{x}}(s)\|_{\mathbb{C}^3\times\mathbb{C}^3\leftarrow\boldsymbol{L}^{1+\alpha}(\Gamma)\times\boldsymbol{L}^{\frac{1+\alpha}{\alpha}}(\Gamma)}\leq C\,|s|\,.$$

The stated pointwise error bound now follows from applying [14, Lemma 5.2] to the representation formula and using the error bound (4.86).

□

Remark 4.6 (Comparison with the original formulation)**.** *In the original paper [57], the presented treatment is applied to the equivalent of the boundary condition (1.17), based on the nonlinearity $\boldsymbol{a}(\boldsymbol{x})=|\boldsymbol{x}|^{\alpha-1}\boldsymbol{x}$, rather than the analysis here, which is based on the equivalent inverted boundary condition (1.19). Analogously to the present analysis, the full discretization in the original paper has the following form. The sequence of boundary densities $(\boldsymbol{\varphi}_+^{\tau,h},\widetilde{\boldsymbol{\psi}}_+^{\tau,h})\in\boldsymbol{V}_h^m\times\boldsymbol{X}_h^m$ for $n\leq N$ is the time-discrete approximation to the solutions of the boundary integral equations, if for all $(\boldsymbol{\eta}_h,\boldsymbol{\xi}_h)\in\boldsymbol{V}_h\times\boldsymbol{X}_h$ it holds that*

$$\left[\begin{pmatrix}\boldsymbol{\eta}_h\\ \boldsymbol{\xi}_h\end{pmatrix},\boldsymbol{C}_{imp}(\partial_t^\tau)\begin{pmatrix}\boldsymbol{\varphi}_+^{\tau,h}\\ \boldsymbol{\psi}_+^{\tau,h}\end{pmatrix}\right]_\Gamma+\left(\boldsymbol{\eta}_h,\boldsymbol{a}\left(\boldsymbol{\varphi}_+^{\tau,h}+\gamma_T\boldsymbol{H}^{inc}\right)\right)_\Gamma=[\gamma_T\boldsymbol{E}^{inc},\boldsymbol{\eta}_h]_\Gamma. \tag{4.87}$$

The solution of this full discretization fulfills similar approximation properties as the presented numerical approximations. Consider the setting and the assumptions of Theorem 4.3. Then, [57, Theorem 2] gives the error estimates

$$\left(\tau\sum_{n=0}^{N}\left\|\left((\partial_t^\tau)^{-1}\left(\boldsymbol{\varphi}_+^{\tau,h}-\boldsymbol{\varphi}\right)\right)_n\right\|^2_{\boldsymbol{X}_\Gamma}+\left\|\left((\partial_t^\tau)^{-1}\left(\boldsymbol{\psi}_+^{\tau,h}-\boldsymbol{\psi}\right)\right)_n\right\|^2_{\boldsymbol{X}_\Gamma}\right)^{1/2} \tag{4.88}$$

$$\leq C\left(\tau^m+h^{\alpha(k+1)}\right). \tag{4.89}$$

The dependencies applying to the constant in the error bounds of Theorem 4.3 also apply to the constant C. Moreover, analogous pointwise bounds follow for alternative boundary densities $(\widetilde{\boldsymbol{\varphi}}_+^{\tau,h},\widetilde{\boldsymbol{\psi}}_+^{\tau,h})$, derived from the fully discrete solution $\boldsymbol{\varphi}_+^{\tau,h}$ and defined through

$$\widetilde{\boldsymbol{\varphi}}_+^{\tau,h}=\boldsymbol{\varphi}_+^{\tau,h},\qquad\widetilde{\boldsymbol{\psi}}_+^{\tau,h}=\boldsymbol{a}(\boldsymbol{\varphi}_+^{\tau,h}+\gamma_T\boldsymbol{H}^{\mathrm{inc}})\times\boldsymbol{\nu}+\gamma_T\boldsymbol{E}^{\mathrm{inc}}.$$

Fully discrete electromagnetic fields $\boldsymbol{E}^{\tau,h}$ and $\boldsymbol{H}^{\tau,h}$, are associated again, defined through the discrete representation formulas (4.46)–(4.47) with $\widetilde{\boldsymbol{\varphi}}_+^{\tau,h}$ and $\widetilde{\boldsymbol{\psi}}_+^{\tau,h}$. By [57, Theorem 3], these numerical solutions

then fulfill, for any $\boldsymbol{x} \in \Omega$ away from the boundary, the error bound

$$\left(\tau \sum_{n=0}^{N} \left| \boldsymbol{E}_n^{\tau,h}(\boldsymbol{x}) - \boldsymbol{E}(\boldsymbol{x}, \underline{t_n}) \right|^2 + \left| \boldsymbol{H}_n^{\tau,h}(\boldsymbol{x}) - \boldsymbol{H}(\boldsymbol{x}, \underline{t_n}) \right|^2 \right)^{1/2} \leq C\tau^{-1} \left(\tau^m + h^{\alpha(k+1)} \right)^{\frac{2\alpha}{1+\alpha}}.$$

where the constant C depends on the same parameters as before. For the concrete form of the error bound to hold, the mild mesh size restriction $h^{4\alpha(k+1)} \leq C\tau$ (which is more restrictive than the mesh size restriction from Theorem 4.4) was assumed.

4.5.3. Unconditional estimates on the numerical solution

The transformed fully discrete boundary densities $(\widetilde{\boldsymbol{\varphi}}^{\tau,h}, \widetilde{\boldsymbol{\psi}}^{\tau,h})$ of the previous section further fulfill an unconditional stability bound, which bounds it in terms of the incident waves without any assumptions on the exact solution. A particular remarkable property of this result is that it does not rely on a positive shift for $m > 2$, since it only requires the weaker positivity result of Lemma 4.4.

Proposition 4.4. *Consider the fully discrete boundary densities $(\boldsymbol{\varphi}_n^{\tau,h}, \boldsymbol{\psi}_n^{\tau,h}) \in \boldsymbol{V}_h^m \times \boldsymbol{X}_h^m$ for all $n \leq N$, solution to the full discretization of the boundary integral equation (4.70), discretized by*

- *Runge–Kutta convolution quadrature based on the m-stage Radau IIA method, and*
- *Raviart–Thomas boundary elements of order k in space.*

Consider again the transformed fully-discrete boundary densities

$$\widetilde{\boldsymbol{\varphi}}^{\tau,h} = \boldsymbol{b}(\boldsymbol{\psi}^{\tau,h} - \gamma_T \boldsymbol{E}^{\mathrm{inc}}) \times \boldsymbol{\nu} + \gamma_T \boldsymbol{H}^{\mathrm{inc}}, \qquad \widetilde{\boldsymbol{\psi}}^{\tau,h} = \boldsymbol{\psi}^{\tau,h},$$

which by Theorem 4.4 approximate the exact solutions $(\boldsymbol{\varphi}, \boldsymbol{\psi})$ of the boundary integral equation (4.32) in the case of sufficient regularity of the exact solution. Without any assumptions on the exact solution $(\boldsymbol{\varphi}, \boldsymbol{\psi})$, these numerical approximations are bounded by

$$\sum_{n=0}^{N} \left\| \widetilde{\boldsymbol{\varphi}}_n^{\tau,h} \right\|_{\boldsymbol{L}^{1+\alpha}(\Gamma)}^{1+\alpha} + \left\| \widetilde{\boldsymbol{\psi}}_n^{\tau,h} \right\|_{\boldsymbol{L}^{\frac{1+\alpha}{\alpha}}(\Gamma)}^{\frac{1+\alpha}{\alpha}} \leq C_\alpha \sum_{n=0}^{N} \left\| \gamma_T \boldsymbol{E}_n^{inc} \right\|_{\boldsymbol{L}^{\frac{1+\alpha}{\alpha}}(\Gamma)}^{\frac{1+\alpha}{\alpha}} + \left\| \gamma_T \boldsymbol{H}_n^{\mathrm{inc}} \right\|_{\boldsymbol{L}^{1+\alpha}(\Gamma)}^{1+\alpha},$$

where the constant C_α depends only on α.

Proof. We start with the full discretization (4.70), test it with the numerical solution for all $n \geq 0$ and take the weighted sum with $\rho = e^{-\tau/T}$, which yields

$$\begin{aligned} &\sum_{n=0}^{\infty} \rho^n \left(\left[\begin{pmatrix} \boldsymbol{\varphi}_n^{\tau,h} \\ \boldsymbol{\psi}_n^{\tau,h} \end{pmatrix}, \left(\boldsymbol{C}_{\mathrm{imp}}^{-}(\partial_t^\tau) \begin{pmatrix} \boldsymbol{\varphi}_h^{\tau} \\ \boldsymbol{\psi}_h^{\tau} \end{pmatrix} \right)^n \right]_\Gamma + \left(\boldsymbol{\psi}_n^{\tau,h}, \boldsymbol{b} \left(\boldsymbol{\psi}_n^{\tau,h} - \gamma_T \boldsymbol{E}_n^{\mathrm{inc}} \right) \right)_\Gamma \right) \\ &\qquad = \sum_{n=0}^{\infty} \rho^n [\gamma_T \boldsymbol{H}_n^{\mathrm{inc}}, \boldsymbol{\psi}_n^{\tau}]_\Gamma. \end{aligned} \tag{4.90}$$

The positivity of the time-discrete operator $\boldsymbol{C}_{\mathrm{imp}}^{-}(\partial_t^\tau)$, seen as a direct consequence of the second identity of Lemma 4.4 applied to the second identity of Lemma 4.6, implies

$$\sum_{n=0}^{\infty} \rho^n \left[\begin{pmatrix} \boldsymbol{\varphi}_n^{\tau,h} \\ \boldsymbol{\psi}_n^{\tau,h} \end{pmatrix}, \left(\boldsymbol{C}_{\mathrm{imp}}(\partial_t^\tau) \begin{pmatrix} \boldsymbol{\varphi}_n^{\tau,h} \\ \boldsymbol{\psi}_n^{\tau,h} \end{pmatrix} \right)^n \right]_\Gamma \geq 0.$$

Neglecting the first summand of (4.90) therefore reduces the left-hand side to the summation of the expression

$$\begin{aligned}
&\left(\boldsymbol{\psi}_n^{\tau,h}, \boldsymbol{b}\left(\boldsymbol{\psi}_n^{\tau,h} - \gamma_T \boldsymbol{E}_n^{\mathrm{inc}} \right) \right)_\Gamma = \left\| \boldsymbol{\psi}_n^{\tau,h} - \gamma_T \boldsymbol{E}_n^{\mathrm{inc}} \right\|_{\boldsymbol{L}^{\frac{1+\alpha}{\alpha}}(\Gamma)}^{\frac{1+\alpha}{\alpha}} + \left(\gamma_T \boldsymbol{E}_n^{\mathrm{inc}}, \boldsymbol{b}\left(\boldsymbol{\psi}_n^{\tau,h} - \gamma_T \boldsymbol{E}_n^{\mathrm{inc}} \right) \right)_\Gamma \\
&\geq \left\| \boldsymbol{\psi}_n^{\tau,h} - \gamma_T \boldsymbol{E}_n^{\mathrm{inc}} \right\|_{\boldsymbol{L}^{\frac{1+\alpha}{\alpha}}(\Gamma)}^{\frac{1+\alpha}{\alpha}} - \left\| \gamma_T \boldsymbol{E}_n^{\mathrm{inc}} \right\|_{\boldsymbol{L}^{\frac{1+\alpha}{\alpha}}(\Gamma)}^{\frac{1+\alpha}{\alpha}} \left\| \boldsymbol{\psi}_n^{\tau,h} - \gamma_T \boldsymbol{E}_n^{\mathrm{inc}} \right\|_{\boldsymbol{L}^{\frac{1+\alpha}{\alpha}}(\Gamma)} \\
&\geq \frac{2}{3} \left\| \boldsymbol{\psi}_n^{\tau,h} - \gamma_T \boldsymbol{E}_n^{\mathrm{inc}} \right\|_{\boldsymbol{L}^{\frac{1+\alpha}{\alpha}}(\Gamma)}^{\frac{1+\alpha}{\alpha}} - C_\alpha \left\| \gamma_T \boldsymbol{E}_n^{\mathrm{inc}} \right\|_{\boldsymbol{L}^{\frac{1+\alpha}{\alpha}}(\Gamma)}^{\frac{1+\alpha}{\alpha}},
\end{aligned}$$

where the final estimate is obtained by the generalized Young's inequality. Rearranging this bound and inserting it into the left-hand side of (4.90) yields

$$\begin{aligned}
\frac{2}{3} \sum_{n=0}^{\infty} \rho^n \left\| \boldsymbol{\psi}_n^{\tau,h} - \gamma_T \boldsymbol{E}_n^{\mathrm{inc}} \right\|_{\boldsymbol{L}^{1+\alpha}(\Gamma)}^{1+\alpha} &\leq C \sum_{n=0}^{\infty} \rho^n \left\| \gamma_T \boldsymbol{E}_n^{\mathrm{inc}} \right\|_{\boldsymbol{L}^{\frac{1+\alpha}{\alpha}}(\Gamma)}^{\frac{1+\alpha}{\alpha}} \\
&\quad + \sum_{n=0}^{\infty} \rho^n [\gamma_T \boldsymbol{H}_n^{\mathrm{inc}}, \boldsymbol{\psi}_n^\tau]_\Gamma.
\end{aligned}$$

We continue by estimating the second summand on the right-hand side by subsequently applying the Hölderlin inequality and Young's inequality, which yields for all $n \in \mathbb{N}$ the estimate

$$\begin{aligned}
[\gamma_T \boldsymbol{H}_n^{\mathrm{inc}}, \boldsymbol{\psi}_n^{\tau,h}]_\Gamma &\leq \left\| \gamma_T \boldsymbol{H}_n^{\mathrm{inc}} \right\|_{\boldsymbol{L}^{1+\alpha}(\Gamma)} \left(\left\| \boldsymbol{\psi}_n^{\tau,h} - \gamma_T \boldsymbol{E}_n^{\mathrm{inc}} \right\|_{\boldsymbol{L}^{\frac{1+\alpha}{\alpha}}(\Gamma)} + \left\| \gamma_T \boldsymbol{E}_n^{\mathrm{inc}} \right\|_{\boldsymbol{L}^{\frac{1+\alpha}{\alpha}}(\Gamma)} \right) \\
&\leq C \left(\left\| \gamma_T \boldsymbol{H}_n^{\mathrm{inc}} \right\|_{\boldsymbol{L}^{1+\alpha}(\Gamma)}^{1+\alpha} + \left\| \gamma_T \boldsymbol{E}_n^{\mathrm{inc}} \right\|_{\boldsymbol{L}^{\frac{1+\alpha}{\alpha}}(\Gamma)} \right) + \frac{1}{3} \left\| \boldsymbol{\psi}_n^{\tau,h} - \gamma_T \boldsymbol{E}_n^{\mathrm{inc}} \right\|_{\boldsymbol{L}^{\frac{1+\alpha}{\alpha}}(\Gamma)}^{\frac{1+\alpha}{\alpha}}.
\end{aligned}$$

The bound for the numerical solution $\boldsymbol{\psi}_n^{\tau,h}$ is now given by absorption and the triangle inequality. Furthermore, applying the bound (4.14) of the nonlinearity $\boldsymbol{b}$ shows the estimate

$$\left\| \widetilde{\boldsymbol{\varphi}}_n^{\tau,h} \right\|_{\boldsymbol{L}^{1+\alpha}(\Gamma)} \leq \left\| \boldsymbol{\psi}_n^{\tau,h} - \gamma_T \boldsymbol{E}_n^{\mathrm{inc}} \right\|_{\boldsymbol{L}^{\frac{1+\alpha}{\alpha}}(\Gamma)} + \left\| \gamma_T \boldsymbol{H}_n^{\mathrm{inc}} \right\|_{\boldsymbol{L}^{1+\alpha}(\Gamma)}.$$

The stated bound is then given by setting the incident wave $(\gamma_T \boldsymbol{E}_n^{\mathrm{inc}}, \gamma_T \boldsymbol{H}_n^{\mathrm{inc}})$ to zero for all $n > N$, outside of the observed time interval. □

4.6. Numerical experiments

Consider the setting of the numerical experiments in [57], which is repeated in the following. The Galerkin discretizations of the electromagnetic boundary integral operators have been realized with the boundary element library Bempp [65]. Let the domain Ω be the complement of two unit cubes, which are shifted from the origin in such a way, that a gap of length $l = 0.5$ separates them. An incoming electric planar wave is initially away from the boundary and interacts with the scatterers. The incoming wave is given by the closed form of the previous chapter (i.e. (3.71)), namely by the expression

$$\boldsymbol{E}^{\text{inc}}(t, x) = e^{-c(t-x_3-t_0)^2}\boldsymbol{e}_1,$$

with the parameters $c = 100$, $\boldsymbol{e}_1 = (1, 0, 0)^T$ and $t_0 = -2$. We enforce the nonlinear boundary condition with multiple parameters α, to present several types of numerical experiments.

Semi-discretization convergence plots in Figure 4.1 and Figure 4.2

We consider the semi-discrete convergence rates in time and space. The errors are estimated by fixing the semi-discretization in time and space in the full discretization (4.70) respectively, and comparing the approximations with appropriate reference solutions. All convergence plots have been computed with $\alpha = 1/2$.

Figure 4.1 shows the time discretization error obtained when fixing a 0-th order Raviart–Thomas elements space-discretization with 252 degrees of freedom in space. A reference solution is computed with the convolution quadrature method based on the 3-stage Radau IIA Runge-Kutta method with $N = 362$ time steps. Using the convolution quadrature method based on the 1- and 2-stage Radau IIA Runge-Kutta method, we compute the numerical solution with $N_j = 16 \cdot \text{round}(2^{j/2})$ time steps (rounded, for $j = 0, ..., 8$) and compare the approximations with the reference solution at the final time $T = 2$ in the origin $\boldsymbol{P} = (0, 0, 0)$.

The predicted orders of $\mathcal{O}(\tau)$ and $\mathcal{O}(\tau^2)$ are only asymptotically achieved, possibly due to the low regularity of the scatterers, which in particular also contain corners. Nevertheless, the two-stage Radau IIA method outperforms the implicit Euler, even for moderately small step sizes τ. The restrictive order reductions of Theorem 4.4 are not observed.

Conversely, Figure 4.2 shows semi-discrete spatial errors, that have been computed by fixing a convolution quadrature time discretization based on the 3-stage Radau IIA Runge-Kutta method with $N = 32$ time steps. A reference solution has been computed by additionally employing a 0-th order Raviart–Thomas elements space-discretization with 11088 degrees of freedom (which corresponds to the mesh width $h = 2^{-4}$) and using the proposed fully discrete boundary integral equation (4.70).

Two types of numerical approximations are compared with this reference solution. The left plot, with the additional numbering I, shows the spatial error of the original formulation of [57], namely the boundary integral equation (4.87). Several grids, corresponding to the mesh widths $h_j = 2^{-j/2}$ for $j = 0, ..., 6$, are used to compute numerical approximations, which are compared to the reference solution on the whole time interval $[0, 3]$. The maximal error (with regards to the time t), is computed again in the origin $\boldsymbol{P} = (0, 0, 0)$. On the right plot of Figure 4.2,

marked with the additional numbering II, an identical error plot is shown for the fully discrete boundary integral equation (4.70) analyzed in this chapter.

Both methods exhibit similar convergence properties, despite the predicted differences of the spatial convergence rates, which are $\mathcal{O}(h^{1/2})$ (from [57] as described in Remark 4.6) for the left plot and $\mathcal{O}(h^{3/4})$ (due to Theorem 4.2) for the right plot respectively. Overall, the numerical evidence indicates that the error behaves in the order of $\mathcal{O}(h)$, which is the rate of the best-approximation error of the 0-th order Raviart–Thomas boundary element space.

Full discretization convergence plots in Figure 4.4 and Figure 4.3

The full discretization error plots are taken from the original paper [57] and were therefore computed with the fully discrete boundary integral equation (4.87). Both numerical formulations ((4.70) and (4.87)) seem to exhibit the same convergence properties in practice, as indicated in Figure 4.2 (compare also the acoustic experiments Figures 2.1–2.2 and Figures 2.3–2.4).
The nonlinear boundary condition is again used with the parameter $\alpha = 0.5$. We observe the interaction of the incoming wave with the scatterers until the final time $T = 3$. Instead of mutually fixing the semi-discretizations and computing two reference solutions, a single reference solution based on a 0-th order Raviart–Thomas boundary element discretization with 6228 degrees of freedom, which corresponds to the mesh width $h = 2^{-7/2}$, was used in combination with $N = 256$ time steps using the 3-stage Radau IIA based Runge–Kutta convolution quadrature method.

Varying the mesh width and time step size reveals the convergence properties of the scheme by comparing the resulting solutions with a reference solution in the origin $\boldsymbol{P} = (0, 0, 0)$.

The convergence plots in Figure 4.4 and Figure 4.3 are obtained by mutually fixing the time step size τ, or the mesh width h respectively.

The error bound of [57, Theorem 2], reformulated in (4.88), predicts a convergence rate of at least $\mathcal{O}(\tau^2 + h^{1/2})$, although the order reductions from Theorem 4.4 could apply and reduce the overall convergence rates in space and time. The exact solution is further unlikely to fulfill the assumptions of [57, Theorem 2], due to the low regularity of the scatterers (which contain corners).

Nevertheless, the empirical space convergence rate in Figure 4.4 is higher than the order of the error bounds $\mathcal{O}(h^{1/2})$ and more accurately described by $\mathcal{O}(h)$. The rapid increase in accuracy for the final data points (also in the second plot of Figure 4.2) might be explained by the close proximity to the reference solution.

For $\tau \to 0$, the empirical time convergence rate in Figure 4.3 approaches $\mathcal{O}(\tau^2)$. The rapid decay of the error in the final data point might be explained by the close proximity to the reference solution.

Altogether, the proposed full discretizations show good convergence properties, despite the obstacles of the covered problem. In the process of computing the numerical solution, several underlying approximations are made during the implementation, such as the quadrature and compression of the boundary element matrices, the iterative solution of the resulting linear systems, Newton's method in each time step and the underlying trapezoidal rule approximating the convolution quadrature weights (C.10). The convergence plots show that these factors can

be controlled in a way that the overall convergence properties of the method are preserved.

Visualization of the wave

This chapter, and with it the main part of this thesis, concludes with Figures 4.5–4.7, which visualize several waves corresponding to different values of α. All images were created using the full discretization (4.70), which was proposed in this chapter. The structure of the plot and the specific time points is taken from the original paper [57, Figure 3], which used the fully discrete boundary integral equation (4.87).

As the time discretization, the convolution quadrature method based on the 3-stage Radau IIA Runge–Kutta method is employed with $N = 256$ time steps, up to the final time $T = 3$. A 0-th order Raviart–Thomas boundary element space with 1620 degrees of freedom, which corresponds to the mesh width $h = 2^{-5/2}$, was used as the space discretization.

To visualize the 3D-scattering, we plot the absolute value of the electric field $\boldsymbol{E}^{\tau,h}$ on the $x_2 = 0.5$ plane, which cuts through the middle of the scatterer, at several time points.

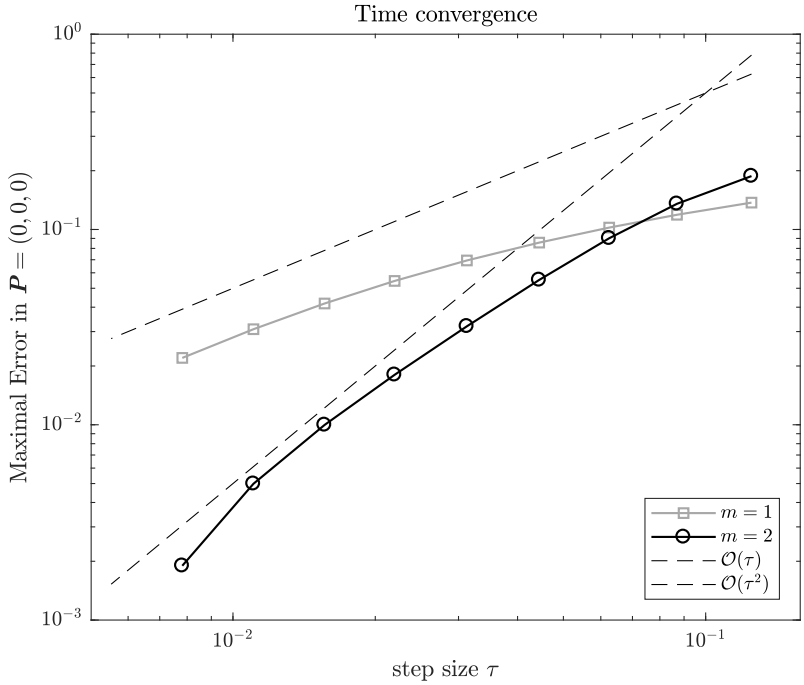

Figure 4.1.: Semi-discrete time convergence plot at time $T = 2$ for $\alpha = 1/2$, obtained by fixing a 0th order Raviart–Thomas boundary element discretization with 252 degrees of freedom.

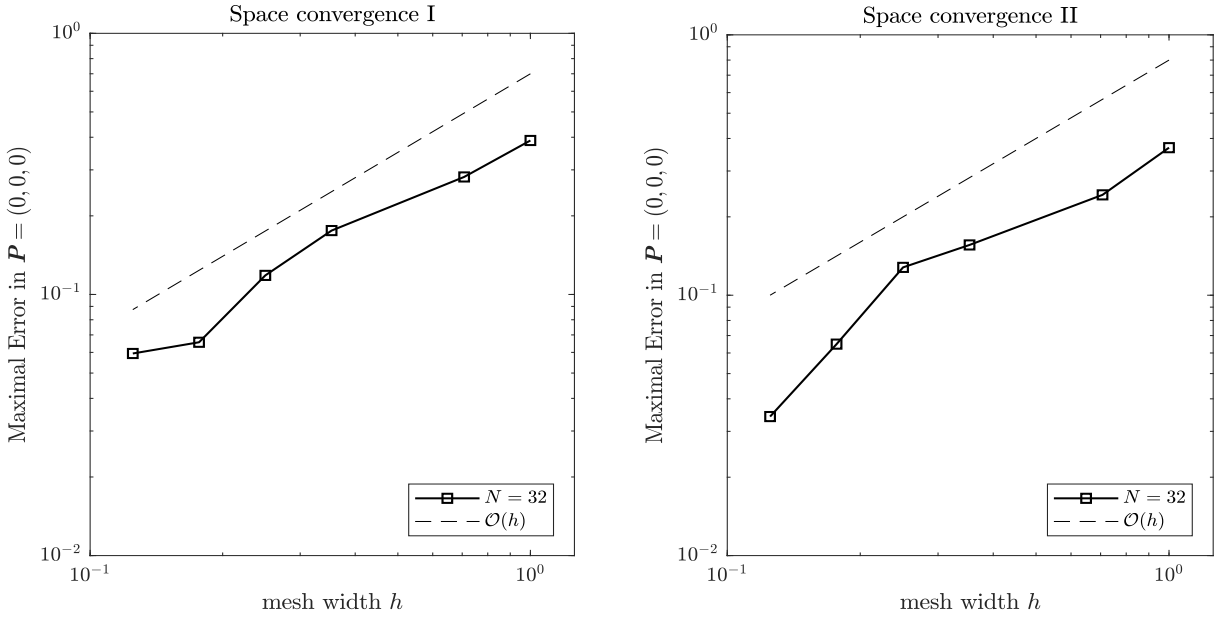

Figure 4.2.: Semi-discrete space convergence plot for $\alpha = 1/2$, obtained by fixing a 3-stage Radau IIA based Runge–Kutta convolution quadrature method time discretization with $N = 32$ time steps. The larger gap between the 4-th and the 5-th data point is caused by the mesh generator embedded in the Bempp library.

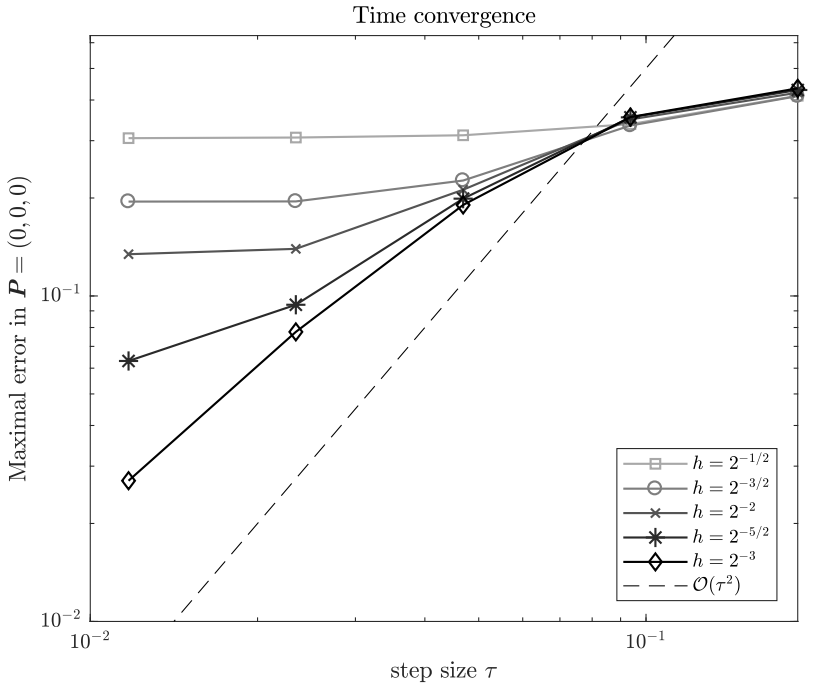

Figure 4.3.: Time convergence plot of the fully discrete system with $\alpha = 1/2$, for 0th order Raviart–Thomas boundary elements and the 2-stage Radau IIA based Runge–Kutta convolution quadrature method. The Figure originally appeared in [57, Figure 2].

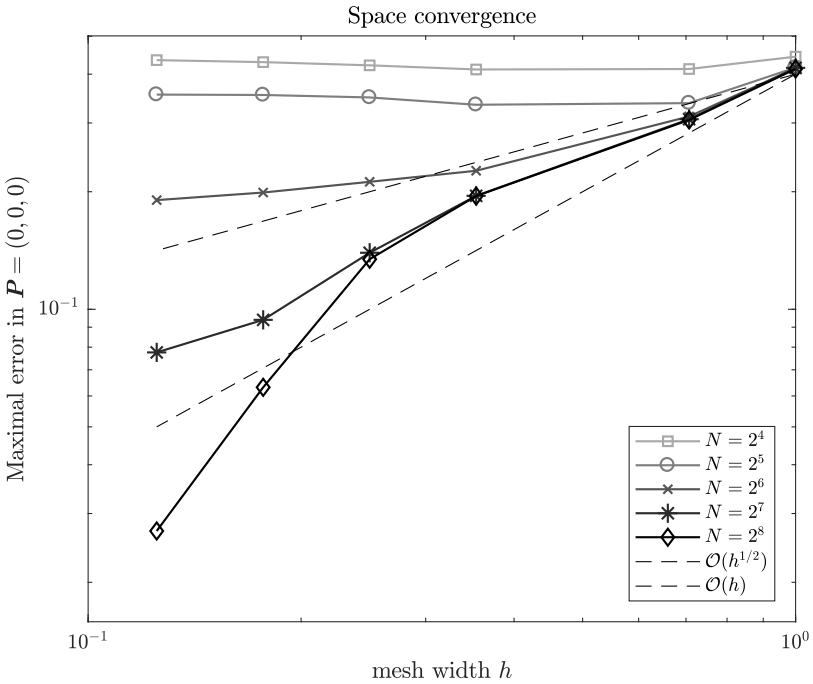

Figure 4.4.: Space convergence plot of the fully discrete system with $\alpha = 1/2$, for 0th order Raviart–Thomas boundary elements and the 2-stage Radau IIA based Runge–Kutta convolution quadrature method. The Figure originally appeared in [57, Figure 1].

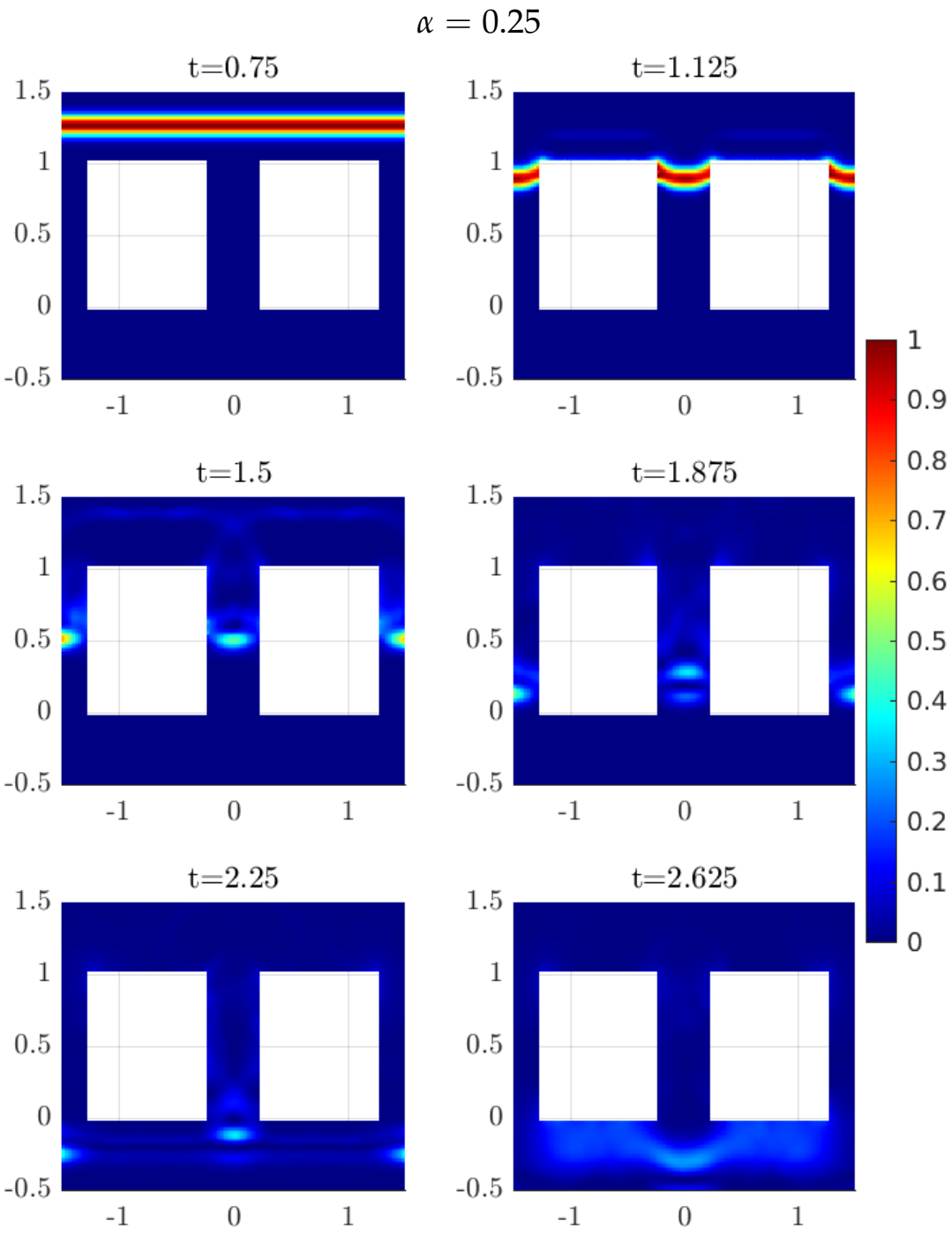

Figure 4.5.: 3D-scattering arising for the parameter $\alpha = 0.25$, with $N = 256$ time steps on the time interval $[0,3]$, using the 3-stage Radau IIA method with the mesh width $h = 2^{-5/2}$, corresponding to 0-th order Raviart–Thomas boundary element space with 1620 degrees of freedom.

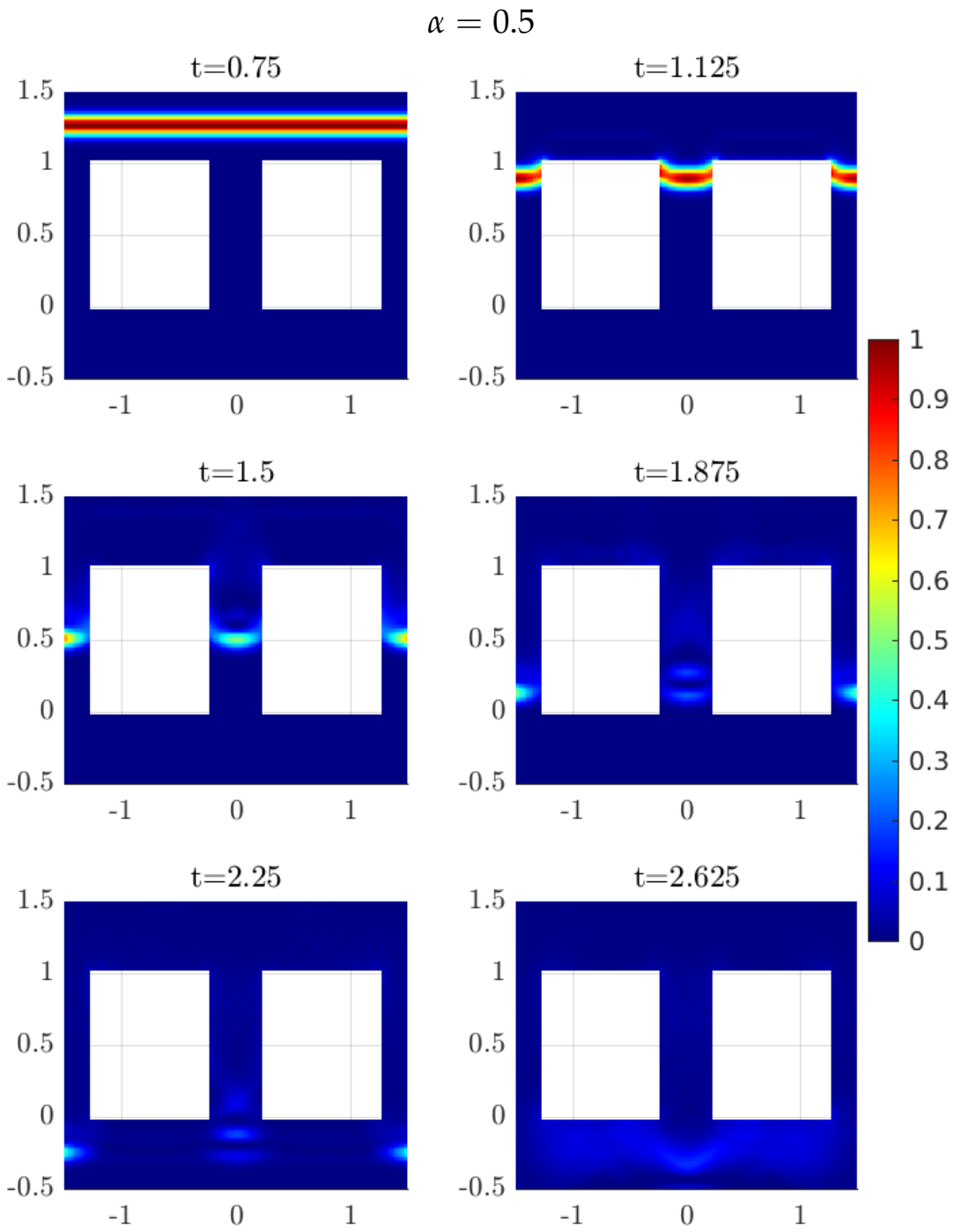

Figure 4.6.: 3D-scattering arising for the parameter $\alpha = 0.5$, with $N = 256$ time steps on the time interval $[0, 3]$, using the 3-stage Radau IIA method with the mesh width $h = 2^{-5/2}$, corresponding to 0-th order Raviart–Thomas boundary element space with 1620 degrees of freedom.

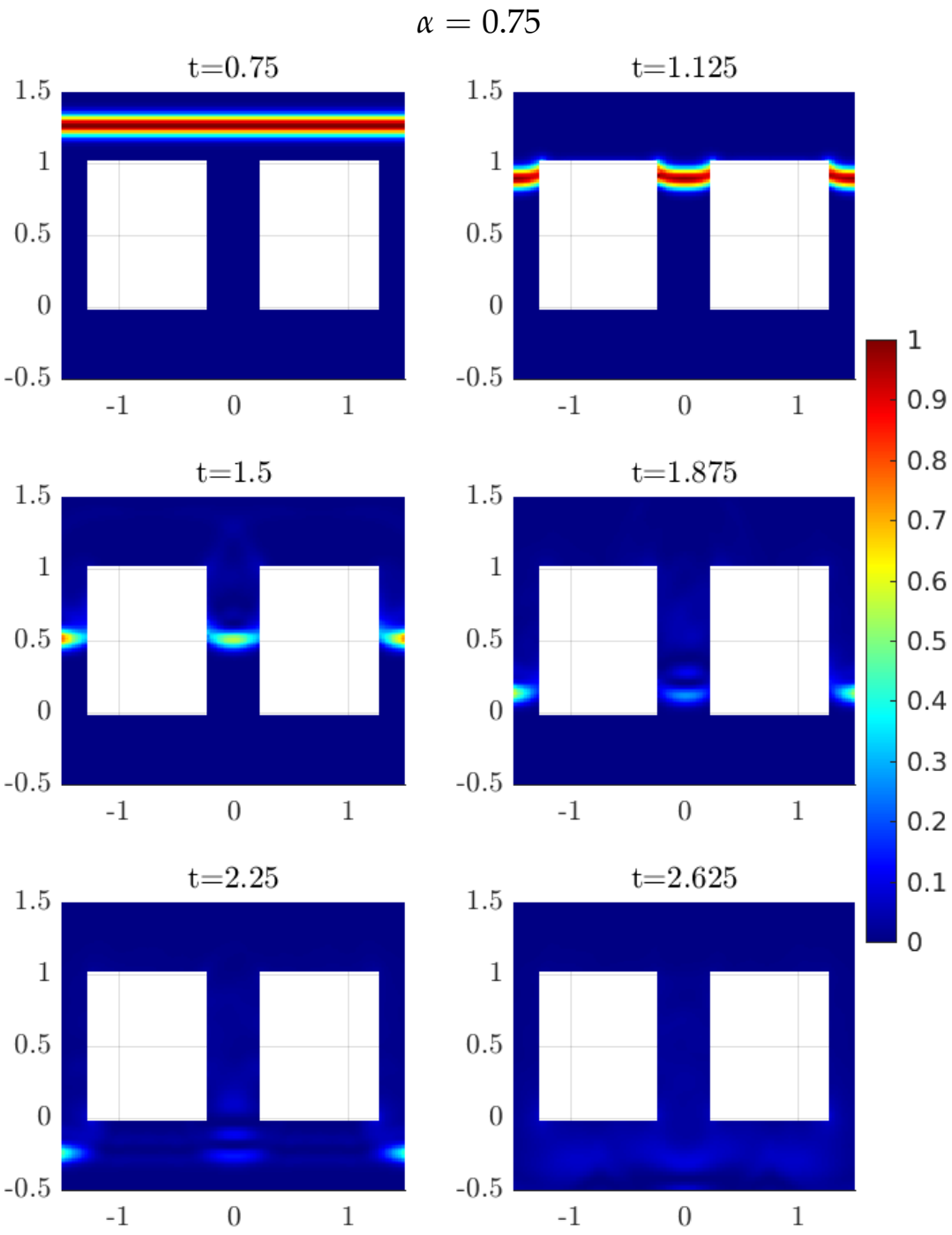

Figure 4.7.: 3D-scattering arising for the parameter $\alpha = 0.75$, with $N = 256$ time steps on the time interval $[0, 3]$, using the 3-stage Radau IIA method with the mesh width $h = 2^{-5/2}$, corresponding to 0-th order Raviart–Thomas boundary element space with 1620 degrees of freedom.

Appendices

The following two appendices describe the notation and fundamental results for continuous and discrete convolutional operators. The structure and large passages in these sections are taken from [59, Section 2.2 & Section 5.1] and are not original results of this thesis. We repeat these sections here for the convenience of the reader to keep the thesis largely self-contained.

A. Temporal Sobolev spaces and operational calculus

We introduce the Heaviside notation of operational calculus and associated temporal Sobolev spaces. Let $\boldsymbol{K}(s)\colon \boldsymbol{X} \to \boldsymbol{X}'$ be an analytic family of bounded linear operators, defined for all s in a complex half space $\mathbb{C}_+$, where $\boldsymbol{X}$ is a Hilbert space.

The analytic operator family $\boldsymbol{K}(s)$ is assumed to be polynomially bounded (with respect to the frequency s) for all $\operatorname{Re} s \geq \sigma_0 > 0$, in the following sense. There exists a real κ, a positive $\nu \geq 0$ and, for every $\sigma > \sigma_0$, there exists a constant $M_\sigma < \infty$ such that

$$\|\boldsymbol{K}(s)\|_{\boldsymbol{X}' \leftarrow \boldsymbol{X}} \leq M_\sigma \frac{|s|^\kappa}{(\operatorname{Re} s)^\nu} \quad \text{for } \operatorname{Re} s \geq \sigma \geq \sigma_0. \tag{A.1}$$

Under this condition, $\boldsymbol{K}(s)$ is guaranteed to be the Laplace transform of a distribution of finite order of differentiation with support on the nonnegative real half-line $t \geq 0$. Hence, for a sufficiently regular function $\boldsymbol{g} : \mathbb{R} \to \boldsymbol{X}$, which vanishes on the negative real half-axis, we use the Heaviside notation of operational calculus, which denotes

$$\boldsymbol{K}(\partial_t)\boldsymbol{g} = (\mathcal{L}^{-1}\boldsymbol{K}) * \boldsymbol{g},$$

for the convolution of the inverse Laplace transform of $\boldsymbol{K}(s)$ with $\boldsymbol{g}$. This notation defines a wide class of temporal differential operators and is motivated by the fact that for $\mathbf{Id}(s) = s$, we have $\mathbf{Id}(\partial_t)\boldsymbol{g} = \partial_t \boldsymbol{g}$, which is the time derivative of $\boldsymbol{g}$.

The composition of two time-dependent operators defined via the Heaviside notation carries through to the Laplace domain. Specifically, for two operator families $\boldsymbol{K}(s)\colon \boldsymbol{X} \to \boldsymbol{Y}$ and $\boldsymbol{L}(s)\colon \boldsymbol{Y} \to \boldsymbol{Z}$ on compatible Hilbert spaces, we have the composition rule

$$\boldsymbol{K}(\partial_t)\boldsymbol{L}(\partial_t)\boldsymbol{g} = (\boldsymbol{K}\boldsymbol{L})\,(\partial_t)\boldsymbol{g}, \tag{A.2}$$

where $\boldsymbol{g} : [0, T] \to \boldsymbol{X}$ is again vanishing on the negative real half-line and sufficiently regular.

Operators defined by the notation of operational calculus require a temporal functional analytic framework, which is provided by temporal Sobolev spaces. Consider the space $\boldsymbol{H}^r(\mathbb{R}, \boldsymbol{X})$ with real order r, the Sobolev space of order r of $\boldsymbol{X}$-valued functions on $\mathbb{R}$. Restricting the Hilbert space on functions which vanish on the negative axis yields the definition

$$\boldsymbol{H}^r_0(0, T; \boldsymbol{X}) = \{\boldsymbol{g}|_{(0,T)} \,:\, \boldsymbol{g} \in \boldsymbol{H}^r(\mathbb{R}, \boldsymbol{X}) \text{ with } \boldsymbol{g} = 0 \text{ on } (-\infty, 0)\}.$$

For the integer order $r \geq 0$, the norm $\|\partial_t^r \boldsymbol{g}\|_{\boldsymbol{L}^2(0,T;\boldsymbol{X})}$ is equivalent to the original norm on $\boldsymbol{H}^r_0(0, T; \boldsymbol{X})$. For $r > 1/2$, we have the continuous embedding $\boldsymbol{H}^r_0(0, T; \boldsymbol{X}') \subset \boldsymbol{C}([0, T]; \boldsymbol{X}')$.

The following identity from [52, Lemma 2.1] clarifies the connection of the Heaviside nota-

tion with the setting of temporal Sobolev spaces. Let the analytic family $\boldsymbol{K}(s)$ fulfill the polynomial bound (A.1) in a half-plane Re $s > 0$, then $K(\partial_t)$ extends by density to a bounded linear operator

$$\boldsymbol{K}(\partial_t) : \boldsymbol{H}_0^{r+\kappa}(0,T;\boldsymbol{X}) \to \boldsymbol{H}_0^r(0,T;\boldsymbol{X}') \tag{A.3}$$

for arbitrary real r. The framework of temporal Sobolev spaces therefore provides an appropriate setting for the Heaviside notation of operational calculus. Moreover, choosing $\sigma = 1/T$ in the Plancherel formula (see [52, Lemma 2.1]), shows that the norm of the operator fulfills the bound

$$\|\boldsymbol{K}(\partial_t)\|_{\boldsymbol{H}_0^r(0,T;\boldsymbol{X}')\leftarrow\boldsymbol{H}_0^{r+\mu}(0,T;\boldsymbol{X})} \leq eM_{1/T},$$

where $M_{1/T}$ is the constant from (A.1).

B. The convolution quadrature method

The prevalence of temporal convolutions $\boldsymbol{K}(\partial_t)\boldsymbol{g}$ throughout the thesis, as defined via (1.2), requires a well understood discretization. Runge–Kutta convolution quadrature methods are used throughout the thesis to approximate temporal convolutions ; cf. (1.2). Let us first recall an m-stage implicit Runge–Kutta discretization of the initial value problem $y' = f(t,y)$, $y(0) = y_0$; see [44]. For the time step size $\tau > 0$, the approximations y^n to $y(t_n)$ at time $t_n = n\tau$, and the internal stages Y^{ni} approximating $y(t_n + c_i\tau)$, are obtained from

$$\begin{aligned} Y^{ni} &= y^n + \tau \sum_{j=1}^m a_{ij} f(t_n + c_j h, Y^{nj}), \qquad i = 1,\dots,m, \\ y^{n+1} &= y^n + \tau \sum_{j=1}^m b_j f(t_n + c_j h, Y^{nj}). \end{aligned}$$

The method is determined by its coefficients, stored in the Butcher-tableau

$$\mathscr{A} = (a_{ij})_{i,j=1}^m, \quad \boldsymbol{b} = (b_1,\dots,b_m)^T, \quad \text{and} \quad \boldsymbol{c} = (c_1,\dots,c_m)^T.$$

The stability function of the Runge–Kutta method is given by the expression $R(z) = 1 + zb^T(\boldsymbol{I}_m - z\mathscr{A})^{-1}\mathbb{1}$, where $\mathbb{1} = (1,1,\dots,1)^T \in \mathbb{R}^m$. We always assume that $\mathscr{A}$ is invertible.

Runge–Kutta methods can be used to construct convolution quadrature methods. Such methods were first introduced in [53] in the context of parabolic problems and were studied for wave propagation problems in [14] and subsequently, e.g., in [11, 13, 17, 18]. Runge–Kutta convolution quadrature was studied for the numerical solution of exterior Maxwell problems in [7, 28] and in the context of an eddy current problem with an impedance boundary condition in [45]. For wave problems, Runge–Kutta convolution quadrature methods such as those based on the Radau IIA methods (see [44, Section IV.5]), often enjoy more favourable properties than their BDF-based counterparts, which are more dissipative and cannot exceed order 2 but are easier to understand and slightly easier to implement.

To construct the convolution quadrature weights, we use the *Runge–Kutta differentiation sym-*

bol

$$\Delta(\zeta) = \Big(\mathscr{A} + \frac{\zeta}{1-\zeta}\mathbb{1}\boldsymbol{b}^T\Big)^{-1} \in \mathbb{C}^{m\times m}, \qquad \zeta \in \mathbb{C} \text{ with } |\zeta| < 1. \tag{B.4}$$

This expression is well-defined for $|\zeta| < 1$ if $R(\infty) = 1 - \boldsymbol{b}^T\mathscr{A}^{-1}\mathbb{1}$ satisfies $|R(\infty)| \leq 1$. In fact, the Sherman–Morrison formula yields for Radau IIA methods

$$\Delta(\zeta) = \mathscr{A}^{-1} - \frac{\zeta}{1-R(\infty)\zeta}\mathscr{A}^{-1}\mathbb{1}\boldsymbol{b}^T\mathscr{A}^{-1} = \mathscr{A}^{-1}(\boldsymbol{I}_m - \zeta\mathbb{1}\boldsymbol{e}_m^T), \tag{B.5}$$

with $\boldsymbol{e}_m^T = (0,...,1) \in \mathbb{R}^m$ and $\boldsymbol{I}_m \in \mathbb{R}^{m\times m}$ denoting the identity matrix. This is well-defined for $|\zeta| < 1$ if $R(\infty) = 1 - \boldsymbol{b}^T\mathscr{A}^{-1}\mathbb{1}$ satisfies $|R(\infty)| \leq 1$, which is seen from the Sherman–Woodbury formula. Moreover, for A-stable Runge–Kutta methods (e.g. the Radau IIA methods), the eigenvalues of the matrices $\Delta(\zeta)$ have positive real part for $|\zeta| < 1$ [14, Lemma 3].

To formulate the Runge–Kutta convolution quadrature for $\boldsymbol{K}(\partial_t)\boldsymbol{g}$, we replace the complex argument s in $\boldsymbol{K}(s)$ by the matrix $\Delta(\zeta)/\tau$ and use the power series expansion

$$\boldsymbol{K}\Big(\frac{\Delta(\zeta)}{\tau}\Big) = \sum_{n=0}^{\infty} \boldsymbol{\mathcal{W}}_n(\boldsymbol{K})\zeta^n. \tag{B.6}$$

The operators $\boldsymbol{\mathcal{W}}_n(\boldsymbol{K}) : \boldsymbol{X}^m \to \boldsymbol{Y}^m$ are used as the convolution quadrature weights. For the discrete convolution of these operators with an appropriate sequence $\boldsymbol{g} = (\boldsymbol{g}^n)$ with $\boldsymbol{g}^n = (\boldsymbol{g}_i^n)_{i=1}^m \in \boldsymbol{X}^m$, we use the notation

$$\big(\boldsymbol{K}(\partial_t^\tau)\boldsymbol{g}\big)^n = \sum_{j=0}^{n} \boldsymbol{\mathcal{W}}_{n-j}(\boldsymbol{K})\boldsymbol{g}^j \in \boldsymbol{Y}^m. \tag{B.7}$$

Given a function $\boldsymbol{g} : [0,T] \to \boldsymbol{X}$, we extend the notation for vectors to the evaluations at the nodes $\boldsymbol{c}$ through

$$\boldsymbol{g}^n = \boldsymbol{g}(\underline{t_n}) = \big(\boldsymbol{g}(t_n + c_i\tau)\big)_{i=1}^m.$$

When convenient, the index n is also denoted as a subindex. The i-th component of the vector $\big(\boldsymbol{K}(\partial_t^\tau)\boldsymbol{g}\big)^n$ is then an approximation to $\big(\boldsymbol{K}(\partial_t)\boldsymbol{g}\big)(t_n + c_i\tau)$; see [13, Theorem 4.2].

If $c_m = 1$, as is the case with Radau IIA methods, the continuous convolution at t_n is approximated by the m-th, i.e. last, component of the m-vector (B.7) for $n-1$:

$$\big(\boldsymbol{K}(\partial_t)\boldsymbol{g}\big)(t_n) \approx \Big[\big(\boldsymbol{K}(\partial_t^\tau)\boldsymbol{g}\big)^{n-1}\Big]_m \in \boldsymbol{Y}. \tag{B.8}$$

An essential property is that the continuous composition rule (A.2) is preserved under this discretization: for two such operator families $\boldsymbol{K}(s)$ and $\boldsymbol{L}(s)$ that map to compatible spaces, we have

$$\boldsymbol{K}(\partial_t^\tau)\boldsymbol{L}(\partial_t^\tau)\boldsymbol{g} = (\boldsymbol{K}\boldsymbol{L})(\partial_t^\tau)\boldsymbol{g}. \tag{B.9}$$

The following error bound for Runge–Kutta convolution quadrature from [14], here directly stated for the Radau IIA methods [44, Section IV.5] and in a Banach space setting, will be the

basis for the temporal error bounds, especially in Chapter 2 and Chapter 3.

Lemma B.1 ([14, Theorem 3]). *Let $\boldsymbol{K}(s) : \boldsymbol{X} \to \boldsymbol{Y}$, $\operatorname{Re} s > \sigma_0 \geq 0$, be an analytic family of linear operators between Banach spaces $\boldsymbol{X}$ and $\boldsymbol{Y}$ satisfying the bound (A.1) with exponents κ and ν. Consider the Runge–Kutta convolution quadrature based on the Radau IIA method with m stages. Let $1 \leq q \leq m$ (the most interesting case is $q = m$) and $r > \max(2q - 1 + \kappa, 2q - 1, q + 1)$. Let $\boldsymbol{g} \in \boldsymbol{C}^r([0, T], \boldsymbol{X})$ satisfy $\boldsymbol{g}(0) = \boldsymbol{g}'(0) = ... = \boldsymbol{g}^{(r-1)}(0) = 0$. Then, the following error bound holds at $t_n = n\tau \in [0, T]$:*

$$\begin{aligned}&\left\| \left[\left(\boldsymbol{K}(\partial_t^\tau)\boldsymbol{g}\right)^{n-1} \right]_m - (\boldsymbol{K}(\partial_t)\boldsymbol{g})(t_n) \right\|_{\boldsymbol{Y}} \\ &\qquad \leq C\, M_{1/T}\, \tau^{\min(2q-1, q+1-\kappa+\nu)} \left(\|\boldsymbol{g}^{(r)}(0)\|_{\boldsymbol{X}} + \int_0^t \|\boldsymbol{g}^{(r+1)}(t')\|_{\boldsymbol{X}} \, \mathrm{d}t' \right).\end{aligned}$$

The constant C is independent of τ and $\boldsymbol{g}$ and M_σ of (A.1), but depends on the exponents κ and ν in (A.1) and on the final time T.

The proof of this approximation result generalizes to the following error bounds for the stages, which is the fundamental approximation result used in Chapter 4.

Lemma B.2 ([13, Theorem 4.2]). *Let $\boldsymbol{K}$ satisfy (3.8) and consider the Runge–Kutta convolution quadrature based on the Radau IIA method with m stages. Let $r > \max(m + 1 + \kappa, m + 1)$ and $\boldsymbol{g} \in \boldsymbol{C}^r([0, T], \boldsymbol{V})$ satisfy $\boldsymbol{g}(0) = \boldsymbol{g}'(0) = ... = \boldsymbol{g}^{(r-1)}(0) = 0$. Then, there exists a $\tau_0 > 0$ such that for $0 < \tau \leq \tau_0$ and $t_n = n\tau \in [0, T]$ the following error bound holds:*

$$\begin{aligned}&\left\| \left(\boldsymbol{K}(\partial_t^\tau)\boldsymbol{g}\right)^n - \boldsymbol{K}(\partial_t)\boldsymbol{g}(\underline{t_n}) \right\| \\ &\qquad \leq C M_{1/T} \tau^{\min(m+1, m+1-\kappa+\nu)} \left(\left\|\boldsymbol{g}^{(r)}(0)\right\| + \int_0^t \left\|\boldsymbol{g}^{(r+1)}(\lambda)\right\| \mathrm{d}\lambda \right),\end{aligned}$$

where $\boldsymbol{K}(\partial_t)\boldsymbol{g}(\underline{t_n}) = (\boldsymbol{K}(\partial_t)\boldsymbol{g}(t_n + c_i\tau))_{i=1}^m$. The constant C is again independent of τ and $\boldsymbol{g}$ and M_σ of (A.1), but depends on the exponents κ and ν in (A.1) and on the final time T.

C. Implementation of the convolution quadrature method

In the following, we describe some aspects regarding the practical implementation of time-discrete boundary integral equations, to realize these numerical solutions. The implementation that has been used for all experiments in this thesis is available under [56].

We give a description of the implementation of a discretization of a forward convolution $\boldsymbol{K}(\partial_t^\tau)\Phi$, whose efficient computation yields effective algorithms to compute boundary densities and fields which solve linear temporal scattering problems, as described in Chapter 2 and in Chapter 3.

The convolution quadrature weights are approximated by discretizing their Cauchy-integral representation with the trapezoidal rule, as already described in the original work [51]. This

gives the following approximation to the weights

$$\boldsymbol{W}_n(\boldsymbol{K}) \approx \frac{\rho^{-n}}{L} \sum_{l=0}^{L-1} \boldsymbol{K}\left(\frac{\Delta(\rho\,\zeta_L^{-l})}{\tau}\right) \zeta_L^{nl}, \quad \text{for } 0 \leq n \leq N, \tag{C.10}$$

where $\zeta_L = e^{2\pi i/L}$.

The parameters ρ and L are chosen during the implementation and arise from the underlying contour integral and the respective trapezoidal rule of the convolution quadrature weights. Whereas L can simply be chosen large enough (with increasing computational cost), the choice of ρ must strike a balance between truncation errors and round-off errors of the approximation of the quadrature weights. For $\rho \to 1$, the quadrature error of the underlying trapezoidal rule deteriorates as the integral contour approaches the stability region of the underlying time stepping method. Conversely for $\rho \to 0$, the finite precision arithmetic leads to a catastrophic cancellation on the right-hand side of (C.10) for large n, accumulating large round-off errors in the process. Effective choices for the parameters are provided already in the original paper [50] and are given by $L = 2N$ and $\rho = \epsilon^{\frac{1}{2N}}$, where ϵ denotes the *machine precision*.

For the computations in Chapter 2 and Chapter 3, these parameter choices have been used.

To evaluate the analytic operator family $\boldsymbol{K}(\Delta(\zeta)/\tau)$, for the matrix valued characteristic function $\Delta(\zeta) \in \mathbb{C}^{m\times m}$ at a point $\zeta \in \mathbb{C}$ inside of the unit circle, it is convenient to diagonalize the characteristic function by

$$\boldsymbol{T}^{-1}\boldsymbol{K}\left(\Delta(\zeta)\right)\boldsymbol{T} = \boldsymbol{K}\left(\boldsymbol{T}^{-1}\Delta(\zeta)\boldsymbol{T}\right), \quad \text{for invertible} \quad \boldsymbol{T} \in \mathbb{C}^{m\times m},$$

which reduces the evaluation $\boldsymbol{K}(\Delta(\zeta)/\tau)$ to evaluating $\boldsymbol{K}(\cdot)$ at the eigenvalues of $\Delta(\zeta)$. Inserting these approximations to the quadrature weights into (B.7) then gives the scheme

$$(\boldsymbol{K}(\partial_t^\tau)\boldsymbol{g})^n \approx \frac{\rho^{-n}}{L} \sum_{l=0}^{L-1} \zeta_L^{ln} \boldsymbol{K}\left(\frac{\Delta(\rho\,\zeta_L^{-l})}{\tau}\right) \left[\sum_{j=0}^{N} \rho^j \boldsymbol{g}^j \zeta_L^{-jl}\right]. \tag{C.11}$$

The sums above are realized efficiently by the fast fourier transform (FFT), which leaves the main computational burden at the evaluations of the Laplace domain operators $\boldsymbol{K}(\cdot)$ at mL scalar frequencies $s_k \in \mathbb{C}$ for $k = 1, \ldots, mL$ (i.e. the eigenvalues of $\boldsymbol{K}(\Delta(\rho\,\zeta_L^{-k})/\tau)$) with positive real part. With respect to the number of time steps N, the algorithm therefore has the complexity $\mathcal{O}(N\log(N))$, though in practise the main part of the computation is often taken by the assembly of the boundary element matrices, which scales with $\mathcal{O}(N)$.

Due to symmetry of the time-harmonic operators with regards to the Laplace parameter s, only half of the Laplace domain evaluations have to be computed. For sufficiently smooth finite signals $\boldsymbol{g}$, the amount of necessary Laplace transforms can further be decreased. More details on these improvements are found in [19].

Setting, for instance, either $\boldsymbol{K}(s) = \boldsymbol{A}_h(s)^{-1}$ or $\boldsymbol{K}(s) = \boldsymbol{\mathcal{U}}_h(s)$ then gives numerical algorithms to approximate the boundary densities $(\boldsymbol{\varphi}, \boldsymbol{\psi})$ or the electromagnetic fields $\boldsymbol{E}, \boldsymbol{H}$, respectively.

To realize the evaluations of the Laplace transforms, time-harmonic solvers, for which established libraries such as Bempp [68] exist, can be employed. The assembled matrices of the

boundary element method are used only once, which avoids the need to store a large amount of quadrature weights in memory (which would be referred to as a *memory tail*). Furthermore, the evaluation and application of the Laplace transforms (corresponding to the solution of a time-harmonic scattering problem in our application) are completely decoupled and can consequently be solved in parallel without the need for any communication between the processes. For further aspects of this approach in the context of wave equations we refer the reader to [10] and [19].

For nonlinear convolution equations such as (4.70), this approach is not directly admissible, since the solution can not be written as a direct forward application of a convolution operator. A discrete nonlinear convolution equation such as $\boldsymbol{K}(\partial_t^\tau)\boldsymbol{\phi}^\tau + \boldsymbol{a}(\boldsymbol{\phi}^\tau) = \boldsymbol{g}$ is solved in a time-stepping manner, by rewriting it for all $n \leq N$ by

$$\boldsymbol{\mathcal{W}}_0(\boldsymbol{K})\boldsymbol{\phi}^n + \boldsymbol{a}(\boldsymbol{\phi}^n) = \boldsymbol{g}^n - \sum_{j=0}^{n-1} \boldsymbol{\mathcal{W}}_{n-j}(\boldsymbol{K})\boldsymbol{\phi}^j \quad \text{in } \boldsymbol{Y}^m. \tag{C.12}$$

Here, we denote $\boldsymbol{g}^n = \big(\boldsymbol{g}(t_n + c_i\tau)\big)_{i=1}^m$ and similarly $\boldsymbol{\phi}^n \approx \big(\boldsymbol{\phi}(t_n + c_i\tau)\big)_{i=1}^m$, where $\boldsymbol{\phi}$ is the assumed solution of the analogous continuous convolution equation. By setting $\boldsymbol{a} = 0$, the above formulation is also admissible for linear convolution equations. Solving this system in the linear case for all $n \leq N$ instead of directly applying (C.11) with the inverse of $\boldsymbol{K}$ has the advantage of only needing to invert $\boldsymbol{K}$ at the single frequency $\frac{\Delta(0)}{\tau}$. Preconditioning the linear system $\boldsymbol{\mathcal{W}}_0(\boldsymbol{K})$ further reduces the amount of time necessary to solve the arising linear systems during the time integration procedure.

In general, with the nontrivial nonlinearity $\boldsymbol{a}$, the nonlinear system is solved iteratively with Newton's method in each time step. Directly computing the convolution on the right-hand side via (C.11) would lead to a computational effort that scales at least quadratically. To manage the convolution on the right-hand side in an efficient way, the method proposed in [43] is used, which reduces the computational effort of the method with respect to the amount of time steps N, to almost linear growth, more specifically $\mathcal{O}(N\log(N)^2)$. A good description of the method and a formulation as a recursive algorithm is given in [69, Section 4.1].

The algorithm described in these references takes the explicit form of a time-stepping scheme, which is described in the following, without a derivation. Analogous to the notation for continuous functions, we use the shorthand notation $\boldsymbol{b}^n = (\boldsymbol{b}_{mn+i})_{i=1}^m$ and $\boldsymbol{\phi}^n = (\boldsymbol{\phi}_{mn+i})_{i=1}^m$ for the vectors $\boldsymbol{b}$ and $\boldsymbol{\phi}$.

Algorithm 1: Solving the discrete convolution equation (C.12)

Input: $\boldsymbol{K}, \boldsymbol{a}, \boldsymbol{g}, N$

Output: $\boldsymbol{\phi}$

1 Initialize $\boldsymbol{\phi} \in \boldsymbol{X}^{mN}$, $\boldsymbol{b}^n = \boldsymbol{g}(t_n + c_i\tau)_{i=1}^m$ for $n = 0, ..., N-1$;

2 **for** $n \leftarrow 1$ **to** N **do**

3 Solve $\boldsymbol{\mathcal{W}}_0(\boldsymbol{K})\boldsymbol{\phi}^{n-1} + \boldsymbol{a}(\boldsymbol{\phi}^{n-1}) = \boldsymbol{b}^{n-1}$; `// by Newton's method`

4 $l \leftarrow \gcd(2^n, n)$;

5 $\boldsymbol{\phi}_{loc} \leftarrow [(\boldsymbol{\phi}_j)_{j=nm-lm+1}^{nm}, 0, ..., 0] \in \boldsymbol{X}^{2lm}$;

6 $(\boldsymbol{b}_j)_{j=nm+1}^{nm+lm} \leftarrow (\boldsymbol{b}_j)_{j=nm+1}^{nm+lm} - \left((\boldsymbol{K}(\partial_t^\tau)\boldsymbol{\phi}_{loc})_j\right)_{j=lm+1}^{2lm}$; `// by` (C.11)

7 **return** $\boldsymbol{\phi}$;

We note that the somewhat unintuitive solution for $\boldsymbol{\phi}^{n-1}$ in the n-th time step stems from (B.8), by which $\boldsymbol{\phi}^{n-1}$ already includes an approximation for $\boldsymbol{\phi}(t_n)$. To compute the solution of the nonlinear discrete convolution equation described in Chapter 4, the parameters $L = 4N$ and $\rho^N = \sqrt{\epsilon}$ were used to compute the right-hand side of Line 6 via (C.11). The additional evaluations of the Laplace transforms are computationally expensive, but ensure the convergence of the method. The evaluations of the Laplace tansform $\boldsymbol{K}(s)$ necessary for the convolutions in Algorithm 1 can be reused. Consequently, $2mL$ (which corresponds to $8mN$ in the used implementation) evaluations are sufficient to execute Algorithm 1, as long as all Laplace transform evaluations can be stored in memory during the execution of the program.

Bibliography

[1] T. Abboud, P. Joly, J. Rodrı, and I. Terrasse. Coupling discontinuous galerkin methods and retarded potentials for transient wave propagation on unbounded domains. *J. Comput. Phys.*, 230(15):5877–5907, 2011.

[2] A. Alonso and A. Valli. Some remarks on the characterization of the space of tangential traces of $h(rot;\omega)$ and the construction of an extension operator. *Manuscripta Math.*, 89(1):159–178, 1996.

[3] H. Ammari, L. Halpern, and K. Hamdache. Thin ferromagnetic films. *Asymptot. Anal.*, 24(3-4):277–294, 2000.

[4] H. Ammari and S. He. Generalized effective impedance boundary conditions for an inhomogeneous thin layer in electromagnetic scattering. *J. Electromagn. Waves Appl.*, 11(9):1197–1212, 1997.

[5] H. Ammari and J.-C. Nédélec. Sur les conditions d'impédance généralisées pour les couches minces. *C. R. Acad. Sci. Paris Sér. 1, Math.*, 322(10):995–1000, 1996.

[6] H. Ammari and J.-C. Nédélec. Generalized impedance boundary conditions for the Maxwell equations as singular perturbations problems. *Comm. Partial Differential Equations*, 24(5-6):24–38, 1999.

[7] J. Ballani, L. Banjai, S. Sauter, and A. Veit. Numerical solution of exterior Maxwell problems by galerkin BEM and Runge–kutta convolution quadrature. *Numer. Math.*, 123(4):643–670, 2013.

[8] A. Bamberger and T. Ha Duong. Formulation variationnelle espace-temps pour le calcul par potentiel retardé de la diffraction d'une onde acoustique (I). *Math. Methods Appl. Sci.*, 8(1):405–435, 1986.

[9] A. Bamberger and T. Ha Duong. Formulation variationnelle pour le calcul de la diffraction d'une onde acoustique par une surface rigide. *Math. Methods Appl. Sci.*, 8(1):598–608, 1986.

[10] L. Banjai. Multistep and multistage convolution quadrature for the wave equation: algorithms and experiments. *SIAM J. Sci. Comput.*, 32(5):2964–2994, 2010.

[11] L. Banjai and M. Kachanovska. Sparsity of Runge-Kutta convolution weights for the three-dimensional wave equation. *BIT*, 54(4):901–936, 2014.

[12] L. Banjai and C. Lubich. An error analysis of Runge-Kutta convolution quadrature. *BIT*, 51(3):483–496, 2011.

[13] L. Banjai and C. Lubich. Runge-Kutta convolution coercivity and its use for time-dependent boundary integral equations. *IMA J. Numer. Anal.*, 39(3):1134–1157, 2019.

[14] L. Banjai, C. Lubich, and J. M. Melenk. Runge–Kutta convolution quadrature for operators arising in wave propagation. *Numer. Math.*, 119(1):1–20, 2011.

[15] L. Banjai, C. Lubich, and J. Nick. Time-dependent acoustic scattering from generalized impedance boundary conditions via boundary elements and convolution quadrature. *IMA J. Numer. Anal.*, 150(1):1–26, 2022.

[16] L. Banjai, C. Lubich, and F.-J. Sayas. Stable numerical coupling of exterior and interior problems for the wave equation. *Numer. Math.*, 129(4):611–646, 2015.

[17] L. Banjai, M. Messner, and M. Schanz. Runge-Kutta convolution quadrature for the boundary element method. *Comput. Methods Appl. Mech. Engrg.*, 245/246:90–101, 2012.

[18] L. Banjai and A. Rieder. Convolution quadrature for the wave equation with a nonlinear impedance boundary condition. *Math. Comp.*, 87(312):1783–1819, 2018.

[19] L. Banjai and S. Sauter. Rapid solution of the wave equation in unbounded domains. *SIAM J. Numer. Anal.*, 47(1):227–249, 2009.

[20] J. T. Beale and S. I. Rosencrans. Acoustic boundary conditions. *Bull. Amer. Math. Soc.*, 80(6):1276–1278, 1974.

[21] J.-P. Berenger. A perfectly matched layer for the absorption of electromagnetic waves. *J. Comput.*, 114(2):185–200, 1994.

[22] F. Brezzi and M. Fortin. *Mixed and hybrid finite element methods*, volume 15 of *Springer Series in Computational Mathematics*. Springer-Verlag, New York, 1991.

[23] A. Buffa and S. H. Christiansen. The electric field integral equation on Lipschitz screens: definitions and numerical approximation. *Numer. Math.*, 94(2):229–267, 2003.

[24] A. Buffa and P. Ciarlet, Jr. On traces for functional spaces related to Maxwell's equations. I. An integration by parts formula in Lipschitz polyhedra. *Math. Methods Appl. Sci.*, 24(1):9–30, 2001.

[25] A. Buffa, M. Costabel, and D. Sheen. On traces for $H(\mathbf{curl}, \Omega)$ in Lipschitz domains. *J. Math. Anal. Appl.*, 276(2):845–867, 2002.

[26] A. Buffa and R. Hiptmair. Galerkin boundary element methods for electromagnetic scattering. In *Topics in computational wave propagation*, pages 83–124. Springer, 2003.

[27] J. F.-C. Chan and P. Monk. Time dependent electromagnetic scattering by a penetrable obstacle. *BIT*, 55(1):5–31, 2015.

[28] Q. Chen, P. Monk, X. Wang, and D. Weile. Analysis of convolution quadrature applied to the time-domain electric field integral equation. *Commun. Comput. Phys.*, 11(2):383–399, 2012.

[29] M. Costabel. Boundary integral operators on lipschitz domains: elementary results. *SIAM J. Math. Anal.*, 19(3):613–626, 1988.

[30] G. Dziuk and C. M. Elliott. Finite element methods for surface pdes. *Acta Numer.*, 22:289–396, 2013.

[31] M. Eller, J. E. Lagnese, and S. Nicaise. Stabilization of heterogeneous Maxwell's equations by linear or nonlinear boundary feedbacks. *Electron. J. Differential Equations*, 2002:Paper–No, 2002.

[32] B. Engquist and J.-C. Nédélec. Effective boundary conditions for acoustic and electromagnetic scattering in thin layers. Technical report, Technical Report of CMAP, 278, 1993.

[33] V. Girault and P. Raviart. *Finite element methods for Navier–Stokes equations*. Berlin, 1986.

[34] F. Z. Goffi, K. Lemrabet, and T. Arens. Approximate impedance for time-harmonic Maxwell's equations in a non planar domain with contrasted multi-thin layers. *J. Math. Anal. Appl.*, pages 124–141, 2020.

[35] F. Z. Goffi, K. Lemrabet, and T. Laadj. Transfer and approximation of the impedance for time-harmonic Maxwell's system in a planar domain with thin contrasted multi-layers. *Asymptot. Anal.*, 101(1-2):1–15, 2017.

[36] T. Ha-Duong. On retarded potential boundary integral equations and their discretisation. In *Topics in computational wave propagation*, pages 301–336. Springer, 2003.

[37] T. Ha-Duong, B. Ludwig, and I. Terrasse. A galerkin bem for transient acoustic scattering by an absorbing obstacle. *Internat. J. Numer. Methods Engrg.*, 57(13):1845–1882, 2003.

[38] W. Hackbusch, W. Kress, and S. A. Sauter. Sparse convolution quadrature for time domain boundary integral formulations of the wave equation. *IMA J. Numer. Anal.*, 29(1):158–179, 2009.

[39] H. Haddar and P. Joly. Effective boundary conditions for thin ferromagnetic layers: the one-dimensional model. *SIAM J. Appl. Math.*, 61(4):1386–1417, 2001.

[40] H. Haddar and P. Joly. Stability of thin layer approximation of electromagnetic waves scattering by linear and nonlinear coatings. *J. Comput. Appl. Math.*, 143(2):201–236, 2002.

[41] H. Haddar, P. Joly, and H.-M. Nguyen. Generalized impedance boundary conditions for scattering by strongly absorbing obstacles: the scalar case. *Math. Models Methods Appl. Sci.*, 15(08):1273–1300, 2005.

[42] H. Haddar, P. Joly, and H.-M. Nguyen. Generalized impedance boundary conditions for scattering problems from strongly absorbing obstacles: The case of Maxwell's equations. *Math. Models Methods Appl. Sci.*, 18(10):1787–1827, 2008.

[43] E. Hairer, C. Lubich, and M. Schlichte. Fast numerical solution of nonlinear volterra convolution equations. *SIAM J. Sci. Statist. Comput.*, 6(3):532–541, 1985.

[44] E. Hairer and G. Wanner. *Solving ordinary differential equations. II*, volume 14 of *Springer Series in Computational Mathematics*. Springer-Verlag, Berlin, 1991. Stiff and differential-algebraic problems.

[45] R. Hiptmair, M. López-Fernández, and A. Paganini. Fast convolution quadrature based impedance boundary conditions. *J. Comput. Appl. Math.*, 263:500–517, 2014.

[46] B. Kovács and C. Lubich. Stable and convergent fully discrete interior–exterior coupling of Maxwell's equations. *Numer. Math.*, 137(1):91–117, 2017.

[47] A. R. Laliena and F.-J. Sayas. Theoretical aspects of the application of convolution quadrature to scattering of acoustic waves. *Numer. Math.*, 112(4):637–678, 2009.

[48] M. A. Leontovich. On one approach to a problem of the wave propagation along the surface. *Academy of Science USSR, Series Physics*, 8:16–22, 1944.

[49] M. A. Leontovich. Approximate boundary conditions for the electromagnetic field on the surface of a good conductor. *Investigations on radiowave propagation*, 2, 1948.

[50] C. Lubich. Convolution quadrature and discretized operational calculus. I. *Numer. Math.*, 52(2):129–145, 1988.

[51] C. Lubich. Convolution quadrature and discretized operational calculus. II. *Numer. Math.*, 52(4):413–425, 1988.

[52] C. Lubich. On the multistep time discretization of linear initial-boundary value problems and their boundary integral equations. *Numer. Math.*, 67(3):365–389, 1994.

[53] C. Lubich and A. Ostermann. Runge-Kutta methods for parabolic equations and convolution quadrature. *Math. Comp.*, 60(201):105–131, 1993.

[54] J.-C. Nédélec. *Acoustic and electromagnetic equations: integral representations for harmonic problems*. Springer, 2001.

[55] H.-M. Nguyen and L. V. Nguyen. Generalized impedance boundary conditions for strongly absorbing obstacle: The full wave equation. *Math. Models Methods Appl. Sci.*, 25(10):1927–1960, 2015.

[56] J. Nick. Accompanying codes provided via GitHub. https://github.com/joergnick/cqExperiments.

[57] J. Nick. Numerical analysis for electromagnetic scattering from nonlinear boundary conditions. *arXiv preprint arXiv:2208.08402*, 2022.

[58] J. Nick, B. Kovács, and C. Lubich. Correction to: Stable and convergent fully discrete interior-exterior coupling of Maxwell's equations. *Numer. Math.*, 147(4):997–1000, 2021.

[59] J. Nick, B. Kovács, and C. Lubich. Time-dependent electromagnetic scattering from thin layers. *Numer. Math.*, 150(4):1123–1164, 2022.

[60] P.-A. Raviart and J. M. Thomas. A mixed finite element method for 2nd order elliptic problems. In *Mathematical aspects of finite element methods (Proc. Conf., Consiglio Naz. delle Ricerche (C.N.R.), Rome, 1975)*, pages 292–315. Lecture Notes in Math., Vol. 606, 1977.

[61] S. Rytov. Calcul du skin-effect par la méthode des perturbations. *J. Phys. USSR*, 2(3):233–242, 1940.

[62] S. A. Sauter and M. Schanz. Convolution quadrature for the wave equation with impedance boundary conditions. *J. Comput. Phys.*, 334:442–459, 2017.

[63] S. A. Sauter and C. Schwab. Boundary element methods. Springer-Verlag, New York, 2011.

[64] F.-J. Sayas. *Retarded potentials and time domain boundary integral equations: A road map*, volume 50 of *Springer Series in Computational Mathematics*. Springer, Heidelberg, 2016.

[65] M. W. Scroggs, T. Betcke, E. Burman, W. Śmigaj, and E. van 't Wout. Software frameworks for integral equations in electromagnetic scattering based on Calderón identities. *Comput. Math. Appl.*, 74(11):2897–2914, 2017.

[66] M. Slodivcka and V. Zemanová. Time-discretization scheme for quasi-static Maxwell's equations with a non-linear boundary condition. *J. Comput. Appl. Math.*, 216(2):514–522, 2008.

[67] M. Slodivcka and S. Durand. Fully discrete finite element scheme for Maxwell's equations with non-linear boundary condition. *J. Math. Anal. Appl.*, 375(1):230–244, 2011.

[68] W. Śmigaj, T. Betcke, S. Arridge, J. Phillips, and M. Schweiger. Solving boundary integral problems with BEM++. *ACM Trans. Math. Software*, 41(2):1–40, 2015.

[69] K. Van Bockstal. *Numerical techniques for partial differential equations in superconductivity and thermoelasticity*. PhD thesis, Ghent University, 2015.

[70] V. Vrábel and M. Slodicka. An eddy current problem with a nonlinear evolution boundary condition. *J. Math. Anal. Appl.*, 387(1):267–283, 2012.

[71] S. Yuferev. *Surface Impedance Boundary Conditions: A Comprehensive Approach*. CRC Press, 09 2009.